Examination of Crystal River Unit #3 Steam Generator Tube Sections

TR-103756
Research Project S413-06

Final Report, January 1994

Prepared by

B&W NUCLEAR TECHNOLOGIES
Special Products & Integrated Services Division
and
THE BABCOCK & WILCOX COMPANY
Nuclear Environmental Services, Inc.

Principal Investigators
P.A. Sherburne
K.R. Redmond

Prepared for

Electric Power Research Institute
3412 Hillview Avenue
Palo Alto, California 94304
and
Florida Power Corporation
15760 West Power Line Street
Crystal River, Florida 34428-6708

EPRI Project Manager

J.P.N. Paine
Steam Generator Reliability Project
Nuclear Power Division

DISCLAIMER OF WARRANTIES AND LIMITATION OF LIABILITIES

This report was prepared by the organizations(s) named below as an account of work sponsored or cosponsored by the Electric Power Institute, Inc. (EPRI). Neither EPRI, any member of EPRI, any cosponsor, the organizations(s) named below, nor any person acting on behalf of any of them:

(a) makes any warranty or representation whatsoever, express or implied, (1) with respect to the use of any information, apparatus, method, process, or similar item disclosed in this report, including merchantability and fitness for a particular purpose, or (2) that such use does not infringe on or interfere with privately owned rights, including any party's intellectual property, or (3) that this report is suitable to any particular user's circumstance; or

(b) assumes responsibility for any damages or other liability whatsoever (including any consequential damages, even if EPRI or any EPRI representative has been advised of the possibility of such damages) resulting from your selection or use of this report or any information, apparatus, method, process, or similar item disclosed in this report.

Organization(s) that prepared this report:

B&W Nuclear Technologies, Inc.
The Babcock & Wilcox Company

ABSTRACT

Portions of seven (7) tubes were removed from the "B" OTSG at CR-3 during Refuel 8 (June 1992) and sent to the Babcock & Wilcox Company's Lynchburg Technology Center (LTC) for a laboratory evaluation. Six of the tubes contained low voltage ECT indications in the free span region between the secondary face of the lower tubesheet (LTSF) and the first tube support plate (TSP). The 7th tube had eddy current indications at the 7th TSP; however, due to difficulties encountered during tube removal, this region of interest was not recovered. The objectives of the laboratory examination were to physically characterize any tube degradation for correlation with field eddy current data, to determine the effect of these defects on the pressure holding capability of the tubing, and to establish the damage mechanism.

The defects responsible for the low voltage eddy current signals in the first span region consisted of small, relatively shallow, isolated patches of OD-initiated IGA. The IGA damage was associated with a non-uniform deposit pattern, concentrated in an area 8 to 18 inches above the secondary face of the lower tube sheet. The corrosion was attributed to low-temperature, reduced-sulfur attack, which probably occurred early in plant life and is no longer active. The bobbin coil eddy current technique was successful in detecting this damage, detecting all IGA patches with depths greater than 50% throughwall and ~80% of those with depths equal to or greater than 40% throughwall. Additionally, lab tests determined that the IGA had almost no effect on the burst strength of the tubing.

ACKNOWLEDGEMENTS

The authors would like to acknowledge and thank Peter Paine of the Electric Power Research Institute (EPRI) and Rocky Thompson of Florida Power Corporation for their guidance throughout this project and for their patience during preparation of the final report. The authors would also like to acknowledge and thank the following people for their contributions to this project: Harry Smith, B&W Nuclear Technologies, and Kenji Krzywosz, EPRI NDE Center, for analysis and interpretation of eddy current data; Ross Davidson, Surface Science Western, for AES and XPS analysis; Sue Hobart, Adams & Hobart, for the review and evaluation of operating chemistry data; and Sidney (Trey) Reeves, B&W Nuclear Environmental Services, metallography.

TABLE OF CONTENTS

ILLUSTRATIONS

Figure | Page

TABLES

SUMMARY

Crystal River Unit 3 (CR-3) is an 860 MWe pressurized water reactor (PWR) plant owned and operated by Florida Power Corporation (FPC). The plant has been operating commercially since March 1977. CR-3 utilizes two (2) Model 177 FA once-through steam generators (OTSG) designed and fabricated by The Babcock & Wilcox Company. Each steam generator has 15,531 Alloy 600 tubes with nominal dimensions of 0.625 inch OD X 0.034 inch wall thickness.

Analysis of Refuel 7 field eddy current data revealed a significant number of indications along the tube free spans in the boiling regions of the steam generators. In particular, numerous indications were observed in the free span between the lower tubesheet secondary face (LTSF) and the first tube support plate (TSP) of the "B" steam generator. Many of these indications were just below the threshold of detection, and were difficult to distinguish from background noise. To investigate these indications further, sections of 6 tubes were removed from the lower part of the "B" steam generator tube bundle during Refuel 8 in May 1992 and submitted for detailed laboratory examination and root cause evaluation. Additionally, an attempt was made to pull a 7th tube which had eddy current indications at the 7th TSP. The area of interest for this tube was not recovered, however, since the tube became stuck in the steam generator during the removal process.

The objectives of the examination were as follows:

1. Physically characterize any tube degradation, particularly damage associated with low signal-to-noise ratio (S/N) indications in the boiling/free span regions, for correlation with field eddy current and ultrasonics data. This included identification of the type of and extent of degradation and the degree of through-wall penetration. This data was used to establish the baseline sensitivity and sizing accuracy of the NDE techniques for this type of defect.

2. Obtain burst pressure data to determine the effect of any significant defects on the pressure holding capability of the tubing.

3. Attempt to establish the damage mechanism responsible for the eddy current indications.

4. Evaluate plant chemistry trends with respect to the degradation observed.

The laboratory examination consisted of eddy current and ultrasonics testing, radiography, dimensional measurements, visual inspection and photography, burst testing, extensive metallography, and corrosion film and deposit analysis.

In parallel with the tube examination, a review of plant chemistry data and hideout return studies were conducted by Adams & Hobart, Consulting Engineers. The purpose in conducting a review of the plant chemistry information was to look for a causal relationship of tube degradion with the steam generator environment.

In addition to the plant chemistry studies, independent reviews of eddy current test data (both historical and present) were carried out by the EPRI NDE Center. The objectives in reviewing historical eddy current data were (1) to establish the approximate date that tube defect indications were first observed,

and (2) to determine if the defect indications are changing in size or in number. The latter objective addresses whether the damage mechanism is active or inactive.

The results obtained in this project can be summarized as follows:

- The defects responsible for the low voltage eddy current signals in the first span region consisted of small, relatively shallow, isolated patches of OD-initiated IGA. The IGA damage was associated with a non-uniform deposit pattern, concentrated in an area 8 to 18 inches above the secondary face of the lower tube sheet.

- The corrosion was attributed to low-temperature, reduced-sulfur attack, which probably occurred early in plant life when resin leakage from the condensate polishing system and poor oxygen control during wet lay-up combined to produce conditions favorable for this type of corrosion. A review of recent plant chemistry data, including hideout return studies, suggests that the present chemistry environment does not support continuation of the reduced sulfur acid attack below the first tube support plate. It is recommended, however, that precautions be taken to ensure that acidic conditions in the lower part of the steam generators do not recur.

- The bobbin coil eddy current technique used for the inservice inspection successfully detected this damage, detecting all IGA patches with depths greater than 50% throughwall and ~80% of those with depths equal to or greater than 40% throughwall.

Section 1

INTRODUCTION

1.1 Background Information

Crystal River Unit 3 (CR-3) is an 860 MWe pressurized water reactor (PWR) plant owned and operated by Florida Power Corporation (FPC). The plant has been operating commercially since March 1977. CR-3 utilizes two (2) Model 177 FA once-through steam generators (OTSG) designed and fabricated by The Babcock & Wilcox Company. Each steam generator has 15,531 Alloy 600 tubes with nominal dimensions of 0.625 inch OD X 0.034 inch wall thickness.

Analysis of Refuel 7 field eddy current data revealed a significant number of indications along the tube free spans in the boiling regions of the steam generators. In particular, numerous indications were observed in the first free span between the lower tubesheet secondary face (LTSF) and the first tube support plate (TSP) of the "B" steam generator. Many of these indications were just below the threshold of detection, and were difficult to distinguish from background noise. To investigate these indications further, sections of 6 tubes were removed from the lower part of the "B" steam generator tube bundle during Refuel 8 in May 1992 and submitted for detailed laboratory examination. In addition, an attempt was made to pull a 7th tube (tube no. 133-33) which had eddy current indications at the 7th TSP. The area of interest for this tube was not recovered, however, since the tube became stuck in the steam generator during the removal process.

A sketch of the pulled tube segments and their approximate elevation in the CR-3 steam generator is provided in Figure 1-1.

1.2 Project Objectives

The objectives of the examination were as follows:

1. Physically characterize any tube degradation, particularly damage associated with low signal-to-noise ratio (S/N) indications in the boiling/free span regions, for correlation with field eddy current and ultrasonics data. This included identification of the type of and extent of degradation and the degree of through-wall penetration. This data was used to establish the baseline sensitivity and sizing accuracy of the NDE techniques for this type of defect.

2. Obtain burst pressure data to determine the effect of any significant defects on the pressure holding capability of the tubing.

3. Attempt to establish the damage mechanism responsible for the eddy current indications.

4. Evaluate plant chemistry trends with respect to the degradation observed.

1.3 Technical Approach

Since the sections of tubing removed from the steam generators were contaminated in service with activated corrosion products from the primary system, the bulk of the tube examination was conducted under controlled conditions at B&W's Lynchburg Technology Center. The examination (Table 1-1)

consisted of eddy current and ultrasonics testing, radiography, dimensional measurements, visual inspection and photography, burst testing, extensive metallography, and corrosion film and deposit analysis.

In parallel with the tube examination, a review of plant chemistry data and hideout return studies were conducted by Adams & Hobart, Consulting Engineers. The purpose in conducting a review of the plant chemistry information was to look for a causal relationship of tube degradion with the steam generator environment.

In addition to the plant chemistry studies, independent reviews of eddy current test data (both historical and present) were carried out by the EPRI NDE Center. The objectives in reviewing historical eddy current data were (1) to establish the approximate date that tube defect indications were first observed, and (2) to determine if the defect indications are changing in size or in number. The latter objective addresses whether the damage mechanism is active or inactive.

1.4 Results Summary

The defects responsible for the low voltage eddy current signals in the first span region consisted of small, relatively shallow, isolated patches of OD-initiated IGA. The IGA damage was associated with a non-uniform deposit pattern, concentrated in an area 8 to 18 inches above the secondary face of the lower tube sheet. The corrosion was attributed to low-temperature, reduced-sulfur attack, which probably occurred early in plant life when resin leakage from the condensate polishing system and poor oxygen control during wet lay-up combined to produce conditions favorable for this type of corrosion. The bobbin coil eddy current technique was successful in detecting this damage, detecting all IGA patches with depths greater than 50% throughwall. Additionally, laboratory tests demonstrated that the IGA has little effect on the burst strength of the tubing.

1.5 Report Organization

Results of the nondestructive and destructive tube examinations are described in Section 2. Evaluation of the data and correlations with eddy current testing and plant chemistry information are included in Section 3. All of the results are discussed in Section 4 and conclusions are presented in Section 5. Eddy current information and individual reports by the EPRI NDE Center and by Adams & Hobart are included in Appendices A through C.

TABLE 1-1: EXAMINATION OUTLINE

TASK 1: NONDESTRUCTIVE PHASE

Receipt Inspection*
Visual Inspection & Photography*
Eddy Current Testing**
Ultrasonic Testing**
X-Ray Radiography**

TASK 2: DESTRUCTIVE PHASE

Task Description	97-91-2 108-32-2	52-51-2 90-28-2	109-30-2	41-44-2	52-51-4 90-28-5	133-33-9	133-33-3 133-33-2
Hand-Pull ECT	X	X	X	X			
OD Descaling	X						
Post-Clean ECT	X						
Liquid Penetrant	X						
Tube Sectioning					X	X	X
Tube Swelling		X			X	X	X
Burst Testing	X						
Deposit Sampling		X			X	X	X
Stereovisual	X	X	X		X	X	X
Tube Sectioning	X	X	X			X	X
SEM/EDS		X	X			X	X
Metallography	X	X	X			X	X
SAM/XPS		X					

* All tube sections

** These examinations were performed only on those tube sections with field eddy current indications

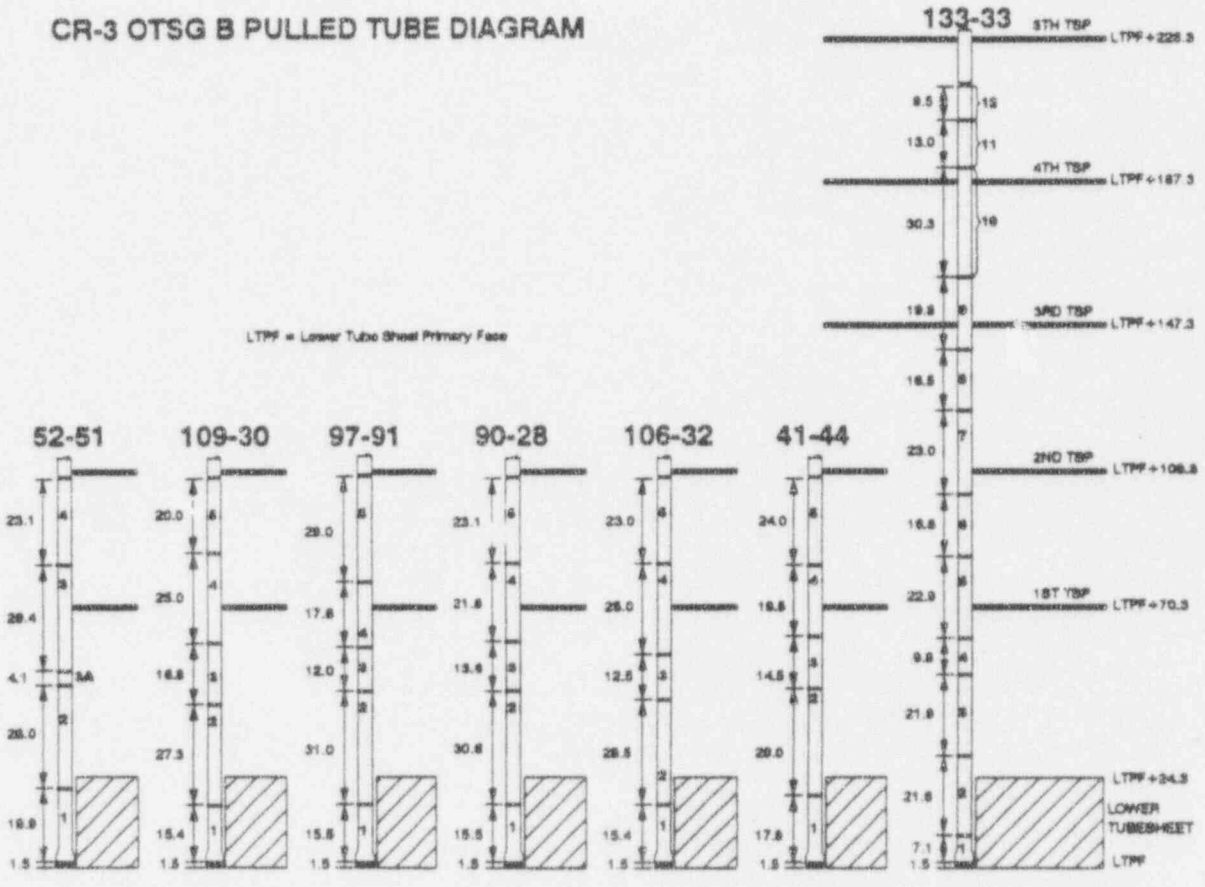

Figure 1-1: CR-3 OTSG B Pulled Tube Diagram

Section 2

TUBE EXAMINATION

2.1 Nondestructive Examinations

2.1.1 Receipt Inspections

The CR-3 tube sections arrived at the Lynchburg Technology Center (LTC) on August 12, 1992. Contact radiation levels on receipt were approximately 200 mR/hr γ and smearable contamination levels were on the order of 500K dpm/100cm^2, requiring much of the initial work to be performed under Radiation Work Permits (RWPs).

The tube segments were measured for length and visually inspected for orientation markings and landmark features (e.g., lower tubesheet secondary face (LTSF) and tube support plate (TSP) regions) for comparison with tube removal records. Once the tube orientation relative to the steam generator tube array was established, each tube segment was notched at an arbitrary 0° position at the bottom to preserve the orientation. Angular convention used throughout this report is clockwise looking at the bottom of the tube. Length measurements and the location of important landmarks were generally verified to within 1/4 inch of the field reported data (see Table 2-1 for lab data).

TABLE 2-1

TUBE RECEIPT INSPECTION RESULTS

Tube No. 52-51			Tube No. 90-28			Tube No. 106-32		
Piece	Length	Landmarks	Piece	Length	Landmarks	Piece	Length	Landmarks
4	23.3		5	23.1		5	23.1	
3	29.1	TSP (16.5)	4	21.8	TSP (9.4)	4	24.8	TSP (11.8)
3A	4.3		3	13.5		3	12.6	
2	27.9	LTSF (2.6)	2	30.8	LTSF (7.5)	2	28.8	LTSF (7.5)
1	19.9		1	15.4		1	15.4	

TABLE 2-1 (cont.)

TUBE RECEIPT INSPECTION RESULTS

Tube No. 97-91

Piece	Length	Landmarks
5	28.9	
4	18.0	TSP (10.6)
3	11.8	
2	30.6	LTSF (7.5)
1	15.5	

Tube No. 109-30

Piece	Length	Landmarks
5	20.0	
4	24.8	TSP (9.5)
3	16.6	
2	27.1	LTSF (7.5)
1	15.3	

Tube No. 41-44

Piece	Length	Landmarks
5	24.0	
4	19.3	TSP (7.5)
3	14.5	
2	28.8	LTSF (5.0)
1	17.6	

Tube No. 133-33

Piece	Length	Landmarks
12	9.4	
11	13.0	
10	29.8	TSP*
9	19.9	TSP (6.0)
8	16.5	
7	22.9	TSP (6.8)
6	16.5	
5	22.9	TSP (8.3)
4	9.8	
3	22.0	
2	21.4	LTSF (15.6)
1	7.0	

*Not verified due to extensive deposit spalling.
Note: Numbers in parentheses are inches to TSP center from the tube bottom end (TBE).

2.1.2 Visual Inspection and Photography

Each tube segment was examined visually and selectively at low power (up to 40X) with a stereomicroscope to characterize surface deposits, visible regions of degradation, dimensional variations, mechanical damage sustained during tube removal and other items of interest. Important results of the examination were documented photographically.

General Appearance

In general, the freespan tube surfaces were covered with a relatively thin layer of black deposit. The outer regions of the deposit were powdery and nonadherent, but the underlying deposit was more tenacious (verified by scraping). These characteristics are typical of magnetite deposits, which form on boiling surfaces in steam generators utilizing AVT water chemistry control. Minor scratches and saw nicks from the tube pulling operation were common to all tube sections as well.

Lower Tubesheet Region (All Tubes)

On all tubes, regions contained within the tubesheet were essentially free of deposits, although some light green deposits were noted on most tubes in the first few inches below the LTSF. The areas void of deposit typically exhibited a copper-colored sheen; this may simply have been due to a thin Ni-Cr oxide film on the metal surface. Some minor pitting was also typically observed within 2 to 3 inches below the LTSF. The LTSF regions for all tubes except 133-33 are shown in Figures 2-1 through 2-6.

1st Freespan Region (Tubes 52-51, 90-28, 97-91, 106-32, 109-30, 41-44)

For all tubes except 133-33, the deposits had a pronounced irregularly-shaped splotchy appearance, resulting from (1) spots where the deposit had spalled off exposing the tube metal and (2) areas where the deposit was thinner and darker than the surrounding bulk deposit giving a scalloped appearance (see Figs. 2-7 through 2-12). There were some subtle tube-to-tube differences in the deposit character as discussed below:

Tube Section 52-51-2: The scalloped patterns were less prevalent in the 0° orientation. Also, coarser scallop patterns were present along the 180° and 270° orientations. A half inch wide circumferential band of relatively smooth uniform deposit was noted 19 inches above the LTSF; immediately adjacent to and on either side of this band, the scallop patterns were very coarse and appeared to have some significant depth (see Fig. 2-13). A 3/8 inch wide circumferential band of apparently deep scallop patterns was observed about 21 inches above the LTSF (see Fig. 2-14).

Tube Section 90-28-2: The scalloped deposit patterns were generally coarser than 52-51-2 and were more prevalent in the 0° and 270° orientations. Also, there was large areas of spalled deposit.

Tube Section 97-91-2: The deposits on this tube section were more uniform than the other tubes. The dark scalloped patterns were not nearly as evident, although there were many tiny spots of spalled deposit.

Tube Section 106-32-2: The deposit patterns on this tube section were very similar to 52-51-2, except that coarser scalloped patterns were most apparent along the 90° orientation.

Tube Section 109-30-2: The deposit patterns on this tube section were quite similar to 90-28-2, with the coarsest scallop patterns present in the 0° orientation.

Tube Section 41-44-2: The deposit patterns on this tube section were very similar to 52-51-2, except that the scallop patterns were more uniformly coarse around the tube circumference. Also, an axial band of spalled deposit was observed along the 0° orientation.

In any case, no defects were identified by visual inspection in any of these tube sections in the first freespan zone; particularly in the area immediately above the LTSF (i.e., the location of the field reported bobbin coil indications).

1st TSP Region (Tubes 52-51, 90-28, 97-91, 106-32, 109-30, 41-44)

In general, the support plate land contact positions were easily visible on these tubes due to the general absence of deposit (see Figs. 2-15 through 2-20). There were no obvious signs of wear or significant pitting in the TSP regions. The deposit patterns described previously generally persisted up to the TSP, then continued on above. Tube-to-tube differences are discussed below.

Tube Section 52-51-3: Tube section 52-51-3 was bowed rather severely just below the TSP and the deposits were severely spalled in this area (see Fig. 2-21). This was probably a result of the tube pulling operation. Deposits above the TSP were similar to those described previously, except the scalloped patterns were much larger (see Fig. 2-22).

Tube Section 90-28-4: There was extensive deposit spalling within the TSP region on this tube section. A typical deposit pattern above the TSP is shown in Figure 2-23).

Tube Section 97-91-4: Deposit spalling within the TSP was also reasonably extensive on this tube. This tube section was different than the others in that the deposit was very uniform, with the exception of some occasional spalling. A typical area is shown in Figure 2-24.

Tube Section 106-32-4: The scalloped deposits persisted above the TSP on this tube, but the patterns were coarser than those in the free span below the TSP. A typical area is shown in Figure 2-25.

Tube Section 109-30-4: Similar to tube section 106-32-4 (see Fig. 2-26).

Tube Section 41-44-4: Some possible, but very minor pitting was noted at the 30° land contact on this tube section. The deposit characteristics were very similar to tube section 106-32-4 (see Fig. 2-27).

Comments on Tube 133-33

In a few locations, the deposit in the first freespan zone on tube 133-33 exhibited characteristics similar to the other tubes, but in general it possessed a relatively uniform, thin deposit layer. The deposit layer appeared to become somewhat thicker with increasing elevation in the steam generator, but above the 3rd TSP essentially all of the deposit had spalled off - probably a result of the tube removal operation. The TSP land contact zones were not nearly as visible on this tube.

2.1.3 Laboratory Eddy Current Testing

All tube segments containing TSP intersections, roll expansion transitions and areas with suspected defects were inspected by eddy current probes to characterize and to accurately locate the defects, and to correlate the lab eddy current data with that obtained in the field. The probes used for the examination were (1) Zetec 0.510" mag-bias universal long cone high frequency (M/ULC/HF) bobbin coils and (2) Zetec 0.520" 3-coil motorized rotating pancake coil (MRPC) probes. Data was acquired and analyzed using Zetec DDA-4 and Eddynet software.

From the examination, two major observations were made:

(1) The defects presented a volumetric (non-cracklike) signature, similar to signals provided by shallow, outside diameter pitting.

(2) The majority of flaws reported in the field were confirmed in the laboratory . No new or different modes of degradation were detected.

Detailed results of the laboratory examination may be found in Appendix A. Note that for brevity, figures (lisajous plots and MRPC terrain maps) are not included in the Appendix.

2.1.4 Ultrasonics Testing

Tube segments containing areas with suspected defects were inspected by ultrasonics. BWNT's rotating probe ultrasonic inspection system (UT-360) was used for both pre-tube pull and post-tube pull examination. The objective was to determine if ultrasonic inspection is a viable technique for detecting defects of the type present in the CR-3 steam generators.

Comparison of the UT (lab and field) data with ECT data showed good correlation between field and lab UT data, but no correlation with ECT data. Most defect indications found with the eddy current probes were not detected with the ultrasonic inspection system. Results of the UT-360 examination are documented in Reference 1.

2.1.5 X-Ray Radiography

X-Ray Radiography was performed on the freespan areas containing eddy current indications and at the 1st TSP regions on all of the tube segments except 133-33. A Norelco 150 Model MG150 industrial radiographic unit with a 150 KV heavy duty double focus x-ray tube was used for this inspection. A double wall radiography technique was used and each area of interest was radiographed in four (4) angular positions (i.e., 0°, 45°, 90°, and 135°). Two sheets of 14" X 17" Type S(R) Kodak high resolution film were loaded into the cassettes to obtain two radiographs of slightly different density for each exposure. Front and back lead screens (5 mils thick) were utilized in the film cassette. For most of the radio-graphs, the exposure conditions were 150 KV tube voltage and 20 ma tube current for 0.9 minutes at a source-to-film distance of 35 inches. These parameters were chosen based on operator experience to obtain high film contrast and good sensitivity. All of the radiographs were carefully inspected on a light box using a hand held magnifying glass.

No defect indications were observed in any of the radiographs. Some tube sections exhibited wispy indications, which may have been due to deposit patterns or residual water (from the ultrasonics testing) on the inside of the tubes. The observed wispy patterns were in no way related to the OD deposit patterns noted previously. Since no service related defects were identified, prints of the x-ray film were not reproduced in this report.

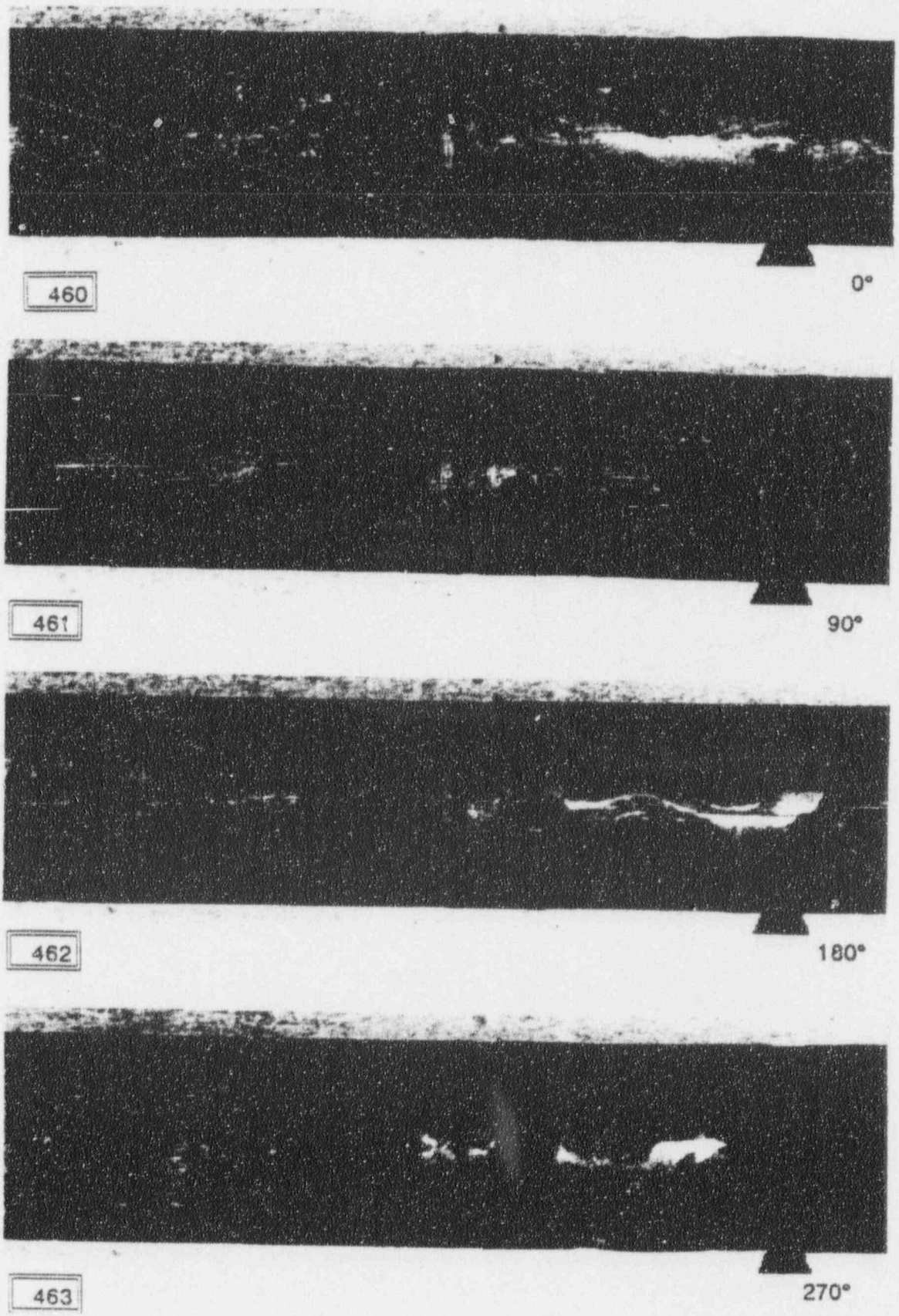

Figure 2-1: Tube Section 52-51-2, LTSF Region As-Received (2.2X; Bottom At Left)

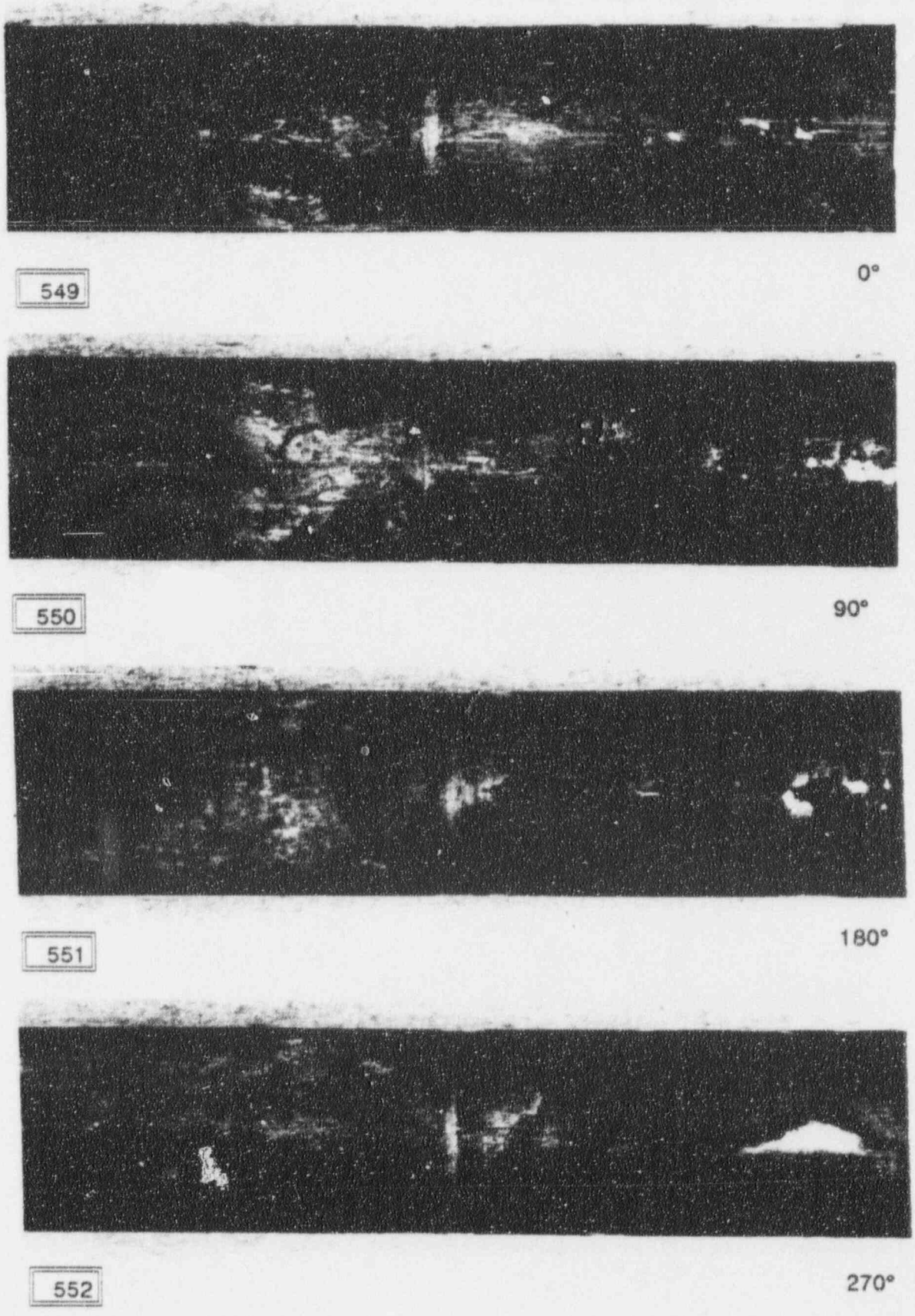

Figure 2-2: Tube Section 90-28-2. LTSF Region As-Received (2.2X; Bottom At Left)

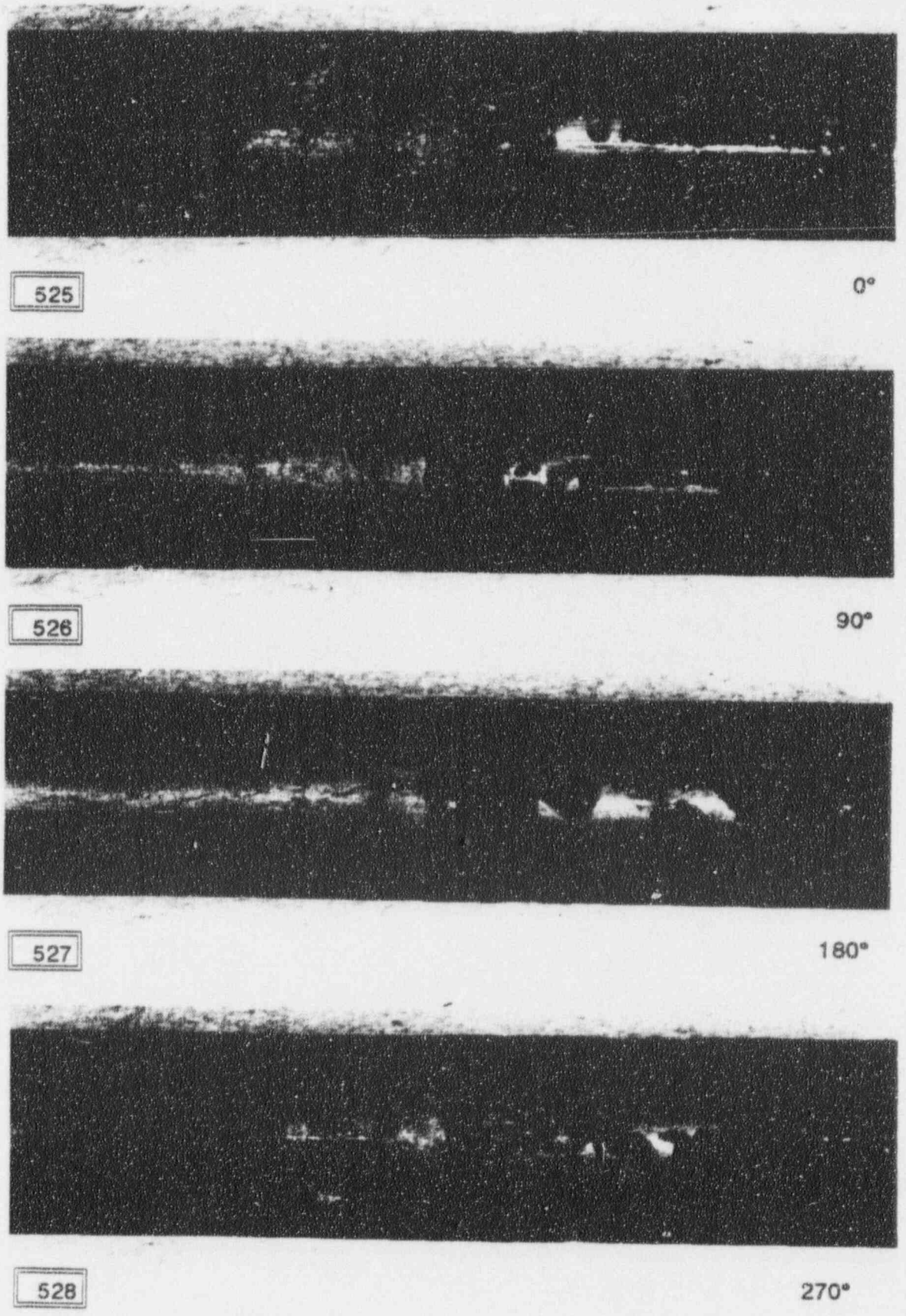

Figure 2-3: Tube Section 97-91-2, LTSF Region As-Received (2.2X; Bottom At Left)

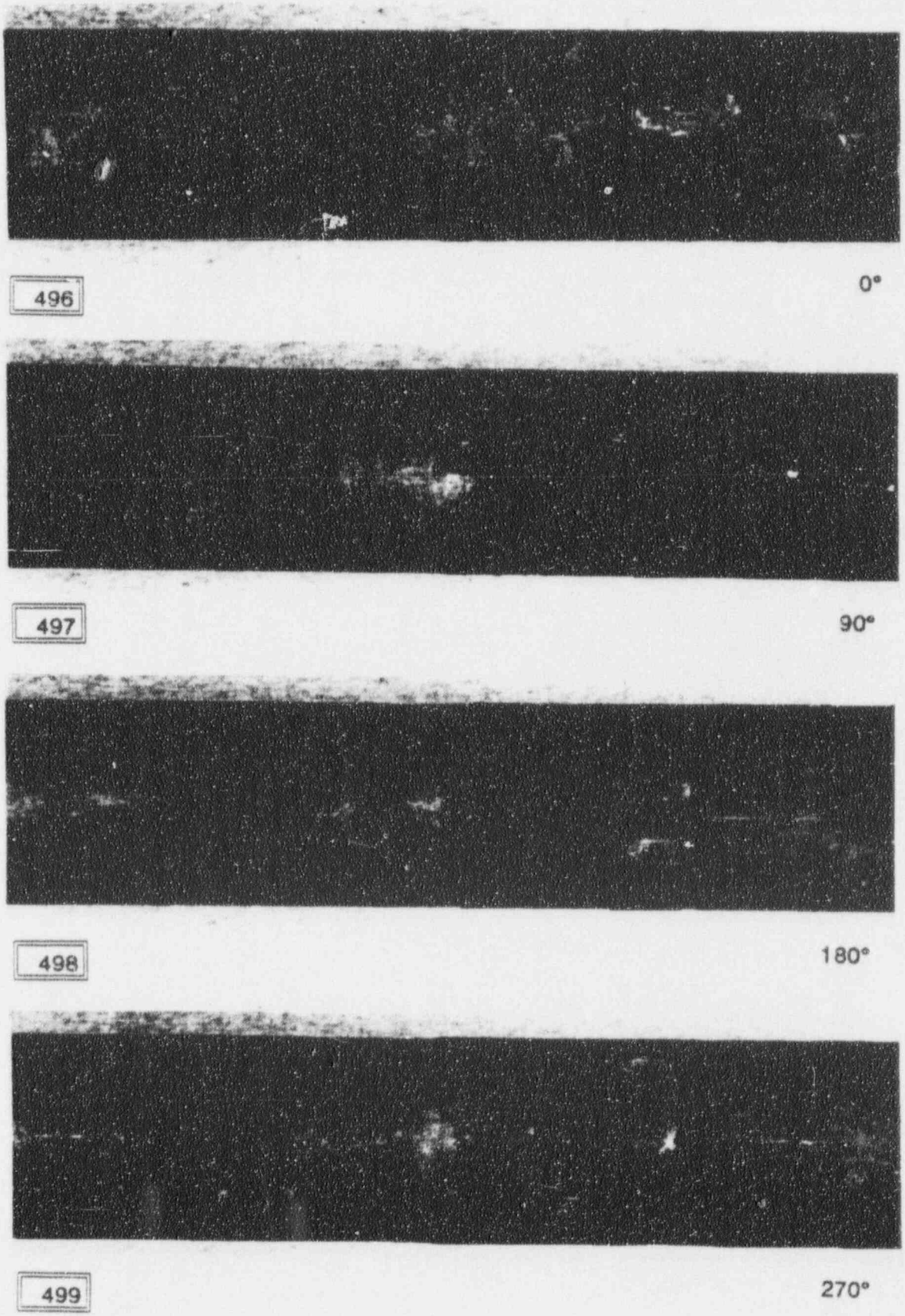

Figure 2-4: Tube Section 106-32-2, LTSF Region As-Received (2.2X; Bottom At Left)

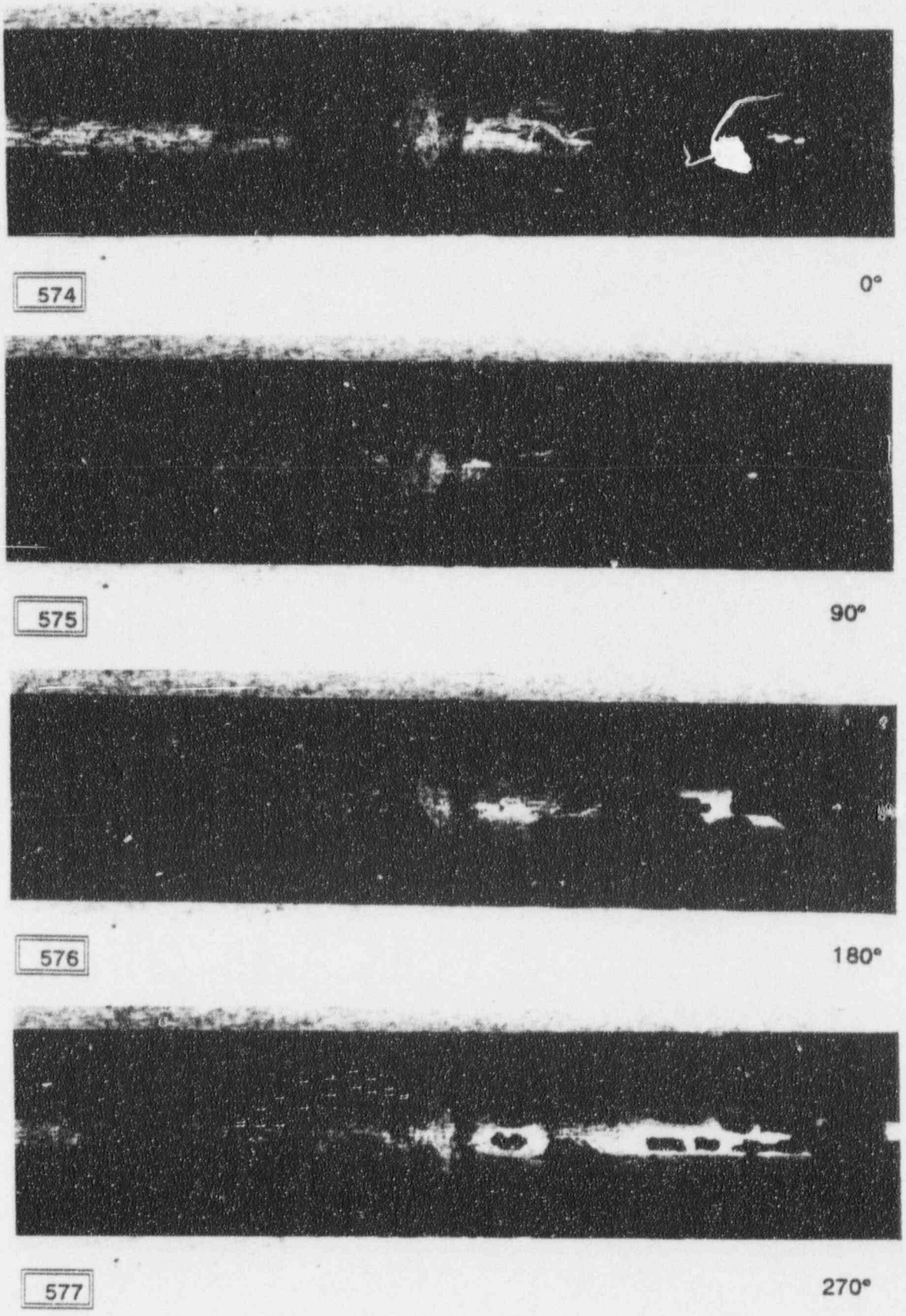

Figure 2-5: Tube Section 109-30-2, LTSF Region As-Received (2.2X; Bottom At Left)

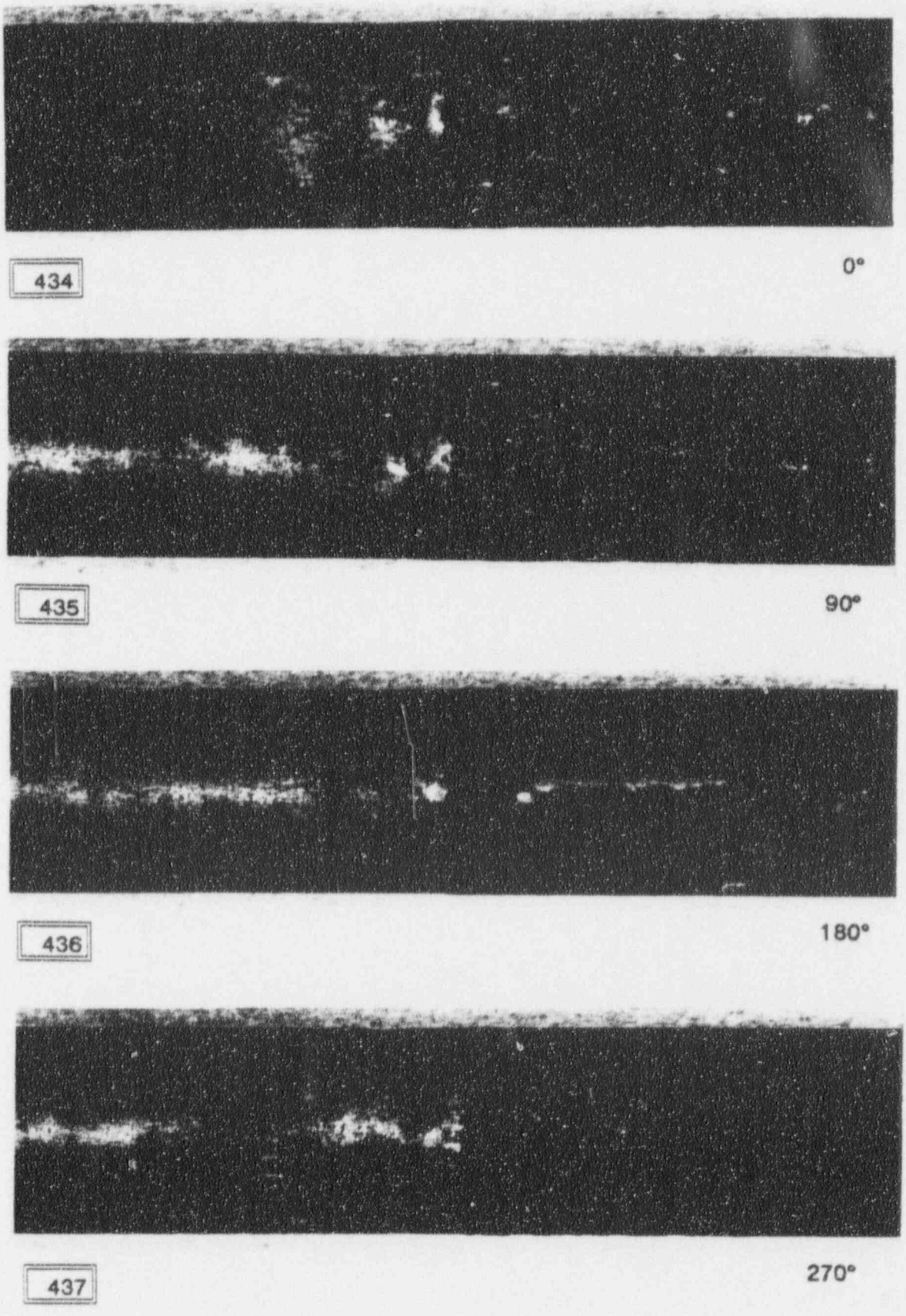

Figure 2-6: Tube Section 41-44-2, LTSF Region As-Received (2.2X; Bottom At Left)

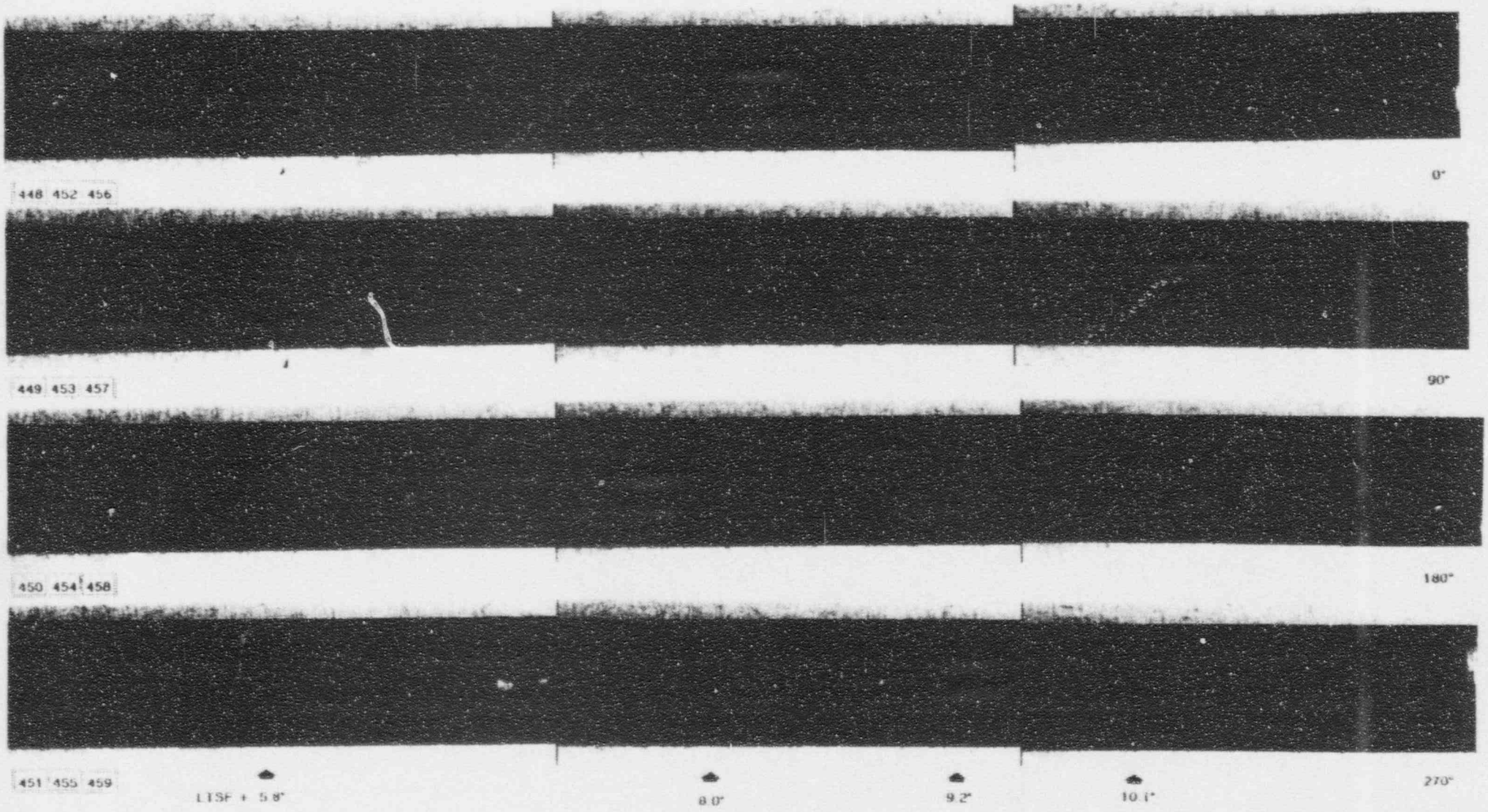

Figure 2-7: Tube Section 52-51-2, Freespan above LTSF As-Received

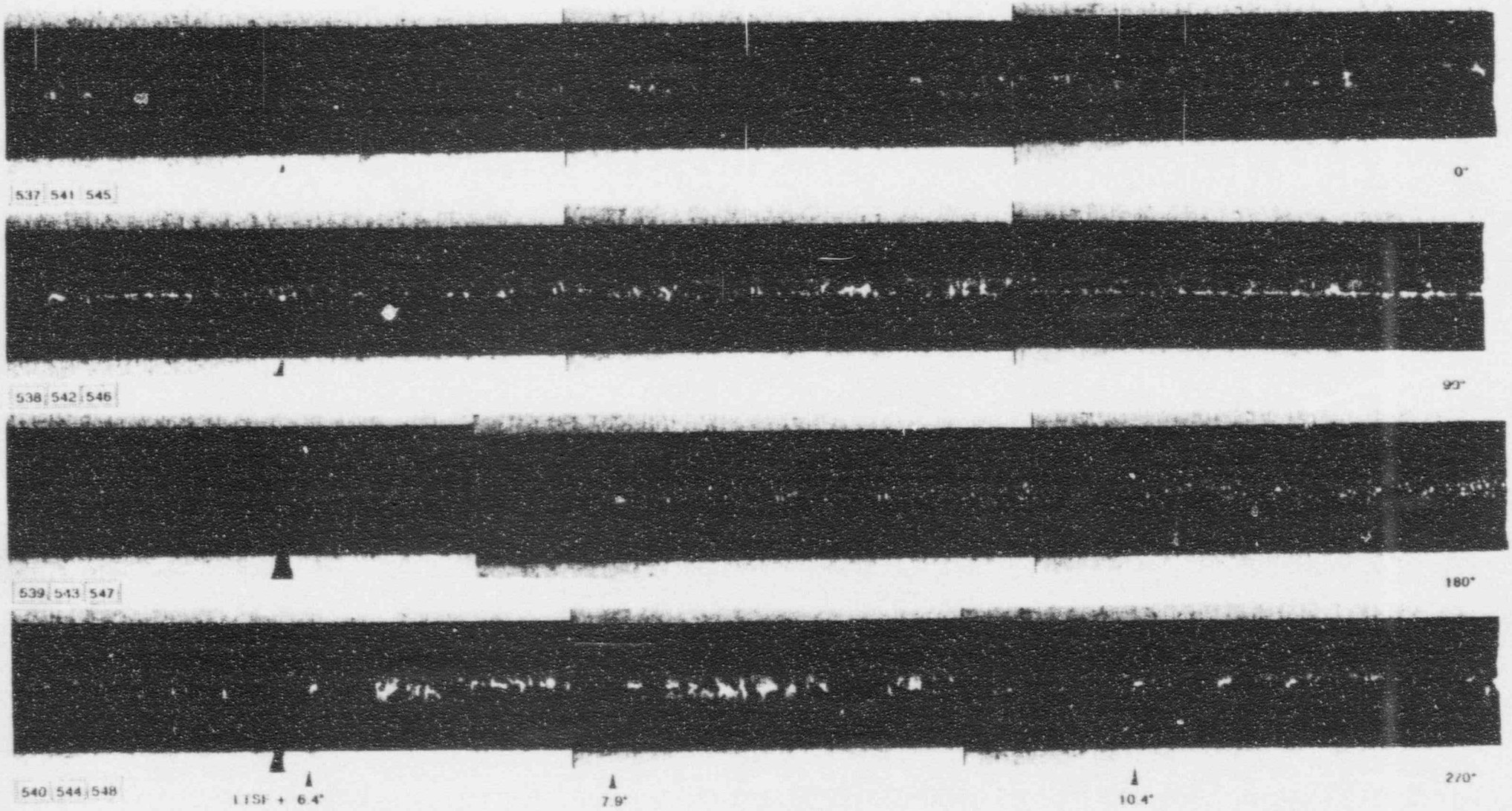

Figure 2-8: Tube Section 90-28-2, Freespan above LTSF As-Received

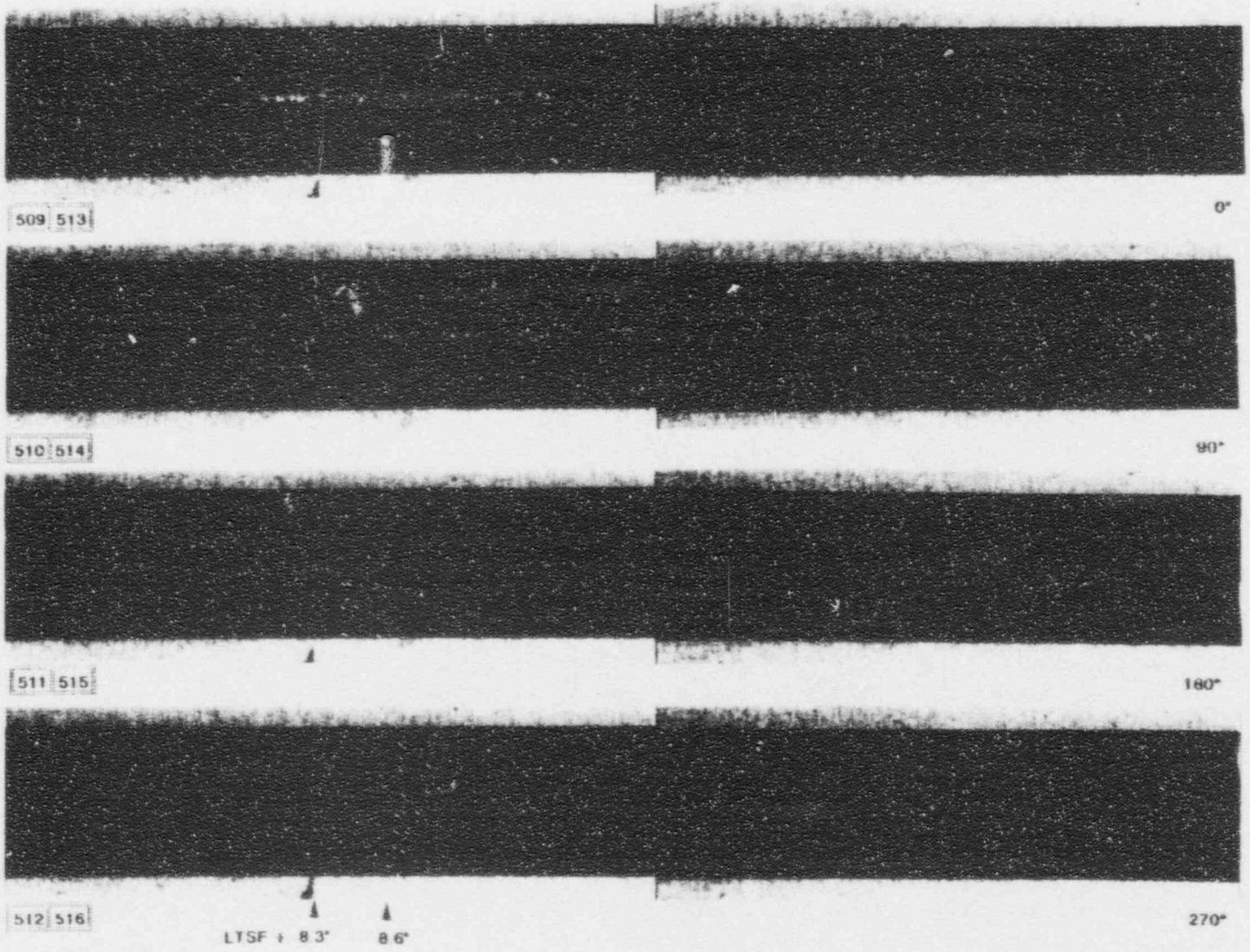

Figure 2-9A:Tube Section 97-91-2, Freespan above LTSF As-Received

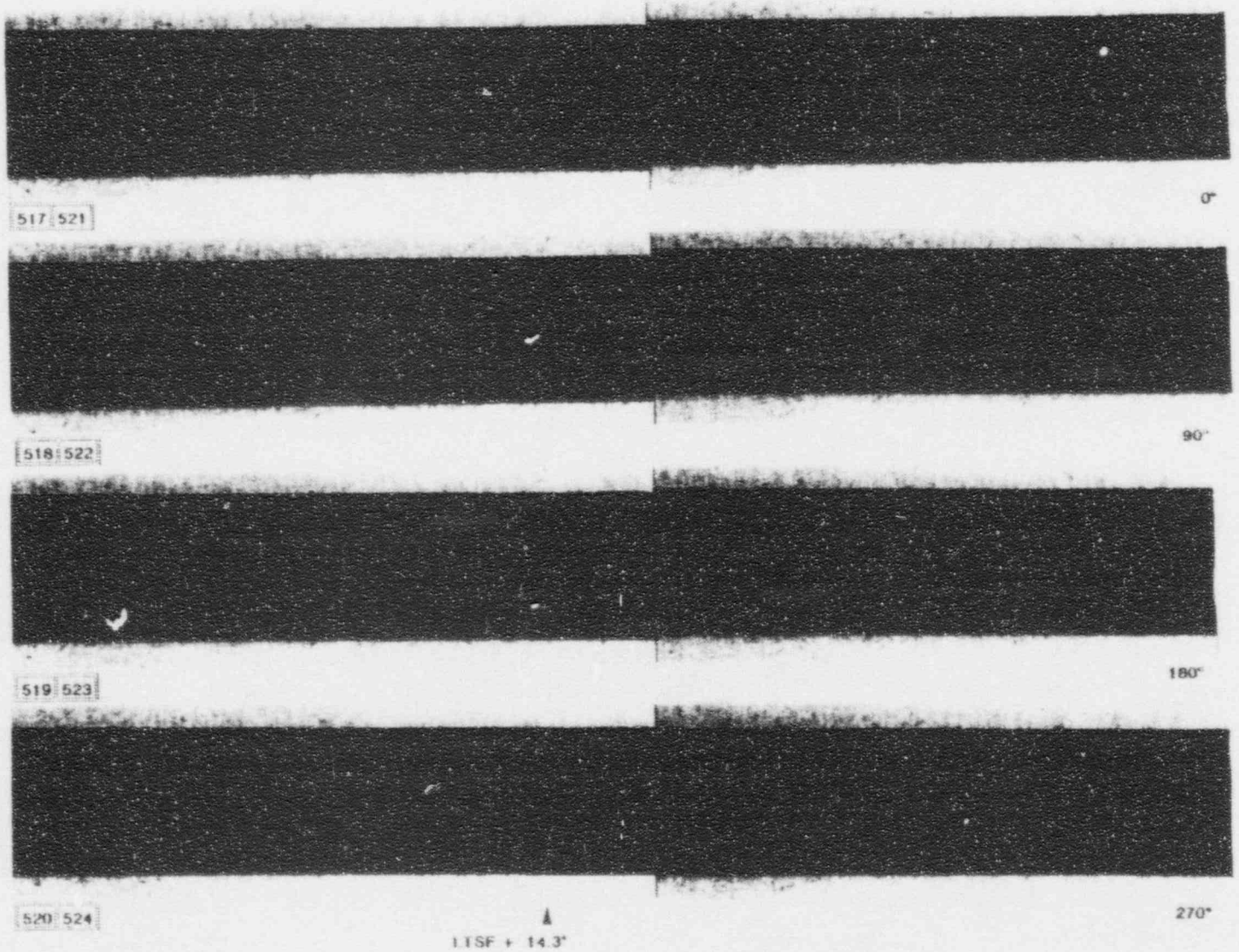

Figure 2-9B: Tube Section 97-91-2, Freespan above LTSF As-Received

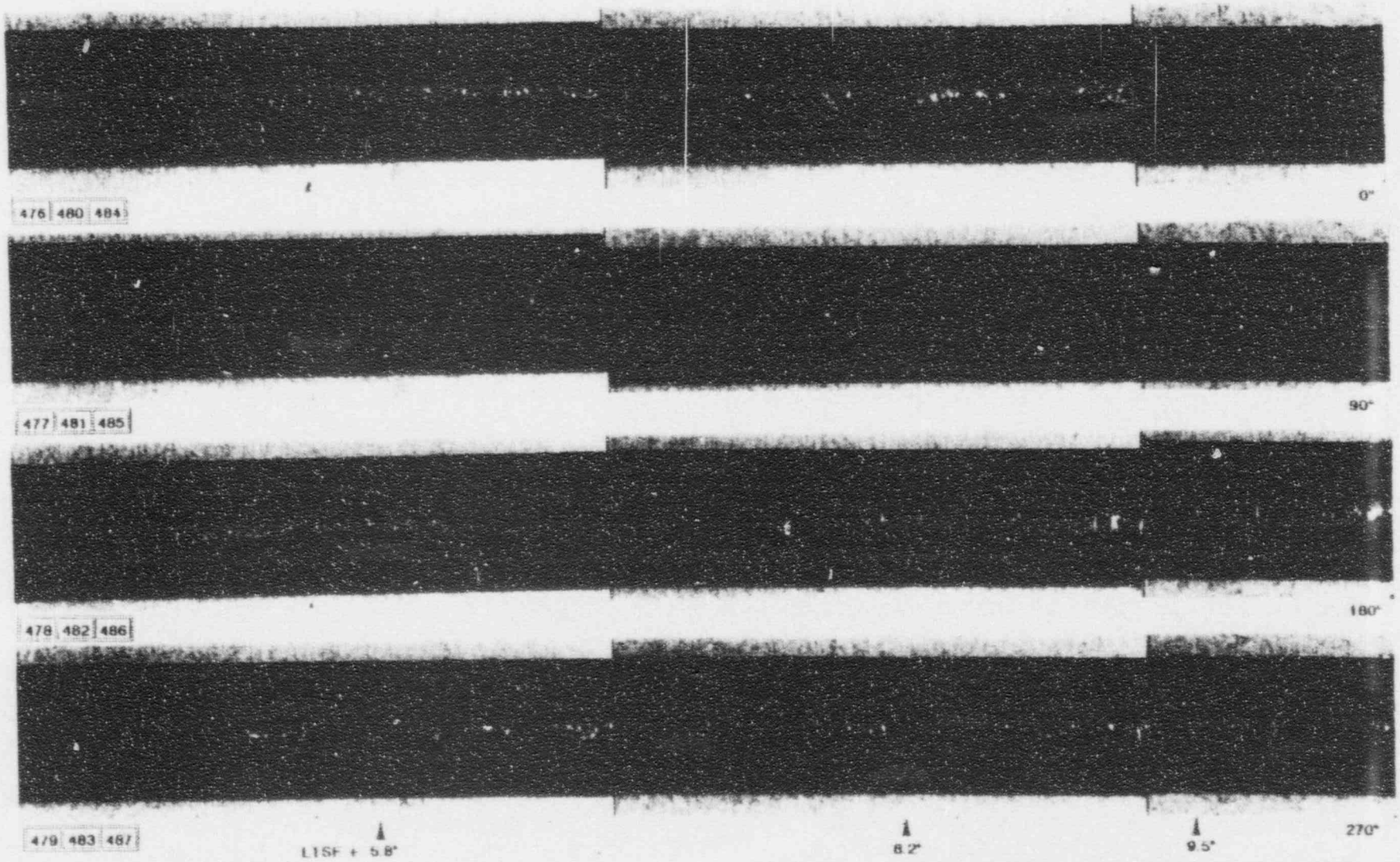

Figure 2-10A: Tube Section 106-32-2. Freespan above LTSF As-Received

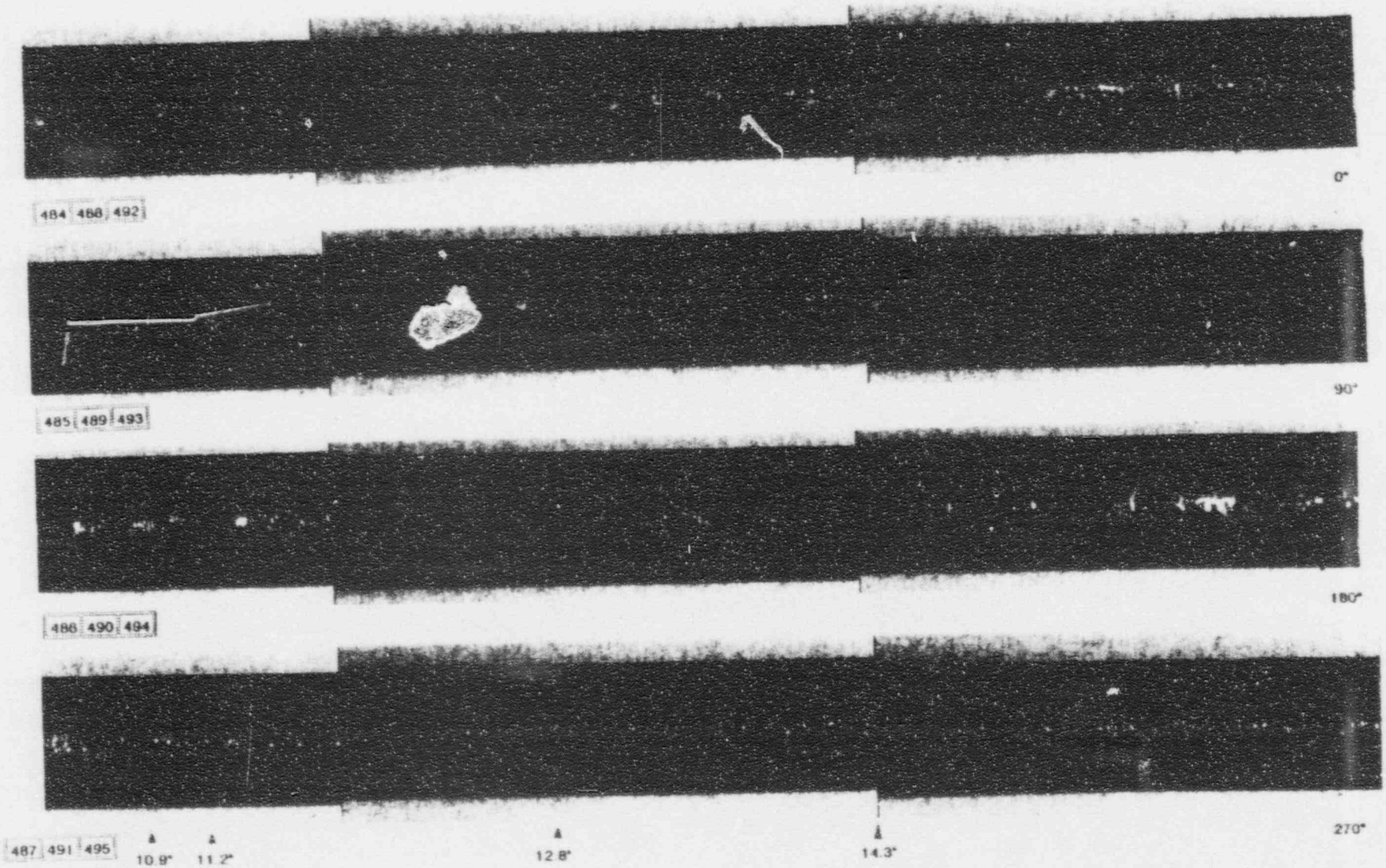

Figure 2-10B: Tube Section 106-32-2, Freespan above LTSF As-Received

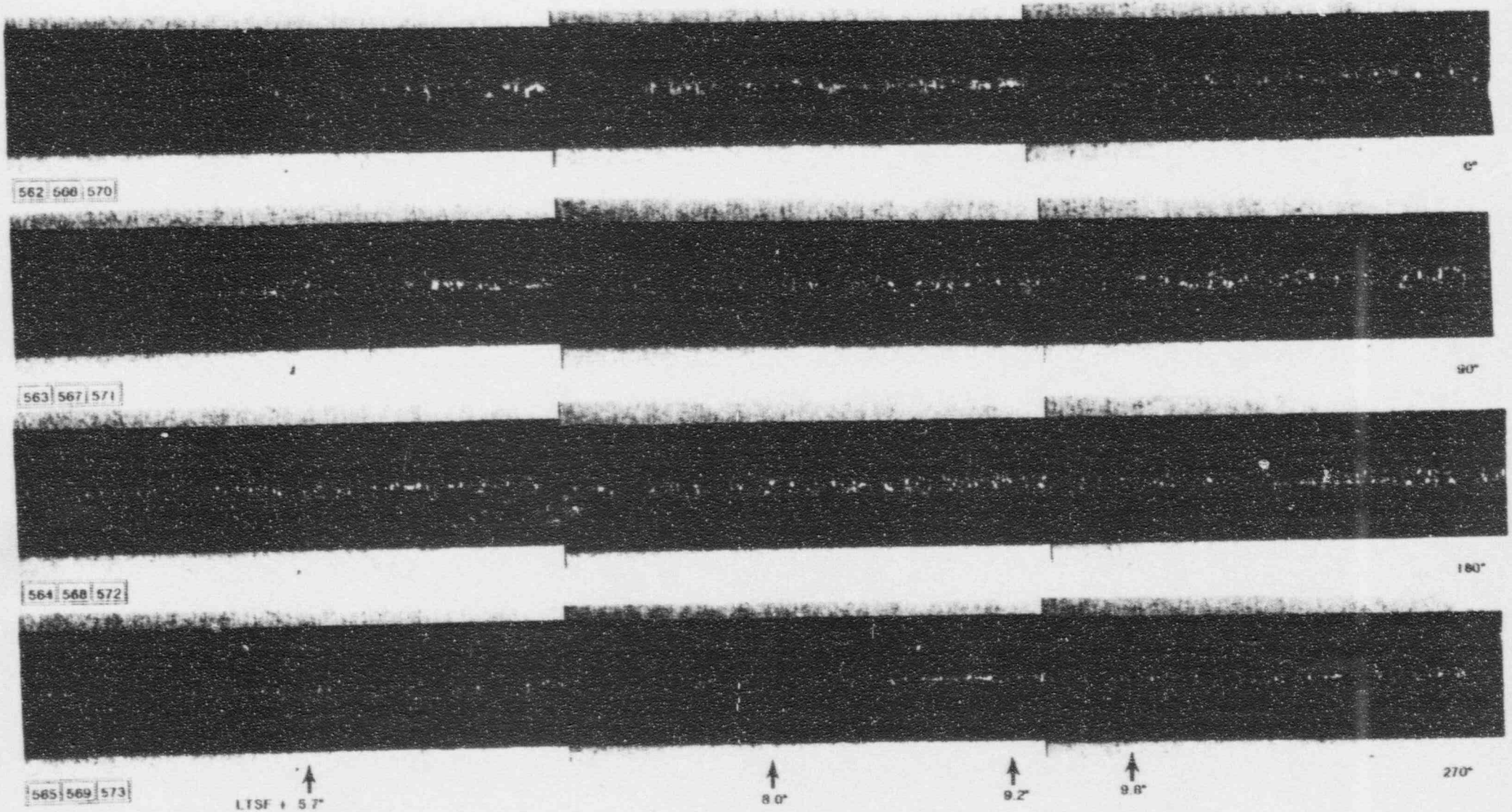

Figure 2-11:Tube Section 109-30-2, Freespan above LTSF As-Received

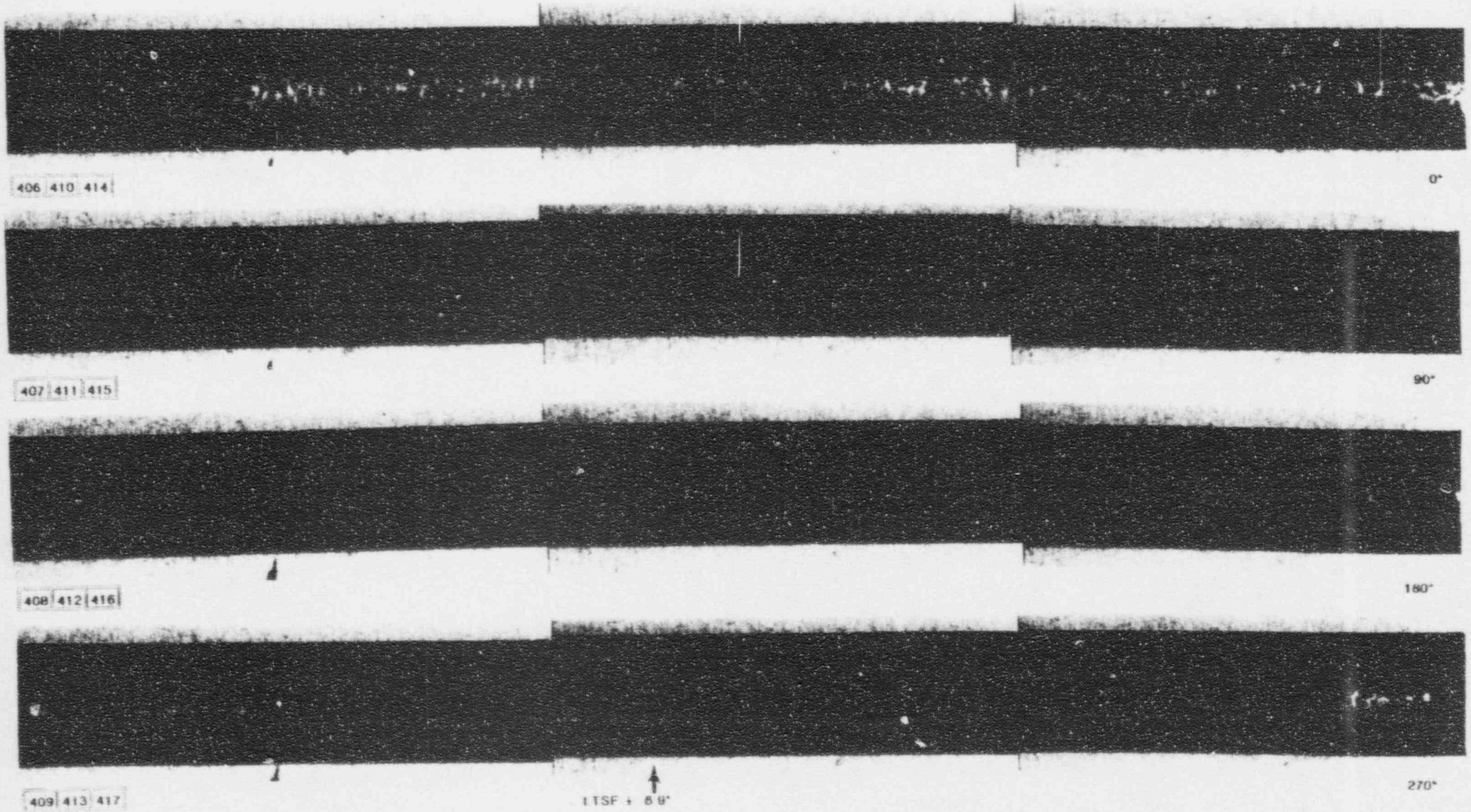

Figure 2-12A: Tube Section 41-44-2, Freespan above LTSF As-Received

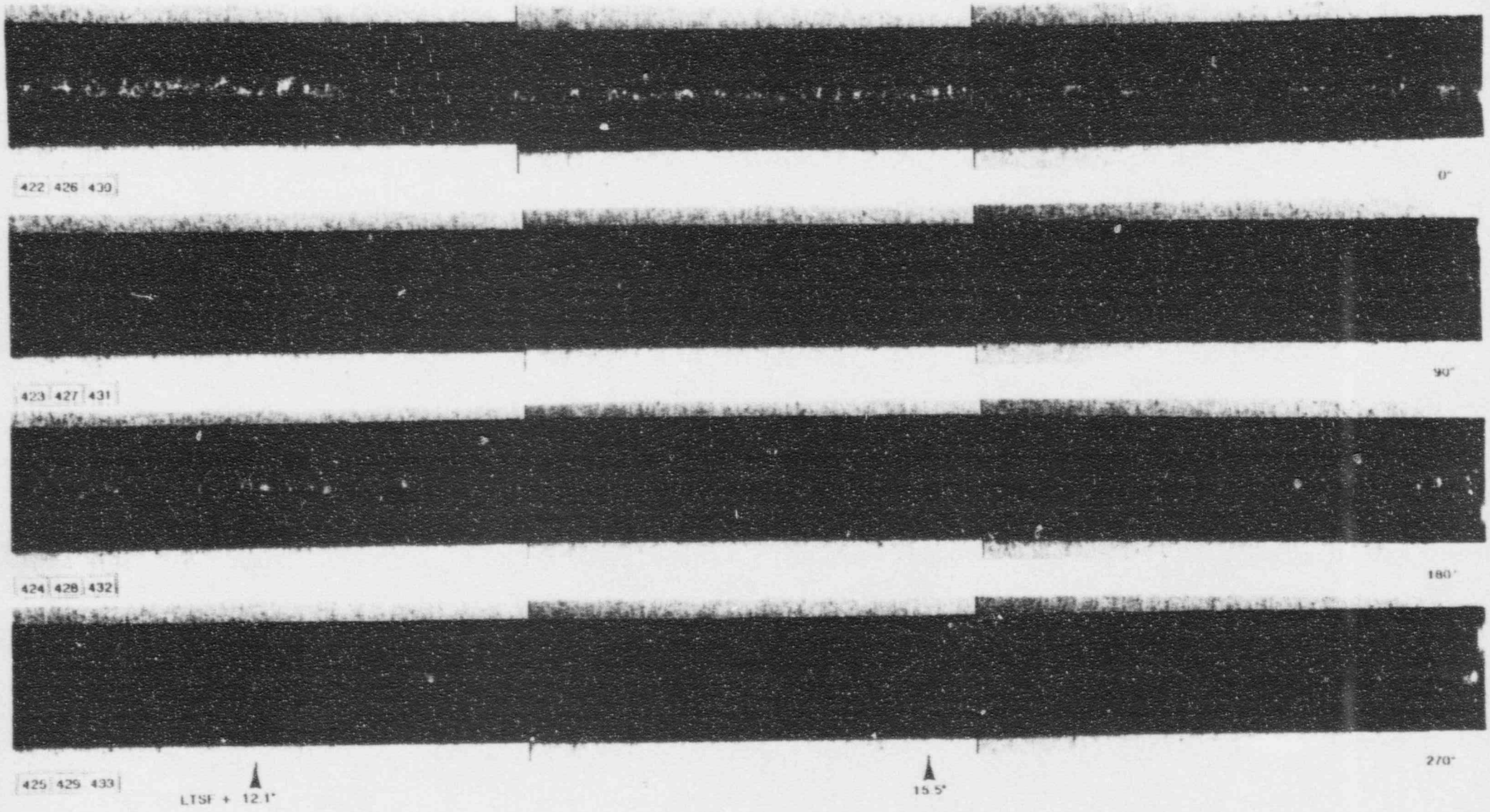

Figure 2-12B: Tube Section 41-44-2, Freespan above LTSF As-Received

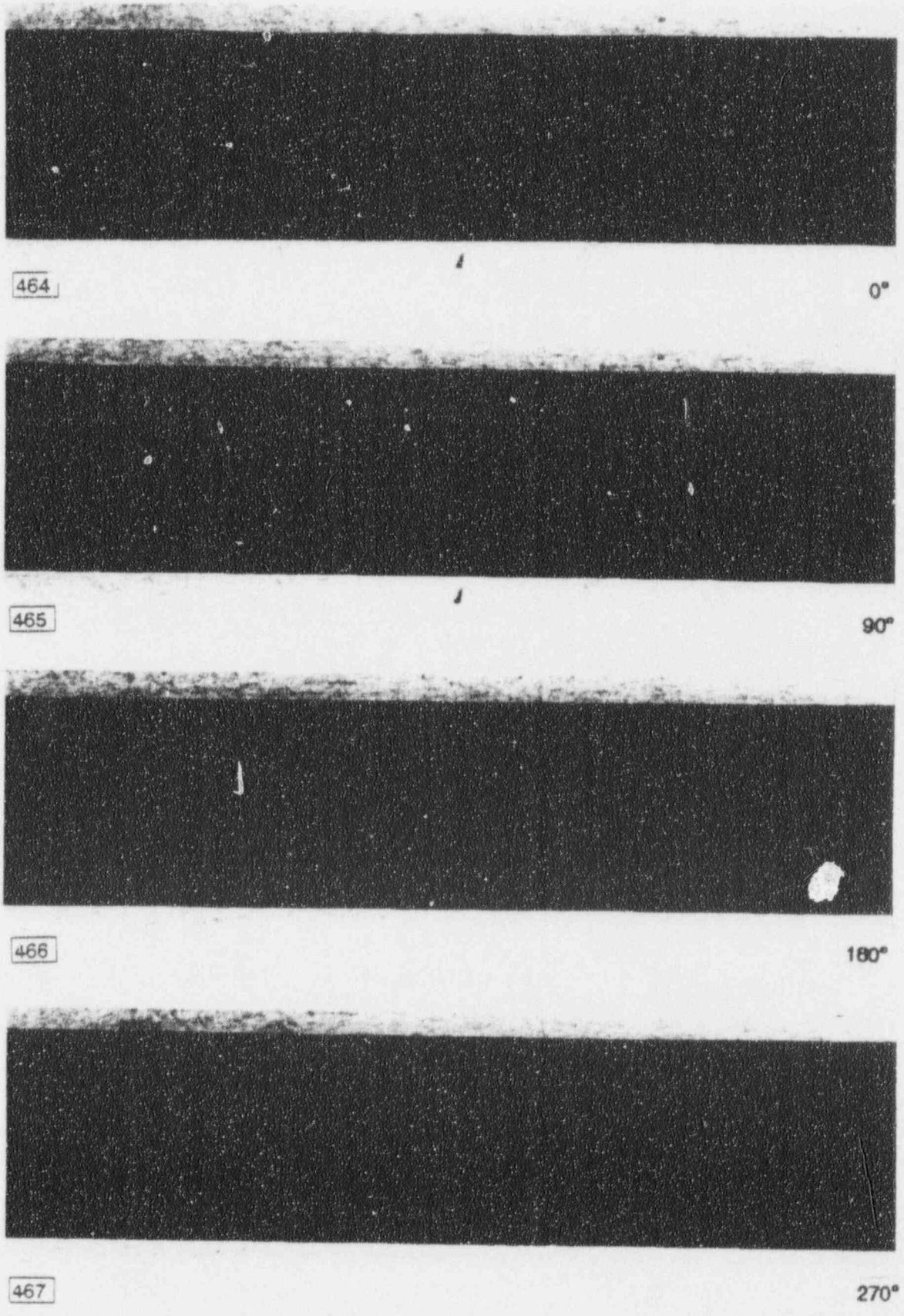

Figure 2-13: 52-51-2, LTSF+19", Circular Band of Non-Uniform Deposits

Figure 2-14: 52-51-2, Possible Pits and Non-Uniform Deposits above LTSF

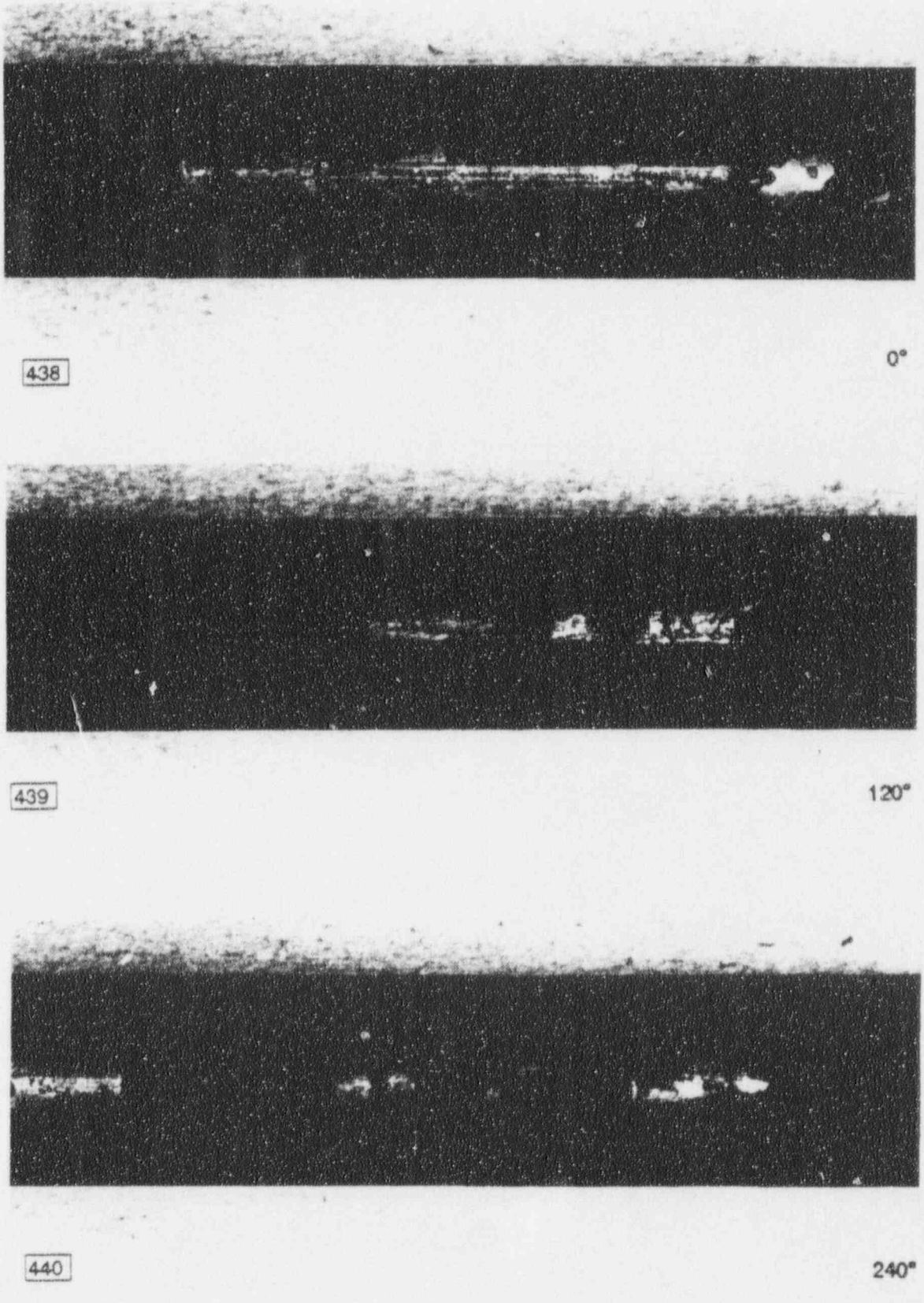

Figure 2-15: Tube Section 52-51-3, TSP Region (As-Received)

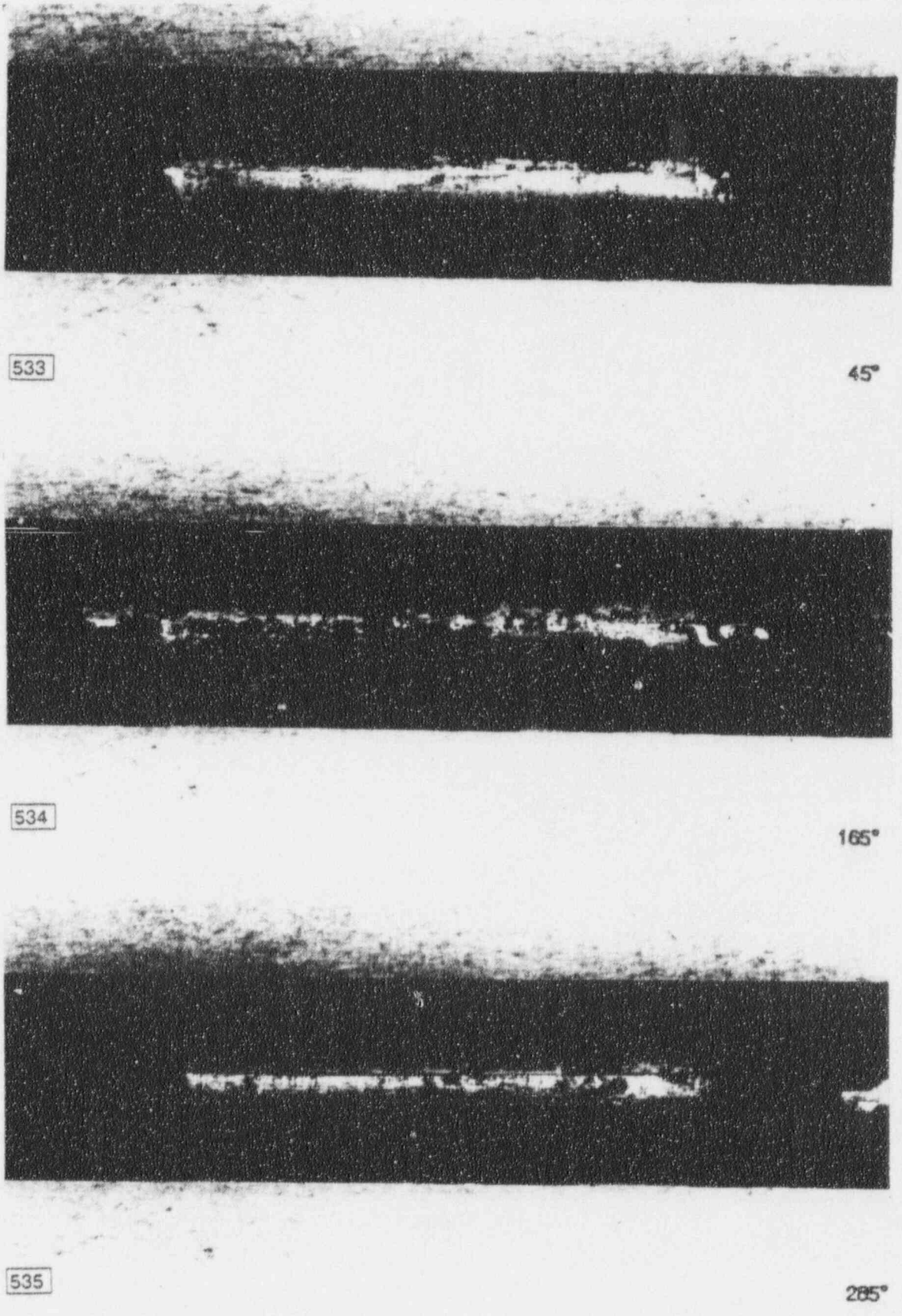

Figure 2-16: Tube Section 90-28-4, TSP Region (As-Received)

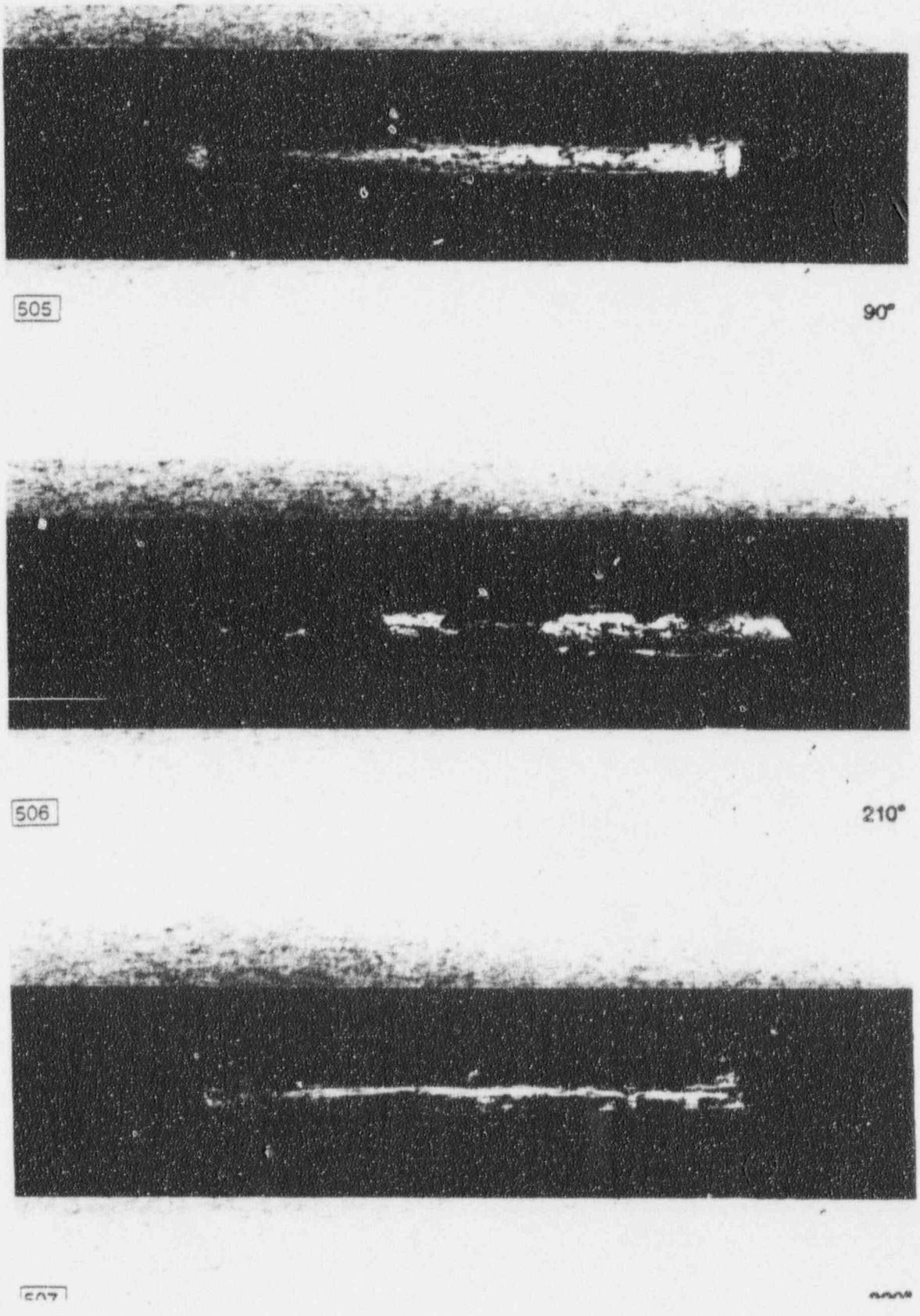

Figure 2-17: Tube Section 97-91-4, TSP Region (As-Received)

45°

469

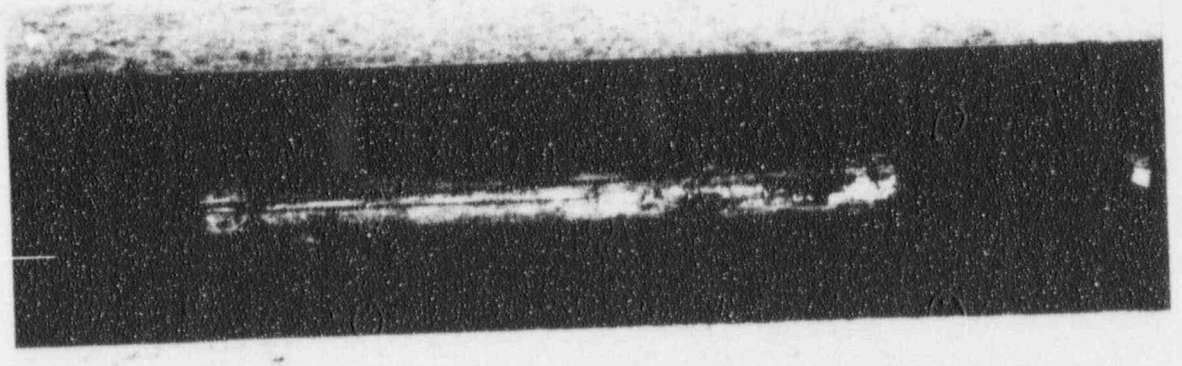

165°

470

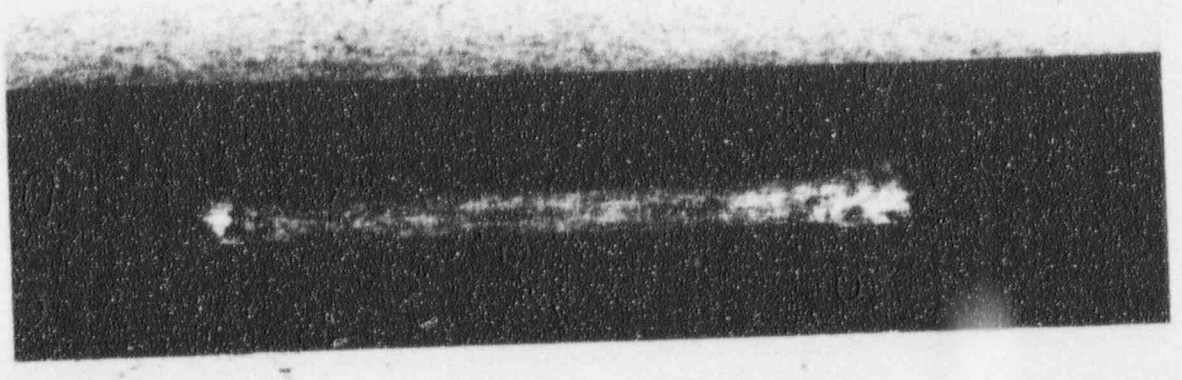

285°

471

Figure 2-18: Tube Section 106-32-4, TSP Region (As-Received)

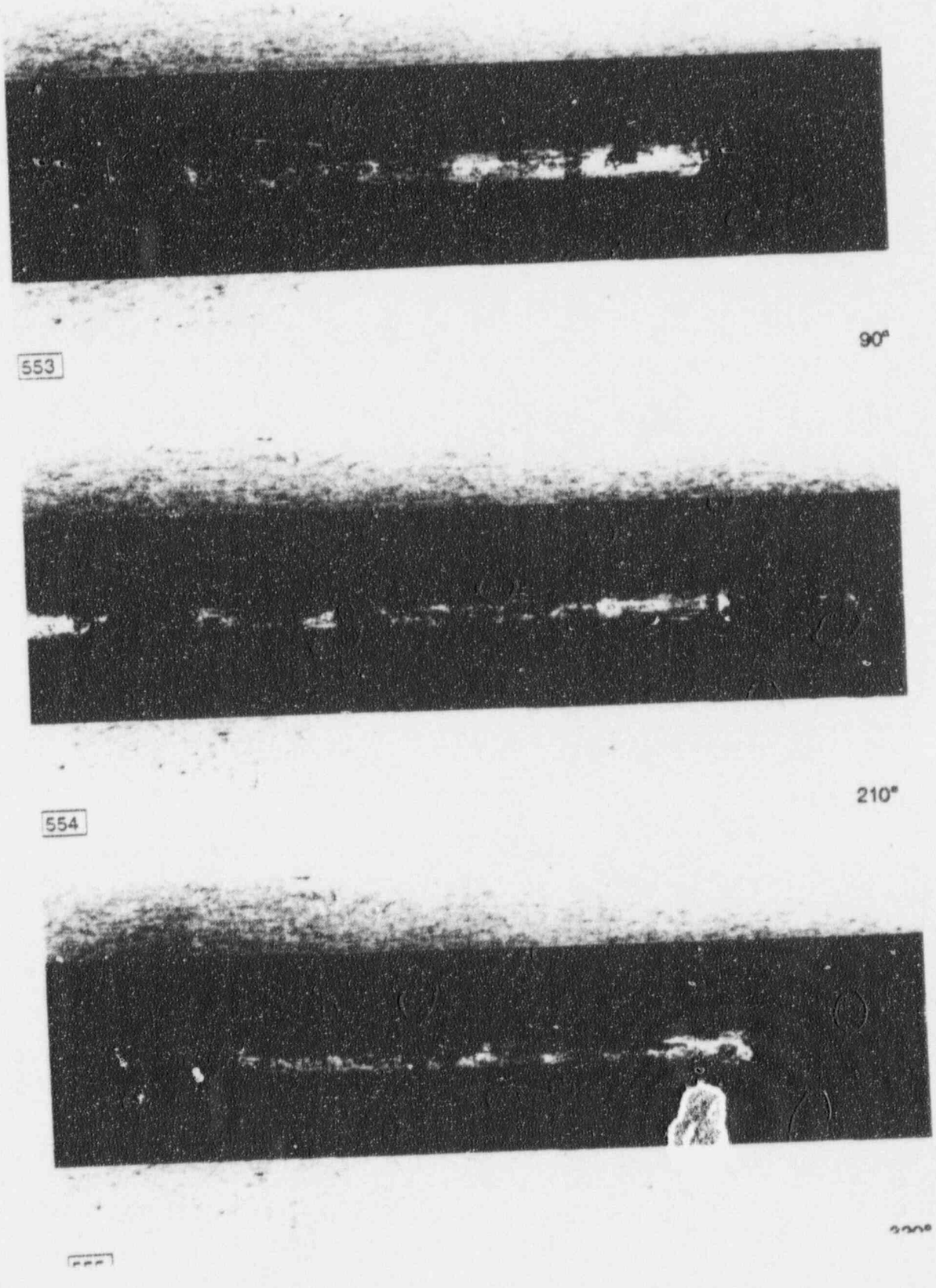

Figure 2-19: Tube Section 109-30-4, TSP Region (As-Received)

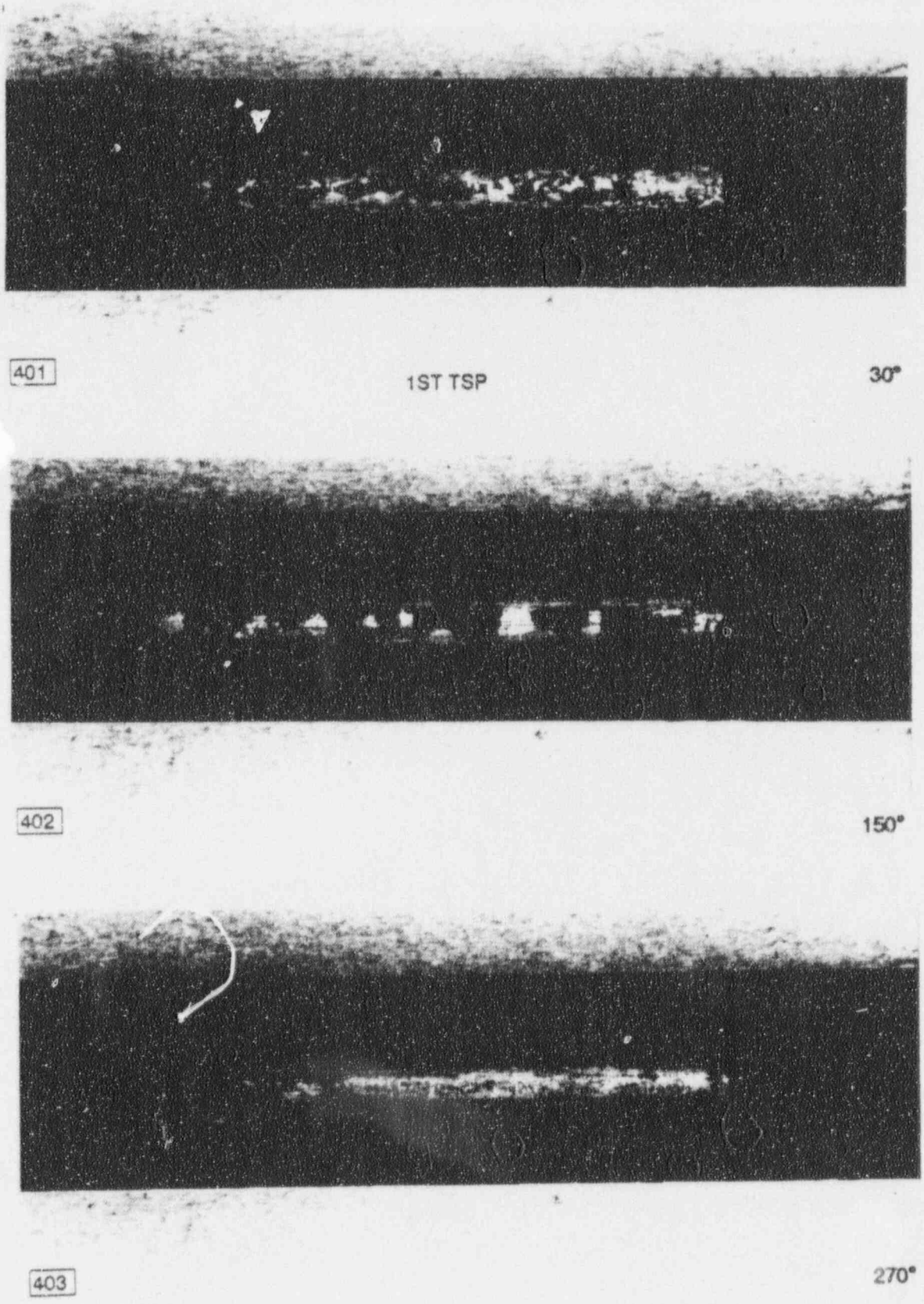

Figure 2-20: Tube Section 41-44-4, TSP Region (As-Received)

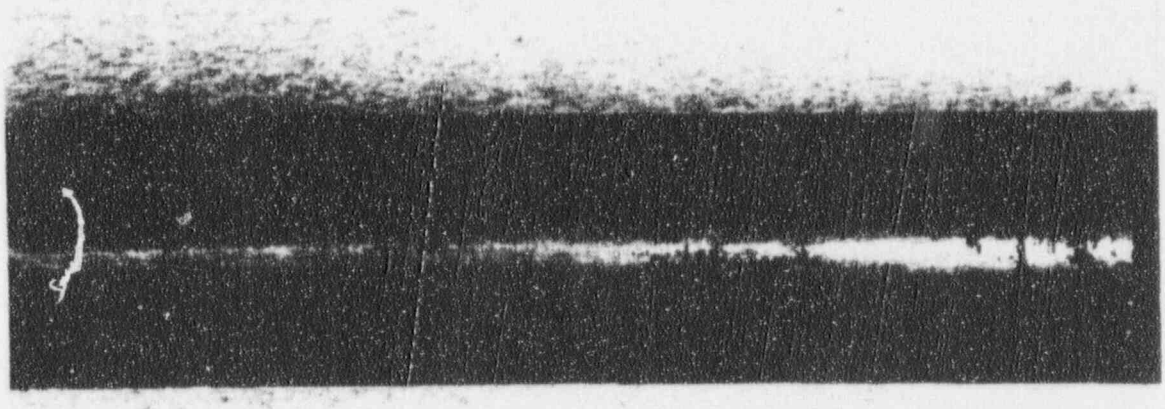

Figure 2-21: 52-51-3, Spalled Deposit at TSP-2¼" Where Tube Was Bowed

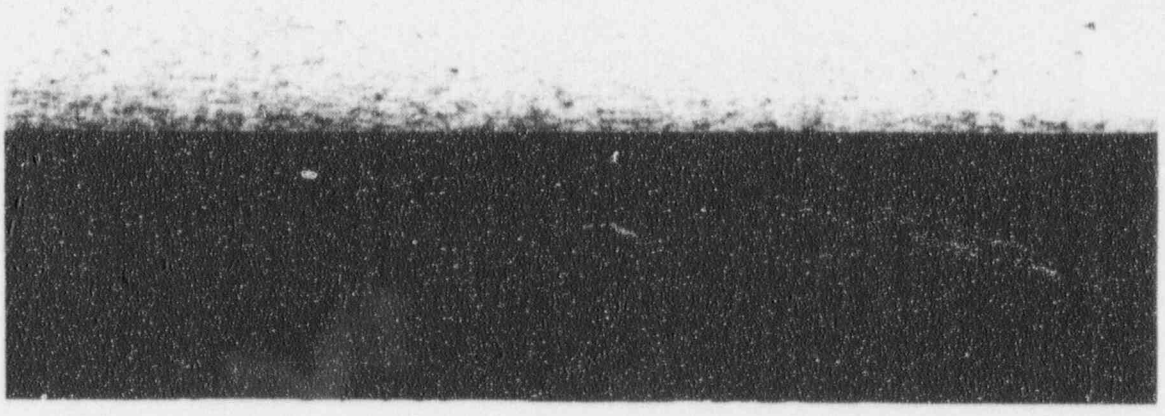

Figure 2-22: 52-51-3, Typ. Deposit above TSP+9½"

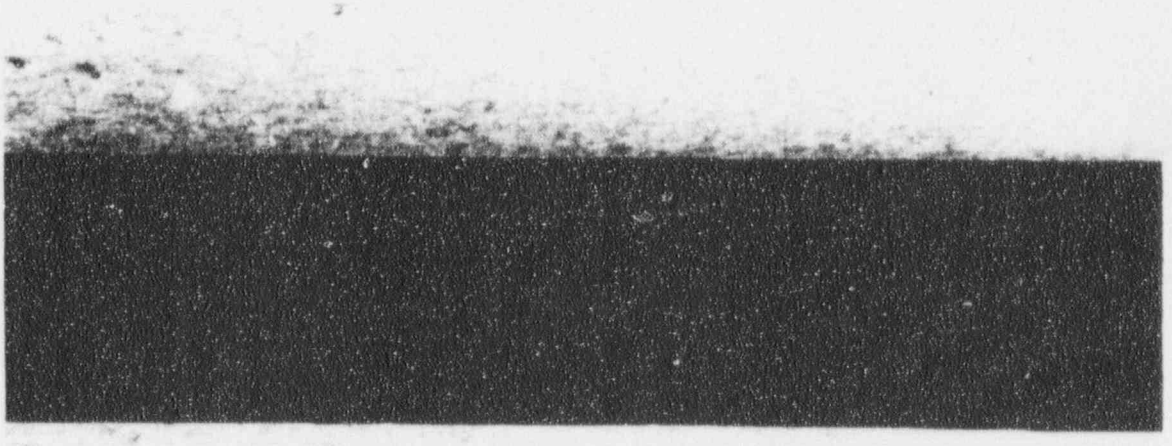

Figure 2-23: 90-28-4, Axial Lines of Slightly Heavier Deposit

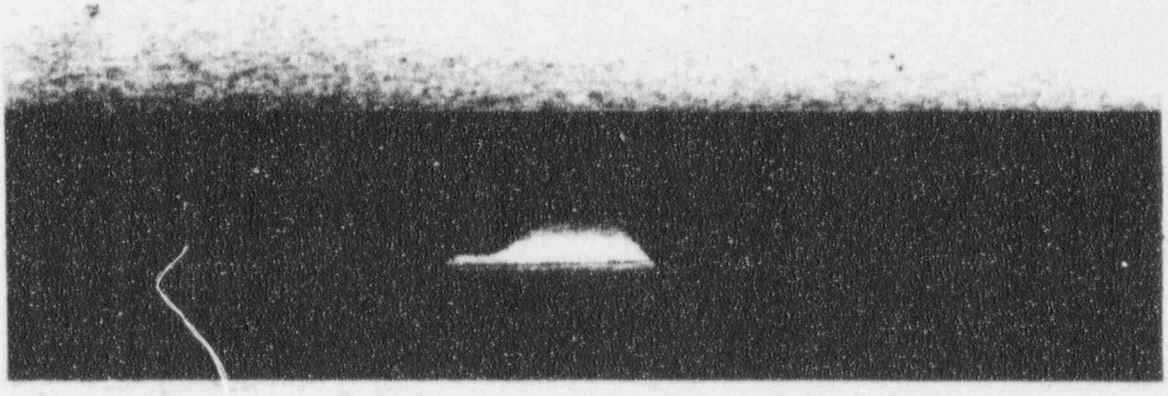

508

300°

Figure 2-24: 97-91-4, Spalled Deposit 1st TSP-5 5/8"

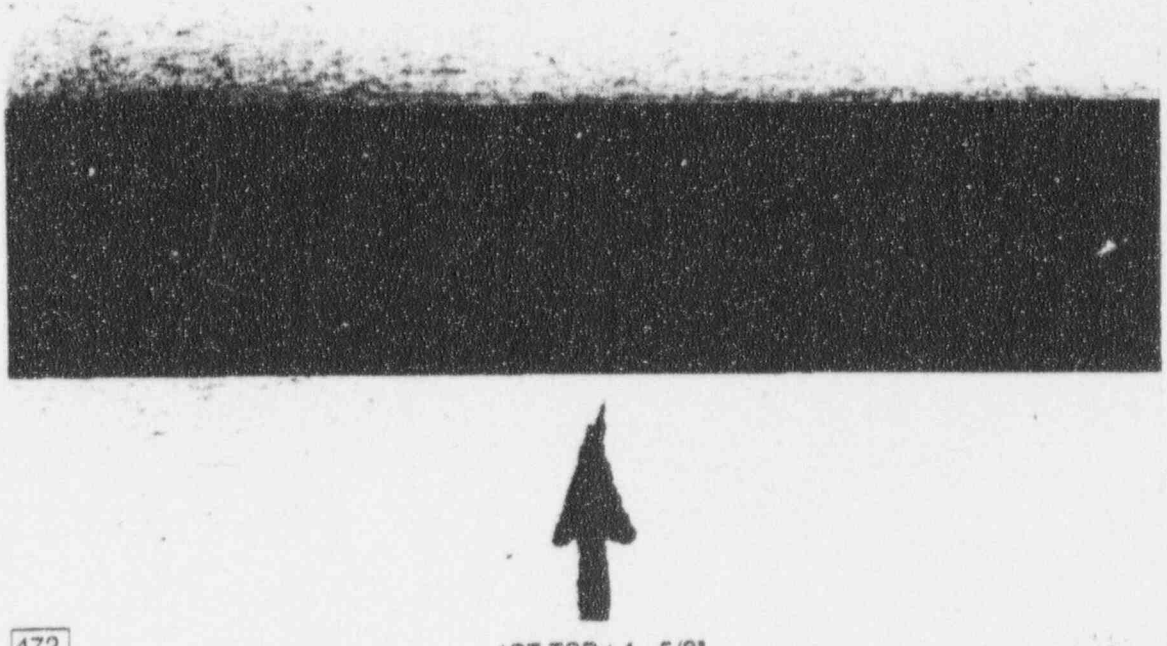

Figure 2-25: 106-32-4, Typical Deposit above TSP

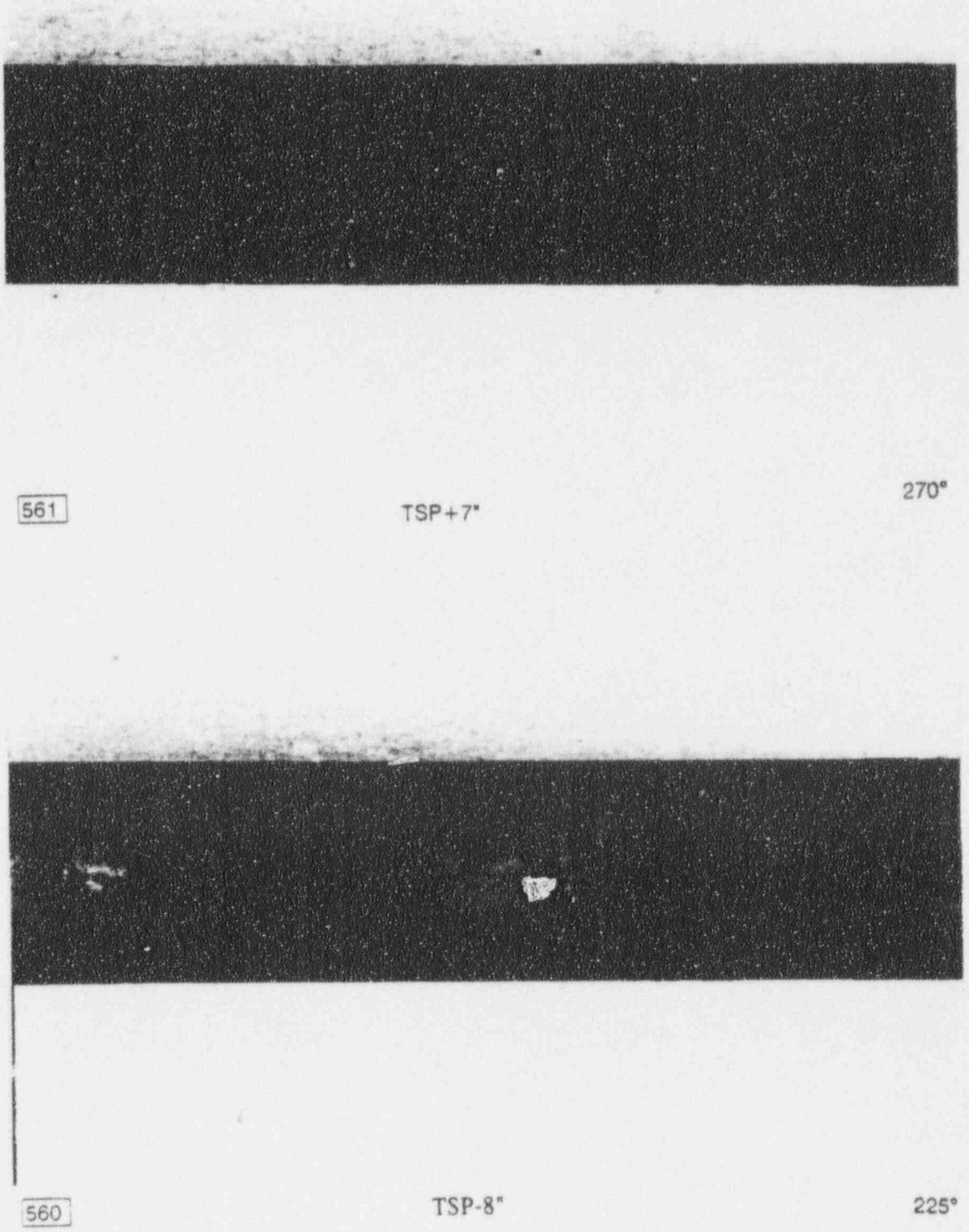

Figure 2-26: 109-30-4, Typical Non-Uniform Deposits Above and Below TSP

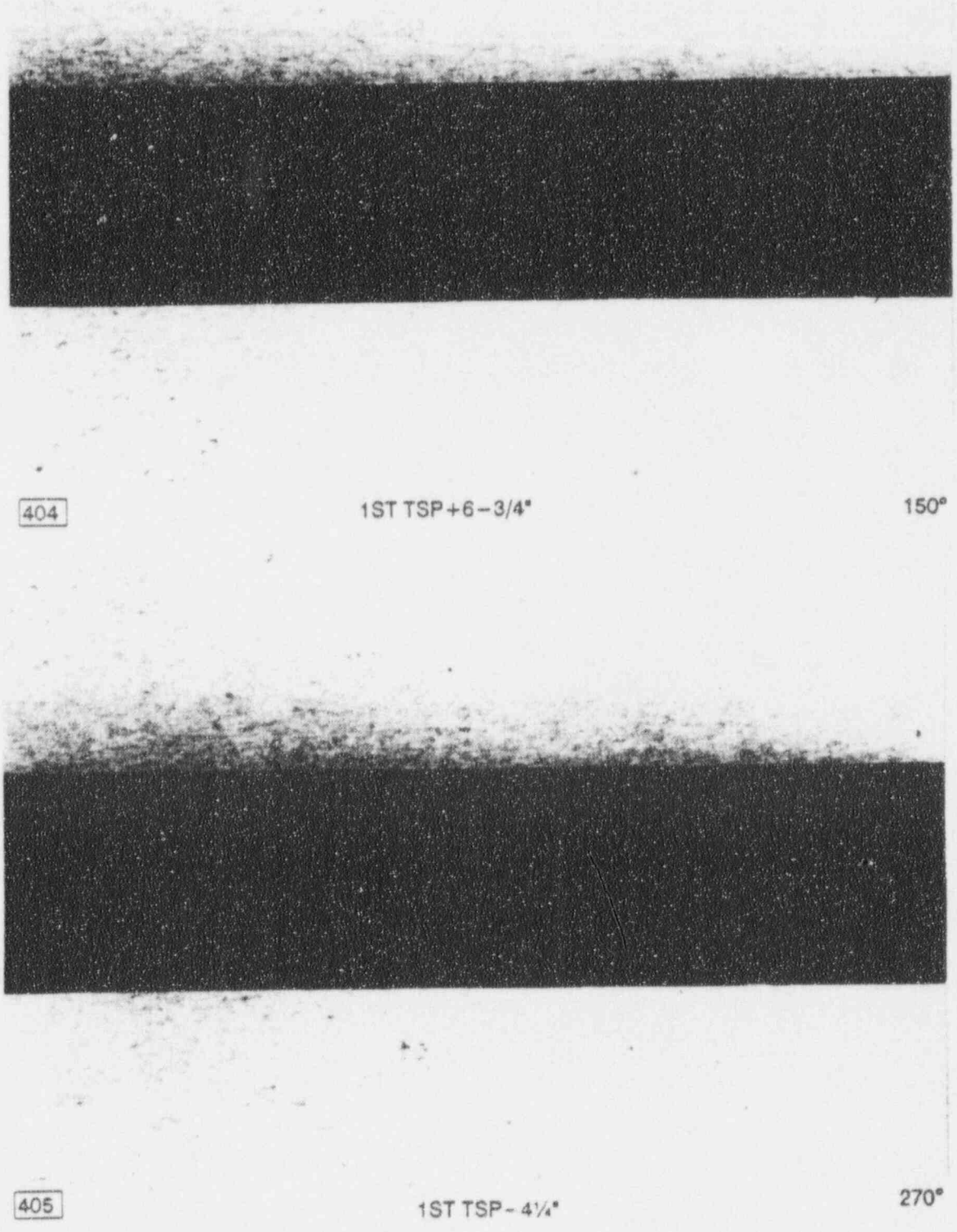

Figure 2-27: 41-44-4, Typical Deposit Above and Below 1st TSP (2.2X)

2.2 Destructive Phase - Methods & Results

2.2.1 Slow-Pull Bobbin Coil Eddy Current Testing

The six tube sections containing eddy current indications in the region above the LTSF were reinspected by bobbin coil eddy current techniques. The axial position of each eddy current indication was more precisely determined by slowly pulling and centering the probe at each indication, then marking the probe sheath at the bottom end of the tube section at the 0° orientation and physically measuring the distance from the mark to the center of the coils. Prior to performing this test, the positioning capability of the probe was demonstrated using a calibration standard. The results are summarized below in Table 2-2:

Table 2-2
RESULTS OF SLOW-PULL BOBBIN COIL INSPECTION

Section No.	Defect Locations (inches above LTSF)							
52-51-2	6.4	8.7	9.9	10.8				
90-28-2	6.1	7.8	10.0	11.5	12.3	13.9	14.4	16.0
106-32-2	6.3	8.6	9.9	11.3	11.6	13.1	14.6	
97-91-2	8.6	8.9	12.0	14.4				
109-30-2	6.0	8.4	9.0	9.6				
41-44-2	6.3	7.6	12.4	16.1				

After completing this test, tube section no. 41-44-2 was archived at the LTC for possible future analysis.

2.2.2 Descaling of Tube Sections 97-91-2 & 106-32-2

Following eddy current testing, tube sections 97-91-2 and 106-32-2 were descaled using a two step cleaning process consisting of a 4 to 8 hour soak in an alkaline permanganate (100 g/l NaOH and 30 g/l $KMnO_4$) solution at 90 to 95°C followed by a short (i.e., less than 10 minute) duration dilute acid (6N HCl inhibited with 2 g/l hexamethylene tetramine) rinse at ~60°C.[1]

As a result of cleaning, the radiation and loose contamination levels on both tube sections were reduced to less than 2 mR/hr (contact γ) and about 1K dpm/100cm^2, respectively. The OD tube deposits were completely removed, although light-colored "stains" were apparent, which generally correlated with the spalled deposit regions and darker scalloped areas noted previously during the visual inspection.

---

[1] This process is not aggressive to the base metal, but is very effective in breaking down the spinel structure associated with corrosion films formed on Ni-Cr-Fe alloys in high temperature pure water.

2.2.3 Post-Cleaning Eddy Current Testing of Tube Sections 97-91-2 & 106-32-2

After descaling, tube sections 97-91-2 and 106-32-2 were reinspected by the bobbin coil eddy current technique described in Section 2.2.1 to establish any effect the OD deposits may have had on the eddy current signals. No significant deposit effect was observed.

2.2.4 Dye Penetrant Inspection of Tube Sections 97-91-2 & 106-32-2

The two (2) descaled tube sections (97-91-2 and 106-32-2) were examined by fluorescent liquid penetrant inspection to identify defects which may not have been detected previously. Liquid penetrant indications were photographed to document their location and orientation, and further characterized by subsequent visual and/or stereovisual examinations.

Other than minor pitting noted in a few locations, no significant defects were identified. There were localized areas exhibiting general surface roughness - possibly a result of IGA. However, only a few of these indications were actually verified to be IGA after swelling and metallographic examination. The results of this inspection are summarized below in Table 2-3; pitting and suspect IGA areas are shown in Figures 2-28 (Section 97-91-2) and 2-29 (Section 106-32-2).

2.2.5 Burst Testing

The two (2) descaled tube sections (97-91-2 & 106-32-2) were pressurized at room temperature to determine burst strength and open existing defects. The tube sections were installed in the burst test sytem using standard Swagelok™ fittings. A pneumatically driven, piston-type hydraulic pump was used to charge an accumulator to approximately 30,000 psi; pressure was applied to the test tube section through a metering valve to achieve pressurization rates on the order of 2,500 psi per second; time to burst the CR-3 tubing was less than 10 seconds. Tube pressure was monitored by a 0 to 30,000 psi Heise gage with an accuracy of $\pm 0.1\%$. Also, a permanent record of each pressurization event was obtained via a pressure transducer connected to a x-y recorder.

Both tube sections burst at relatively high pressures - 12,400 and 11,400 psi for sections 97-91-2 and 106-32-2, respectively. Both tube sections exhibited significant uniform plastic deformation; tube section 106-32-2 ruptured in classical "fishmouth" fashion, but tube section 97-91-2 exhibited a more localized pinhole failure.

Table 2-3
LIQUID PENETRANT INSPECTION RESULTS

Tube Section 97-91-2:

Axial Position*	Angular Position	Description
-0.1	140°	Superficial pitting below LTSF
0.0	270°	White surface deposit; no defect
8.4	90°	Minor pitting adjacent to axial scratch
8.9	45°	Superficial pitting
9.6	135°	One small pit with white deposit inside
11.4	90°	Small pits within an axial scratch
13.3	350°	Superficial pitting and localized surface roughness
13.8	0°	Localized minor surface roughness
14.5	0°	Localized minor surface roughness

Tube Section 106-32-2:

Axial Position*	Angular Position	Description
0.1	10°	White surface deposit; no defect
0.1	315°	White surface deposit; no defect
0.4	200°	White surface deposit; no defect
6.4	70°	Superficial pitting and localized surface roughness**
6.4	280°	Superficial pitting and localized surface roughness
8.6	90°	Single pit with localized surface roughness
8.8	90°	Single pit with localized surface roughness
9.0	90°	Superficial pitting and localized surface roughness
9.8	200°	Superficial pitting and localized surface roughness
10.0	30°	Superficial pitting and localized surface roughness
11.4	10°	Superficial pitting and localized surface roughness
11.8	180°	Superficial pitting and localized surface roughness
13.2	150°	Superficial pitting and localized surface roughness
14.4	20°	Superficial pitting and localized surface roughness
14.9	135°	Localized surface roughness

* Relative to LTSF, inches

** Verified to be IGA after swelling or bursting, and subsequent metallographic examination.

2.2.6 Tube Swelling & Deposit Collection

Seven (7) tube sections as identified in Table 2-4 below were pressurized at room temperature to achieve yielding and swell the tube sufficiently to spall off OD deposits and open up any existing defects. To prevent chemical contamination of surface deposits, deionized water was utilized as the working fluid.

The tubes reached yield at pressures of about 6,500 psi, then were plastically swelled to a diametrical expansion of about 10%. The maximum pressure applied to each tube section was 8,400 psi, with the exception of number 90-28-2, which sprung a pinhole leak at 8,050 psi; the leak location was LTSF + 10.2 inch and 330°, which was within 1/4 inch of the uppermost field reported eddy current indication (see Fig. 1-1). In general, the OD tube deposits spalled off in small flakes, leaving behind a relatively clean surface; the deposits were collected and dried, then weighed to the nearest milligram.

Table 2-4
SWELLED TUBE SECTIONS & COLLECTED DEPOSITS

Tube Section	Areas of Interest for Deposit	Deposit Weight (mg)
52-51-2	Freespan area above LTSF	850
52-51-4	Freespan area above 1st TSP intersection	1697
90-28-2*	Freespan area above LTSF	382
90-28-5	Freespan area above 1st TSP intersection	778
133-33-3/2	Freespan area above LTSF	340
133-33-9**	Freespan areas adjacent to TSP	321
133-33-9**	3rd TSP intersection	1537

* This tube section sprung a pinhole leak at 8,050 psi.
** Highest available TSP intersection with visible deposits.

Note: Prior to swelling tube section 52-51-2, a 2-3/4 inch long section was removed from the top due to a throughwall saw nick (from tube removal). Also, prior to performing any swelling of 52-51-4, 90-28-5 and 133-33-3, ring sections were isolated near the top of each section for metallographic and SEM/EDS characterization of the OD deposits.

In addition to the deposit flakes collected from the swelled tube sections, other bulk deposit samples were collected as shown in Table 2-5 below. These additional deposit samples were obtained by scraping the tube surface with a razor knife thoroughly cleaned in ethanol.

Table 2-5
OTHER COLLECTED DEPOSITS

Tube Section	Areas of Interest for Deposit	Deposit Weight (mg)
52-51-2	Green deposits just below LTSF	4
90-28-2*	Green deposits just below LTSF	7
133-33-3	Primary deposits*	6

* Obtained after longitudinally splitting and clam shelling a two inch long section of tube; the primary side deposit was extremely thin.

2.2.7 Post Burst/Swell Test Visual & Stereovisual Inspections

The burst/swelled tube sections were inspected visually and at low power (i.e., magnifications up to 40X) with a stereomicroscope to identify, precisely locate and further characterize any defects, which may have opened up.

Representative mosaics of tube sections 97-91-2, 106-32-2, and 52-51-2, are shown in Figures 2-30 through 2-32. As stated in Section 2.2.2, light-colored "stains" were present over much of the OD surface on the descaled tube sections; these stains generally correlated with the spalled deposit regions and darker scalloped areas noted previously during the visual inspection. The stereovisual inspection revealed defects within some of these light stains. Most of the degradation was in the form of small IGA patches, although some minor pitting was occasionally observed. It was also observed that some of the defects were located at axial scratches. These scratches were most likely created during tube installation since fresh scratches caused by tube removal would have been observed in the initial examination but were not. A total of 17 and 56 potential defect areas were identified on burst tube sections 97-91-2 and 106-32-2, respectively. Representative defect areas are shown at higher magnification in Figures 2-33. All defect information is summarized in Table 2-6 below.

Table 2-6: STEREOVISUAL INSPECTION SUMMARY

Note: Axial position is given relative to the LTSF; axial extent is given in mils.

Tube Section: 97-91-2

ID No.	Position Axial	Position Angular	Extent Axial	Extent Angular	Description	ID No.	Position Axial	Position Angular	Extent Axial	Extent Angular	Description
AA	18.1	285°	9.1	0.4	Possible minor pit	M	7.1	320°	19.7	3.3	Minor IGA patch
Y	16.5	20°	5.9	0.7	Possible minor pit	*K	6.6	225°	49.8	3.8	Small IGA patch
*W	14.1	105°	60.6	9.6	Small IGA patch	I	5.6	355°	5.7	0.9	Minor IGA patch
U	11.6	245°	54.1	9.6	Small IGA patch	*G	3.3	20°	13.1	0.7	Minor IGA patch
*T	11.5	90°	61.0	13.6	Small IGA patch	*E2	2.8	20°	2.6	1.1	Minor IGA patch
*S	11.4	95°	11.2	0.1	Minor pitting	*E1	2.8	285°	10.1	3.3	Minor IGA patch
R1	9.3	350°	15.9	2.7	Minor IGA patch	*D	2.6	350°	27.8	1.3	Minor IGA patch
*P	8.4	90°	73.2	15.2	Small IGA patch	*B	1.1	285°	16.3	2.5	Minor pitting
*O	8.1	15°	75.8	12.8	Small IGA patch						

* Defects associated with axial scratches.

Tube Section: 105-32-2

ID No.	Position Axial	Position Angular	Extent Axial	Extent Angular	Description	ID No.	Position Axial	Position Angular	Extent Axial	Extent Angular	Description
BG	16.6	90°	29.5	3.1	Small IGA patch	*AG1	8.7	85°	9.8	1.5	Small IGA patch
BF	16.5	30°	34.6	4.5	Small IGA patch	AE	7.9	225°	63.7	11.5	Small IGA patch
BD	15.6	50°	32.2	6.4	Small IGA patch	AD	7.7	60°	26.0	9.6	Small IGA patch
BC	15.5	30°	31.3	6.4	Small IGA patch	AC2	7.6	220	97.9	6.4	Small IGA patch
BB	15.0	90°	30.4	5.8	Small IGA patch	AC1	7.5	60°	53.0	7.5	Small IGA patch
BA	14.9	35°	43.2	7.1	Small IGA patch	AB	7.3	70°	53.9	4.0	Small IGA patch
AZ	14.8	45°	32.4	5.1	Small IGA patch	AA	7.1	200°	40.0	9.0	Small IGA patch
AY	14.6	220°	55.3	16.1	Small IGA patch	Z	6.9	180°	52.4	9.6	Small IGA patch
AX	14.3	30°	39.9	9.6	Small IGA patch	Y	6.4	85°	14.5	1.6	Minor IGA patch
AV	13.6	60°	39.8	9.6	Small IGA patch	X2	6.3	65°	70.8	11.0	Minor IGA patch
AU	13.4	45°	47.2	11.2	Small IGA patch	X1	6.3	50°	16.0	7.8	Small IGA patch
AT	13.2	135°	59.8	10.3	Small IGA patch	V2	5.3	125°	40.8	5.3	Small IGA patch
*AR	12.3	90°	44.9	12.8	Small IGA patch	V1	5.2	45°	8.8	2.1	Minor pit
AQ2	11.8	180°	46.7	11.2	Small IGA patch	T	4.1	60°	6.6	1.0	Minor pit
AQ1	11.6	90°	29.4	4.8	Small IGA patch	R	0.0	290°	15.4	4.0	Minor IGA patch
*AP	11.3	20°	70.6	8.0	Small IGA patch	Q	-0.6	190°	17.1	3.2	Small pit
*AO	11.1	90°	25.3	6.4	Small IGA patch	O	-1.6	210°	2.9	3.1	Minor IGA patch
AN	10.9	240°	32.4	8.7	Small IGA patch	N	-1.8	270°	5.4	1.0	Minor IGA patch
*AM3	10.9	0°	29.2	3.2	Small IGA patch	M1	-2.3	305°	8.8	0.8	Minor IGA patch
AM2	10.8	45°	16.1	3.0	Small IGA patch	L	-2.3	280°	29.1	8.8	Minor pitting
AM1	10.7	180°	16.6	1.6	Small IGA patch	K	-2.4	310°	24.2	7.6	Small IGA patch
AM1	10.7	125°	25.8	2.9	Small IGA patch	J	-2.6	105°	9.5	5.8	Small pit
AL2	10.5	25°	48.1	4.6	Small IGA patch	I	-2.8	40°	14.1	5.3	Small IGA patch
AL1	10.4	75°	19.1	2.3	Small IGA patches	H	-2.9	120°	9.7	3.8	Minor IGA patch
AK	10.0	25°	63.2	13.5	Small IGA patch	*G1	-3.3	160°	8.3	6.5	Minor pitting
AJ	9.7	190°	58.4	9.3	Small IGA patch	F	-3.4	160°	12.0	9.3	Minor IGA patches
AH	8.9	69°	55.9	5.7	Small IGA patch	E	-3.9	145°	18.2	3.4	Small IGA patch
AG2	8.7	100°	62.3	7.3	Small IGA patch	*C	-5.4	350°	6.7	4.9	Minor pitting

* Defects associated with axial scratches

For tube sections 52-51-2 and 90-28-2, the deposits spalled in such a manner that a splotchy pattern of adhering deposit remained on the tube surface. The adhering deposit areas correlated precisely with the thin, dark, scallop shaped deposits noted during the initial visual inspection. Additional patterns of dark stains, with essentially no associated deposit, were also noted; these areas appeared to correlate quite well with the spotty patterns of spalled deposit previously noted. The stereovisual inspection revealed defects within some of the scallop shaped deposit regions. Essentially all the degradation was in the form of small IGA patches, although it is possible minor pitting, as observed on the other two tube sections, may not have been visible due to obstructing deposits. Again, several of the IGA patches were located at "old-appearing" axial scratches, which were most likely created during tube installation. A total of 17 and 24 potential defect areas were identified on tube sections 52-51-2 and 90-28-2, respectively (see Figs. 2-34 & 2-35); the defects are summarized in Table 2-7 below.

Table 2-7: STEREOVISUAL INSPECTION SUMMARY

Note: Axial position is given relative to the LTSF; axial extent is given in mils.

Tube Section: 52-51-2

ID No.	Position Axial	Position Angular	Extent Axial	Extent Angular	Description	ID No.	Position Axial	Position Angular	Extent Axial	Extent Angular	Description
Z	18.0	270°	9.1	0.4	Possible minor pit	*L	11.4	180°	33.5	1.4	Small IGA patch
*X	16.5	315°	40.3	2.0	Small IGA patch	*K2	11.0	250°	27.3	2.1	Small IGA patch
*V	15.8	240°	60.6	3.8	Small IGA patch	*K1	10.9	180°	42.7	5.7	Small IGA patch
*U	15.4	315°	32.7	4.8	Small IGA patch	*I2	10.0	330°	47.5	7.6	Small IGA patch
*S	14.7	315°	63.7	8.3	Small IGA patch	I1	10.0	270°	52.9	7.6	Small IGA patch
*R	14.1	250°	38.9	3.7	Small IGA patch	G	9.0	315°	36.9	7.2	Small IGA patch
*P	13.1	200°	43.9	5.3	Small IGA patch	*F	8.8	350°	82.4	5.3	Small IGA patch
*N2	12.5	190°	31.4	3.2	Small IGA patch	D	8.5	265°	60.9	8.4	Small IGA patch
N1	12.3	260°	35.8	1.4	Small IGA patch	B	-0.8	10°	38.6	2.0	Minor IGA patches

Tube Section: 90-28-2

ID No.	Position Axial	Position Angular	Extent Axial	Extent Angular	Description	ID No.	Position Axial	Position Angular	Extent Axial	Extent Angular	Description
*AF	17.2	150°	28.9	2.0	Small IGA patch	*S1	12.8	110°	27.8	1.5	Small IGA patch
AD2	16.1	180°	52.4	3.5	Small IGA patch	*Q	12.3	340°	59.2	3.1	Small IGA patch
*AD1	16.1	315°	na	na	Small IGA patch	*O	11.8	340°	51.7	1.5	Small IGA patch
AB	15.5	340°	54.4	8.3	Small IGA patches	*N	11.6	100°	60.8	4.3	Small IGA patch
Z	15.1	325°	38.2	1.3	Small IGA patch	*M	11.4	290°	58.1	8.7	Small IGA patch
X2	14.6	340°	38.0	2.0	Small IGA patch	K	10.8	290°	31.8	3.6	Small IGA patch
X1	14.4	110°	53.1	0.7	Small IGA patch	I	10.4	200°	62.5	4.7	Small IGA patch
V2	14.1	270°	55.5	3.1	Small IGA patch	H	10.2	10°	58.7	4.5	Small IGA patch
V1	14.0	350°	51.9	4.4	Small IGA patch	G	10.1	330°	79.1	8.1	Small IGA patch
*T2	13.2	110°	44.0	7.6	Small IGA patch	*E	7.8	340°	70.9	7.9	Small IGA patch
T1	13.2	330°	28.5	0.1	Small IGA patch	C	6.2	20°	53.2	2.0	Small IGA patch
S2	12.9	350°	39.9	1.7	Small IGA patch	*B	6.1	315°	63.0	4.1	Small IGA patch

* Defects associated with scratches

2.2.8 Tube Sectioning

As defects were identified and selected for specific analyses, they were sectioned into smaller specimens of working size. Sectioning was performed with either a slow speed diamond saw or a high-speed abrasive cut-off saw For tube specimens which were to be used for deposit analyses, sectioning was performed dry or with deionized water to prevent chemical contamination of the deposits. Sectioned

specimens were stored in clearly labeled clean plastic bags to prevent loss and/or confusion of the samples. Sectioning diagrams were maintained for each tube section and defect area examined.

All of the defect specimens from the first freespan region identified in Tables 2-6 and 2-7 were utilized for metallography, except specimens 52-51-2F and 90-28-2N, which were analyzed by SEM/EDS and SAM/XPS. In addition, two (2) specimens were isolated on 109-30-2 based on the laboratory slow-pull bobbin coil ECT data; these defect specimens correlated with the field reported bobbin coil indications at LTSF + 8 inches (27% TW; 0.94 V; Specimen B) and LTSF + 9.2 inches (S/N; 0.54 V; Specimen D) for metallographic examination by incremental grinding. Detailed sectioning diagrams for tube sections 52-51-2, 109-30-2, 90-28-2, 97-91-2 and 106-32-2 are shown in Figures 2-36 through 2-38. Additional ring sections were taken from tube sections 52-51-4, 133-33-3 and 133-33-9 for characterization of the OD deposits by metallography and SEM/EDS.

2.2.9 Metallography

Selected samples were mounted in Epomet (a thermoset resin), and prepared for metallographic examination using standard techniques. Deionized water was utilized as the grinding and polishing lubricant for preservation of corrosion product chemistry within defect regions on tube specimens subsequently used for microchemical analyses. The specimens were examined as-polished on the metallograph at magnifications up to 1,000X to characterize defects and deposit morphology. Selected grinding planes on specimens 109-30-2D and 109-30-2B were etched electrolytically in 5% nital solution to reveal the grain structure, then re-examined to establish the defect path relative to the grain boundaries.

Step Grinding Results (109-30-2D & 109-30-2B)

IGA patches were identified on both of these specimens (see Figure 2-39). The IGA exhibited a classic thumbnail shape. The IGA had maximum depths of 40% and 50% throughwall for 109-30-2D and 109-30-2B, respectively.

A summary of the metallography results for these specimens is provided in Table 2-8.

Table 2-8
SUMMARY OF INCREMENTAL GRIND & POLISH DATA

Grind No.	Axial Position	Remarks	Defect Extent			Grind No.	Axial Position	Remarks	Defect Extent		
			Circ. Extent	Depth (%TW)	Vol. (10^{-4} in^3)				Circ. Extent	Depth (%TW)	Vol. (10^{-4} in^3)
Specimen 109-30-2D:						Specimen 109-30-2B:					
8	10.00	IGA Patch at 285°	9°	24%	6.3	10	8.38	IGA Patch at 275°	5	38%	4.0
9	10.02	IGA Patch at 285°	9°	40%	8.5	11	8.39	IGA Patch at 275°	11	46%	11.7
10	10.03	IGA Patch at 285°	6°	32%	3.5	12	8.41	IGA Patch at 275°	12	50%	13.8
11	10.04	IGA Patch at 285°	6°	40%	5.9	13	8.42	IGA Patch at 275°	9	35%	9.1
12	10.06	IGA Patch at 285°	3°	40%	2.7	14	8.44	IGA Patch at 275°	2	10%	0.8
						15	8.46	IGA Patch at 275°	2	3%	0.1
				Total:	26.9					Total:	39.2

Results on 1st Freespan Regions (52-51-2, 90-28-2, 97-91-2 & 106-32-2)

The majority of defects identified by stereovisual inspection (as well as the type of damage) were confirmed by metallography (see Figure 2-40). Again, tube degradation was primarily in the form of small patches of "thumbnail-shaped" IGA. A total of 108 defects were confirmed, with maximum and minimum depths of 62% and 1% throughwall, respectively, with an overall average depth of 28% and a standard deviation of 16%. Metallography data is summarized in Table 2-9.

Table 2-9
FIRST SPAN METALLOGRAPHY SUMMARY

52-51-2			90-28-2			97-91-2			106-32-2					
ID	Type	Depth	ID	Type	Depth	ID	Type	Depth	ID	Type	Depth	ID	Type	Depth
Z	Pit	NDD	AF	IGA	51%	AA	Pit	NDD	BG	IGA	11%	AG1	IGA	N/A
X	IGA	32%	AD	IGA	24%	Y	Pit	NDD	BF	IGA	17%	AE	IGA	24%
V	IGA	N/A	AD	IGA	49%	W	IGA	54%	BD	IGA	31%	AD	IGA	25%
U	IGA	26%	AB	IGA	30%	U	IGA	48%	BC	IGA	30%	AC2	IGA	22%
S	IGA	33%	Z	IGA	30%	T	IGA	44%	BB	IGA	17%	AC1	IGA	18%
R	IGA	18%	X2	IGA	24%	S	Pit	1%	BA	IGA	20%	AB	IGA	18%
P	IGA	33%	X1	IGA	62%	R1	IGA	4%	AZ	IGA	22%	AA	IGA	17%
N2	IGA	19%	V2	IGA	46%	P	IGA	46%	AY	IGA	36%	Z	IGA	51%
N1	IGA	40%	V1	IGA	49%	O	IGA	54%	AX	IGA	32%	Y	IGA	8%
L	IGA	13%	T2	IGA	53%	M	IGA	16%	AV	IGA	29%	X2	IGA	49%
K2	IGA	19%	T1	IGA	46%	K	IGA	29%	AU	IGA	39%	X1	IGA	27%
K1	IGA	45%	S2	IGA	28%	I	IGA	4%	AT	IGA	31%	V2	IGA	14%
I2	IGA	52%	S1	IGA	23%	G	IGA	5%	AR	IGA	19%	V1	Pit	NDD
I1	IGA	28%	Q	IGA	45%	E2	IGA	5%	AQ2	IGA	46%	T	Pit	NDD
G	IGA	34%	O	IGA	45%	E1	IGA	5%	AQ1	IGA	24%	R	IGA	NDD
F*	IGA	53%	N*	IGA	60%	D	IGA	8%	AP	IGA	42%	—	—	—
D	IGA	34%	M	IGA	27%	B	Pit	6%	AO	IGA	12%	Q	Pit	7%
—	—	—	K	IGA	18%	—	—	—	AN	IGA	36%	O	IGA	3%
B		38%	I	IGA	46%				AM3	IGA	25%	N	IGA	15%
			H	IGA	37%				AM2	IGA	22%	M1	IGA	3%
			G	IGA	53%				AM1	IGA	12%	L	Pit	14%
			E	IGA	50%				AM1	IGA	16%	K	IGA	17%
			C	IGA	56%				AL2	IGA	16%	J	Pit	5%
			B	IGA	12%				AL1	IGA	10%	I	IGA	31%
			—	—	—				AK	IGA	40%	H	IGA	3%
									AJ	IGA	38%	G1	Pit	4%
									AH	IGA	29%	F	IGA	9%
									AG2	IGA	40%	E	IGA	23%
												C	Pit	7%

Statistics:

Maximum	F	IGA	53%	X1	IGA	62%	O,W	IGA	53%	Z		IGA		51%
Minimum	L	IGA	13%	B	IGA	12%	S	Pit	1%	O, M1, H		IGA		3%
Average			32%			40%			22%					22%
S. Dev. (σ)			12%			14%			21%					13%

NDD = No Detectable Degradation; N/A = Data not available; Boldface/Shaded = Burst location; — = LTSF
* Sp[illegible]a utilized for SEM/EDS & SAM/XPS; depth estimated from SEM of fracture surface.

2.2.10 SEM/EDS/WDS

Selected specimens were examined at higher magnifications in the SEM for characterization of defect and OD tube deposit micromorphology. The EDS (Energy Dispersive Spectrometer) and WDS (Wavelength Dispersive Spectrometer) attachments to the SEM were utilized for qualitative analysis of deposits and corrosion products to establish elemental composition and distribution within defect regions and other areas of interest. The examination included analysis of existing tube or defect surfaces, as well as metallographically prepared cross sections.

IGA Defect Surfaces (Specimens 52-51-2F, P & 90-28-2B, N)

Typical IGA regions are shown after swelling in Figures 2-41 through 2-44. The intergranular nature of the fracture surfaces is readily apparent. At higher magnifications an obvious grain boundary film was noted (see Figs. 2-43 and 2-44). EDS analysis of the grain facets indicated chromium, oxygen and nickel were the major corrosion film constituents. However, significant levels of iron, sulfur, aluminum, silicon and carbon were also detected.

As noted previously, although the majority of the deposit spalled away from the tube as a result of swelling, "stains" were left on the tube OD surface where the scalloped areas of dark thin deposit had been. It was noted that the IGA patches were contained entirely within these stained regions, although there were obviously large numbers of "stained" regions which had not developed IGA. A ring of deposit typically remained on the surface outlining each stain (see Fig. 2-45). EDS analysis indicated the heavier deposits in this surrounding ring were rich in aluminum, silicon and oxygen; lower levels of base metal elements were also detected. Within the ring of heavier deposit (i.e., within the stain itself) and on the tube surface outside of the stain, a EDS fingerprint more typical of oxidized I-600 was observed, although the chromium appeared to be somewhat enriched relative to base metal composition. It was also noted that the area within the stain exhibited a higher oxygen peak and had slightly higher silicon and aluminum levels than the tube surface outside of the stain.

IGA Defect Cross-Sections (Specimens 109-30-2B, D)

One (1) grinding plane from each of these specimens was inspected by SEM/EDS. Typical patches of IGA are shown in Figures 2-46 and 2-47. EDS analysis of the grain boundary corrosion products revealed very high sulfur levels (see also Fig. 2-48). Sulfur enrichment at the grain boundaries is further illustrated by the sulfur line scans in Figures 2-46 and 2-47.

OD Deposit Cross-Sections (109-30-2, 52-51-4, 90-28-5, 133-33-3 & 9)

Metallography and SEM/EDS results on these metallography specimens revealed a relatively thin (about 1 mil thick or less) porous deposit layer. The deposits on specimen 133-33-3 were slightly thinner on average than the other specimens, while specimen 133-33-8 exhibited slightly thicker (up to 1.5 mil) deposits. Typical deposit cross sections are shown in Figure 2-49. The porosity levels were highest at the outer surface, giving the outer deposit a "fluffy" appearance, and decreased to very low levels near the deposit/tube interface.

For the most part, the deposits appeared to be a single phase, with iron and oxygen as the major elemental constituents (see Figs. 2-50 through 2-53); trace levels of chromium, nickel, copper, and silicon were also detected. It was interesting to observe that a thin layer (perhaps on the order of 1 μm thick) of deposit at the tube/deposit interface was typically enriched in chromium and nickel relative to the bulk deposit (see esp. Fig. 2-52). Very infrequently, a copper-rich secondary phase, which was generally

present as discrete particles in the deposit, was observed on most of the samples. In specimen 109-30-2D a copper-rich particle appeared to be present as an oxide (see Fig. 2-50), while small particles of apparent metallic copper were observed in one location on specimen 133-33-8 (see Fig. 2-53). No sulfur was detected in the bulk deposit by EDS.

OD Deposit Flakes (52-51-2, 52-51-4, 133-33-3 & 9)

SEM/EDS results indicated the outer flake surfaces were rough and porous, giving the deposit a "fluffy" appearance (see Figs. 2-54 through 2-57). The outer surfaces were comprised chiefly of iron and oxygen. The inner surfaces were smooth with the circumferential grinding marks replicated in the deposit surface; composition of the inner surfaces were also predominantly iron and oxygen, but enriched with chromium and nickel relative to the outer deposit surface. Traces of aluminum, silicon and titanium were also occasionally detected on the flake inner surfaces, but no significant amounts of sulfur were found.

2.2.11 SAM/XPS

Two (2) selected defect specimens were examined by SAM (Scanning Auger Microscopy) and focused XPS (X-ray Photoelectron Spectroscopy) for characterization of in-situ grain boundary and OD surface corrosion films. The inner and outer surfaces of OD tube deposit flakes from a total of four (4) locations in both defect and non-defected regions were also analyzed by SAM/XPS. After spalling and light rinsing in ethanol, no additional specimen preparation was performed on the flake specimens prior to performing the analysis. Qualitative and semi-quantitative analyses were performed using both SAM and XPS to establish elemental composition. The original sample surfaces were analyzed by SAM/XPS, sputtered to remove a few angstroms of deposit and then reanalyzed. Some additional sputtering and reanalyses were performed to depth profile selected elements on the defect specimens. Electron binding energies for detected elements were determined by XPS to establish their oxidation states and subsequent inference of the chemical compounds present.

IGA Defect Specimens 52-51-2F1 & 90-28-2N1

The major elemental constituents of the grain boundary corrosion film were nickel, oxygen, chromium, iron, and carbon (see Table 2-10A through 2-10D). Energy shifts in the XPS spectra for Ni, Cr and O indicated the bulk of the film was probably composed of $Ni(OH)_2$, with significant levels of Cr_2O_3 as well. After short sputter times, the chromium content approached levels that would be expected in the base metal (i.e., chromium was not depleted significantly, see Fig. 2-58). Conversely, nickel was generally depleted slightly relative to base metal composition (see Fig. 2-59). This was also apparent in the Ni/Cr ratios, which were generally slightly lower for the grain boundary film as compared to reference spectra taken on fresh ductile fracture surfaces; average values were 3.0 (σ = 0.6) and 4.5 (σ = 0.8) for the grain boundary film and ductile fracture surface, respectively.

Lower levels of sulfur and titanium, and trace levels of chlorine were also consistently detected throughout the grain boundary corrosion film. Generally, sulfur levels peaked after a short sputter at levels of about 3 to 5 atom percent. XPS results indicated the sulfur was present predominantly as sulfate, but with appreciable quantities of sulfide. Silicon was also detected in significant quantities, but tended to be more prevalent near the OD tube surface and in the outer region of the film, indicating it was probably a surface contaminant which washed into the defect region from the outside surface. Low to trace levels of copper, calcium and phosphorous were only occasionally detected.

Auger spectra collected on the OD tube surfaces indicated that areas with residual deposits were predominantly composed of iron and oxygen, with significant levels of copper, nickel, silicon and carbon

(see Table 2-11). No chromium was detected in these regions. Low to trace levels of sulfur, chlorine and titanium were also detected.

Table 2-10A
SAM RESULTS ON TUBE SPECIMEN 52-51-2F1 DEFECT SURFACES - AREA 1

Analysis Location	Time (min)	Sputter Depth (nm)	Elemental Composition (Atomic %)									Ratios	
			Ni	Cr	Fe	O	C	S	Si	Cl	Ti	Ni/Ni_o	Cr/Cr_o
Near OD Surface	0	0	10.0	3.4	1.0	24.0	52.0	0.4	9.1	0.1	0.3	0.1	0.2
	1	30	22.0	7.5	1.9	26.0	30.0	4.3	7.7		0.9	0.3	0.4
	2	60	32.0	12.0	3.9	28.0	17.0	3.8	3.0	0.1	0.7	0.4	0.7
	5	150	34.0	12.0	6.4	30.0	11.0	3.1	1.7	0.1	1.0	0.5	0.7
	10	300	36.0	14.0	7.9	28.0	9.4	3.3		0.1	1.3	0.5	0.8
Mid-Crack	0	0	12.0		1.6	27.0	48.0	0.6	11.0	0.1		0.2	0.0
	1	30	48.0	15.0	4.8	18.0	10.0	3.4			0.8	0.7	0.9
	2	60	51.0	16.0	4.8	16.0	8.1	3.4		0.1	0.8	0.7	0.9
	5	150	54.0	15.0	4.6	11.0	13.0	2.4		0.1	0.9	0.7	0.9
	10	300	66.0	17.0	7.2	3.1	5.4	0.7		0.1	0.6	0.9	1.0
Crack Tip	0	0	16.0	3.7	1.9	26.0	45.0	0.7	6.6	0.2	0.6	0.2	0.2
	1	30	49.0	13.0	4.1	18.0	12.0	3.3		0.2	0.8	0.7	0.8
	2	60	49.0	16.0	5.4	16.0	9.1	3.0		0.1	1.6	0.7	0.9
	5	150	58.0	13.0	5.9	9.6	10.0	2.0		0.3	1.4	0.8	0.8
	10	300	60.0	17.0	6.5	4.8	8.0	1.2		0.3	2.3	0.8	1.0

Analysis Location	Time (min)	Sputter Depth (nm)	Elemental Composition (Weight %)									Ratios	
			Ni	Cr	Fe	O	C	S	Si	Cl	Ti	Ni/Ni_o	Cr/Cr_o
Near OD Surface	0	0	27.0	8.1	2.6	17.6	28.7	0.6	14.6	0.1	0.7	0.4	0.5
	1	30	42.8	12.9	3.5	13.3	12.0	4.6	8.9		1.4	0.6	0.8
	2	60	51.7	17.2	6.0	12.3	5.6	3.4	2.9	0.1	0.9	0.7	1.1
	5	150	52.5	16.4	9.4	12.6	3.5	2.6	1.6	0.1	1.3	0.7	1.1
	10	300	52.6	18.1	11.0	11.2	2.8	2.6		0.1	1.6	0.7	1.2
Mid-Crack	0	0	31.9		4.0	19.8	26.1	0.9	17.4	0.1		0.4	0.0
	1	30	63.7	17.6	6.1	6.5	2.7	2.5			0.9	0.9	1.1
	2	60	65.1	18.1	5.8	5.6	2.1	2.4		0.1	0.8	0.9	1.2
	5	150	68.0	16.7	5.5	3.8	3.3	1.7		0.1	0.9	0.9	1.1
	10	300	72.7	16.6	7.5	0.9	1.2	0.4		0.1	0.5	1.0	1.1
Crack Tip	0	0	37.8	7.8	4.3	16.8	21.8	0.9	9.3	0.2	1.2	0.5	0.5
	1	30	65.9	15.5	5.2	6.6	3.3	2.4		0.1	0.9	0.9	1.0
	2	60	63.2	18.3	6.6	5.6	2.4	2.1		0.1	1.7	0.8	1.2
	5	150	70.6	14.0	6.8	3.2	2.5	1.3		0.2	1.4	0.9	0.9
	10	300	69.1	17.3	7.1	1.5	1.9	0.8		0.2	2.2	0.9	1.1

Table 2-10B
SAM RESULTS ON TUBE SPECIMEN 52-51-2F1 DEFECT SURFACES - AREA 2

Analysis Location	Time (min)	Sputter Depth (nm)	Elemental Composition (Atomic %)									Ratios	
			Ni	Cr	Fe	O	C	S	Si	Cl	Ti	Ni/Ni_s	Cr/Cr_s
Near OD Surface	0	0	10.0	3.3	1.4	26.0	47.0	0.6	12.0	0.1	0.6	0.1	0.2
	1	30	29.0	10.0	3.1	31.0	17.0	4.2	4.4	0.2	0.7	0.4	0.6
	2	60	36.0	14.0	2.9	31.0	9.6	3.4	2.1	0.2	1.1	0.5	0.8
	5	150	44.0	14.0	4.9	24.0	8.0	2.7	1.2		1.1	0.6	0.8
	10	300	48.0	14.0	4.4	20.0	9.2	2.0		0.1	1.6	0.7	0.8
Mid-Crack	0	0	25.0	4.3	1.0	23.0	40.0	0.6	6.5	0.1		0.3	0.3
	1	30	38.0	13.0	3.8	22.0	17.0	4.3	0.7	0.1	1.0	0.5	0.8
	2	60	47.0	12.0	5.2	18.0	13.0	3.8			1.5	0.6	0.7
	5	150	52.0	16.0	5.5	11.0	13.0	2.0		0.1	1.6	0.7	0.9
	10	300	57.0	16.0	6.2	5.6	13.0	1.0		0.1	1.6	0.8	0.9
Crack Tip	0	0	12.0	4.1	1.4	25.0	46.0	0.6	11.0	0.1		0.2	0.2
	1	30	40.0	8.9	3.5	19.0	22.0	2.5	3.1	0.1	0.8	0.6	0.5
	2	60	45.0	12.0	3.9	18.0	15.0	3.7	1.3	0.1	1.4	0.6	0.7
	5	150	48.0	15.0	4.9	14.0	14.0	3.7			1.1	0.7	0.9
	10	300	48.0	16.0	5.0	14.0	12.0	3.3		0.1	1.2	0.7	0.9

Analysis Location	Time (min)	Sputter Depth (nm)	Elemental Composition (Weight %)									Ratios	
			Ni	Cr	Fe	O	C	S	Si	Cl	Ti	Ni/Ni_s	Cr/Cr_s
Near OD Surface	0	0	25.0	7.3	3.3	17.7	24.1	0.8	17.9	0.1	1.2	0.3	0.5
	1	30	49.7	15.2	5.1	14.5	6.0	3.9	4.5	0.2	1.0	0.7	1.0
	2	60	54.8	15.9	4.2	12.9	3.0	2.8	1.9	0.1	1.4	0.7	1.2
	5	150	60.8	17.1	6.4	9.0	2.3	2.0	1.0		1.2	0.8	1.1
	10	300	64.5	16.7	5.6	7.3	2.5	1.5		0.1	1.8	0.9	1.1
Mid-Crack	0	0	51.6	7.9	2.0	12.9	16.9	0.7	8.0	0.1		0.7	0.5
	1	30	57.4	17.4	5.5	9.1	5.3	3.5	0.6	0.1	1.2	0.8	1.1
	2	60	64.0	14.5	6.7	6.7	3.6	2.8			1.7	0.9	0.9
	5	150	65.4	17.8	6.6	3.8	3.3	1.4		0.1	1.6	0.9	1.1
	10	300	68.5	17.0	7.1	1.8	3.2	0.7		0.1	1.6	0.9	1.1
Crack Tip	0	0	29.9	9.1	3.3	17.0	23.5	0.8	16.3	0.1		0.4	0.6
	1	30	61.7	12.2	5.1	8.0	6.9	2.1	2.9	0.1	1.0	0.8	0.8
	2	60	63.1	14.9	5.2	6.9	4.3	2.8	1.1	0.1	1.6	0.8	1.0
	5	150	63.5	17.6	6.2	5.1	3.8	2.7			1.2	0.9	1.1
	10	300	63.1	18.6	6.3	5.0	3.2	2.4		0.1	1.3	0.8	1.2

Table 2-10C
SAM RESULTS ON TUBE SPECIMEN 90-28-2N1 DEFECT SURFACES - AREA 1

Analysis Location	Time (min)	Sputter Depth (nm)	Elemental Composition (Atomic %)									Ratios	
			Ni	Cr	Fe	O	C	S	Si	Cl	Ti	Ni/Ni_b	Cr/Cr_b
Near OD Surface	0	0	9.9			20.0	62.0	0.7	5.7		1.3	0.1	0.0
	1	30	21.0	8.1	2.8	21.0	41.0	3.2	2.1	0.3	1.2	0.3	0.5
	2	60	37.0	18.0	5.3	23.0	13.0	3.4		0.4	0.4	0.5	1.1
	5	150	50.0	20.0	6.9	13.0	7.9	1.5		0.1	0.9	0.7	1.2
	10	300	51.0	18.0	6.7	11.0	11.0	1.0		0.1	1.7	0.7	1.1
Mid-Crack	0	0	13.0			19.0	62.0	0.6	3.8	0.5	1.5	0.2	0.0
	1	30	17.0	4.2	0.9	19.0	54.0	1.5	2.3	0.3	0.9	0.2	0.2
	2	60	30.0	10.0	3.3	18.0	34.0	3.6		0.3	0.9	0.4	0.6
	5	150	38.0	13.0	3.7	16.0	27.0	3.6		0.3	0.9	0.5	0.8
	10	300	41.0	15.0	4.6	12.0	24.0	2.3		0.3	1.6	0.6	0.9
Crack Tip	0	0	14.0	4.8	1.2	18.0	58.0	0.5	3.6	0.6		0.2	0.3
	1	30	22.0	7.1	2.0	19.0	47.0	2.1	1.0	0.4	0.7	0.3	0.4
	2	60	35.0	16.0	4.4	16.0	24.0	3.5		0.3	0.6	0.5	0.9
	5	150	45.0	16.0	5.1	13.0	18.0	1.7		0.3	0.7	0.6	0.9
	10	300	52.0	16.0	6.5	7.7	16.0	1.2		0.2	0.7	0.7	0.9

Analysis Location	Time (min)	Sputter Depth (nm)	Elemental Composition (Weight %)									Ratios	
			Ni	Cr	Fe	O	C	S	Si	Cl	Ti	Ni/Ni_b	Cr/Cr_b
Near OD Surface	0	0	30.1			16.6	38.6	1.2	10.3		3.2	0.4	0.0
	1	30	42.8	14.6	5.4	11.7	17.1	3.6	2.6	0.3	2.0	0.6	0.9
	2	60	53.4	23.0	7.3	9.0	3.8	2.7		0.3	0.5	0.7	1.5
	5	150	61.7	21.9	8.1	4.4	2.0	1.0		0.1	0.9	0.8	1.4
	10	300	63.3	19.8	7.9	3.7	2.8	0.7		0.1	1.7	0.8	1.3
Mid-Crack	0	0	37.2			14.8	36.3	0.9	6.5	0.7	3.5	0.5	0.0
	1	30	41.6	9.1	2.1	12.7	27.0	2.0	3.4	0.4	1.8	0.6	0.3
	2	60	52.9	15.6	5.5	8.7	12.3	3.5		0.3	1.3	0.7	1.0
	5	150	58.4	18.0	5.5	6.8	8.7	3.1		0.2	1.2	0.8	1.2
	10	300	59.0	19.1	6.3	4.7	7.1	1.8		0.2	1.9	0.8	1.2
Crack Tip	0	0	36.0	10.9	2.9	12.6	30.5	0.7	5.5	0.7		0.5	0.7
	1	30	46.3	13.2	4.0	10.9	20.2	2.4	1.3	0.4	1.2	0.6	0.9
	2	60	53.6	21.7	6.4	6.7	7.5	2.9		0.2	0.7	0.7	1.4
	5	150	61.7	19.4	6.7	4.9	5.1	1.3		0.2	0.8	0.8	1.3
	10	300	65.8	17.9	7.8	2.7	4.1	0.8		0.1	0.7	0.9	1.2

Table 2-10D
SAM RESULTS ON TUBE SPECIMEN 90-28-2N1 DEFECT SURFACES - AREA 2

Analysis Location	Time (min)	Sputter Depth (nm)	Elemental Composition (Atomic %)									Ratios	
			Ni	Cr	Fe	O	C	S	Si	Cl	Ti	Ni/Ni_b	Cr/Cr_b
Near OD Surface	0	0	10.0	4.4		19.0	61.0	1.2	4.0	0.3		0.1	0.3
	1	30	25.0	9.0	2.8	23.0	35.0	3.2	0.5	0.3	1.3	0.3	0.5
	2	60	31.0	13.0	4.2	27.0	19.0	3.2	0.6	0.3	0.6	0.4	0.8
	5	150	37.0	15.0	4.2	24.0	16.0	2.7		0.5	0.7	0.5	0.9
	10	300	41.0	16.0	4.4	19.0	15.0	2.2		0.6	1.3	0.6	0.9
Mid-Crack	0	0	14.0	3.1		19.0	57.0	0.6	4.1	0.9	1.2	0.2	0.2
	1	30	19.0	4.9		18.0	53.0	1.6	2.3	0.9	0.7	0.3	0.3
	2	60	28.0	10.0	2.6	17.0	38.0	3.9	0.9	0.8	0.8	0.4	0.6
	5	150	30.0	13.0	3.1	17.0	29.0	4.8	0.6	0.7	1.2	0.4	0.8
	10	300	37.0	16.0	4.2	14.0	24.0	4.1		0.6	0.9	0.5	0.9
Crack Tip	0	0	16.0	6.0	1.6	21.0	47.0	2.3	4.2	0.1	0.9	0.2	0.4
	1	30	23.0	9.9	3.0	17.0	4.0	4.3	1.8	0.3	1.0	0.3	0.6
	2	60	33.0	16.0	3.9	20.0	22.0	3.6	0.5	0.1	1.0	0.5	0.9
	5	150	38.0	16.0	4.7	17.0	21.0	3.3		0.2	0.5	0.5	0.9
	10	300	42.0	17.0	5.3	13.0	18.0	2.7		0.1	1.0	0.6	1.0

Analysis Location	Time (min)	Sputter Depth (nm)	Elemental Composition (Weight %)									Ratios	
			Ni	Cr	Fe	O	C	S	Si	Cl	Ti	Ni/Ni_b	Cr/Cr_b
Near OD Surface	0	0	29.2	11.4		15.1	36.4	1.9	5.6	0.5		0.4	0.7
	1	30	47.8	15.2	5.1	12.0	13.7	3.3	0.5	0.3	2.0	0.6	1.0
	2	60	51.3	19.0	6.6	12.2	6.4	2.9	0.5	0.3	0.8	0.7	1.2
	5	150	55.7	20.0	6.0	9.8	4.9	2.2		0.5	0.9	0.7	1.3
	10	300	58.4	20.2	6.0	7.4	4.4	1.7		0.5	1.5	0.8	1.3
Mid-Crack	0	0	37.4	7.3		13.8	31.2	0.9	5.2	1.5	2.6	0.5	0.5
	1	30	45.0	10.3		11.6	25.7	2.1	2.6	1.3	1.4	0.6	0.7
	2	60	48.7	15.6	4.6	8.7	14.5	4.0	0.8	0.9	1.2	0.7	1.1
	5	150	50.6	19.4	5.0	7.8	10.0	4.4	0.5	0.7	1.6	0.7	1.3
	10	300	55.0	21.1	5.9	5.7	7.3	3.3		0.5	1.1	0.7	1.4
Crack Tip	0	0	37.9	12.6	3.6	13.6	22.8	3.0	4.8	0.1	1.7	0.5	0.8
	1	30	51.9	19.8	6.4	10.5	1.8	5.3	1.9	0.4	1.8	0.7	1.3
	2	60	51.6	22.2	5.8	8.5	7.0	3.1	0.4	0.1	1.3	0.7	1.4
	5	150	56.0	20.9	6.6	6.8	6.3	2.7		0.2	0.6	0.7	1.3
	10	300	58.6	21.0	7.0	4.9	5.1	2.1		0.1	1.1	0.8	1.4

Areas on the OD tube surface, which were essentially free of deposit, were composed primarily of nickel, oxygen, chromium, iron, and carbon as was the grain boundary corrosion film (see Table 2-11). Low levels of sulfur (below 1 at%), were consistently observed throughout the OD corrosion film. Significant levels of silicon and titanium, and low levels of chlorine, calcium, phosphorous and copper were occasionally detected. The nickel and chromium levels were similar to those observed in the grain boundary corrosion film (i.e., exhibited nickel depletion, see Fig. 2-60).

Table 2-11
SAM RESULTS ON TUBE OD SURFACES

Tube Section & Analysis Location	Sputter Time (min)	Depth (nm)	Elemental Composition (Upper Table: atom % - Lower Table: weight %)												Elemental Ratios	
			Ni	Cr	Fe	O	C	S	Si	Cl	Ti	Cu	Ca	P	Ni/Ni	Cr/Cr
52-51-2F1 Tube Outer Surface Deposit-free Area	0	0	16.0	3.0	2.5	29.0	41.0	0.7	7.9			1.0			0.2	0.2
	0.5	15	30.0	7.2	6.4	37.0	8.0	0.7	8.3	0.2	1.8		0.5		0.4	0.4
	2	60	30.0	16.0	6.9	37.0	5.8	0.8	2.9		0.8			0.6	0.4	0.9
	5	150	35.0	17.0	6.9	35.0	5.7	0.8			0.4			0.5	0.5	1.0
	10	300	38.0	20.0	6.0	31.0	5.5	0.4			0.4				0.5	1.2
	0	0	37.6	6.2	5.6	18.6	19.7	0.9	8.9	0.0		2.5			0.5	0.4
	0.5	15	49.6	10.5	10.1	16.7	2.7	0.6	8.6	0.2	2.4		0.6		0.7	0.7
	2	60	46.3	21.9	10.1	15.6	1.8	0.7	2.1		1.0			0.5	0.6	1.4
	5	150	51.2	22.0	9.6	14.0	1.7	0.6			0.5			0.4	0.7	1.4
	10	300	53.1	24.8	8.0	11.8	1.6	0.3			0.5			0.0	0.7	1.6
90-28-2N1 Tube Outer Surface Deposit-free Area	0	0	2.8		1.6	18.0	75.0	0.4	2.4						0.0	0.0
	0.5	15	23.0	7.6	6.5	26.0	35.0	0.7	1.0						0.3	0.4
	2	60	30.0	10.0	11.0	34.0	12.0	0.1			1.5		0.9		0.4	0.6
	5	150	39.0	13.0	10.0	30.0	6.5	0.4						0.4	0.5	0.8
	10	300	47.0	15.0	9.1	23.0	5.1	0.4		0.2					0.6	0.9
	0	0	10.8		5.9	18.9	59.2	0.8	4.4						0.1	0.0
	0.5	15	45.1	13.2	12.1	13.9	14.0	0.7	0.9						0.6	0.9
	2	60	47.7	14.1	16.6	14.7	3.9	0.1			1.9		1.0		0.6	0.9
	5	150	55.7	16.5	13.6	11.7	1.9	0.3						0.3	0.7	1.1
	10	300	61.4	17.3	11.3	8.2	1.4	0.3		0.2					0.8	1.1

OD Deposit Flake Specimens 52-51-2, 52-51-4, 133-33-3 & 133-33-9

After a light sputter, the outer flake surfaces were found to be predomiantly composed of iron, oxygen and carbon (see Table 2-12). Carbon is normally present in high quantities as the result of handling and/or exposure to the atmosphere, and is probably of no significance to this analysis. Lower levels of nickel, copper, silicon, titanium and sulfur were also detected on the outer surfaces. Energy shifts determined by XPS indicated the copper may have been present as CuO. The sulfur levels were generally quite low (i.e., < 1.0 at%). Low levels of zinc and trace levels of chlorine and calcium were occasionally detected. However, chromium was virtually absent at the outer surface with the exception of one analysis point on a flake from above the 1st TSP on 52-51 (52-51-4).

The inner flakes surfaces were of similar composition, with the following exceptions: (1) nickel levels were generally higher, (2) significant levels of chromium were detected in most cases, and (3) besides sulfur and titanium, other elements (e.g., copper, silicon, zinc and chlorine) were not found in appreciable quantities. Significant point-to-point variations in composition were noted on both surfaces by both SAM and XPS.

Table 2-12
SAM RESULTS ON OD DEPOSIT FLAKE SURFACES

Tube Section & Analysis Location	Sputter Time (min)	Sputter Depth (nm)	Elemental Composition (Upper Table: atom % - Lower Table: weight %) Ni	Cr	Fe	O	C	S	Si	Cl	Ti	Cu	Ca	Zn	P
52-51-2 Deposit Flake:															
Outer Surface	0	0	2.4		13.0	20.0	57.0		4.7			2.9			
	0.5	15	3.5		39.0	36.0	15.0	0.5	2.9			2.3			
Inner Surface	0	0	14.0		3.1	22.0	61.0	0.3		0.2					
	0.5	15	13.0	24.0	5.0	42.0	15.0	0.5			2.7				
Outer Surface	0	0	6.4		33.2	14.6	31.3		6.0			8.4			
	0.5	15	6.1		64.4	17.0	5.3	0.5	2.4			4.3			
Inner Surface	0	0	39.2		8.3	16.8	34.9	0.5		0.3					
	0.5	15	23.2	38.0	8.5	20.4	5.5	0.5			3.9				
133-33-3 Deposit Flake:															
Outer Surface	0	0	3.9		26.0	25.0	43.0	0.7	0.7	0.2			0.2		
	0.5	15	1.9		52.0	38.0	6.8	0.6		0.2	0.8				
Inner Surface	0	0	16.0		2.6	22.0	57.0	0.9	0.2	0.2	1.1				
	0.5	15	12.0	32.0	7.9	38.0	7.2	0.2		0.2	2.0				
Outer Surface	0	0	8.6		54.7	15.1	19.5	0.8	0.7	0.3			0.3		
	0.5	15	3.0		77.0	16.1	2.2	0.5		0.2	1.0				
Inner Surface	0	0	42.4		6.6	15.9	30.9	1.3	0.3	0.3	2.4				
	0.5	15	19.5	46.0	12.2	16.8	2.4	0.2		0.2	2.7				

TABLE 2-12 (Continued)

Tube Section & Analysis Location	Sputter Time (min)	Sputter Depth (nm)	Elemental Composition (Upper Table: atom % - Lower Table: weight %) Ni	Cr	Fe	O	C	S	Si	Cl	Ti	Cu	Ca	Zn	P
133-33-9 Deposit Flake:															
Outer Surface	0	0	2.2		13.0	20.0	62.0				0.7	3.0			
	0.5	15	2.5		39.0	36.0	22.0				1.3				
Inner Surface	0	0	13.0		12.0	19.0	55.0	0.6							
	0.5	15	21.0	15.0	9.0	36.0	18.0	0.3			1.0				
Outer Surface	0	0	6.0		33.9	14.9	34.7				1.6	8.9			
	0.5	15	4.5		67.5	17.8	8.2				1.9				
Inner Surface	0	0	31.6		27.7	12.6	27.3	0.8							
	0.5	15	36.6	23.2	14.9	17.1	6.4	0.3			1.4				
52-51-4 Deposit Flake (Outer Surface):															
Area 1	0	0	2.1		22.0	29.0	40.0	0.4	0.7	0.2	1.3	1.9	0.4	1.9	
	0.5	15	0.8		49.0	41.0	8.1	0.2							0.7
Area 2	0	0	3.7	7.2	24.0	37.0	22.0	0.4	2.9		0.8	1.3	0.9	1.1	
	0.5	15	2.9	8.6	42.0	39.0	4.5	0.4	1.9		0.9		0.8		
Area 1	0	0	4.6	0.0	46.2	17.4	18.1	0.5	0.7	0.3	2.3	4.5	0.6	4.7	
	0.5	15	1.3	0.0	76.8	18.4	2.7	0.2							0.6
Area 2	0	0	7.0	12.0	43.1	19.0	8.5	0.4	2.6		1.2	2.7	1.2	2.3	
	0.5	15	4.5	11.8	62.0	16.5	1.4	0.3	1.4		1.1		0.8		
52-51-4 Deposit Flake (Inner Surface):															
Area 1	0	0	21.0			22.0	54.0	0.7	2.0						
	0.5	15	44.0		3.2	34.0	17.0	0.4		0.1	0.8				
Area 2	0	0	11.0		6.8	20.0	60.0	0.3				1.7			
	0.5	15	4.4		34.0	33.0	28.0	0.4							
Area 1	0	0	53.3			15.2	28.1	1.0	2.4						
	0.5	15	72.5		5.0	15.3	5.7	0.4		0.1	1.1				
Area 2	0	0	29.6		17.4	14.7	33.0	0.4				4.9			
	0.5	15	8.5		62.6	17.4	11.1	0.4							

2.2.12 Bulk Deposit Analyses

Several techniques were used to analyze bulk tube deposits collected from both defect and non-defect tube sections to establish elemental composition and the chemical compounds present, as well as the density and amount of open porosity.

A number of elemental analysis techniques were utilized to establish the concentrations of selected transition elements, alkali and alkali earth metals typically found in nuclear steam generating systems. The techniques used and analyzed elements are summarized below in Table 2-13. These analyses were performed at B&W's Alliance Research Center (ARC).

Table 2-13
SUMMARY OF ELEMENTAL ANALYSIS TECHNIQUES AND PURPOSE

ANALYSIS TECHNIQUE	PURPOSE
Atomic Emission Spectroscopy (AES): by Inductively Coupled Plasma (ICP-AES) by Flame Emission Spectroscopy (ES)	Quantitative Elemental Analysis Al, Ca, Cr, Cu, Fe, Pb, Mg, Mn, Ni, P, Ti, & Zn Na & K
ISE (Ion Selective Electrode)	Quantitative Elemental Analysis (Cl)
Gravimetric Analysis	Quantitative Elemental Analysis (Si)
Combustion/Thermal Conductivity	Quantitative Elemental Analysis (C)
Turbidimetric Analysis	Quantitative Elemental Analysis (S)
X-Ray Fluorescence (XRF)	Qualitative Elemental Analysis (all elements > atomic number 11)

Compound analysis techniques included X-Ray Diffraction (XRD), Fourier Transform Spectroscopy (FTIR) and Raman Spectroscopy. The purpose of XRD was to identify crystalline compounds, such as metal oxides and/or sulfides present in concentrations of a few weight percent or more; XRD was performed at B&W's ARC. FTIR and Raman analysis were intended to identify crystalline, as well as amorphous compounds. In particular, FTIR would be expected to identify various molecular species such as sulfate, silicate, phosphate and borate and other oxyanions. It was expected that Raman analysis would help establish chemical composition, stoichiometry, and other crystallographic phases which may have been present in the metal oxides. Both FTIR and Raman analyses were performed at AECL's Whiteshell Laboratories.

Density, both bulk and skeletal, as well as open porosity volume and pore size distribution were quantified in selected deposit samples by mercury porosimetry. This analysis was performed at AECL's Chalk River Laboratories.

Selected deposit samples were also sent to Rockwell International for Mossbauer Spectroscopy to establish the oxidation state of iron in the deposits. This analysis was to be performed under separate contract

established by EPRI directly with Rockwell. However, results of this analysis were not available for this report.

Lastly, gamma spectroscopy was performed to identify and quantify the radioisotopes present in the primary side deposits.

A total of nine (9) deposit samples, as identified below, were utilized for analysis by selected analysis techniques as discussed above.

Three (3) samples from the first freespan regions above the LTSF. These included:

- One (1) sample from tube section 52-51-2 exhibiting IGA damage.
- One (1) sample from tube section 90-28-2 exhibiting IGA damage.
- One (1) sample from tube section 133-33-3, which did not exhibit IGA damage.

Three (3) samples were taken from higher regions in the steam generator for comparison with the first span deposits. These included:

- One (1) sample from the second freespan region above the 1st TSP on tube section 52-51-4;
- One (1) sample from the 3rd and 4th freespan regions around the 4th TSP on tube section 133-33-9;
- One (1) sample from the 3rd TSP intersection on tube section 133-33-9.

Two (2) samples of the light-green colored deposits from the tube sheet crevice region just below the LTSF on tube sections 52-51-2 and 90-28-2.

One (1) sample of primary side deposit collected off a 2-inch long segment from tube section 133-33-9.

The results of the deposit analyses are summarized in Tables 2-14 and 2-15. The elemental analyses indicated the major elements were iron and oxygen (calculated as a balance). This is consistent with the XRD and FTIR analysis results, both of which detected major peaks for magnetite (Fe_3O_4).[2] For all samples except the 90-28-2 1st freespan deposit, the atom ratio of O/Fe was about where it should be (i.e., 1.33); this sample may have contained some excess moisture. The next most prevalent element was nickel, which was typically present in quantities of a few weight percent. Chromium and copper were also detected consistently, but at levels typically below 1%. Low levels ($< 0.5\%$) of potassium, silicon and carbon were routinely detected, as were trace levels ($\leq 0.1\%$) of all other elements analyzed except phosphorous, which was not detected. Based on this limited analysis, most elements did not exhibit an appreciable tendency to partition to specific areas of the generator. Nickel, chromium, silicon and sulfur all tended to be present in slightly greater quantities at lower elevations, while the opposite behavior was noted for copper. The distribution of elements with respect to steam generator elevation is illustrated graphically in Figure 2-61.

---

[2]No spectra could be obtained by backscatter Laser Raman Spectroscopy due to the intense absorption of light by the magnetite, which is black.

The mercury porosimetry analysis results indicated skeletal densities on the order of 4 to 4.7 g/cm^3; this is just slightly lower than the density of magnetite (5.2 g/cm^3). Bulk densities were significantly lower (about 3 to 3.7 g/cm^3), indicating open porosity levels of about 20% to 25%, with a pore diameter range of ~0.1 to 0.7 μm. The slightly lower skeletal densities might be partially explained by the presence of some closed porosity. In general, the densities increased, while porosity levels decreased, with increasing steam generator elevation.

Table 2-14
DEPOSIT ANALYSIS RESULTS

Analyses	SAMPLE LOCATION						Analysis Technique
	52-51-2 Freespan*** Above LTSF	90-28-2 Freespan*** Above LTSF	133-33-3 Freespan Above LTSF	52-51-4 Freespan Above 1st TSP	133-33-9 Freespan Near 3rd TSP	133-33-9 Freespan At 3rd TSP	
Elemental Analyses (wt %):							
Fe	68.10%	55.88%	65.53%	70.55%	69.39%	70.53%	ICP
O*	26.98%	36.23%	26.94%	25.92%	26.63%	25.01%	By Balance
Ni	3.01%	5.52%	4.75%	1.90%	2.20%	2.06%	ICP
Cr	0.57%	0.87%	1.42%	0.50%	0.32%	0.25%	ICP
Cu	0.25%	0.45%	0.14%	0.14%	0.60%	1.15%	ICP
K	0.18%	0.17%	0.17%	0.17%	0.16%	0.18%	FAA
Si	0.19%	0.27%	0.29%	0.07%	0.06%	0.11%	Gravimetric
C	0.22%	0.24%	0.24%	0.28%	0.22%	0.22%	Combustion
Cl	0.05%	0.11%	0.06%	0.08%	0.08%	0.06%	Electrode
Na	0.06%	0.06%	0.06%	0.07%	0.05%	0.06%	FAA
S	0.07%	0.06%	0.05%	0.04%	*	0.01%	Turbidimetric
Al	0.06%	0.07%	0.04%	0.03%	0.03%	0.04%	ICP
Ca	0.05%	0.06%	0.06%	0.05%	0.05%	0.04%	ICP
Pb	0.00%	0.01%	0.01%	0.00%	0.01%	0.01%	ICP
Mg	0.07%	0.07%	0.07%	0.07%	0.07%	0.08%	ICP
Mn	0.06%	0.06%	0.09%	0.06%	0.07%	0.12%	ICP
Ti	0.04%	0.04%	0.06%	0.05%	0.03%	0.03%	ICP
Zn	0.03%	0.03%	0.03%	0.01%	0.02%	0.02%	ICP
P	**	**	**	**	**	**	ICP
Compound Analyses:							
Fe_3O_4	Major	Major	Major	Major	Major	Major	XRD/FTIR
O/Fe Ratio	1.38	2.27	1.44	1.28	1.34	1.24	Calculated
Density Analysis (g/cm^3):							
Bulk	3.11	-	-	3.02	3.74	-	Hg Poros.
Skeletal	4.31	-	-	4.04	4.68	-	Hg Poros.
Open Porosity	27.8%	-	-	25.3%	20.1%	-	Hg Poros.
	0.12-0.69 μm	-	-	0.12-0.59 μm	0.12-0.68 μm	-	Hg Poros.

* Below 40 ppm; detection threshold

** Insufficient sample available.

*** Green deposits at LTSF were Fe & Ni by XRF; insufficient sample for XRD.

Table 2-15

GAMMA SCAN RESULTS ON ID TUBE DEPOSITS FROM TUBE SECTION 133-33-3

Isotope	Specific Activity (μC_i /gm)	Activity Contribution
Co-60	1,587.00	71.8%
Co-58	546.20	24.7%
Sb-125	41.59	1.9%
Mn-54	19.97	0.9%
Ce-144	9.72	0.4%
Co-57	6.22	0.3%
TOTAL	2,210.70	100.0%

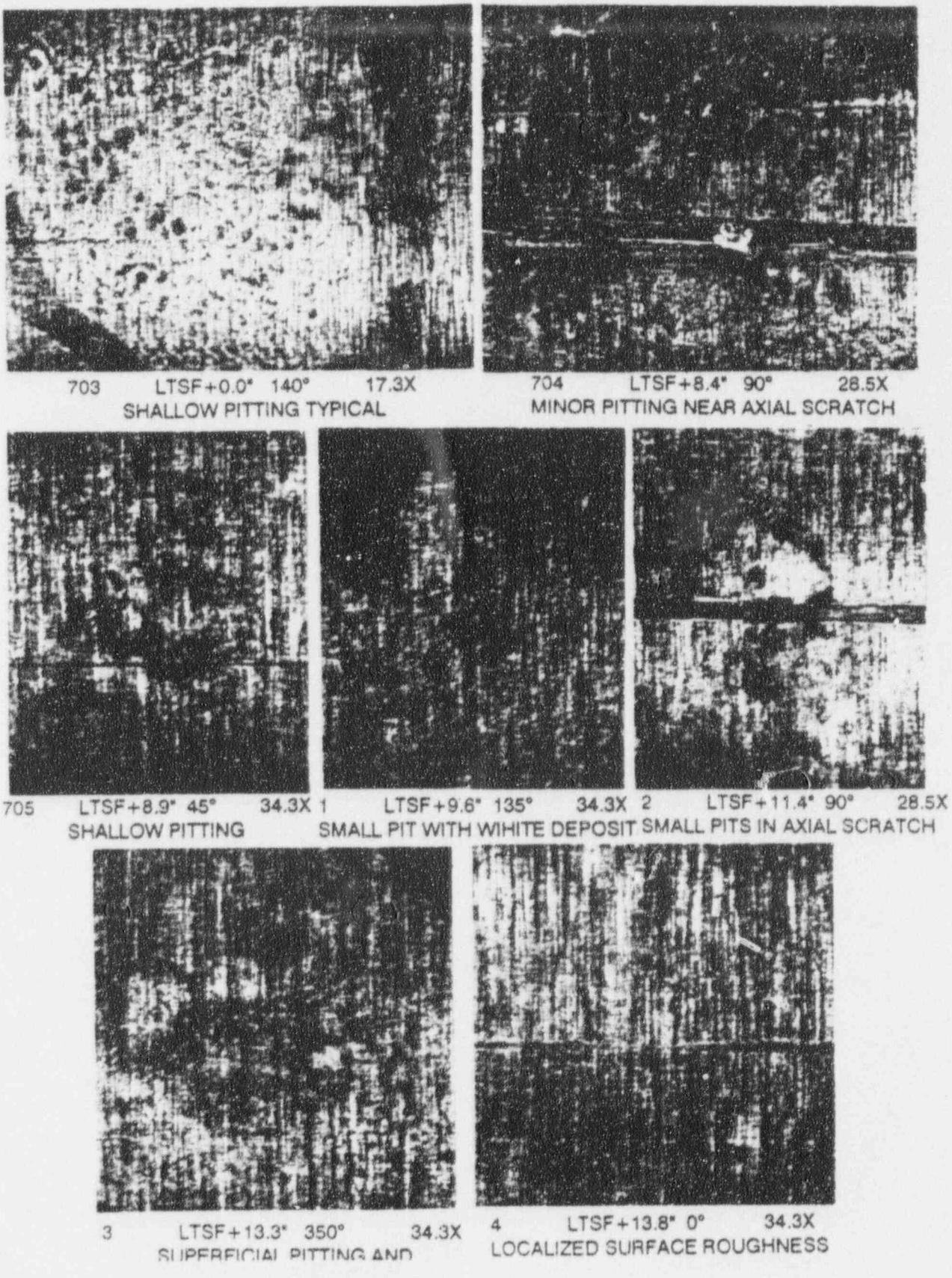

Figure 2-28: Liquid Penetrant Inspection (LPI) Results on Tube Section 97-91-2

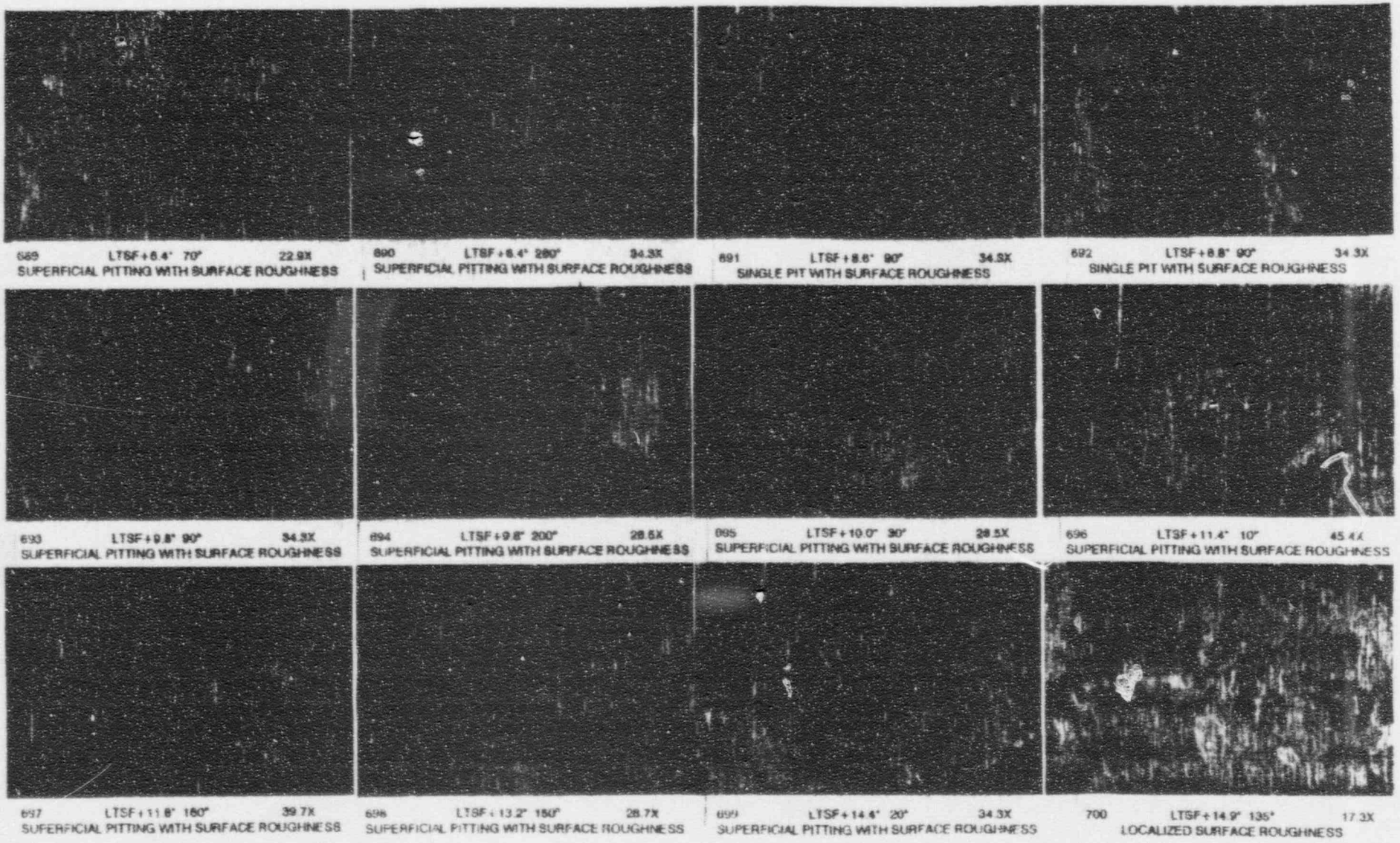

Figure 2-29: LPI Results on 106-32-2

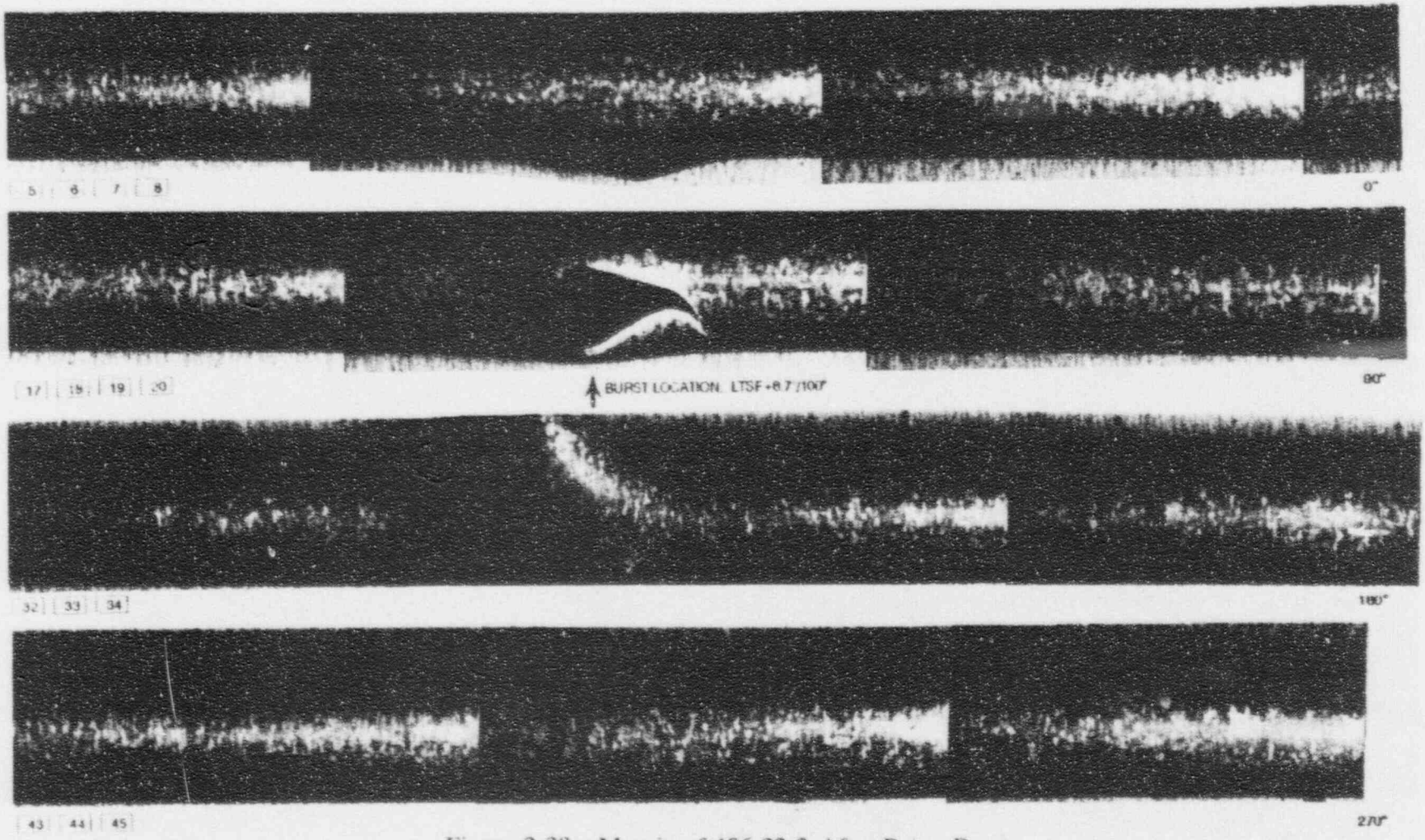

Figure 2-30: Mosaic of 106-32-2 After Being Burst

NOTE IGA PATCHES CONTAINED WITHIN
WHITE DEPOSIT STAINS (SURFACE
APPEARS SLIGHTLY ETCHED)
AFTER DESCALING AND AFTER BURST

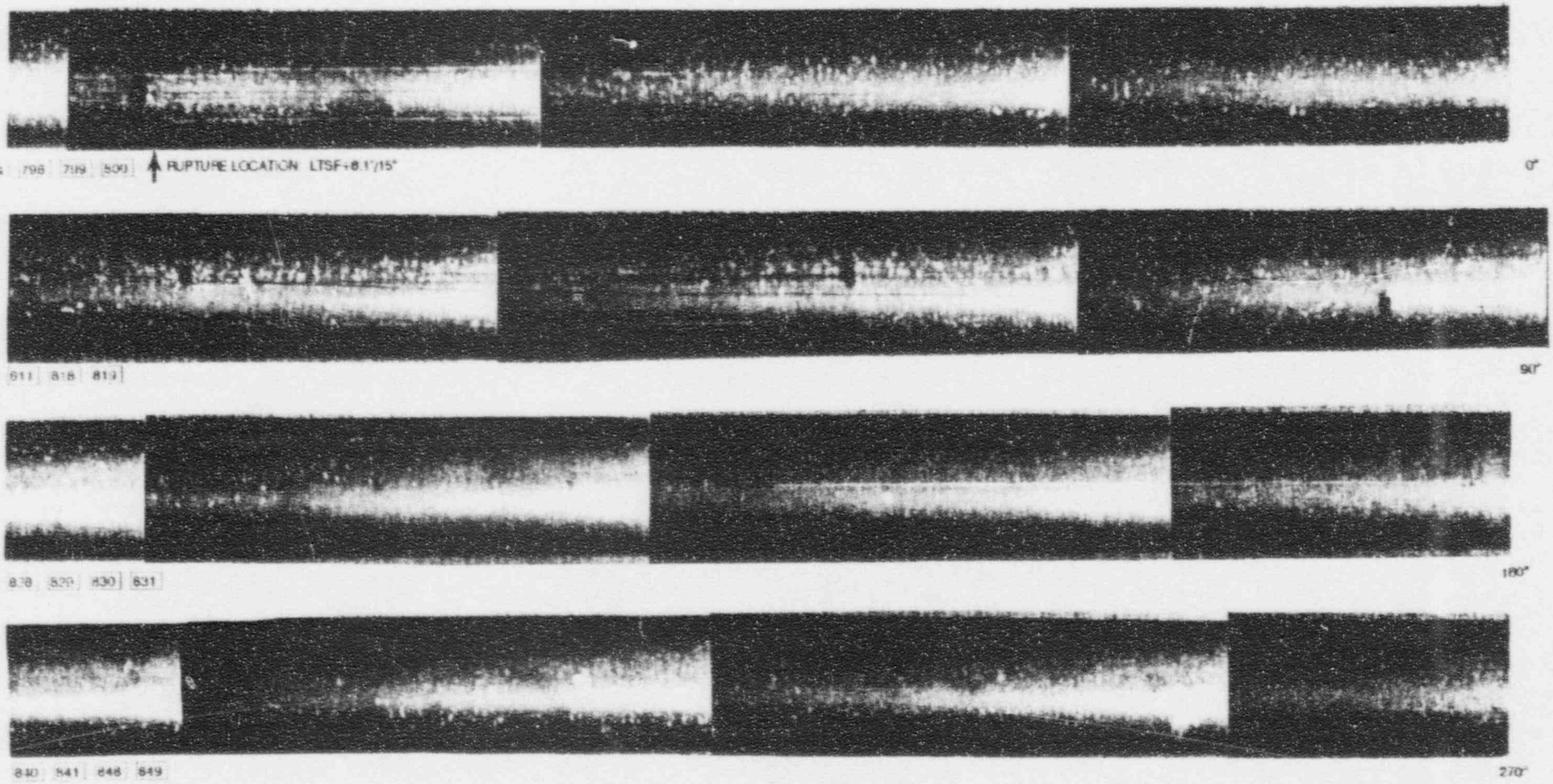

Figure 2-31: Mosaic of 97-91-2 After Being Burst

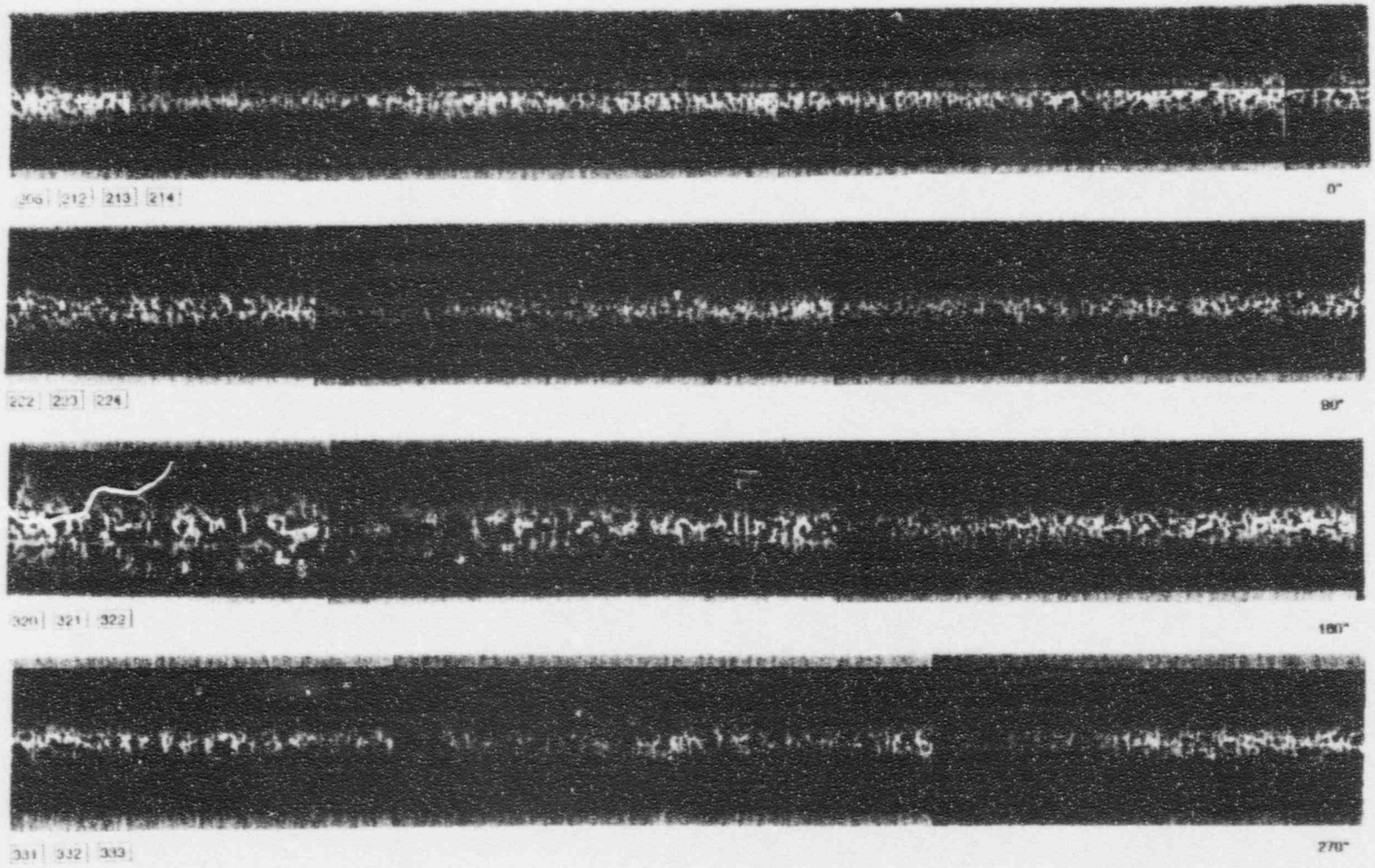

Figure 2-32: Mosaic of 52-51-2 After Swelling

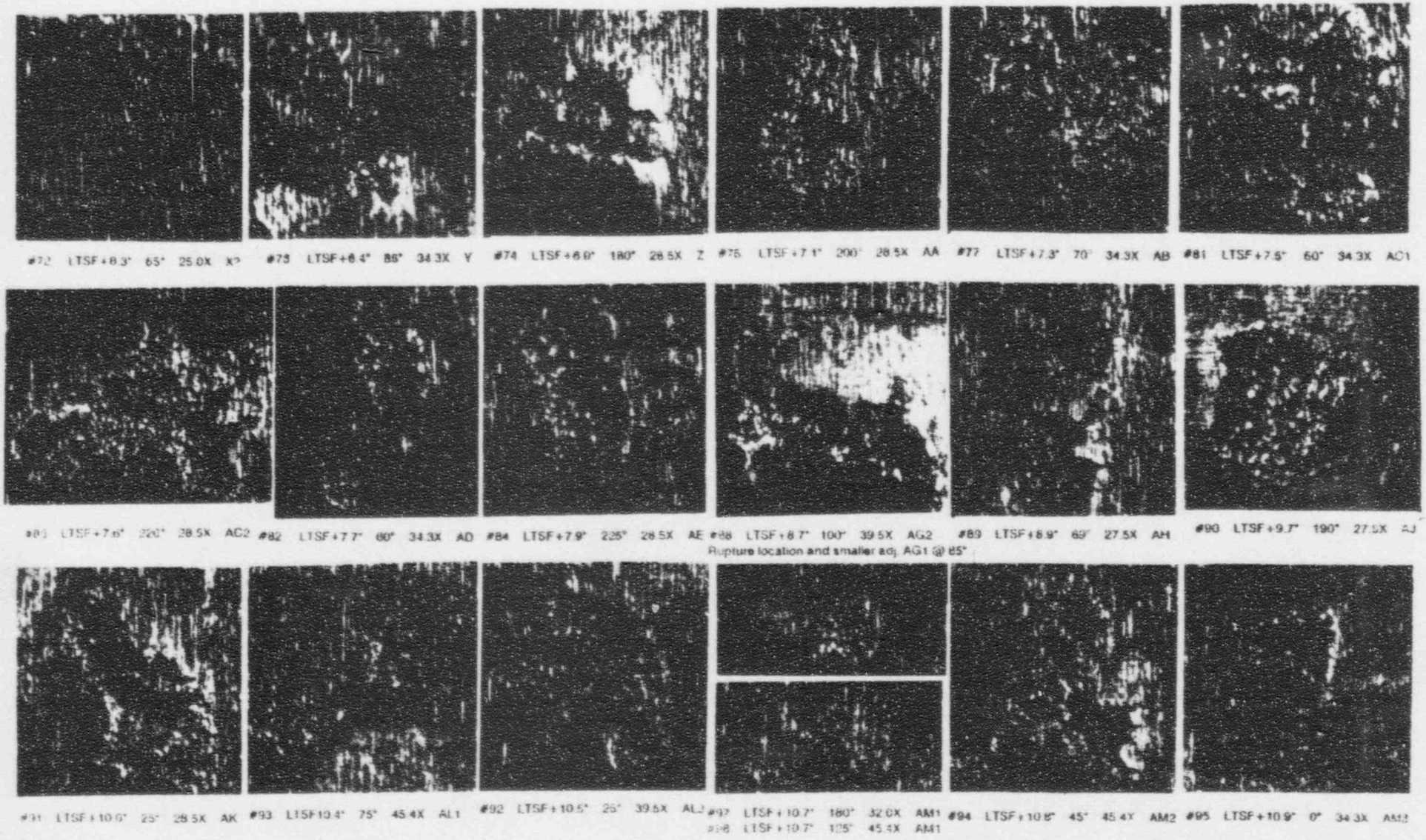

Figure 2-33: Stereovisual Result on 106-32-2 After Bursting

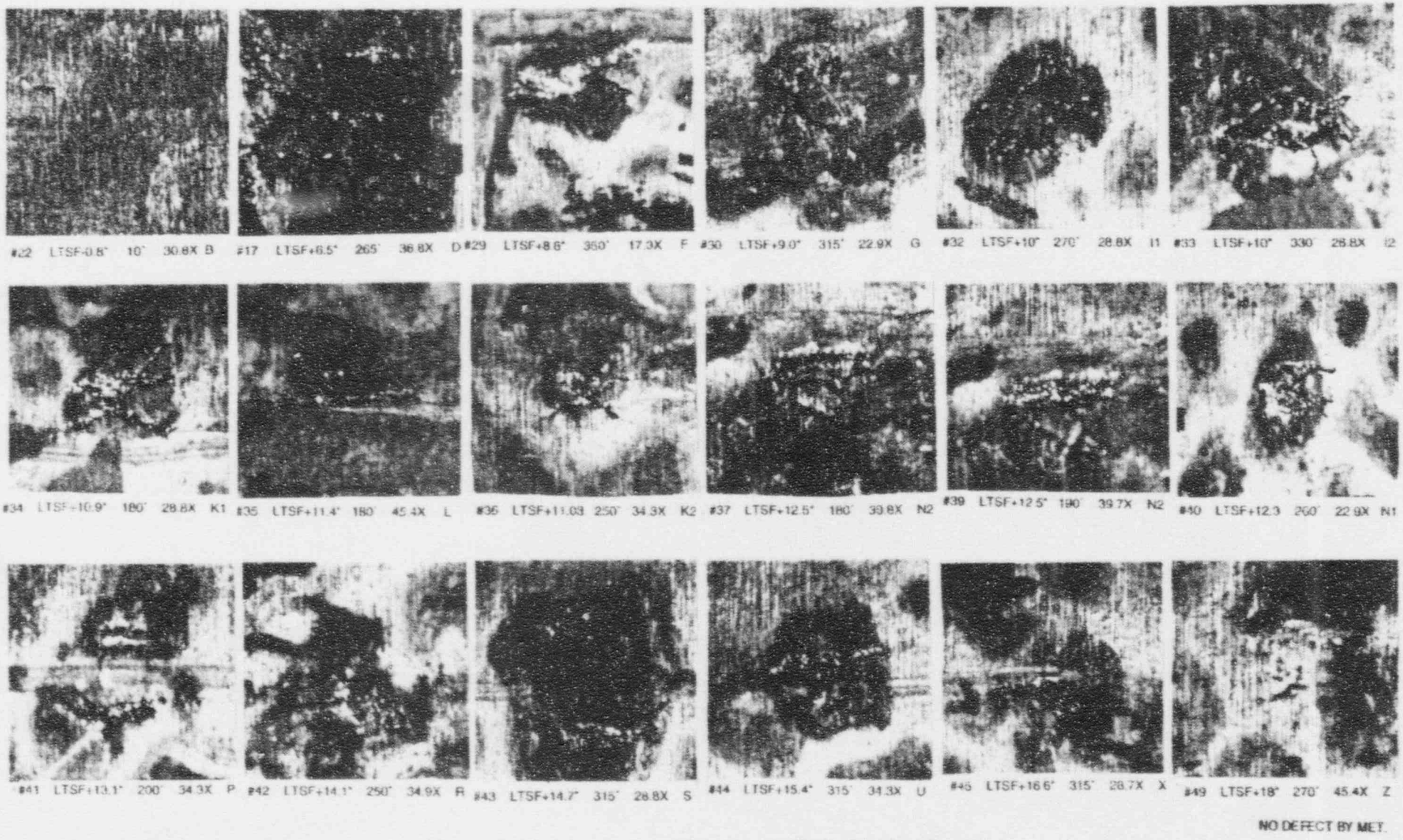

Figure 2-34: Stereovisual Result on 52-51-2 After Swelling

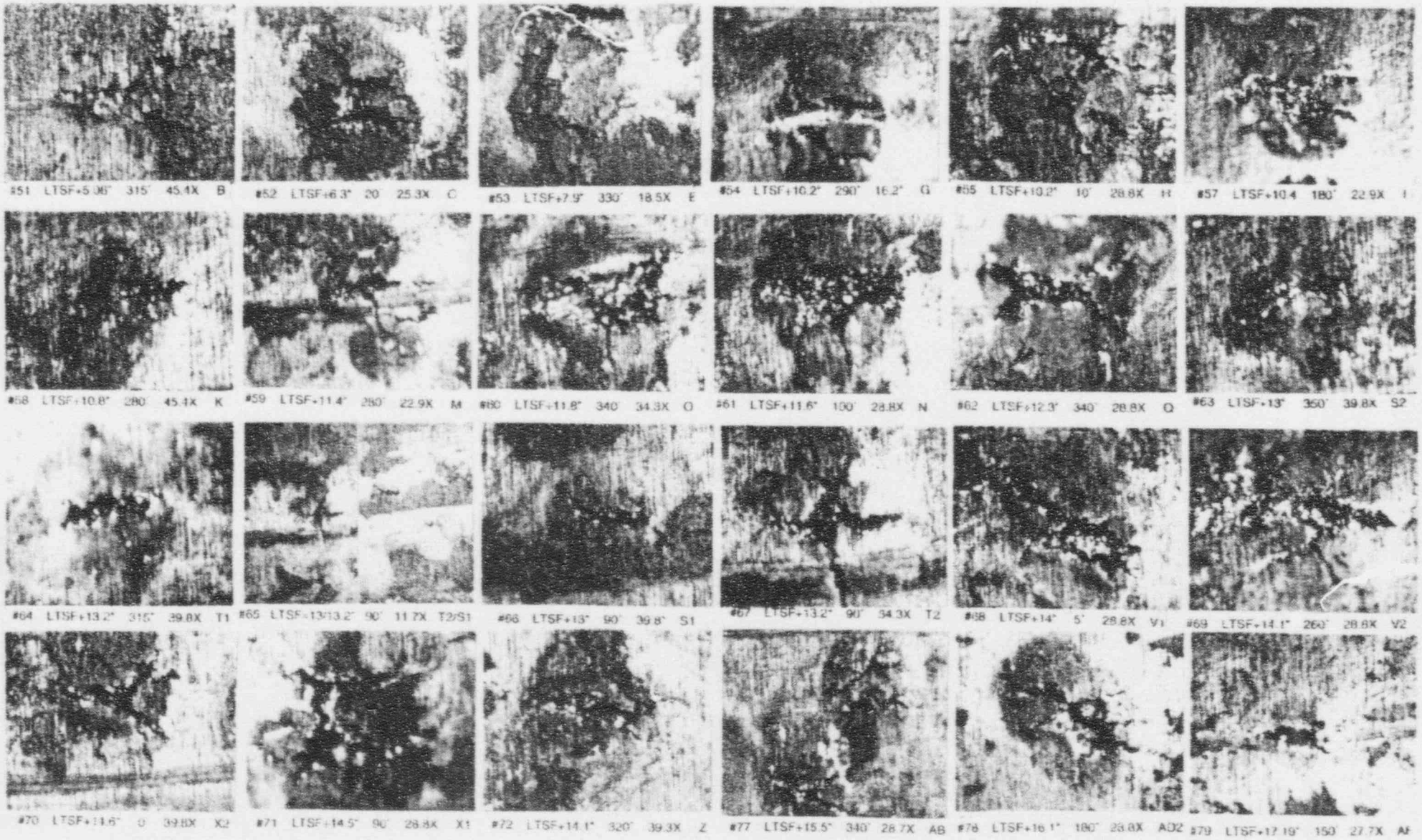

Figure 2-35: Stereovisual Result on 90-28-2 After Swelling

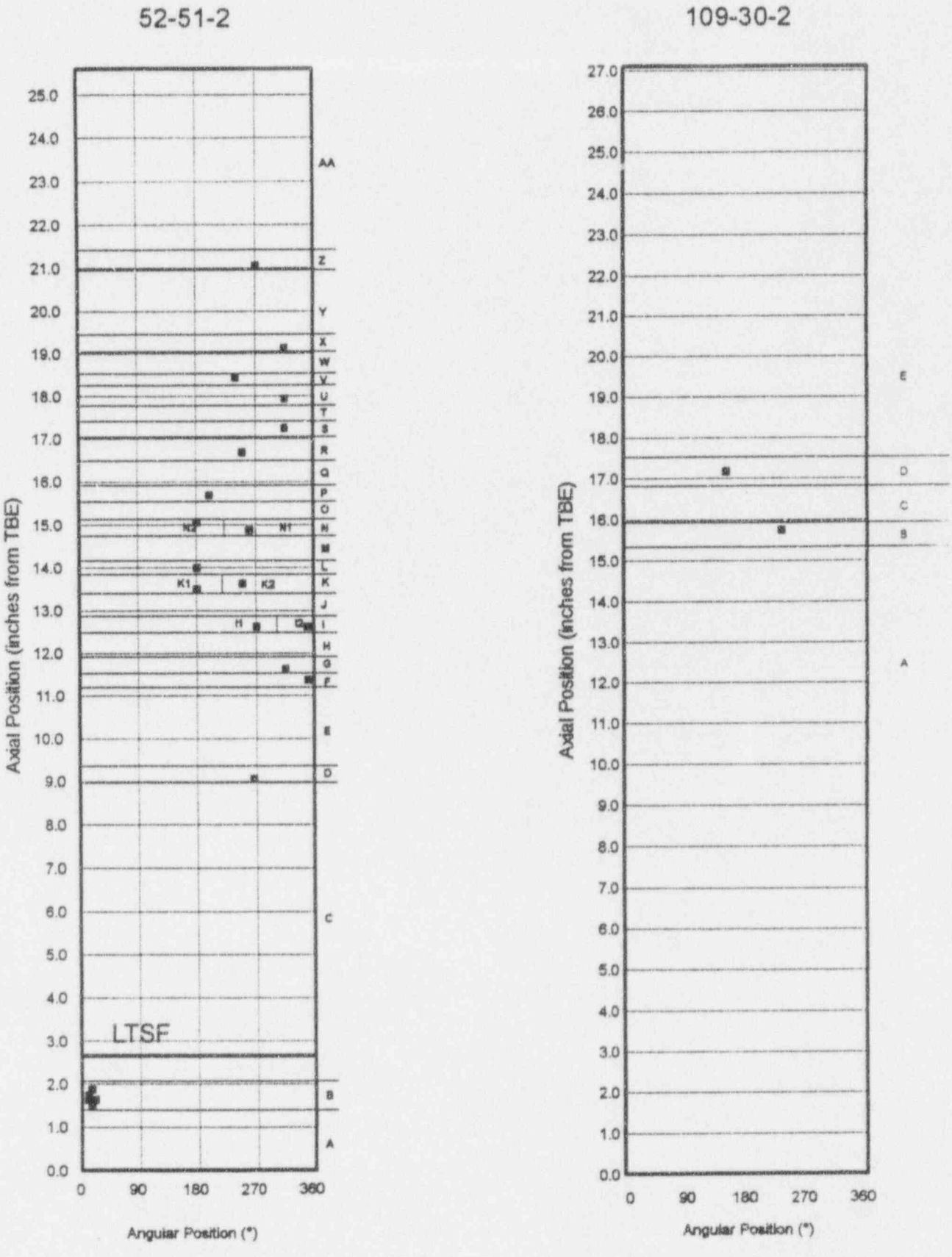

Figure 2-36: Sectioning Diagrams for 52-51-2 & 109-30-2

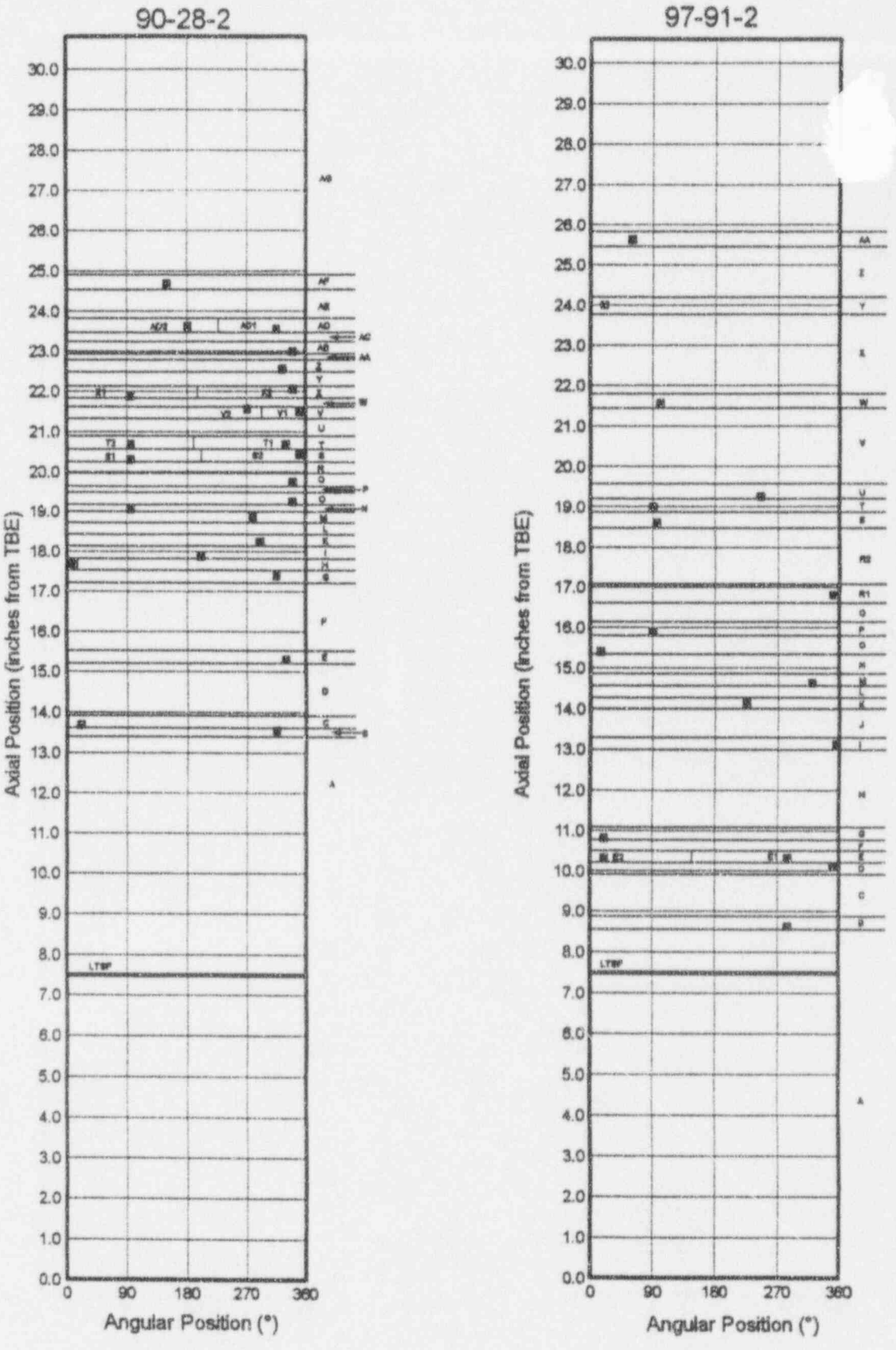

Figure 2-37: Sectioning Diagrams for 90-28-2 & 97-91-2

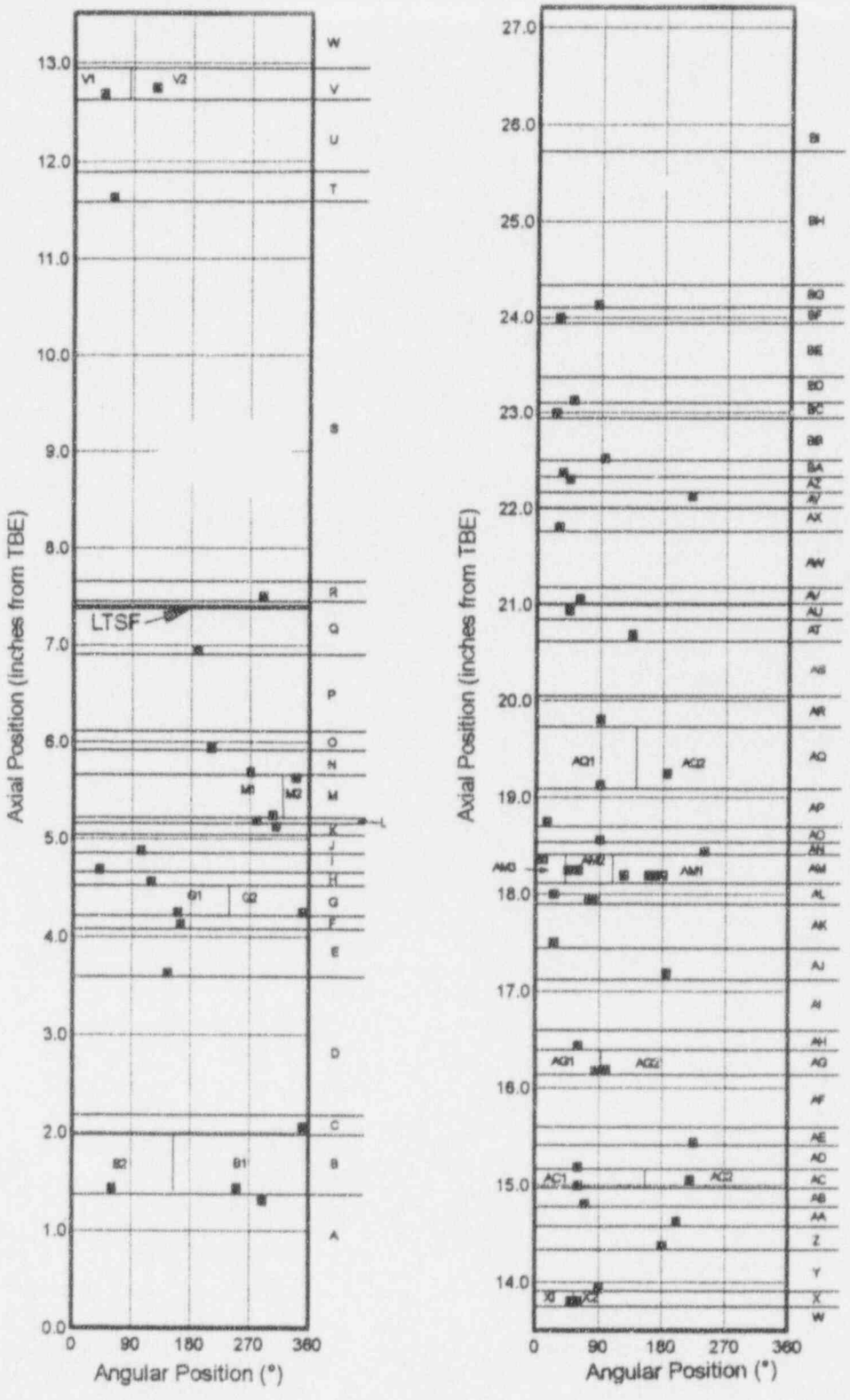

Figure 2-38: Sectioning Diagram for 106-32-2

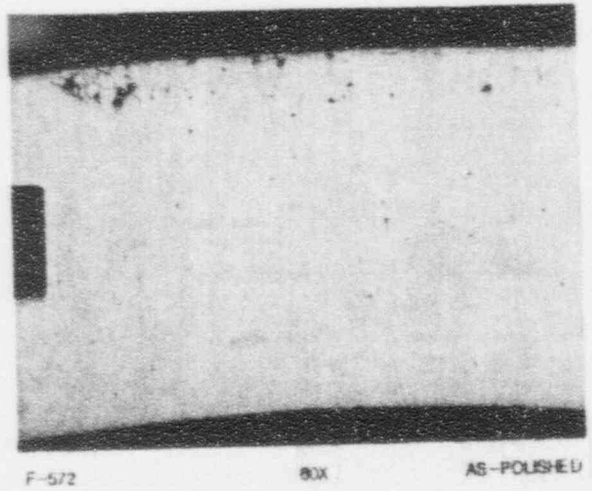

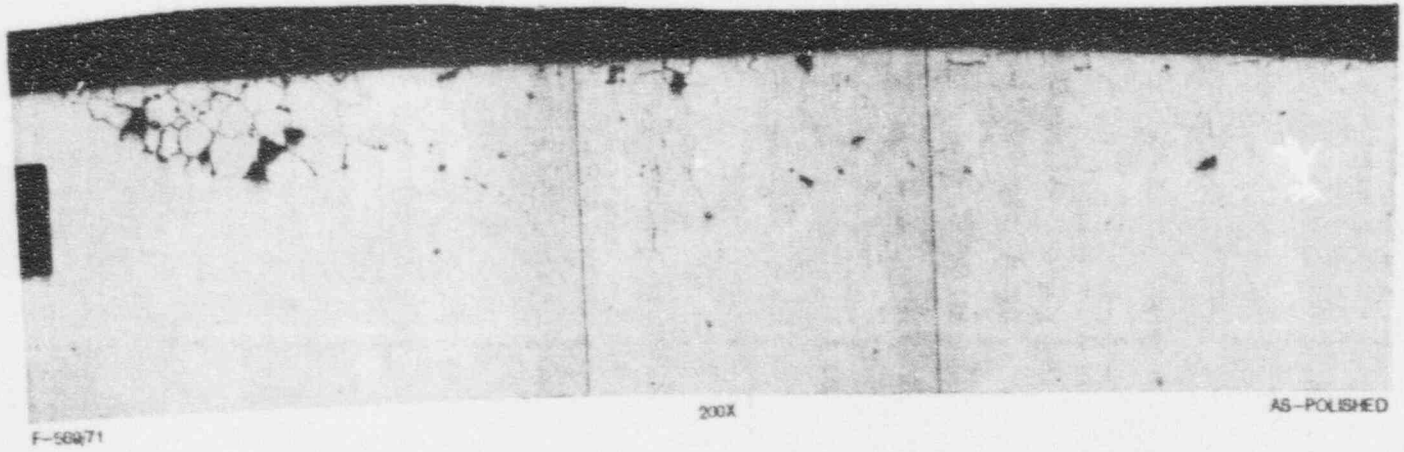

F-58971

Figure 2-39: Specimen 109-30-2D, 8th Grind, IGA Patch at 280°

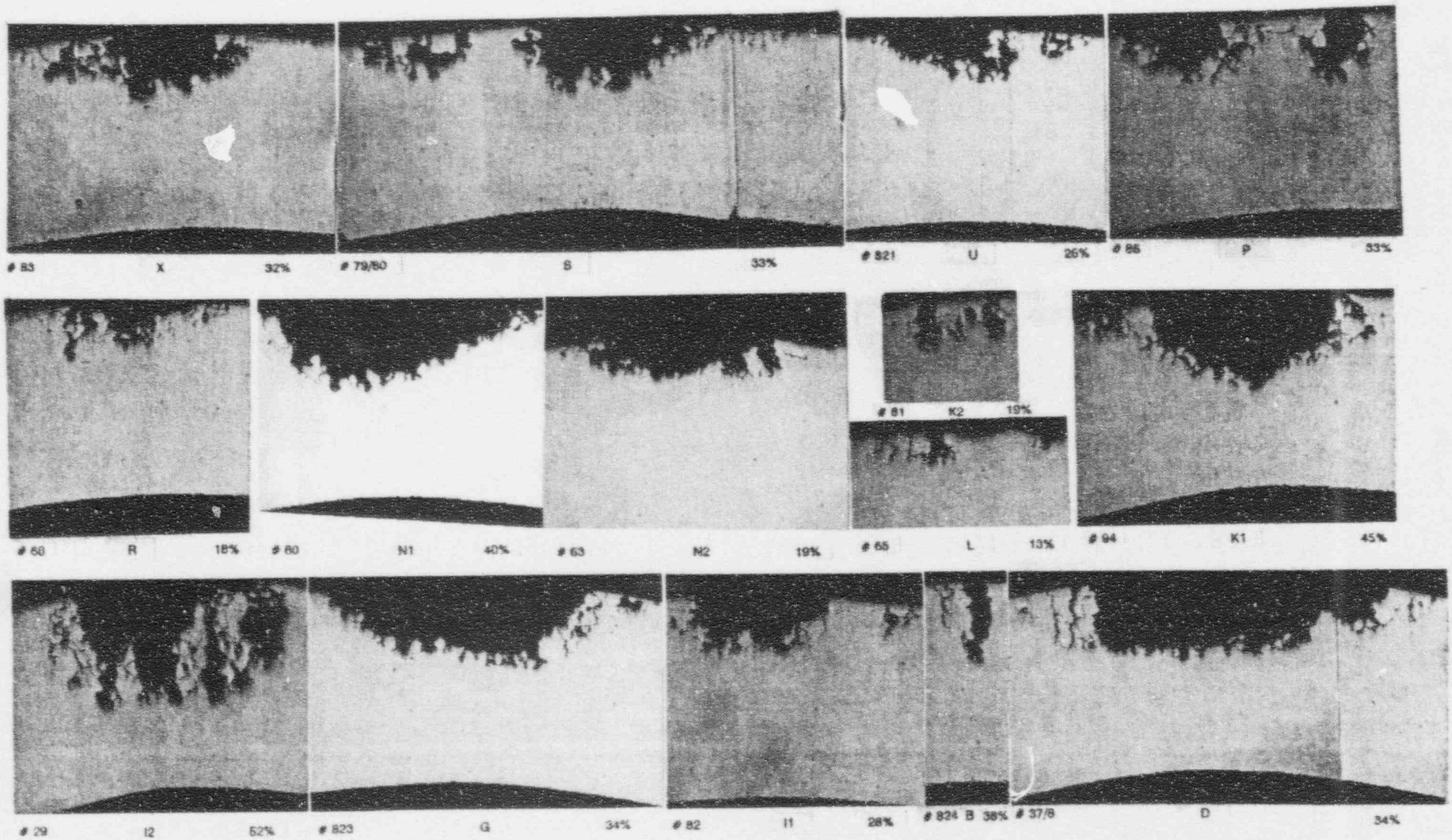

Figure 2-40: Metallography Results on 52-51-2 (63X)

NOTE IGA CONTAINED WITHIN STAIN AND ADJACENT CRACK

BSE IMAGE

BSE IMAGE

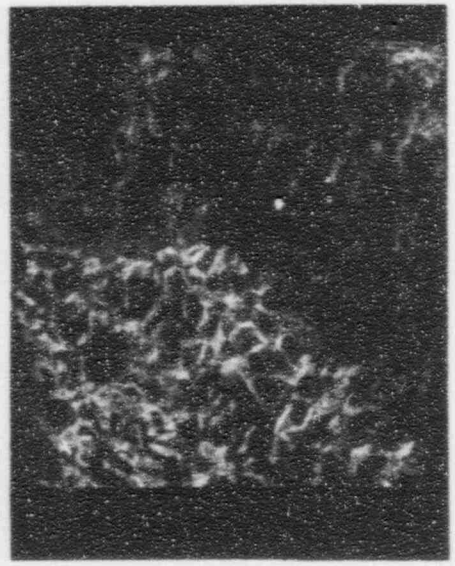

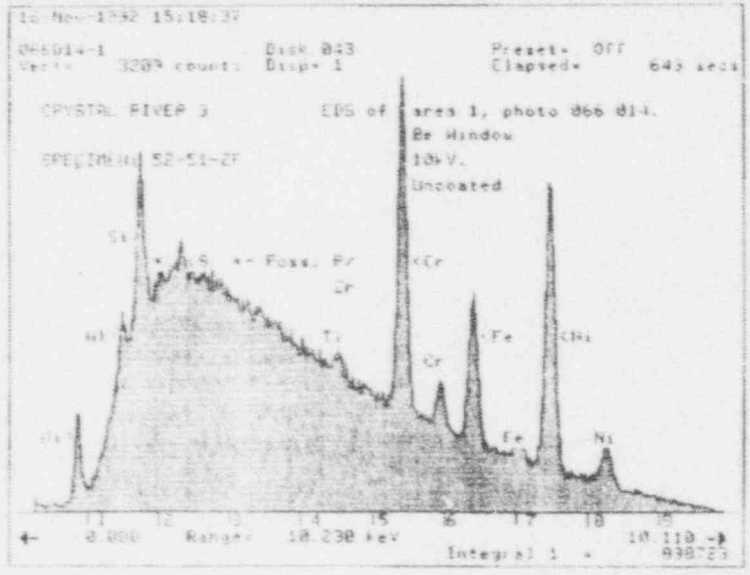

NOTE SI AND Al PEAKS ALSO LOW S PEAK

Figure 2-41: SEM/EDS Results on Specimen 52-51-2F (IGA Patch at LTSF+8.8" and 350°)

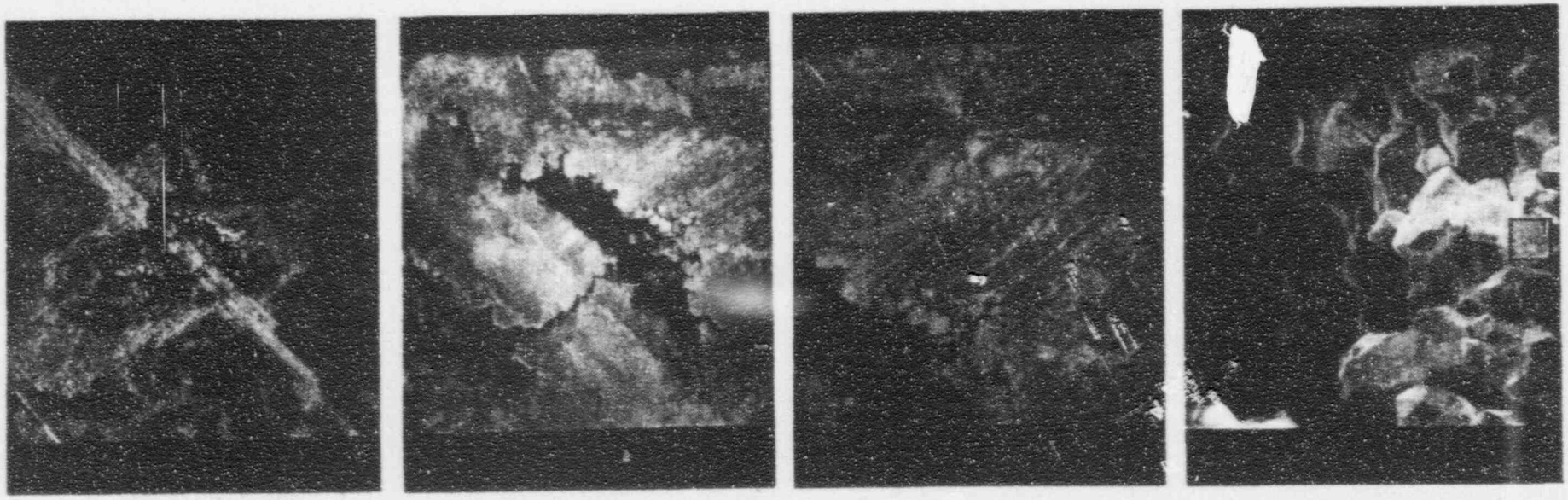

NOTE DARK STAINS SURROUNDING IGA AND ADJACENT SCRATCH

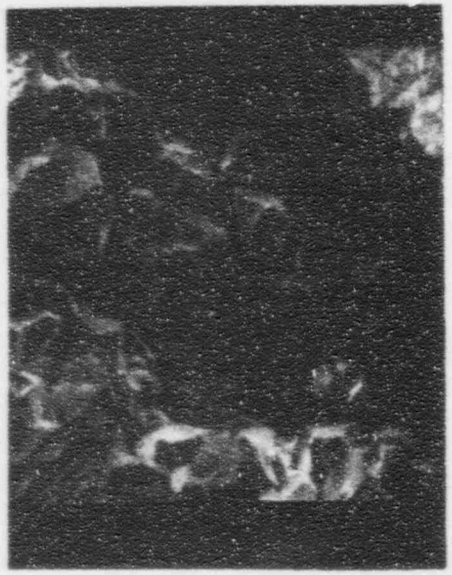

NOTE HIGH S IN GRAIN BOUNDARY CORRSION FILM

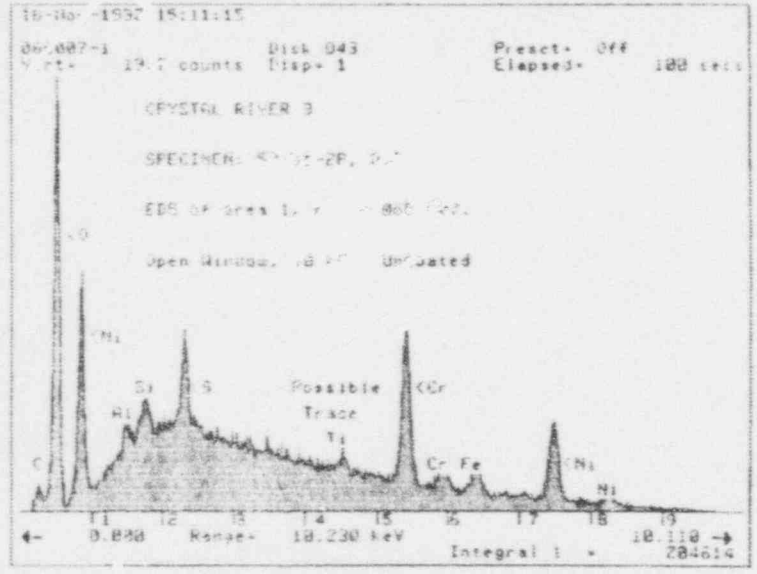

Figure 2-42: SEM/EDS Results on Specimen 52-51-2P
(IGA Patch at LTSF+13.1" and 200°)

NOTE STAINS

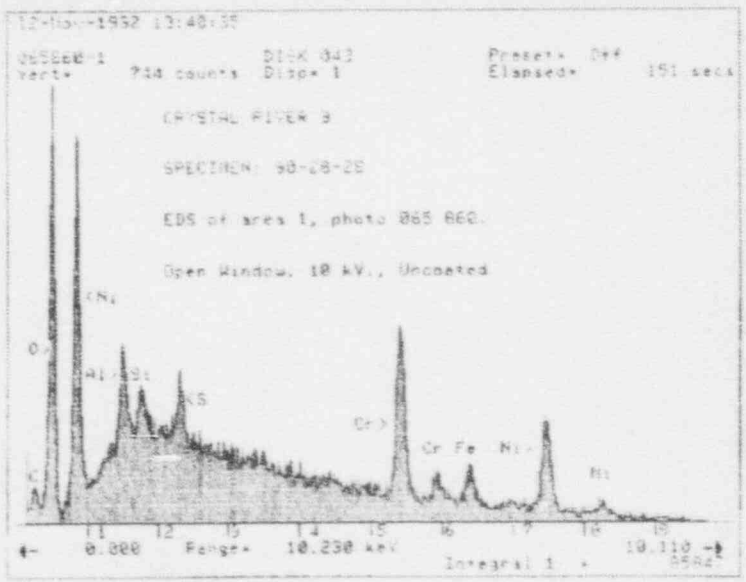

NOTE GRAIN BOUNDARY CORROSION FILM AND SULFUR INDICATIONS

Figure 2-43: SEM/EDS Results on Specimen 90-28-2B (IGA Patch at LTSF+5.1" and 315°)

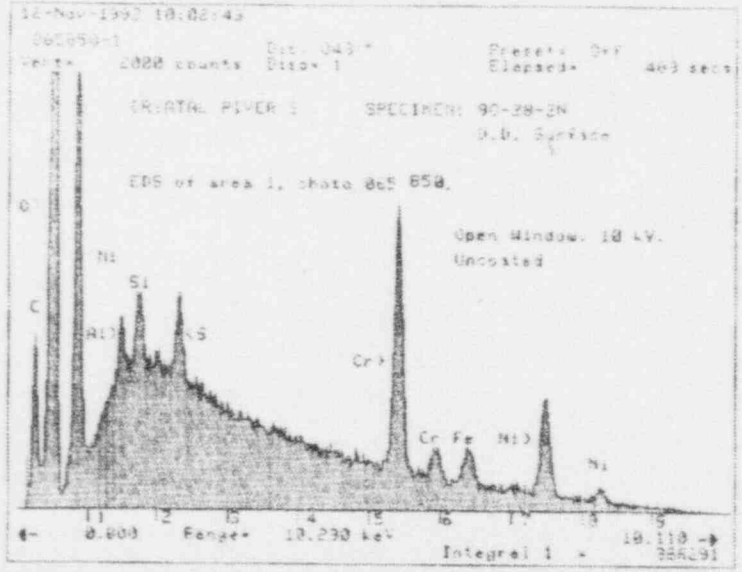

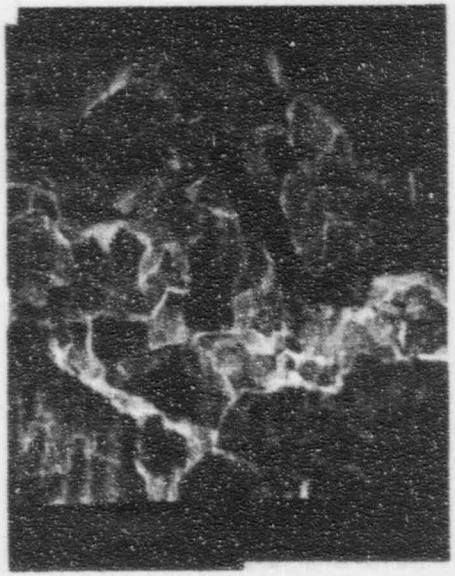

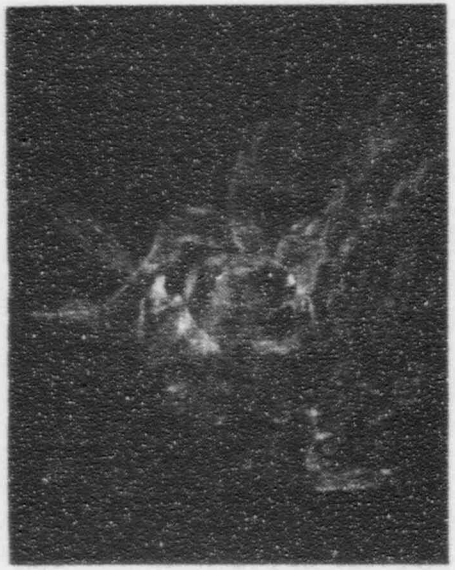

NOTE GRAIN BOUNDARY CORROSION FILM AND SULFUR INDICATIONS ABOVE

Figure 2-44: SEM/EDS Results on Specimen 90-28-2N (IGA Patch at LTSF+11.6" and 100°)

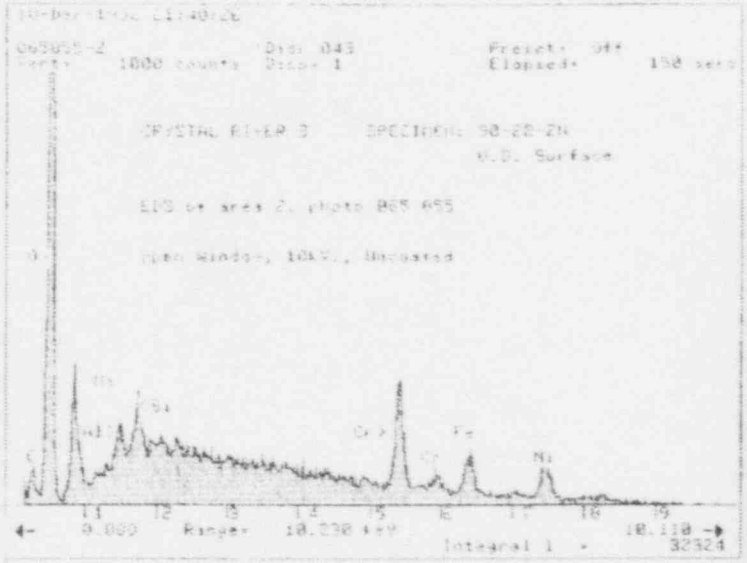

[2] INNER PORTION ON STAIN
SOME Si AND Al; SLIGHTLY Cr-RICH

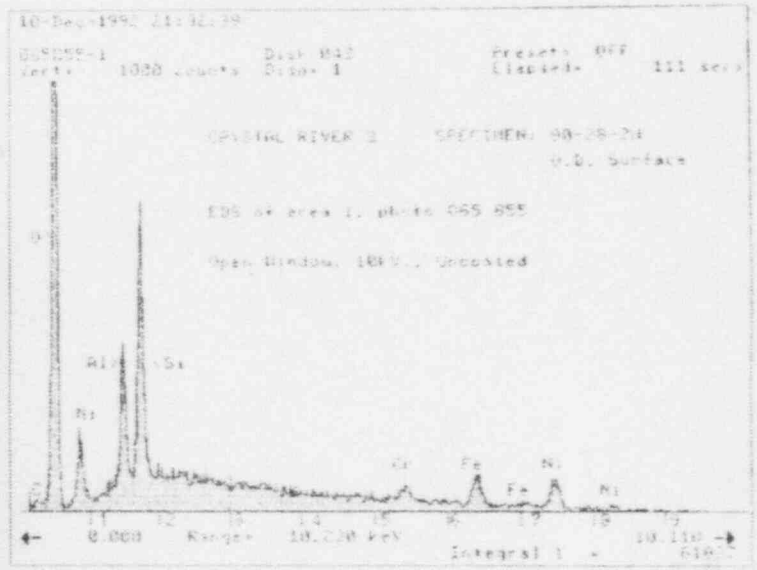

[1] OUTER RING HIGH Si AND Al

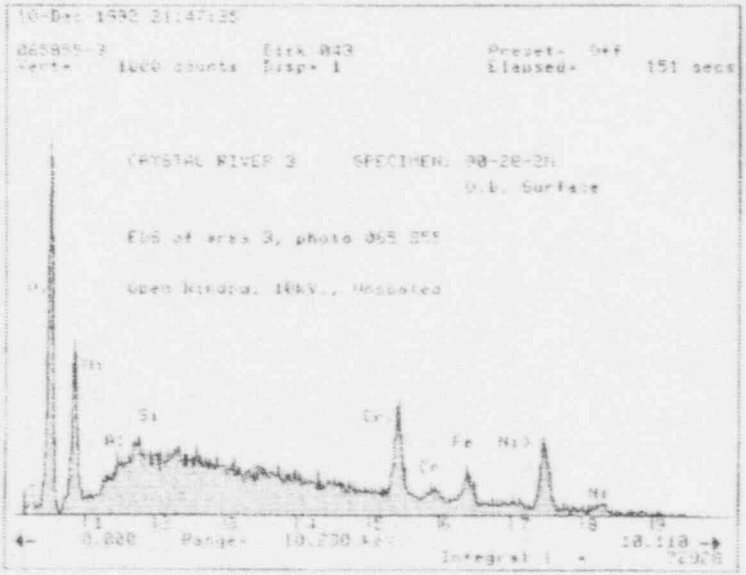

[3] "CLEAN" TUBE OD SURFACE
LOW Si AND Al; Ni/Cr/Fe RATIO
ABOUT SAME, BUT LOWER O

Figure 2-45: SEM/EDS Results on Specimen 90-28-2N
OD Tube Surface

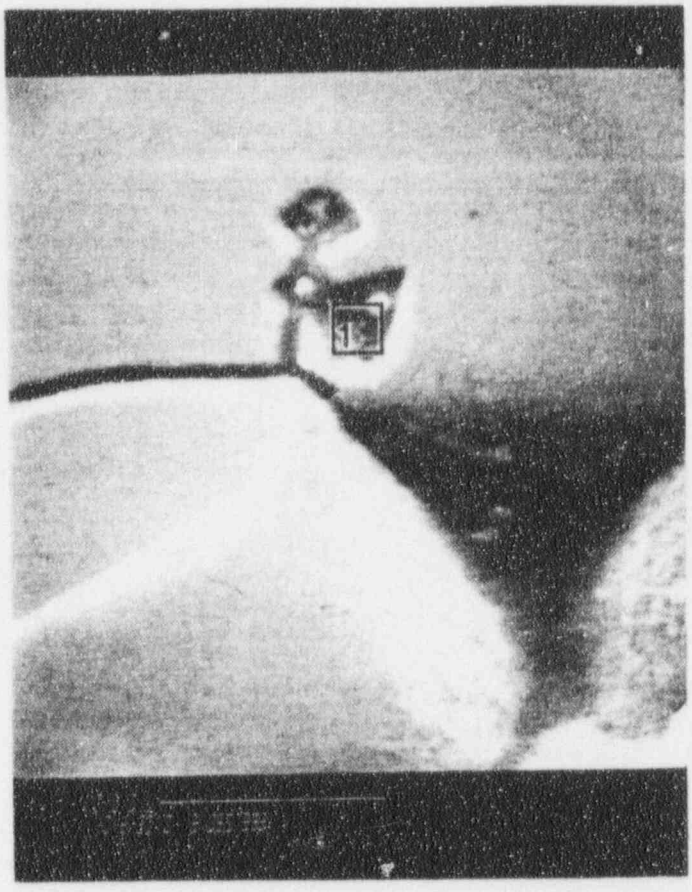

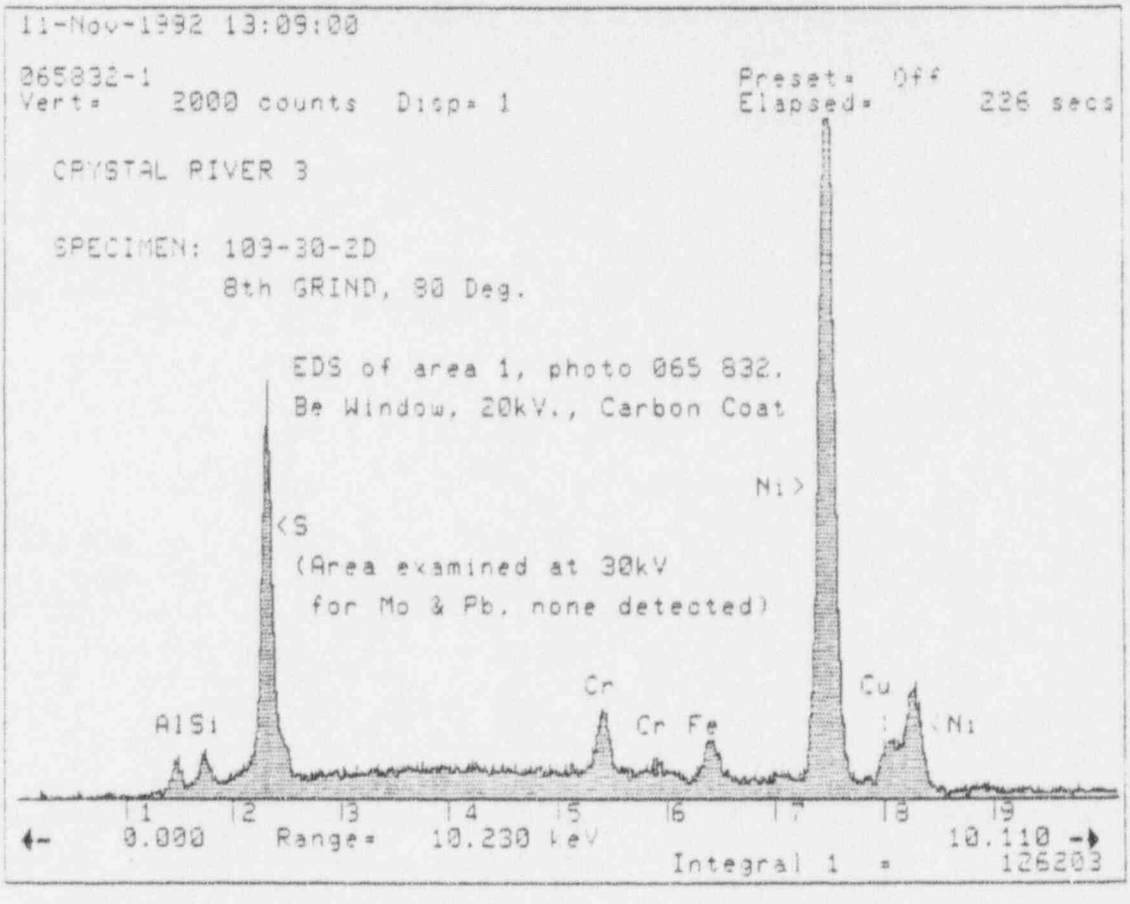

Figure 2-46: SEM/EDS Results on Specimen 109-30-2B, 10th Grind, 270° IGA Patch
(Note high sulfur peak in corrosion product at grain boundary)

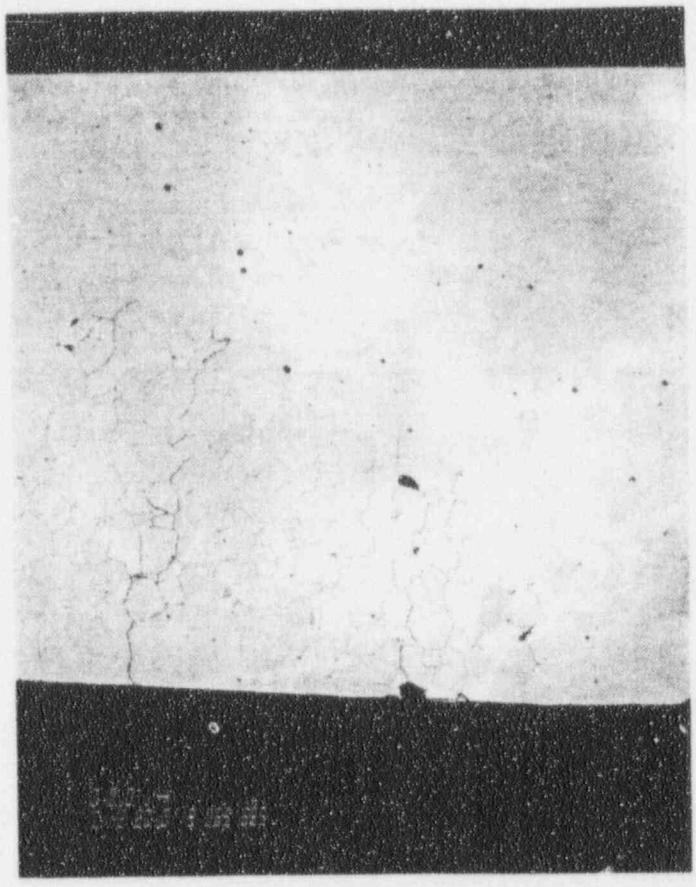

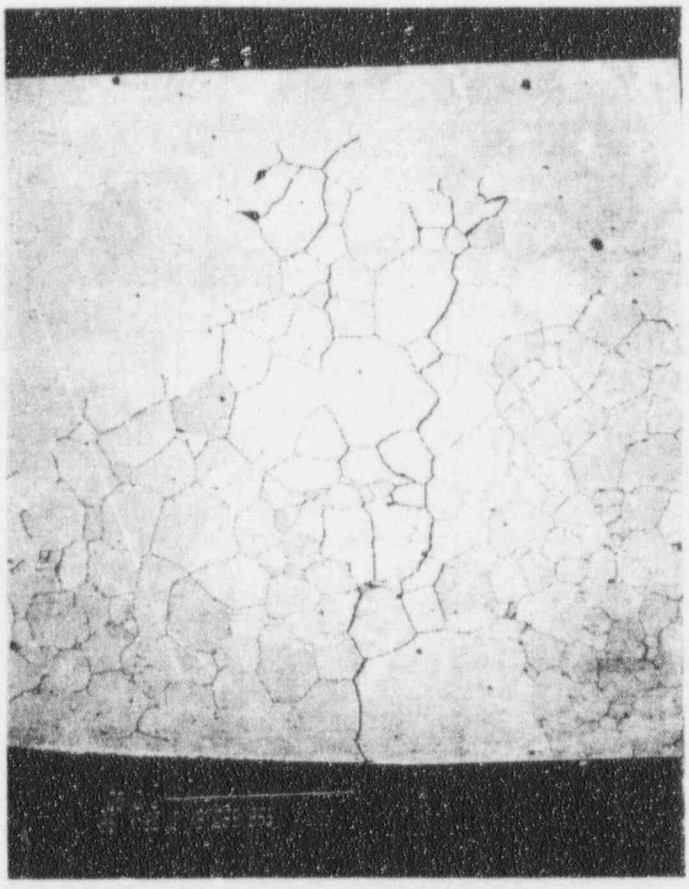

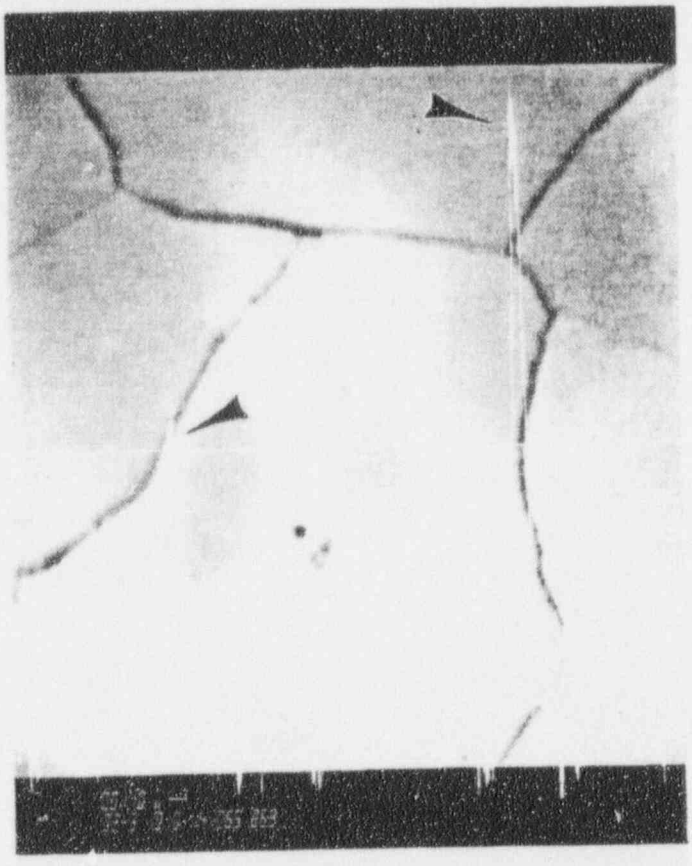

SULFUR LINE SCAN

Figure 2-47: SEM/EDS Results on Specimen 109-30-2B, 8th Grind, 80° IGA Patch
(Note sulfur enrichment at grain boundaries)

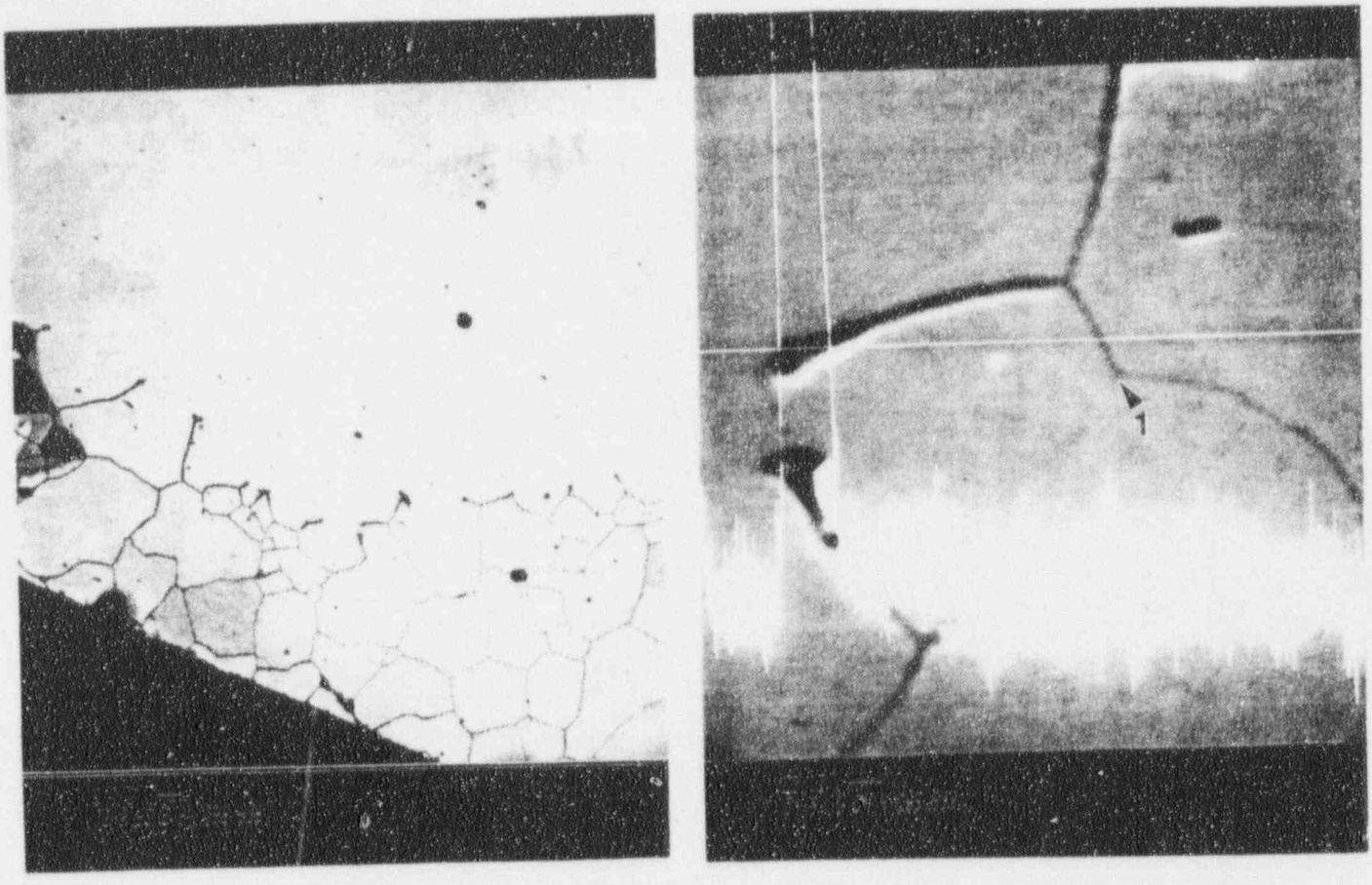

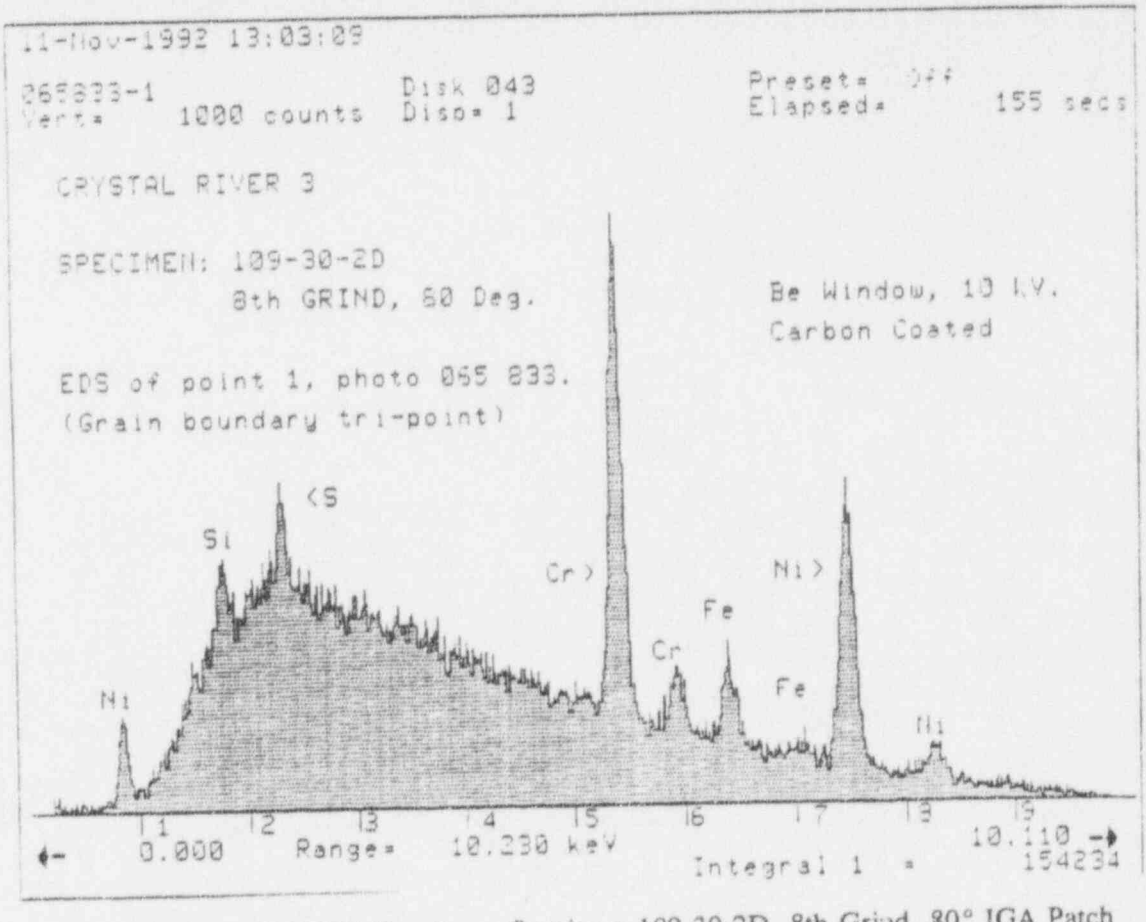

Figure 2-48: SEM/EDS Results on Specimen 109-30-2D, 8th Grind, 80° IGA Patch (Note indications of sulfur at grain boundaries)

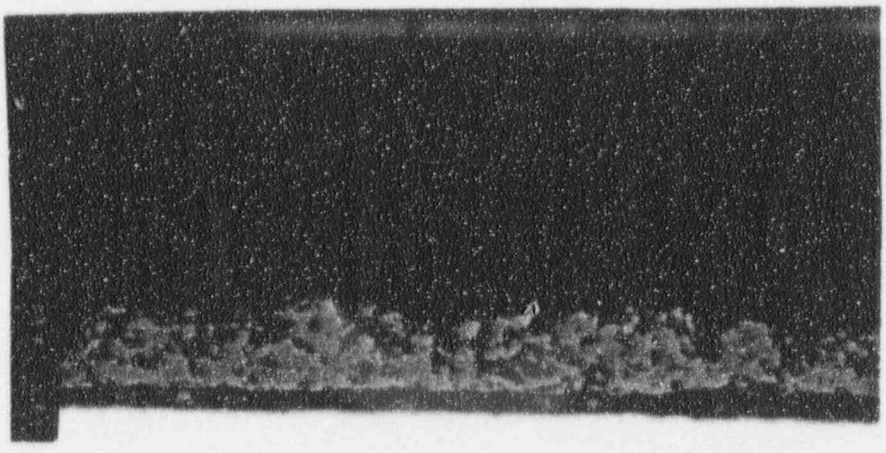

90-28-5b

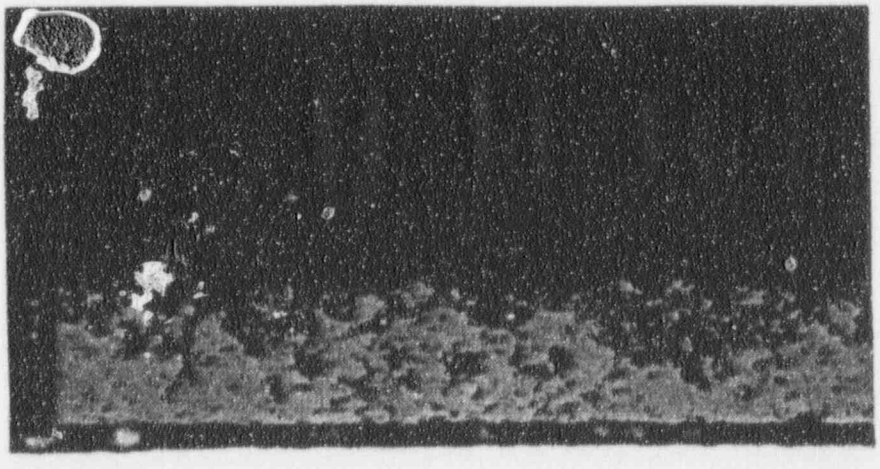

52-51-4b

Figure 2-49: Typical Deposit Cross Sections (630X)

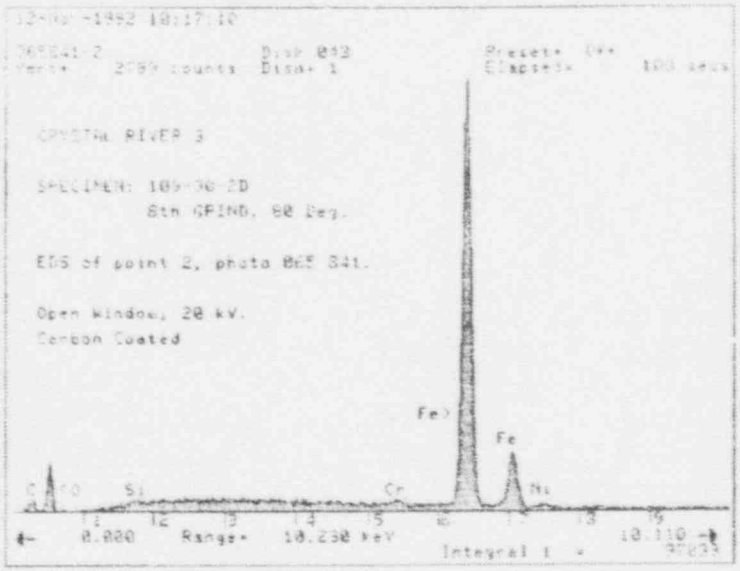

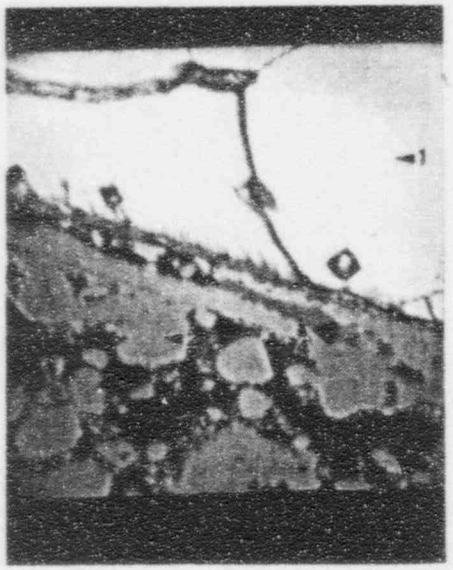

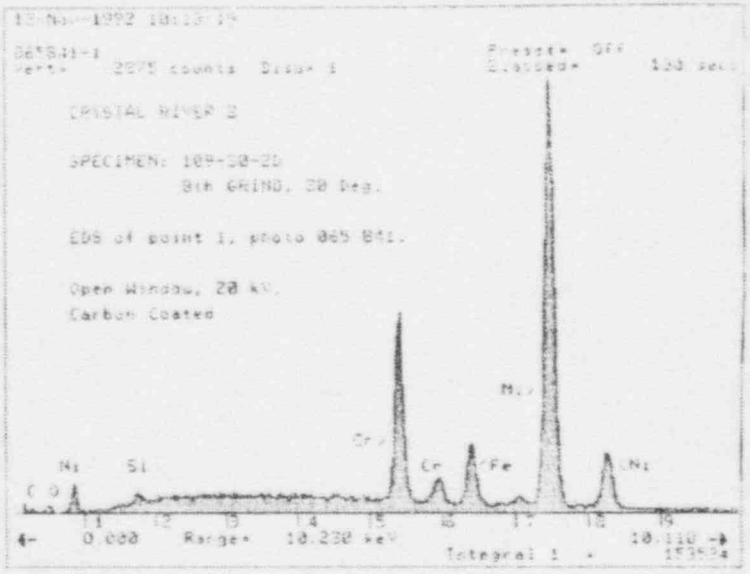

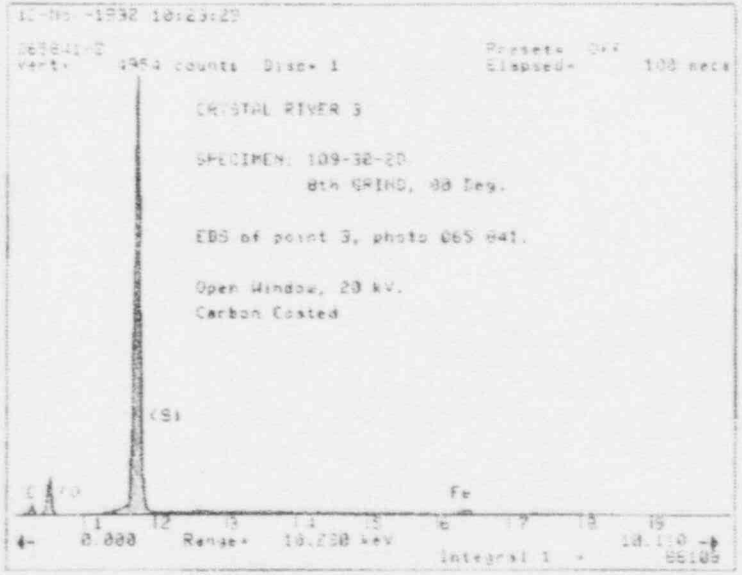

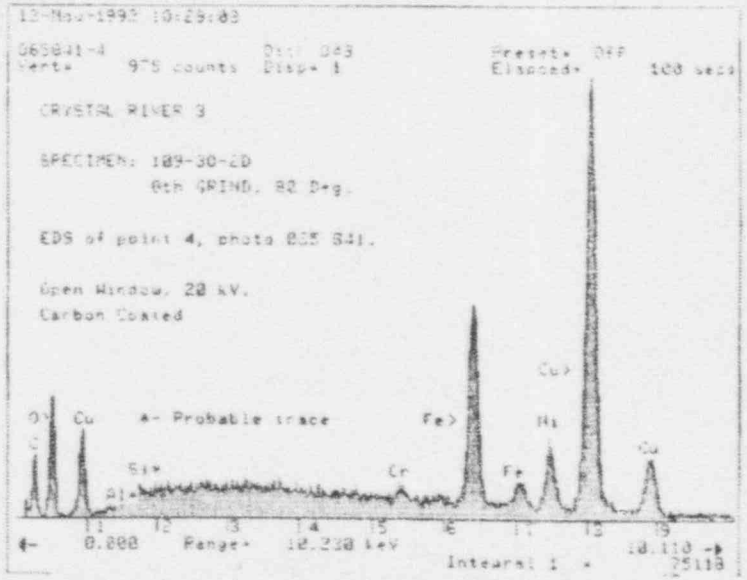

Figure 2-50: SEM/EDS Results on Specimen 109-30-2D, 8th Grind, 80° IGA Patch

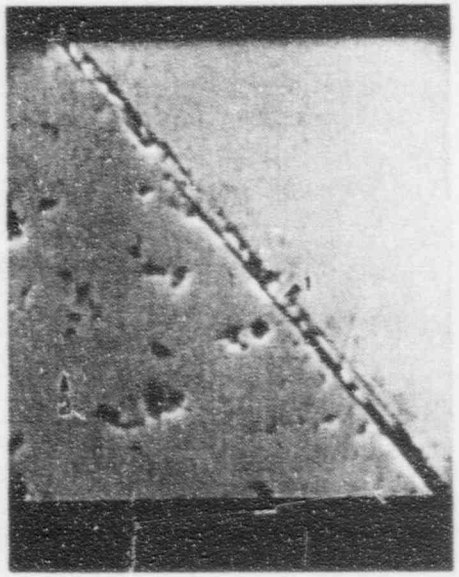

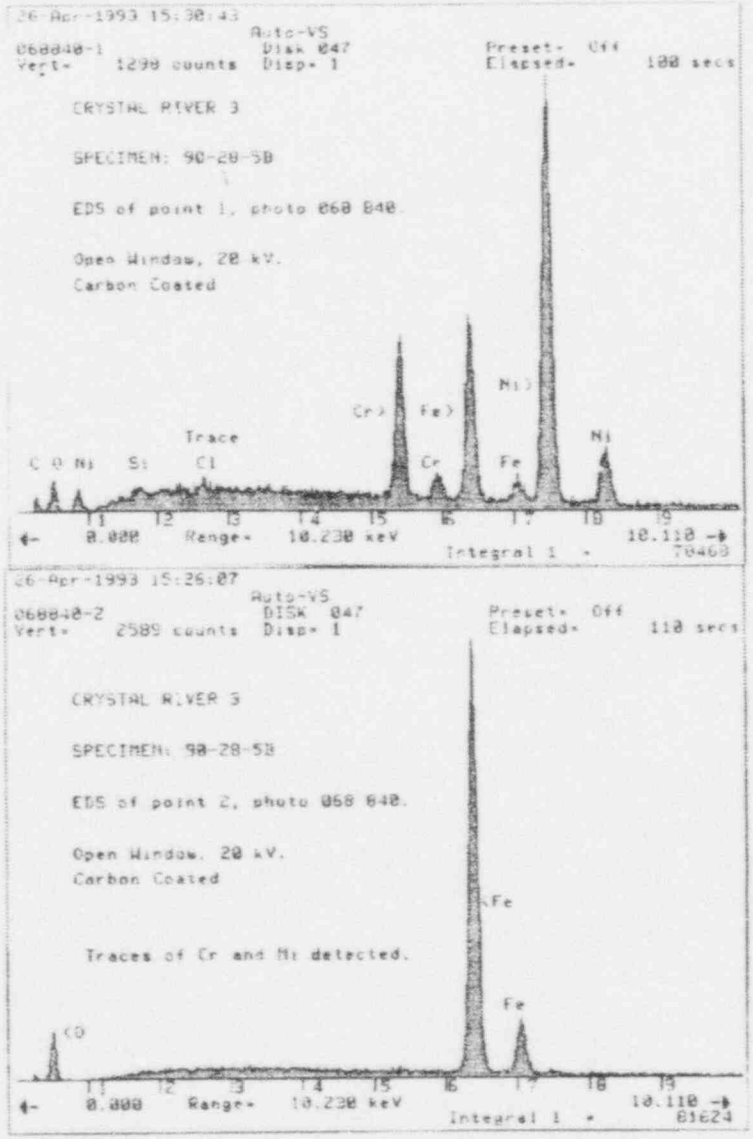

Figure 2-51: SEM/EDS Results on Specimen 90-28-5, 2nd Span
Note: Enriched Ni & Cr Levels immediately adjacent to Tube OD Surface

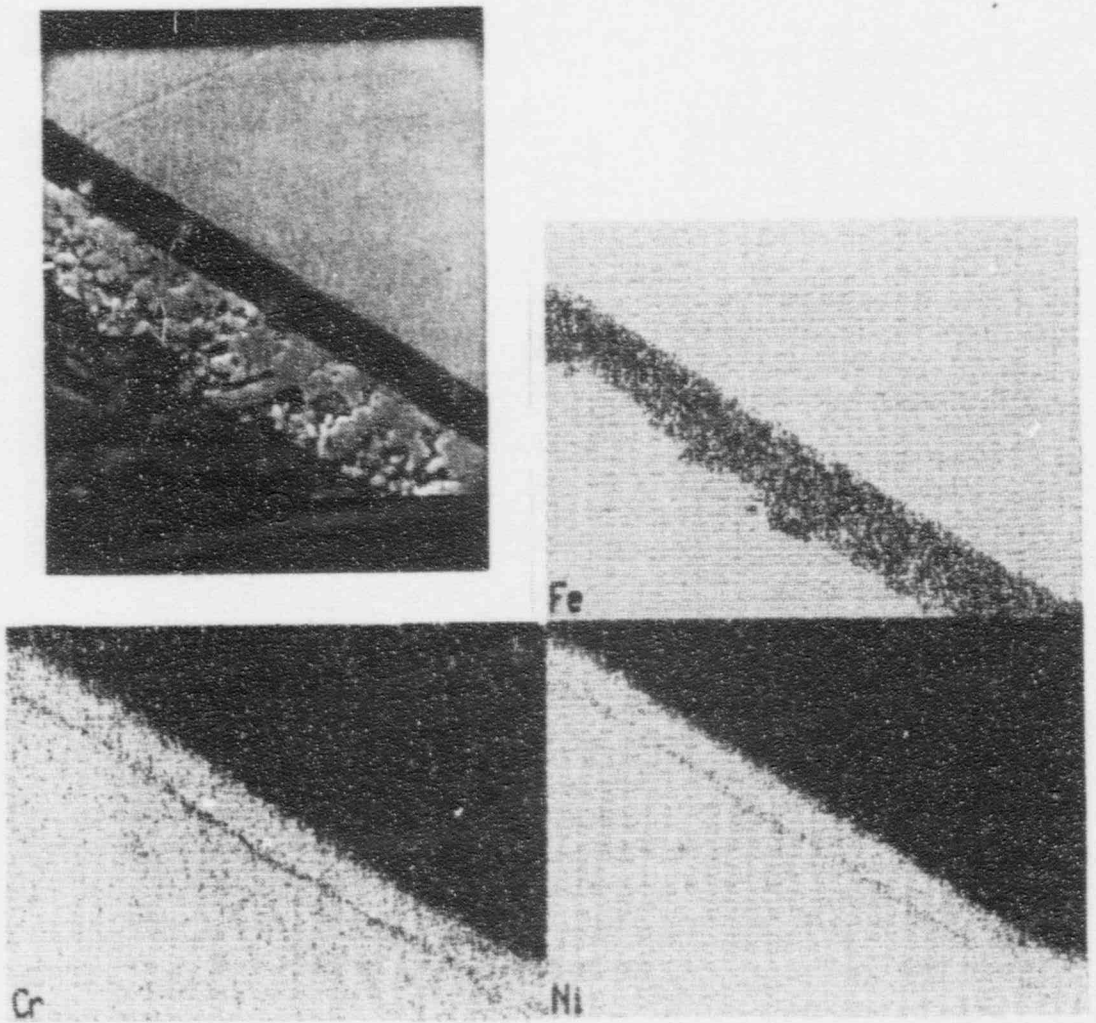

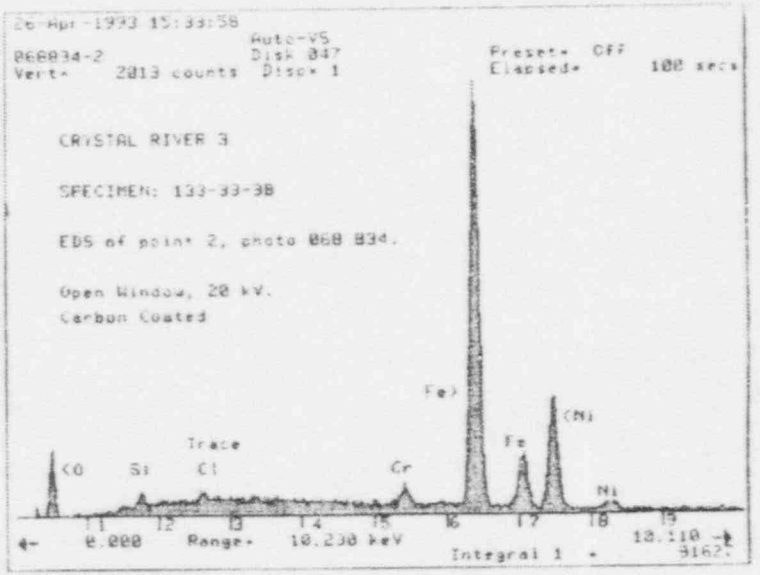

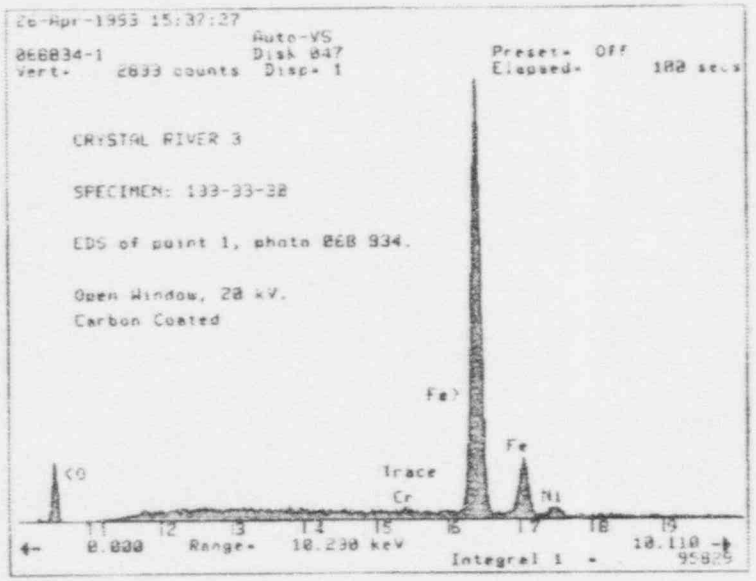

Figure 2-52: SEM/EDS Results on Specimen 133-33-3B, 1st Span
Note: Enriched Ni & Cr Levels immediately adjacent to Tube OD Surface

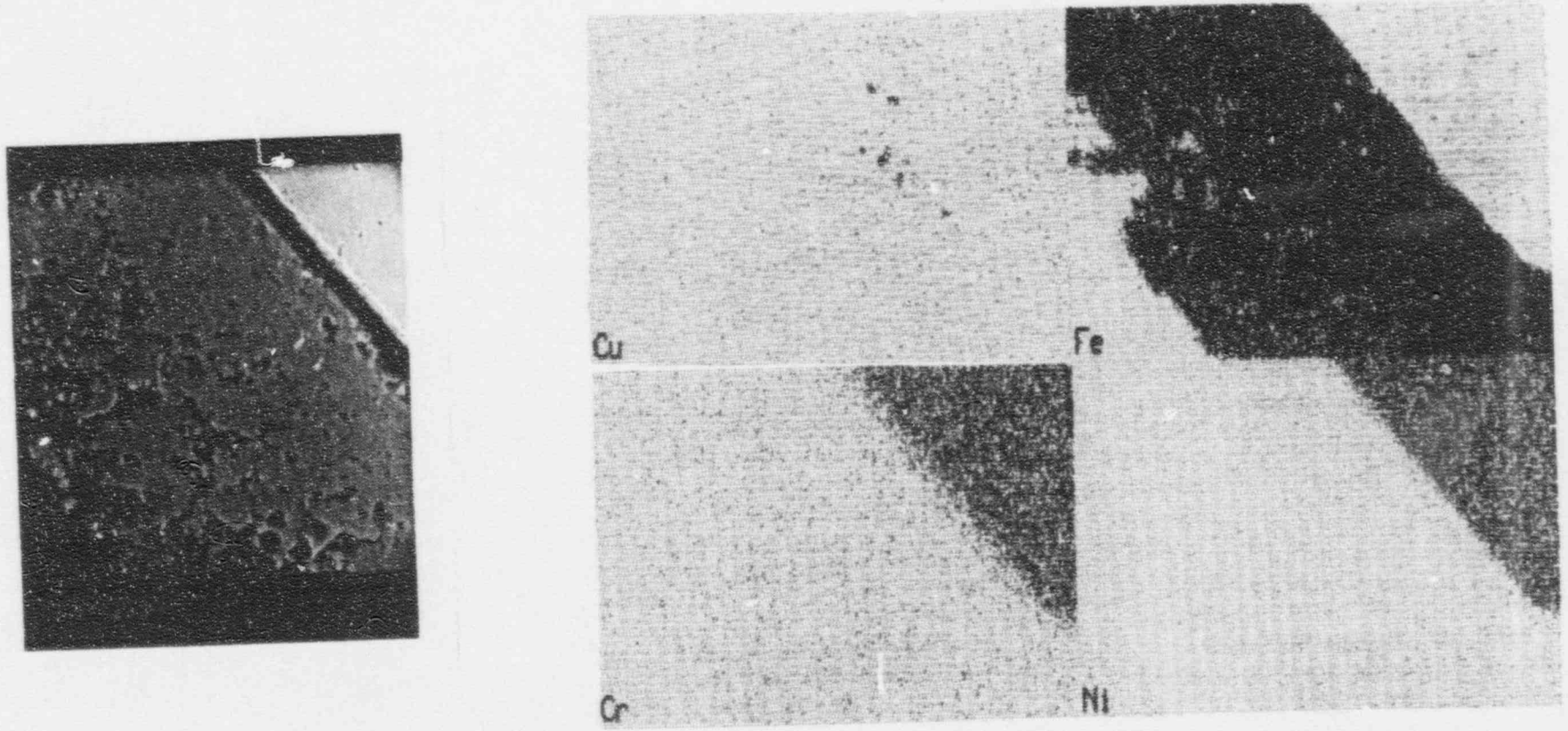

Figure 2-53: SEM/EDS Results on Specimen 133-33-3B, 1st Span

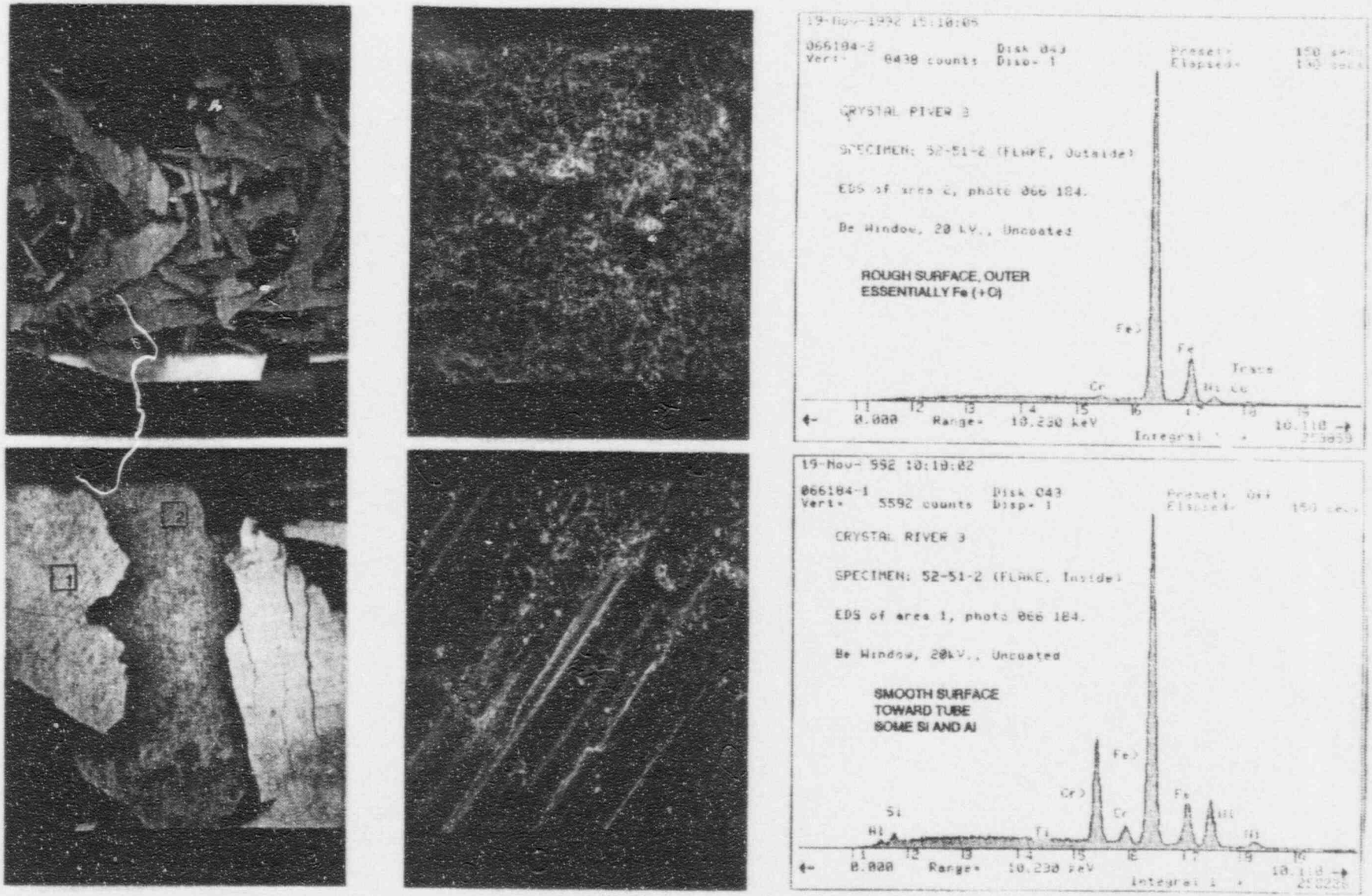

Figure 2-54: SEM/EDS Results on OD Deposit Flake from 52-51-2

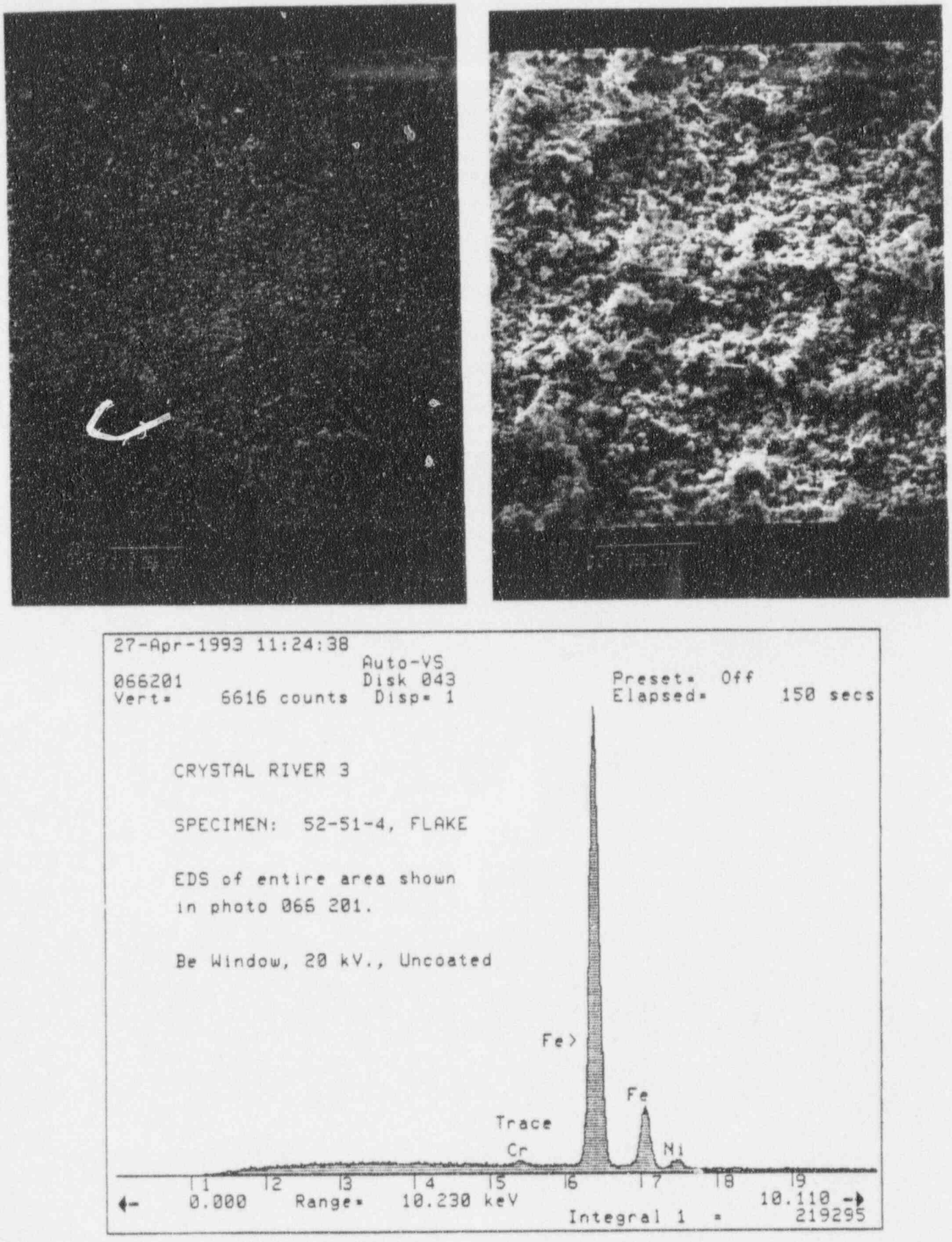

Figure 2-55A: Outer Deposit Flake Surface from Specimen 52-51-4

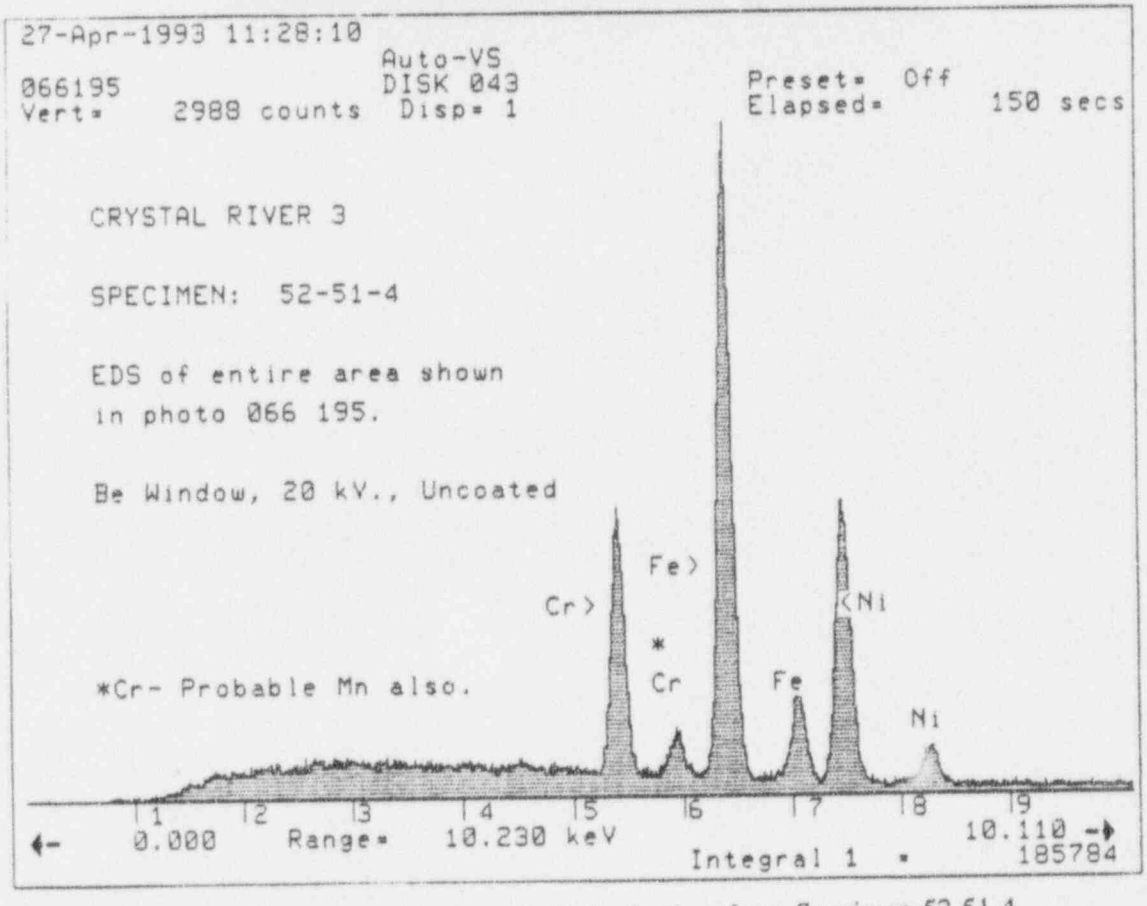

Figure 2-55B: Inner Deposit Flake Surface from Specimen 52-51-4

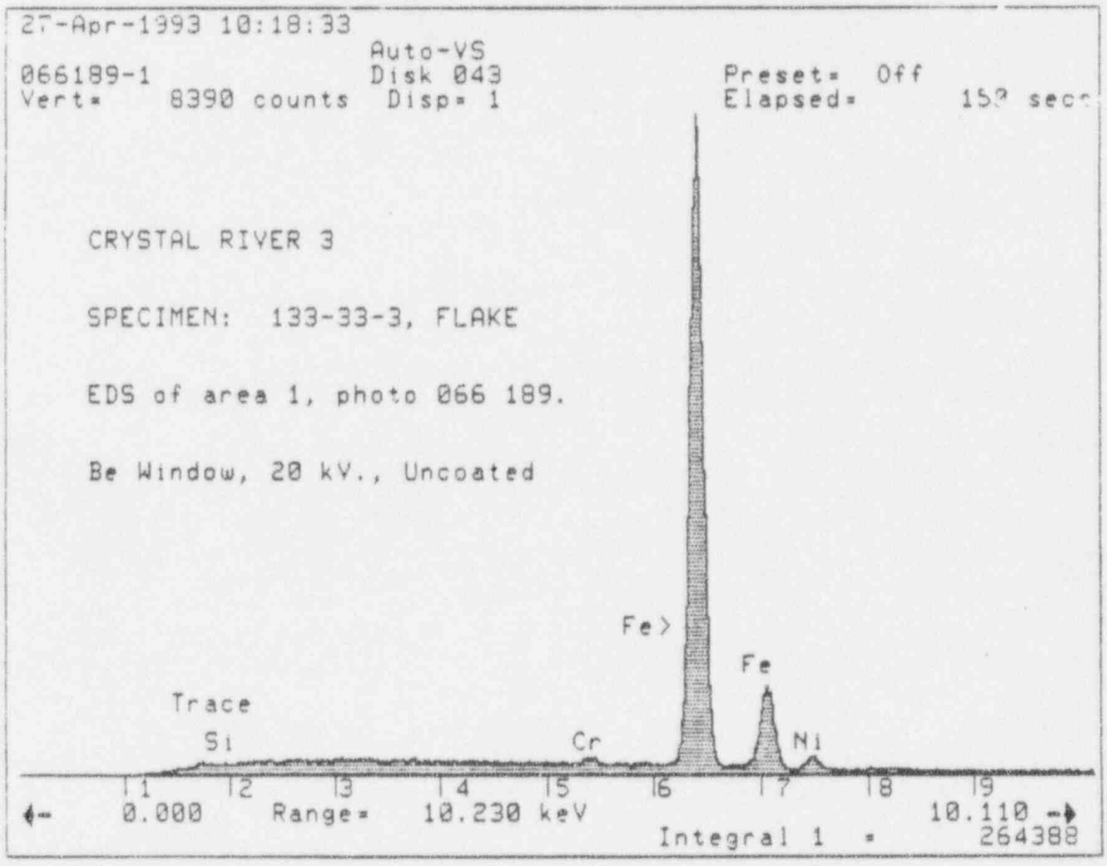

Figure 2-56A: Outer Deposit Flake Surface from Specimen 133-33-3

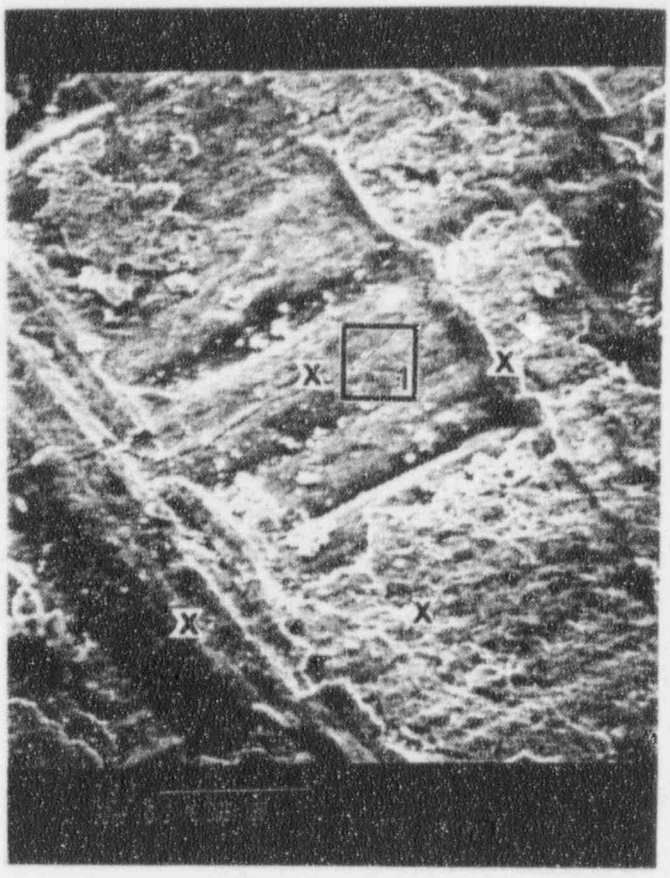

"X" MARKS LOCATIONS OF
DIFFERENT COMPOSITIONS
PREDOMINANTLY Ni/Cr/Fe RATIOS

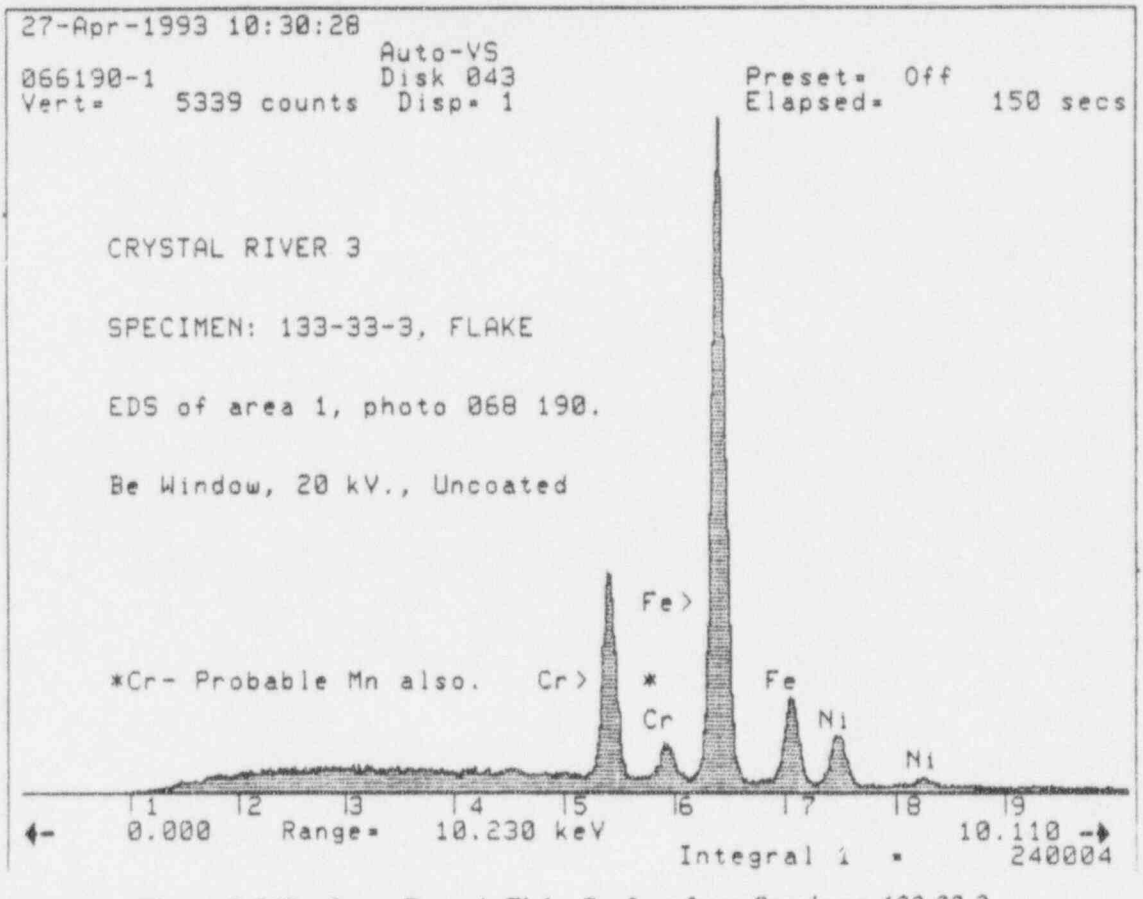

Figure 2-56B: Inner Deposit Flake Surface from Specimen 133-33-3

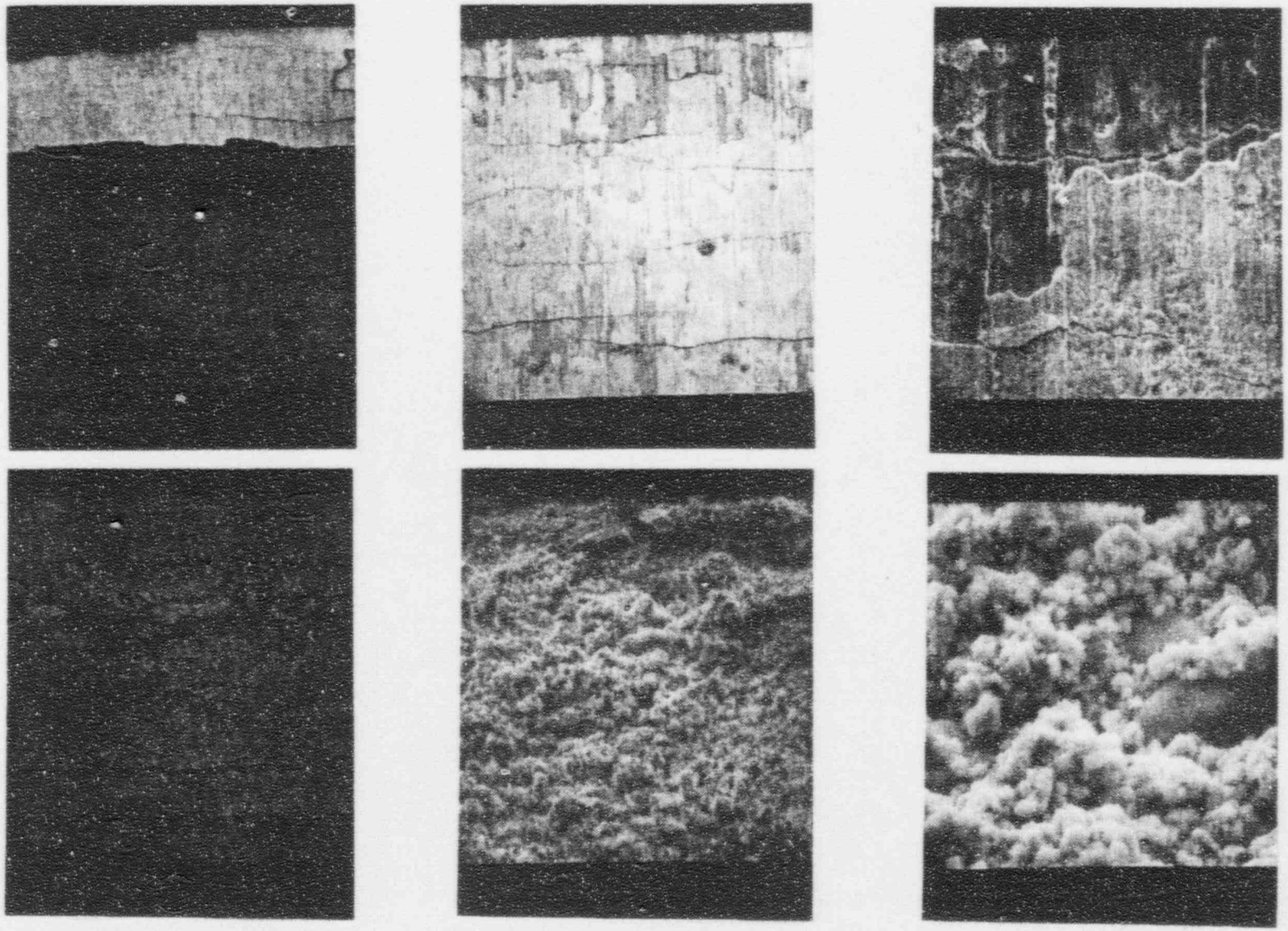

Figure 2-57A: Inner (Top) & Outer (Bottom) Deposit Flake Surfaces from Specimen 133-33-9

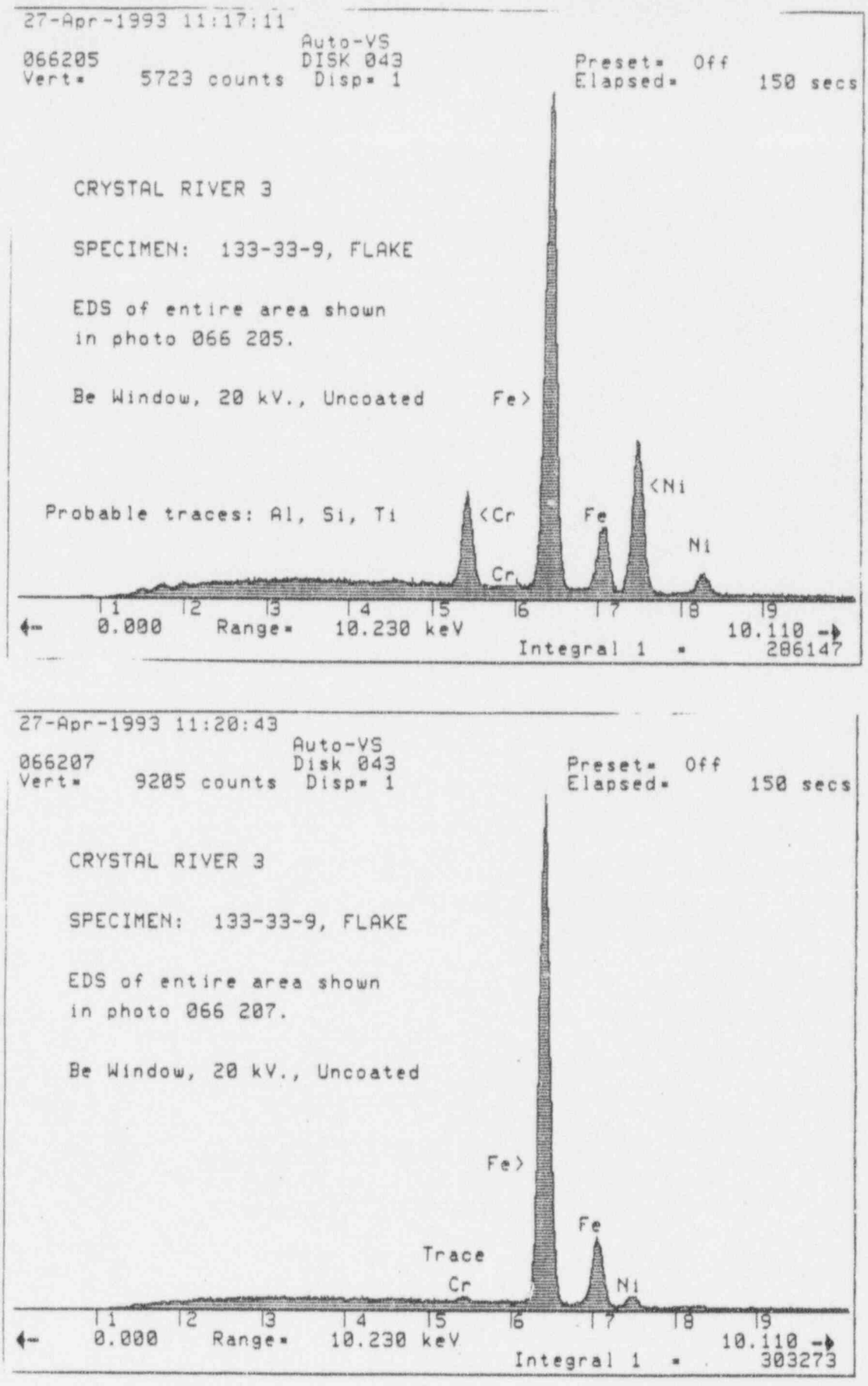

Figure 2-57B: Inner (Top) & Outer (Bottom) EDS Results on Deposit Flake Surfaces from Specimen 133-33-9

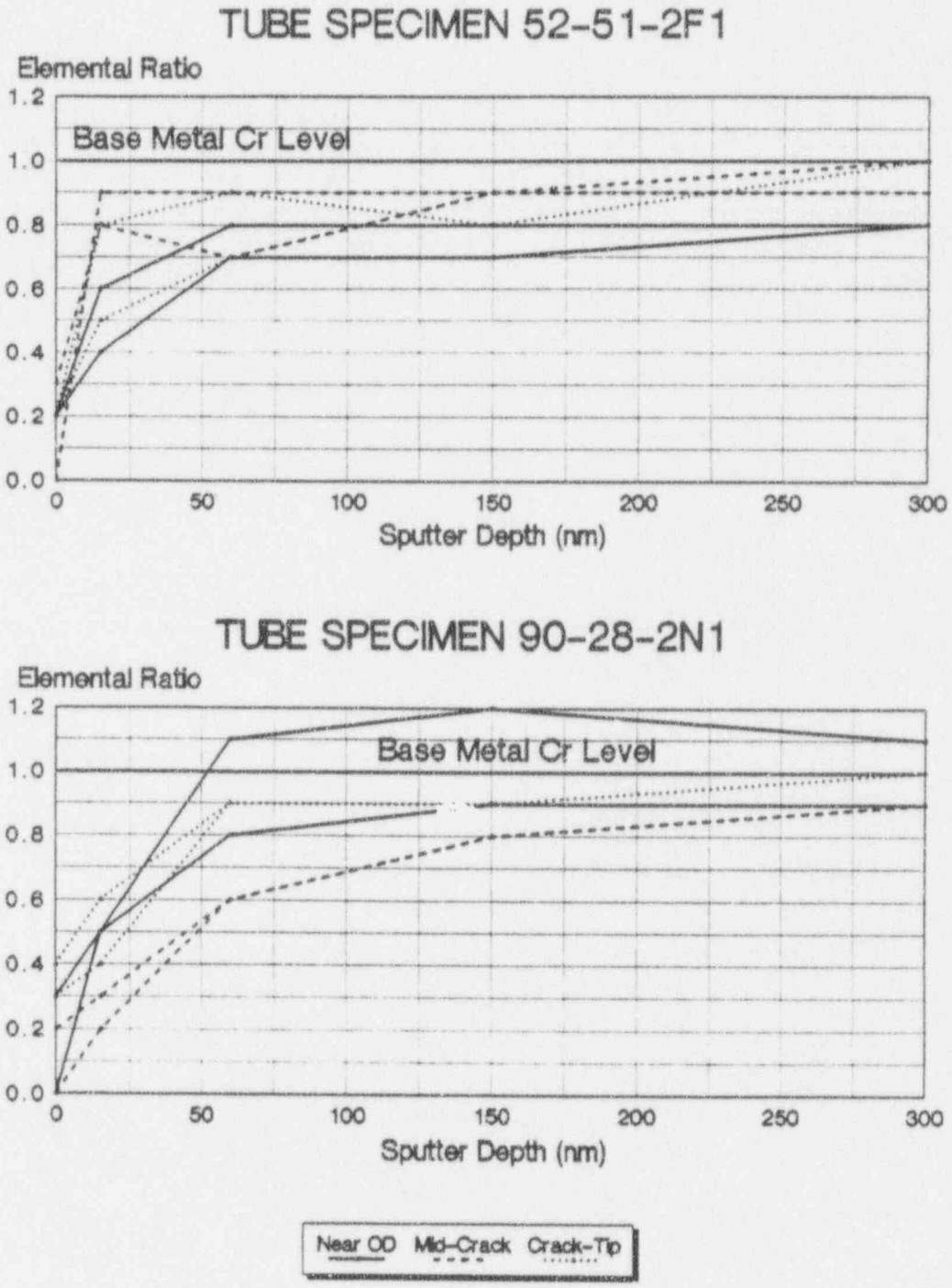

Figure 2-58: Elemental Ratio of Chromium in Grain Boundary Corrosion Film Relative to Base Metal

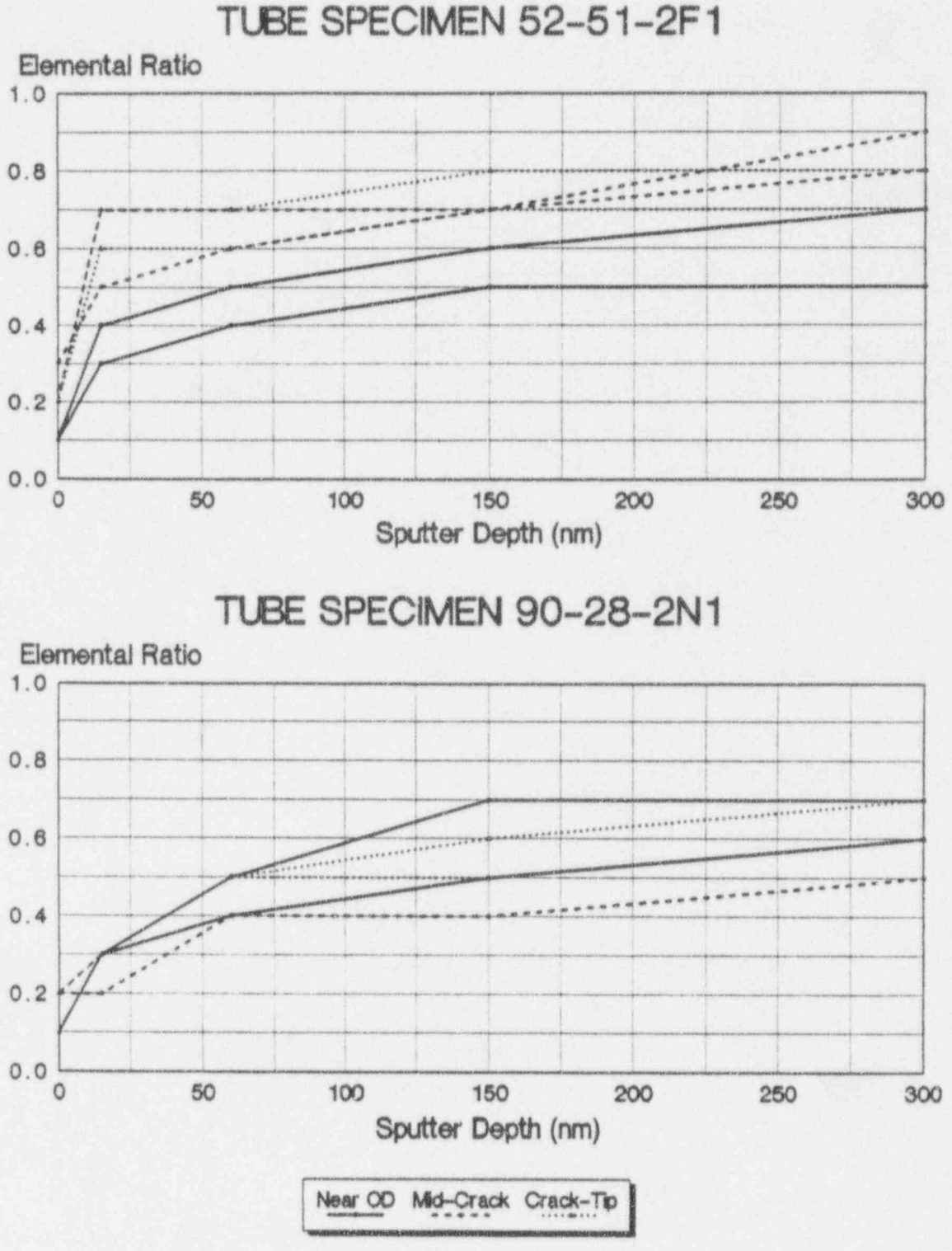

Figure 2-59: Elemental Ratio of Nickel in Grain Boundary Corrosion Film Relative to Base Metal

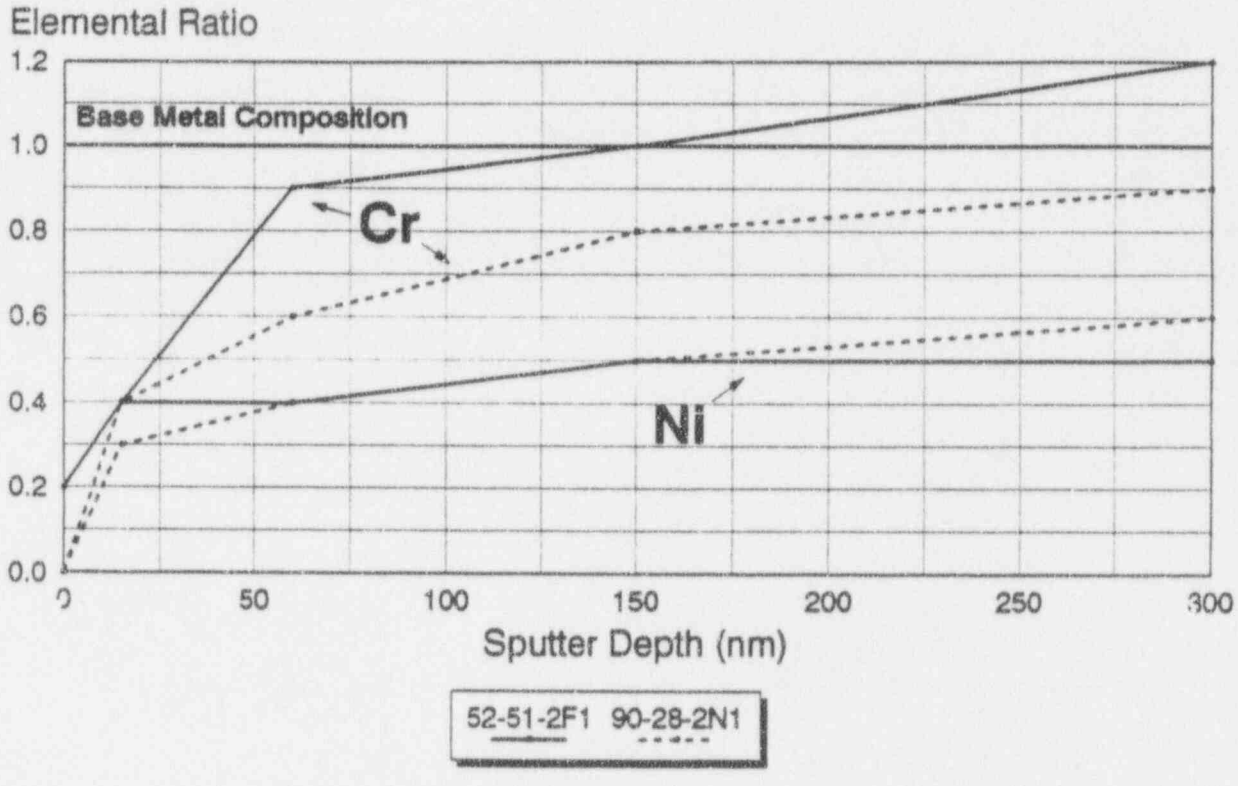

Figure 2-60: Elemental Ratios of Chromium & Nickel in OD Surface Corrosion Film Relative to Base Metal

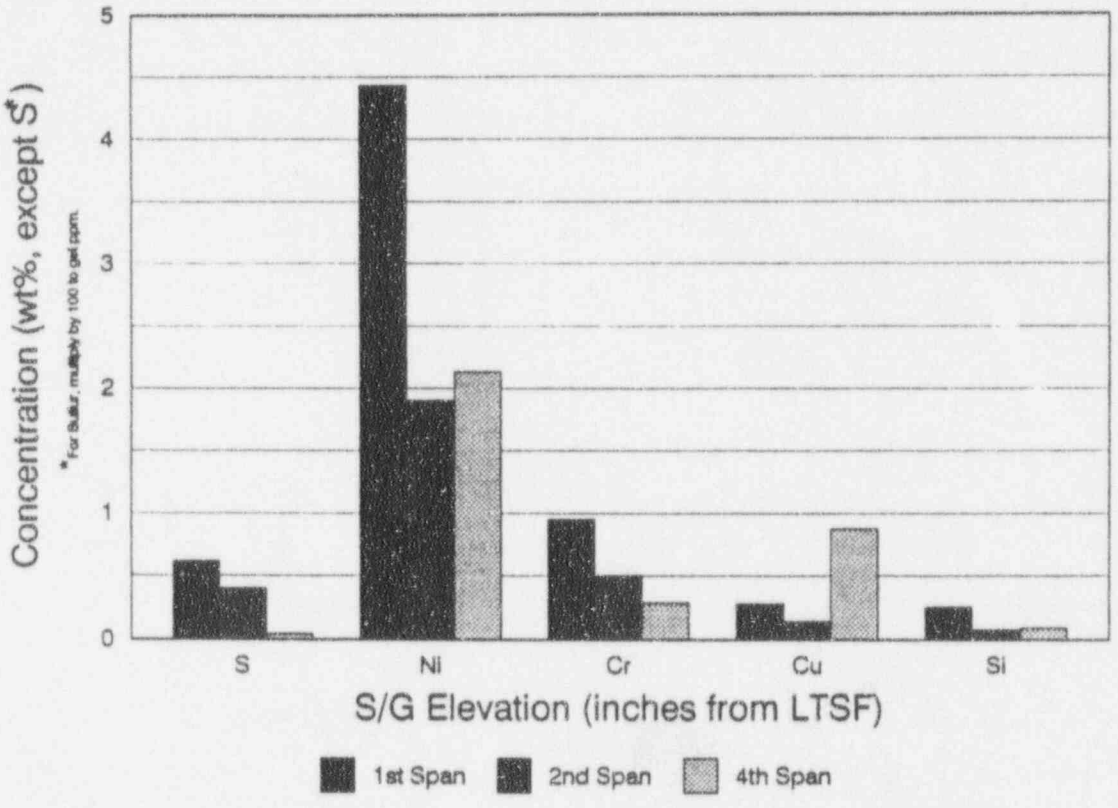

Figure 2-61: Elemental Distribution in OD Tube Deposits with respect to Steam Generator Elevation

Section 3

DATA ANALYSIS AND EVALUATION

3.1 Summary of Tube Degradation

Tube damage was predominantly in the form of isolated, small patches of OD initiated intergranular attack (IGA), although some minor pitting was observed in a few instances. The IGA exhibited, in general, a classical "thumbnail" shape. A total of one-hundred eight (108) defects were observed in four tube sections with maximum and minimum depths of 62% and 1% throughwall, respectively and an overall average depth of 28% (σ = 16%). The defect depths approximated a normal distribution (see Fig. 3-1). Damage was primarily confined to the first free span region, although a few small defects were found within a few inches below the LTSF. The majority of the defects and those with any significant volume were concentrated in a region extending about 6 to 18 inches above the LTSF (see Fig. 3-2). It was also observed that many of the IGA patches were located along "old-appearing" axially oriented scratches, which were probably created during tube installation.

3.2 Correlations with Eddy Current Testing

In order to correlate the destructive examination data with the eddy current results, the defects were first grouped into sixty (60) "eddy current distinguishable" defects (i.e., defects spaced sufficiently far apart so as to be detected as separate indications by eddy current) as shown in Table 3-1.[3] The scatter plot shown in Figure 3-3 shows a general correlation between defect volume and depth as might be expected. In addition, this graph also illustrates that eddy current (field bobbin data) was more effective at detecting those defects with significant volumes. This also would be expected since bobbin coil eddy current is a volume sensitive NDE technique. In general, defects with volumes of $\sim 40(10^{-6})$ in^3 or greater and depths of $\sim$22% or greater were detected reliably (83%) by field bobbin coil. Detectability was somewhat worse for smaller (i.e., less volume) defects with the same depth range; for example, defects with volumes in the range of ~ 10 to $40(10^{-6})$ in^3 and depths of $\sim$22% or greater were detected at about a 48% frequency. This is further illustrated in the bar graphs of Figure 3-4, which provide a general indication of bobbin coil detectability (combined field and lab data). Detectability increases with increasing defect depth and volume. The combined bobbin coil data, shows defects with depths of 41% to 50% throughwall were detected at a frequency of about 75%, while all deeper defects were detected.

MRPC data showed similar behavior, but in general its detectability was lower than bobbin coil (see Fig. 3-5). It had been observed previously by eddy current analysts that many of the field MRPC indications fell along a single angular position; this could easily be explained by the tendency for IGA patches to initiate at pre-existing axial scratches as noted in Section 3.1. A complete summary of eddy current detectability is provided in Table 3-2.

---

[3] The criteria used for this compilation of data was an axial spacing of about 0.3 inches. The volume of each defect was estimated by assuming an ellipsoid shape for the IGA. For defects which were combined to form a composite "eddy current distinguishable" defect, axial extent and depths were determined by a weighted average (based on volume) and circumferential extents were summed.

TABLE 3-1

SUMMARY OF EDDY CURRENT DISTINGUISHABLE DEFECTS

Tube Section No.	Defect No.	Position		Defect Extent				Eddy Current Results			
								Bobbin Coil		MRPC	
		Axial (inches)	Circ. (°)	Axial (mils)	Circ. (°)	Depth (%TW)	Vol. (10^{-6} in^3)	Field	Lab	Field	Lab
90-28-2	AF	17.2	150°	28.9	2.0	51%	3.0		S/N		
	AD2/1	16.1	180°/315°	52.4	3.5	37%	6.9				S/N
	AB	15.5	340°	54.4	8.3	30%	13.8				
	Z	15.1	325°	38.2	1.3	30%	1.5		S/N		
	X2/1	14.6	340°/110°	45.6	2.7	43%	5.4		S/N		S/N
	V2/1	14.0	270°/350°	53.7	7.5	48%	19.8				
	T2/1	13.2	110°/330°	36.3	7.8	50%	14.5				
	S2/1	12.9	350°/110°	33.9	3.2	26%	2.9		S/N		
	Q	12.3	340°	59.2	3.1	45%	8.5		S/N		
	O/N/M	11.5	340°/100°/290°	58.5	14.5	43%	37.5		S/N		S/N
	K	10.8	290°	31.8	3.6	18%	2.1		S/N		
	I/H/G	10.2	200°/10°/330°	71.5	17.3	49%	62.3	S/N	S/N	S/N	S/N
	AFC*	9.2								S/N	
	E	7.8	340°	70.9	7.9	50%	28.8	46%	36%	S/N	S/N
	C/B	6.1	20°/315°	56.5	6.1	41%	14.5	S/N	S/N	S/N	S/N
	AFC*	1.0							S/N		
52-51-2	X	16.5	315°	40.3	2.0	32%	2.6				S/N
	U	15.3	315°	32.7	4.8	26%	4.2				
	S	14.7	315°	63.7	8.3	33%	17.9				
	R	14.1	250°	38.9	3.7	18%	2.7		S/N		S/N
	P	13.1	200°	43.9	5.3	33%	7.9				
	N2/1	12.4	180°/260°	33.6	4.6	30%	4.8				
	L	11.4	180°	33.5	1.4	13%	0.6				S/N
	K2/1	11.0	250°/180°	42.7	7.8	45%	15.4				
	I2/1	10.0	350°/270°	49.7	15.2	42%	32.9	S/N		S/N	S/N
	G/F	8.9	315°/350°	69.9	5.7	47%	19.3	S/N	S/N	S/N	
	AFC*	7.9						S/N	S/N	S/N	S/N
	D	6.5	265°	60.9	8.4	34%	17.9	S/N	S/N	S/N	S/N
	B	-1.0	20°	38.6	2.0	38%	3.0				
97-91-2	W	14.1	105°	60.6	9.6	54%	32.0	67%	S/N	S/N	S/N
	AFC*	12.3									S/N
	U/T/S	11.5	245°/90°/95°	58.2	26.0	46%	70.9		S/N	S/N	S/N
	R1	9.3	350°	11.0	6.1	4%	0.3			S/N	S/N
	AFC*	8.6						S/N	S/N	S/N	S/N
	P/O	8.3	90°/15°	74.4	18.0	50%	68.8	67%	S/N		

TABLE 3-1 (Continued)

Tube Section No.	Defect No.	Position		Defect Extent				Eddy Current Results			
		Axial (inches)	Circ. (°)	Axial (mils)	Circ. (°)	Depth (%TW)	Vol. (10^{-6} in^3)	Bobbin Coil		MRPC	
								Field	Lab	Field	Lab
97-91-2 (cont.)	M	7.1	320°	19.7	3.3	16%	1.1				
	K	6.6	225°	49.8	3.8	29%	5.7				
	I	5.6	355°	6.7	2.4	4%	0.1				
	G	3.3	20°	13.1	0.7	5%	0.0				
	E2/1/D	2.8	20°/285°/350°	13.5	5.7	6%	0.5				
	B	1.1	285°	16.3	2.5	6%	0.2				
	AFC*	-1.7							S/N		
106-32-2	BG/BF	16.6	90°/30°	55.1	7.6	15%	6.2				
	BD/BC	15.6	50°/30°	63.5	12.8	31%	25.5				
	BB/BA/AZ	14.9	90°/35°/45°	35.3	12.9	20%	9.4				
	AY	14.6	220°	55.3	16.1	36%	32.9	S/N	S/N		
	AX	14.3	30°	39.9	9.6	32%	12.6				
	AT/AU/AV	13.2	135°/45°/60°	46.8	42.3	34%	69.2	S/N	S/N	S/N	
	AR	12.3	90°	44.9	12.8	19%	11.2			S/N	
	AQ2/1	11.7	180°/90°	38.1	16.0	35%	21.9			S/N	
	AP/AO	11.2	20°/90°	48.0	14.4	27%	19.2	S/N			
	AN/AM 3/2/1	10.8	240°/0°/50°/45° 125°/180°/170°	26.5	31.9	27%	23.5	S/N	S/N	S/N	
	AL2/1	10.5	25°/80°/75°	27.7	10.2	11%	3.2			S/N	
	AJ/AK	9.9	190°/25°	61.3	22.8	39%	56.0	S/N	S/N	S/N	
	AG2/AH	8.8	100°/60°	59.1	13.0	35%	27.6		S/N	S/N	S/N
	AFC*	8.2								S/N	
	AE/AD/AC2	7.7	225°/60° 220°	62.5	27.5	24%	42.4	S/N	S/N		
	AC1/AB	7.4	60°/70°	53.5	11.5	18%	11.4				
	Z/AA	7.0	180°/200°	46.2	18.6	34%	30.0				
	X2/Y/X1	6.4	65°/85°/50°	33.7	20.4	28%	19.8	S/N	S/N	S/N	S/N
	V2	5.3	125°	40.8	2.1	14%	1.2			S/N	S/N
	Q	-0.6	190°	17.1	3.2	7%	0.4				
	N	-1.8	270°	5.4	1.0	15%	0.1				
	L/K/J i/H	-2.3	280°/310°/105° 40°/120°	17.3	31.3	14%	7.8				
	F	-3.4	160°	12.0	9.3	9%	1.0				
	E	-3.9	145°	18.2	3.4	23%	1.5				
	C	-5.4	350°	6.7	4.9	7%	0.2				

* AFC = Apparent False Call

TABLE 3-2

EDDY CURRENT DETECTABILITY SUMMARY

Eddy Current Technique	Criteria	Size (%TW)	Total No. Defects	FIELD		LAB		COMBINED	
				No. Detected	Percent Detected	No. Detected	Percent Detected	No. Detected	Percent Detected
Bobbin Coil	Depth	0-10	8	0	0%	0	0%	0	0%
		11-20	12	0	0%	1	8%	1	8%
		21-30	11	4	36%	5	45%	6	55%
		31-40	14	4	29%	5	35%	5	36%
		41-50	13	6	46%	9	69%	10	77%
		51-60	2	1	50%	2	100%	2	100%
		Total:	60	15	25%	22	37%	24	40%
	Volume (10^{-6} in^3)	0-12	34	0	0%	7	21%	7	21%
		13-24	13	6	46%	5	38%	6	46%
		25-36	7	4	57%	5	71%	6	86%
		37-48	1	1	100%	1	100%	1	100%
		49-60	2	2	100%	2	100%	2	100%
		61-72	3	2	67%	3	100%	3	100%
		Total:	60	15	25%	23	38%	25	42%
MRPC	Depth	0-10%	8	1	13%	1	13%	1	13%
		11-20%	12	3	25%	3	25%	5	42%
		21-30%	11	2	18%	1	9%	2	18%
		31-40%	14	5	36%	4	29%	7	50%
		41-50%	13	8	62%	9	69%	10	77%
		51-60%	2	1	50%	1	50%	1	50%
		Total:	60	20	33%	19	32%	26	43%
	Volume (10^{-6} in^3)	0-12	34	3	9%	6	18%	8	24%
		13-24	13	6	46%	3	23%	6	46%
		24-36	7	4	57%	5	71%	5	71%
		37-48	1	0	0%	0	0%	0	0%
		49-60	2	2	100%	1	50%	2	100%
		61-72	3	3	100%	2	67%	3	100%
		Total:	60	18	30%	17	28%	24	40%

In an independent review of the eddy current data (Appendix B), Krzywosz similarly concluded that "the MRPC detected IGA patches better than bobbin coils", and that "no reliable IGA depth estimate was demonstrated with the bobbin coil."

3.3 Review of Prior Eddy Current Data

A number of reviews of historical eddy current data for the CR-3 steam generators were done (2,3,4) in an attempt to answer the following questions:

(1) When did the observed defects initiate?

(2) Is the corrosion process active or inactive?

Only a limited number of tubes having defect indications had been inspected in the interval between the baseline inspection (1976) and the May 1992 refueling outage. Only 3 of the 6 tubes removed from the B steam generator (52-51, 106-32, and 109-30) had eddy current data from the 2 previous outages (3/89 and 4/90). Thirty-seven tubes in the B steam generator had eddy current data from the previous outage (4/90).

An earlier review (2), carried out in 1990 for 4 tubes (40-47, 46-46, 52-51, and 52-81), concluded that the defect indications recorded for these 4 tubes during the April 1990 refueling outage were definitely present as early as March 1980, but were not present at the time of the baseline inspection (1976). From this limited review, one could conclude that the defects in those tubes occurred between 1976 and 1980.

Krzywosz (3) performed an independent review of prior eddy current data for the 3 pulled tubes (52-51, 106-32, and 109-30) to determine if the IGA could be attributed to a one-time event. To account for different probe sizes and cable lengths used in the 3 inspections, he normalized the 600 kHz channel data for a 100% calibration hole to 5 volts peak-to-peak at a phase angle of 40°. From his review (Appendix B), he concluded the following:

(1) The eddy current indications confirmed as IGA patches by metallurgical test results were present in 1989.

(2) The IGA patches have not grown since 1989, but have remained stable and dormant.

(3) There were no new detectable IGA indications since 1989.

In Reference 4, eddy current signals were compared for indications detected during both the 4/90 and 5/92 refueling outages. Based on the indications that could be compared, the average %TW growth was 2%, with a standard deviation of 17%, while the average signal voltage decreased by 0.21 volts. Based on this information, it was concluded in Reference 4 that there is no evidence indicating defect growth.

The reviews summarized above are consistent in their conclusions, viz., the patches of IGA present on the B steam generator tubes initiated prior to March 1989, possibly earlier than March 1980, and are currently dormant. Based on the information presented in Reference 3, new patches of IGA are not initiating in the first tube span of the B steam generator.

3.4 Effect of Defects on Pressure Holding Capability of Tubing

The two tube sections which were burst tested exhibited relatively high burst pressures (see tabularized data below).

TABLE 3-3

BURST TEST DATA

Tube Section No.	Burst Pressure	Defect Information		
		No.	Depth	Length
97-91-2	12,400 psi	O	54% TW	75.6 mils
106-32-2	11,400 psi	AG2	40% TW	62.3 mils

Since no defect-free CR-3 tubing was burst tested, nor were any tensile tests of the pulled tube sections performed, a direct correlation to burst pressure degradation could not be made. However, virgin (i.e., defect-free) OTSG tubing with a nominal wall thickness of 37.5 mils would be expected to have a burst pressure of ~11,300 psi based on typical values of yield (50 ksi) and ultimate (100 ksi) strengths for stress relieved Alloy 600 tubing (5). Therefore, it can be concluded that no significant degradation in burst pressure was exhibited by the defected CR-3 tubing.

Furthermore, burst pressure is highly dependent (exponential relationship) upon defect length, as well as depth. Since these defects are, in general, very short (< 3 mm) their effect on burst pressure would be expected to be minimal. The expected drop in burst pressure associated with the above defects is small (~18% decrease based on an empirical relationship developed by D. Azodi et al), which is consistent with the observed burst pressures (6).

3.5 Plant Chemistry Data Review

As part of the overall workscope, Florida Power Corporation and EPRI contracted with Adams and Hobart to review obtainable chemistry data for the period from 1977 to 1982 (Fuel Cycles 1 - 4) and attempt to correlate the data with the pulled tube examination results. Additionally, Adams & Hobart were tasked to review chemistry hideout return data from 1988 to the present and to evaluate the risk of reinitiating and/or propagating the observed IGA in the current operating environment.

As is the usual case with historical data reviews, data from early plant operations was limited and did not cover all impurity species considered today to be important with respect to steam generator corrosion. Nevertheless, the following inferences were drawn by Adams and Hobart (see Appendix C for the complete report):

1. Evidence of high concentrations of non-chloride anionic impurities was found in the early feedwater chemistry data.

2. Hydrazine concentrations in the feedwater during the 1977 to 1982 time period were high which, when combined with suspected instances of resin throw from the polishers, could have led to the reduction of sulfates to the more reactive sulfides.

3. While sulfate was not monitored between 1977 and 1986, cation conductivity was high during this period and not accounted for by measured chloride concentrations. This would suggest that elevated levels of sulfate may have been present. It would also indicate that acidic species, whether sulfate or other anions, may have been available in sufficient concentrations to produce an acidic environment in the concentrating films on the steam generator tubes.

These inferences appear to be consistent with the surface film analyses discussed in Section 2.2.11; viz., appreciable quantities of sulfide were present in the corrosion films. The corrosion films analyzed were also depleted in nickel, suggesting they formed in the presence of an acidic environment.

Adams & Hobart further concluded (Paragraph 4.2 of Appendix C) that "The low-temperature ($< 180°F$), acidic, reduced sulfur attack on the tubing freespan below the first tube support should not be progressing at present" inasmuch as "the sludge pile chemistry environment would not support continuation of the reduced sulfur acid attack below the first tube support."

3.6 Susceptibility of CR-3 Steam Generator Tubing to IGA

Following fabrication, the CR-3 once-through steam generators were subjected to a full-furnace stress relief at 600 to 620°C for 8 hours (at temperature) to reduce residual stresses. This step in the manufacturing process resulted in precipitation of the chromium carbides, leaving the grain boundaries depleted in chromium content; i.e.,"sensitized". This type of microstructure has been shown to have improved resistance to SCC in caustic environments. Following an extensive review of laboratory data and operating plant experience, Koch and Miglin (7) concluded that "in caustic environments in which mill-annealed Alloy 600 undergoes intergranular stress corrosion cracking (IGSCC), sensitized and thermally treated Alloy 600 is far less susceptible to IGSCC (than mill-annealed Alloy 600)." There have not, in fact, been any documented cases of caustic IGSCC in operating OTSGs.

The "sensitized" Alloy 600 microstructure is, however, susceptible to intergranular attack (IGA, IGSCC) in acidic solutions containing reduced sulfur oxyanions, even when the sulfur is present in small quantities (8). This form of corrosion has been observed at 3 operating plants (TMI-1, ANO-1, and Oconee 1), all of which have once-through steam generators with sensitized Alloy 600 tubing. At TMI-1, the attack was intergranular and initiated from the primary side (tube ID). It was postulated that the corrosion occurred with the plant shut down, the reactor coolant level lowered, and the RCS open to the air (9,10). The source of sulfur was identified as sodium thiosulfate, $Na_2S_2O_3$, from the containment spray system that had accidently leaked into the RCS.

At Arkansas Nuclear One-1, intergranular attack occurred from the secondary side of the tubes in the upper regions of the steam generator. Based on examination of pulled tubes, it was postulated that the IGA was caused by sulfur oxyanions at ambient temperatures during a long layup period (8,11). The source of sulfur was thought to be the condensate polishing system; i.e., either regenerant chemicals or thermally degraded resin fines.

Localized regions, ~0.020" X 0.040" X 20% TW, of intergranular penetrations were identified just within the lower tubesheet crevice on the OD of a tube removed from the Oconee 1-B steam generator in 1981. Surface chemistry analysis suggested that "the localized intergranular attack may be due to a synergistic interaction of chlorine, sulfur, and possibly silicon" (12).

Basically, sulfur-induced corrosion mechanisms can be divided into at least two regimes: (1) reduced sulfur IGA of sensitized Alloy 600 in oxygenated environments at low temperatures (< 170°F), and (2) IGSCC, wastage, and pitting in deaerated acidic sulfate solutions at high temperatures (13,14). Corrosion at high temperatures by acid sulfates has been implicated at Millstone 2 (15,16), Connecticut Yankee (17), and St. Lucie 1 (18), and investigated extensively in the laboratory (19). However, the high temperature mechanisms typically result in severe general corrosion or wastage (19,20), which is not consistent with the CR-3 defect morphology.

Corrosion of Alloy 600 by reduced sulfur species requires the presence of one or more aggressive species such as sulfite, thiosulfate, sulfide, or polythionate. The most common source of sulfur species, however, are sulfates ($SO_4^=$). Sulfates are unintentionally introduced into the steam generators via several sources, including makeup water, condenser leaks, improper regeneration of makeup demineralizers and condensate polishers, and leakage of cation resins or cation resin fragments from the demineralizers and condensate polishers (21). In high temperature deaerated environments, in the presence of reducing chemicals such as hydrogen or hydrazine, sulfates are not thermodynamically stable and can be reduced to a more reactive state; e.g., sulfides. In these environments, silica may act as a catalyst in accelerating the reduction of sulfates to the more reactive sulfides (22).

As noted earlier, the most common mode of attack by reduced sulfur species is intergranular corrosion in an oxygenated environment at temperatures less than 170°F. However, more recent studies by Sala, Combrade, et.al. (22,23), suggest that sulfides inhibit the formation of protective oxides in deaerated caustic and neutral environments as well, leaving the alloy more susceptible to intergranular attack by other species, e.g., caustic, at normal operating temperatures. Thus, for the CR-3 steam generators, corrosion by species other than reduced sulfur oxyanions cannot be entirely ruled out.

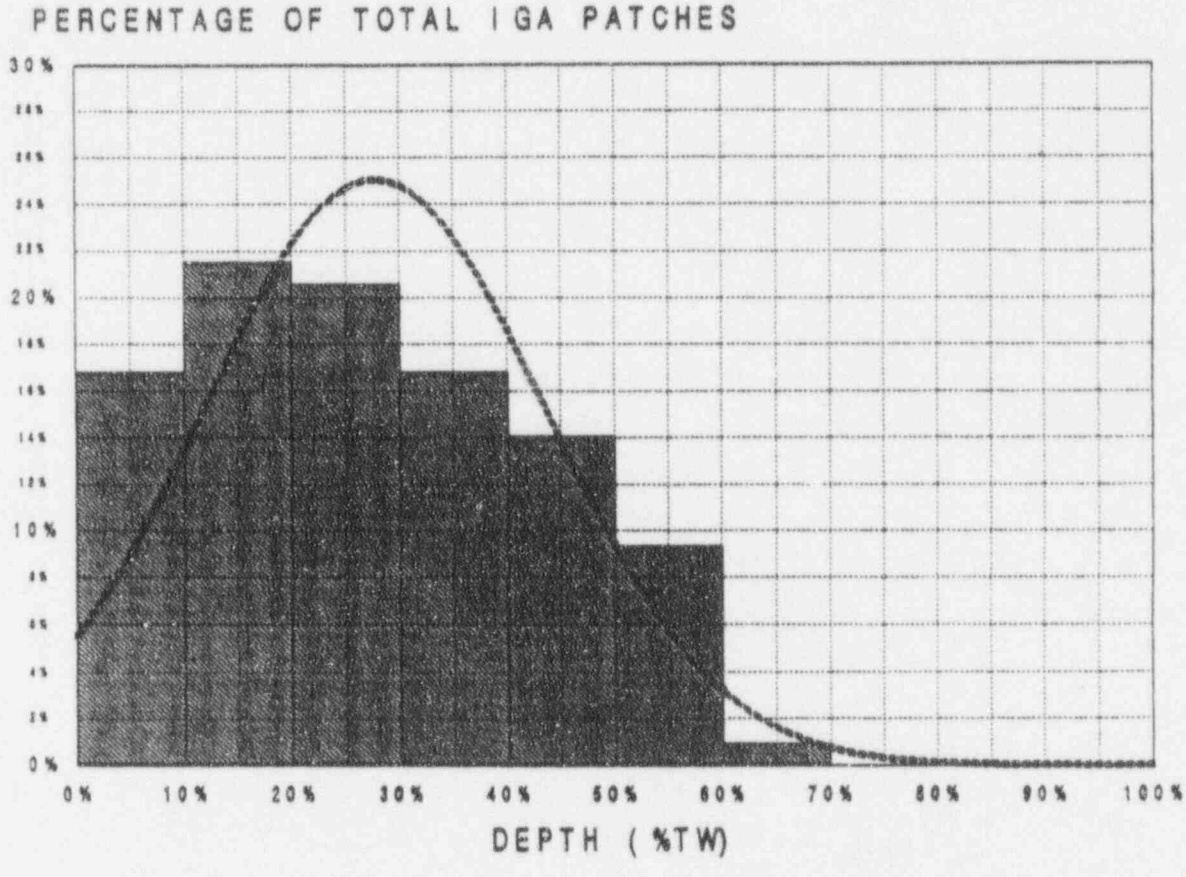

Figure 3-1: Distribution of IGA Patch Depths (107 Defects)

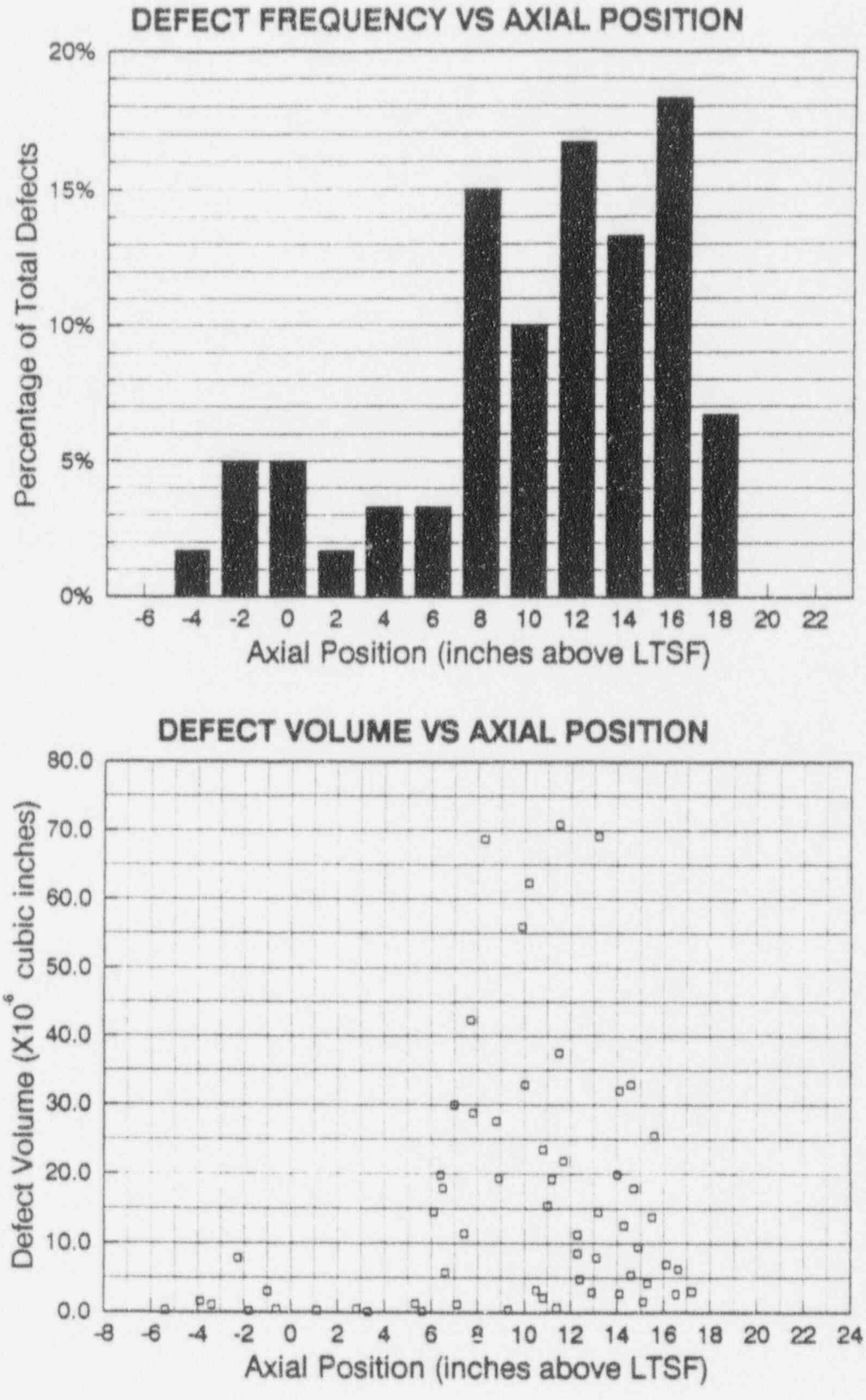

Figure 3-2: Defect Frequency and Volume Vs. Axial Position

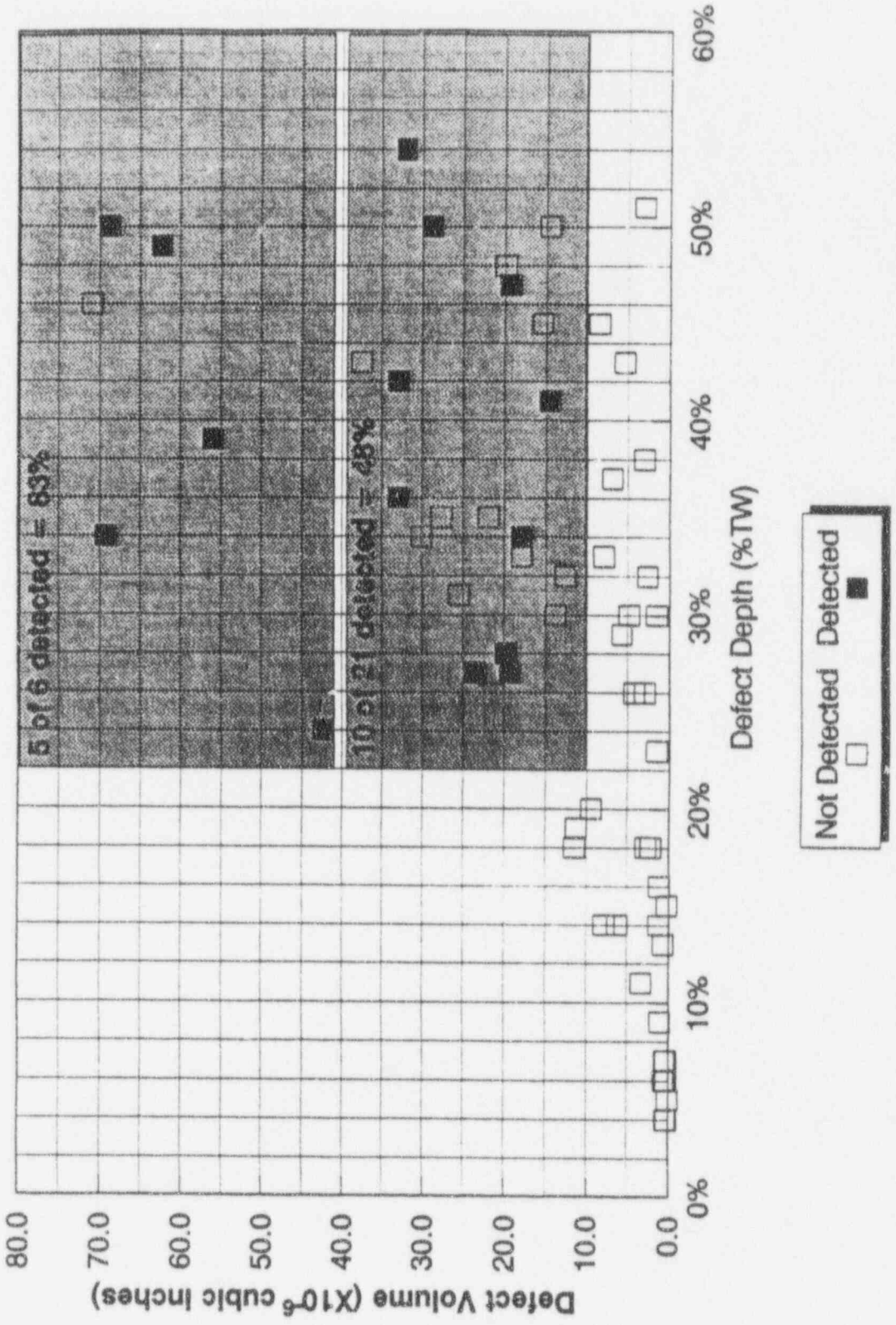

Figure 3-3: Defect Volume vs Defect Depth

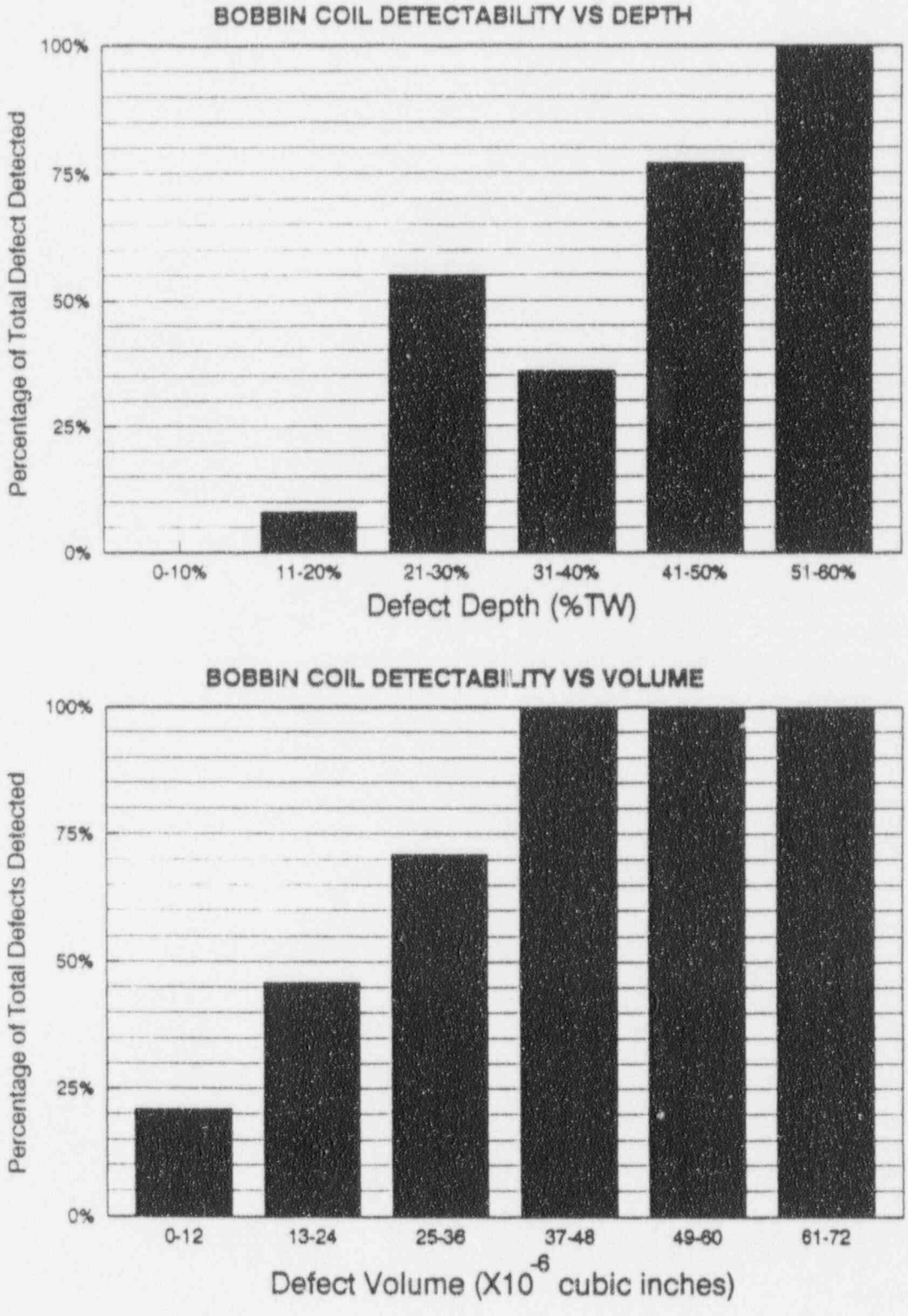

Figure 3-4: Bobbin Coil Detectability vs Depth and Volume
(Detectability based on both field and lab data)

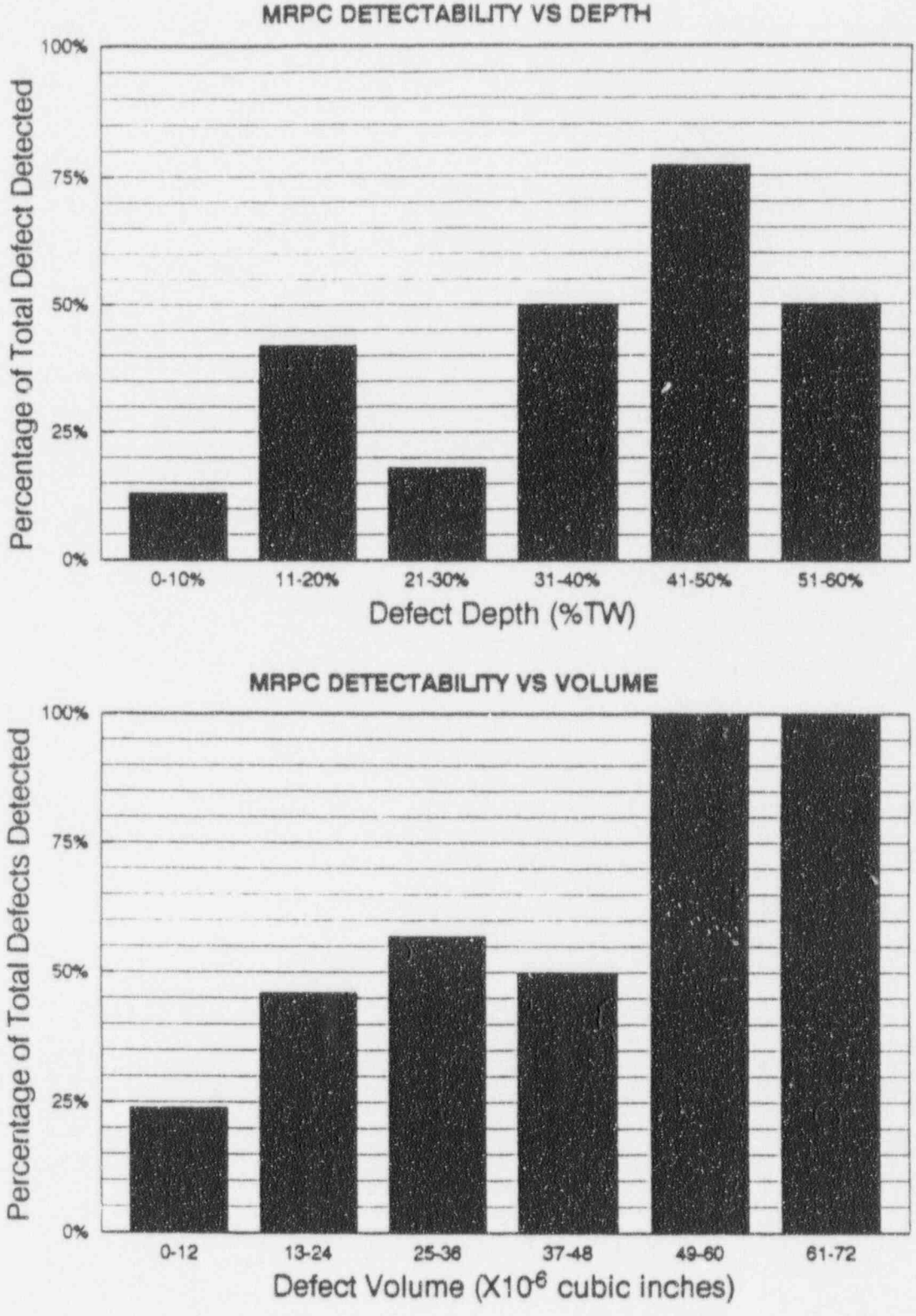

Figure 3-5: MRPC Detectability vs Depth and Volume
(Dectability based on both field and lab data)

Section 4

DISCUSSION OF RESULTS

As noted in Section 2, the majority of the "spots" of intergranular attack were contained within a region extending about 6 to 18 inches above the lower tubesheet secondary face (LTSF) of the "B" steam generator. Coincidentally, the affected tubes appear to be within the sludge pile (Figure 4-1) as it would have existed in the late 1970's through the early 1980's (24). This would suggest a relationship, either direct or indirect, between the occurrence of IGA and the sludge pile.

The IGA was confined to spots on the OD tube surface where the deposits were thinner than the bulk deposit, giving a scalloped appearance to the deposit. Underneath these deposits, the surface of the tube appeared to be "stained." These stained areas were enriched in chromium and surrounded by rings of deposit rich in silica and alumina. After descaling, the tube metal in the "stained" regions appeared to have been chemically etched.

Significant levels of sulfur were found to be incorporated in the tube OD surface and grain boundary corrosion films. Levels of 2 to 5 wt% sulfur were typically observed on the IGA fracture surfaces, while levels in the OD corrosion film were substantially lower (less than 1 wt%, predominantly as sulfate although some sulfide was also detected). It was also observed that the corrosion films were, in general, depleted in nickel and enriched with chromium (Figure 4-2). This behavior was slightly more pronounced for the OD corrosion film. This provides an indication that the corrosion films were not formed under strongly caustic conditions (25,26), but could have formed in mildly alkaline to acidic solutions.

As discussed in Section 3.6, the presence of sulfur in the grain boundary corrosion films is significant in that stress-relieved (sensitized) Alloy 600 is quite susceptible to intergranular attack by sulfur oxyanions. In general, acidic-oxidizing conditions (27) and temperatures less than ~170°F (77°C) are required for reduced sulfur IGA (27). As noted in the previous paragraph, acidic conditions would be consistent with the corrosion film chemistry observed on the CR-3 tubes. In addition, deposits in one IGA location revealed the presence of copper oxide, which may also be indicative of localized oxidizing conditions.

As noted in Section 3.3, historical eddy current data, although limited, suggests that corrosion damage in the B steam generator occurred prior to March 1980. Assuming this is correct, the observed IGA would have occurred under conditions that would have been present during and shortly after intial startup. A review of plant operating information (i.e., operating procedures, layup practices, maintenance records, etc.) during the period from startup through 1983 (28) determined that several incidences occurred during which one of the steam generators might have boiled dry following a loss of feedwater event[4]. Such an event could explain the relationship of the defects to the sludge pile mentioned earlier. Following a loss of feedwater transient and subsequent loss of inventory in the affected steam generator, boiling in the sludge pile could have "splattered" the sludge onto adjacent tube surfaces where they would have "baked on", forming sites for underdeposit corrosion. A similar event occurred at Indian Point No. 3 in 1981 (29) where it was concluded that "in the inner core region of the steam generators some sludge had spattered and then caked on the tubes, because of some local thermohydraulic condition, such as local boiling, during a previous operation. The sludge deposits on the tubes acted as crevices and promoted

---

[4] An Emergency Feedwater Initiation and Control (EFIC) system was installed at CR-3 in 1985 to provide for automatic initiation of emergency feedwater.

wastage corrosion beneath them, when the oxygen concentration was high at the time of cool down."

Since the observed corrosion most likely occurred during plant shutdown (possibly during or following an event such as that described above), air ingress during shutdown operations or during the subsequent lay-up period could have created conditions favorable to attack by sulfur oxyanions, assuming that reduced sulfur species were present. It is known that wet lay-up practices in the period following initial startup resulted in poor oxygen control (30). In addition, it has been observed recently that oxygen excursions to 1000 ppb in the condensate occur at ~250°F during cooldown (30).

The same study of plant operations referenced previously (31) found that there were numerous incidents where resin leakage from the condensate polishers may have occurred and frequent repair/maintenance of resin traps in the 1981-1982 time frame. Thus, condensate polishing operations would be a likely source of resin ingress.[5] Hydrogen form cation resins provide an interesting candidate source for the sulfur contamination in that they can release significant amounts of sulfur (they contain better than 10 wt% sulfur) upon thermal decomposition over a temperature range of ~170°F to 536°F (31,32). Also, breakdown of the resins proceeds through a melted form that could partially coat the tube surface (31). This could explain the stains observed on the CR-3 tubes, which may have resulted in localized under-bead attack of the tubes during the initial stages of the melting process and interference with subsequent deposition processes. The enriched-chromium scale observed within these stains is also consistent with this form of attack (31).

Fresh attack of Alloy 600 by sulfur oxyanions would generally produce a film containing very high levels of sulfur as sulfide (i.e., > 10 wt%) (8). Since this was not observed in the CR-3 tubes, it seems probable that the IGA had not occurred recently, and some of the sulfur had been washed away. This would be consistent with the prior eddy current data and could also explain the lower levels of sulfur on the OD tube surface compared to the grain boundary films.

---

[5] Several modifications to the condensate polishing operations were made in 1982, including the change to a gel type resin that is not regenerated, but replaced when exhausted.

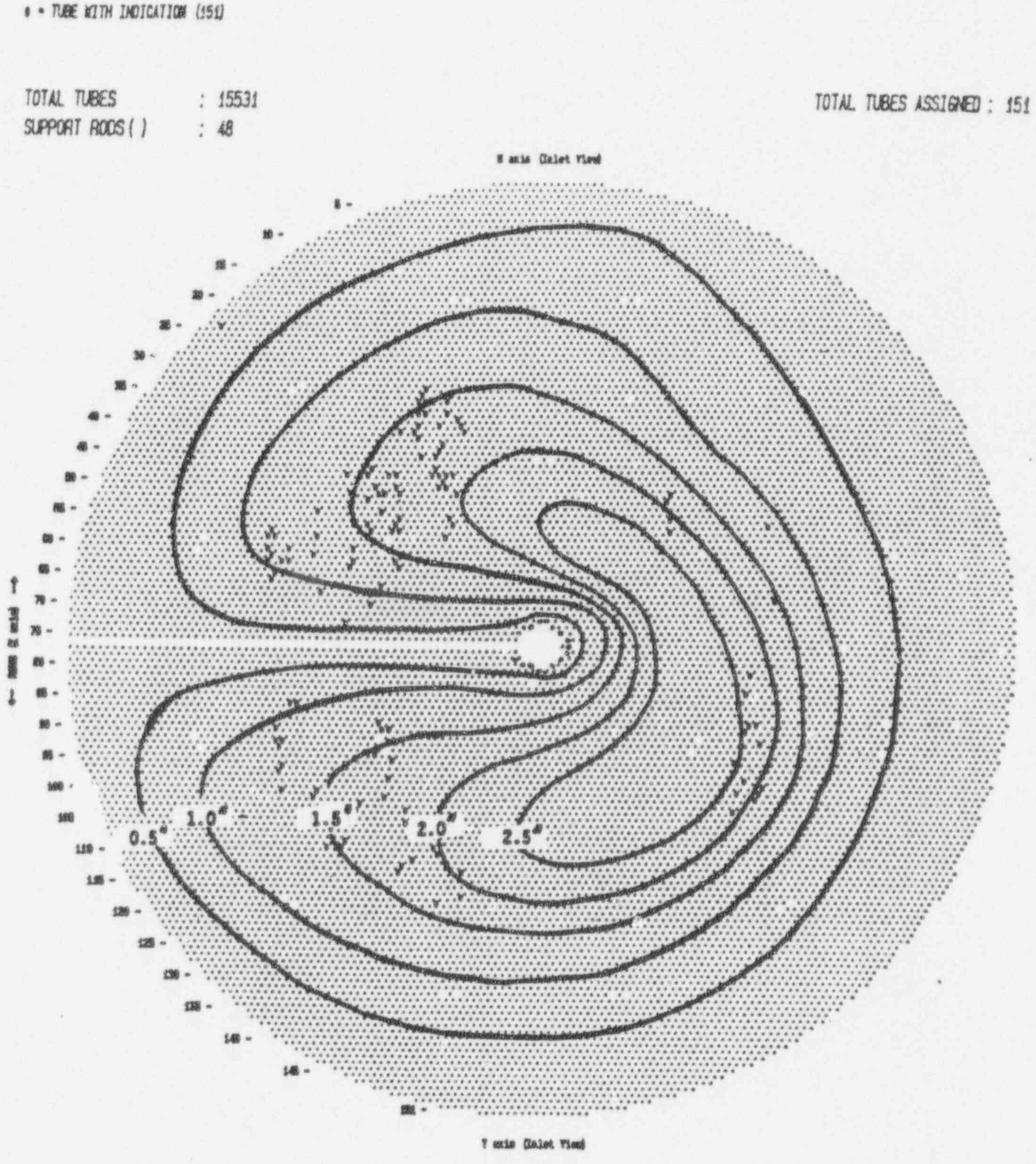

Figure 4-1: Superposition of Sludge Contour Map from 5/83 and Map for 1st Span ECT Indications

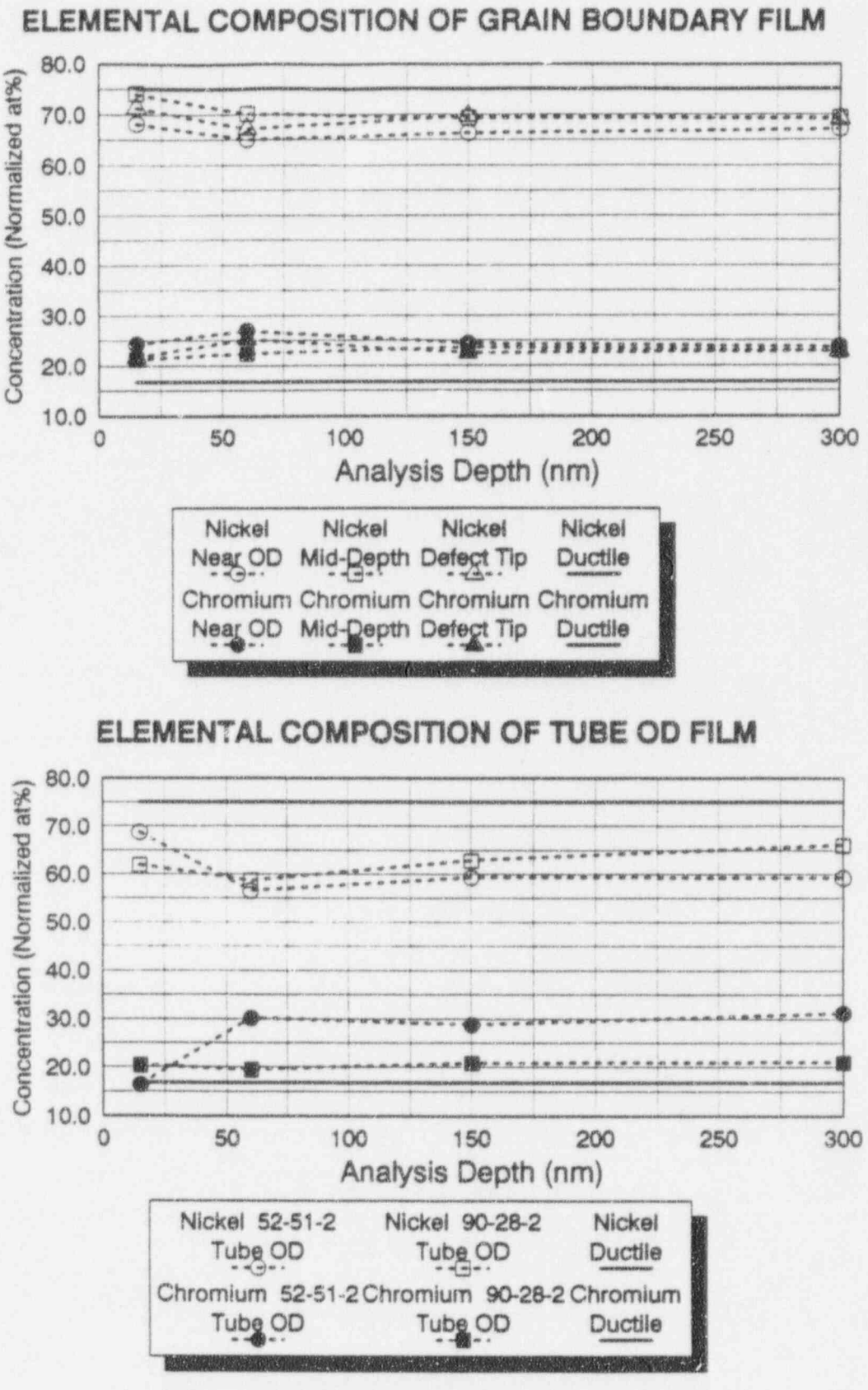

Figure 4-2: Nickel and Chromium Composition of Grain Boundary and Tube OD Surface Corrosion Films

Section 5

CONCLUSIONS/RECOMMENDATIONS

In summary, several observations were made during the tube examination and later that are pertinent to the damage mechanism, including:

- Tube wall degradation in the first span region of the CR-3 B steam generator is in the form of small, relatively shallow, isolated patches of OD-initiated IGA.

- Throughwall penetration ranged from 1% to 62%, with an average depth of 28% and having axial and circumferential extents of less than 0.1 inch.

- The damage was concentrated in an area extending 6 to 18 inches above the secondary face of the lower tube sheet and was associated with a non-uniform deposit pattern; specifically, spots of thinner deposit with an underlying chromium-rich scale surrounded by a ring of silica and alumina deposits.

- The grain boundary and tube OD surface corrosion films contained significant amounts of sulfur, and were depleted in nickel and enriched in chromium indicating an acidic to mildly alkaline environment.

- Review of prior eddy current data suggests that the IGA initiated as early as 1980 and is currently dormant or at least growing very slowly.

Based on these observations, the following conclusions were reached:

- The observed corrosion was likely caused by reduced sulfur species at a temperature of less than 170°F sometime during the period from startup (1977) to early 1980, probably closer to the latter. It is postulated that the steam generator boiled dry during a loss-of-feedwater transient. During either the boildown or during the subsequent feeding, the sludge, which was still light and fluffy (or mud-like) vs the piles of spalled deposit observed later on, splattered (or geysered) up and deposited on the tube walls. This established sites for subsequent underdeposit corrosion.

- The sludge and tube deposits contained significant levels of sulfate from chronic leakage of cation resin from the condensate polishers (or a significant sulfur intusion occurred). The sulfate was subsequently reduced to sulfides by hydrazine (or other, including silica or metal ions). Corrosion could then have occurred following concentration of the sulfides under the deposit during a period of poor oxygen control (e.g., during cooldown or heatup operations).

  Conversely, resin beads or fines could have adhered to the tube wall during the boildown, melted, and provided local acidic conditions and sulfur species that subsequently attacked the affected tubes during or following cooldown operations.

- Propagation ceased when conditions were no longer favorable to corrosion (sulfides were depleted, e.g.).

Additional information obtained during the examination includes the following:

- Bobbin coil detectability was good and improved with increasing defect depth and volume; all defects with depths greater than 50% throughwall were detected by bobbin coil.

- In general, detectability with the MRPC was not as good as with the bobbin coil probe, although defects with the largest affected volumes were reliably detected with both probes.

- The influence on tube burst pressure for these defects is relatively small (i.e., less than a 20% decrease).

On the basis of the information obtained during this project, it is recommended that the following actions be taken:

- Those tubes with defect indications in the first span of the B steam generator should be inspected during subsequent refueling outages to confirm that the corrosion identified in this report is dormant. Changes in ECT phase angle or voltage for a particular indication, or an increase in the number of detectable indications should be cause for additional investigation.

- Hideout return chemistry should be monitored for the recurrence of acidic conditions in the lower portion of the steam generator.

- Selected tubes with defect indications at higher elevations should be removed for laboratory analysis to determine whether such indications are similar to those from the first span, or whether they are a different phenomenon.

- Current BOP operating procedures and design features should be critically evaluated to (1) minimize the introduction of resin beads or fragments into the steam generators, and (2) minimize the ingress of oxygen during all phases of plant operation. Caution should be exercised in adopting high hydrazine chemistry since excess hydrazine can act to reduce sulfates to the more active sulfur species.

- EPRI Project S305-9 evaluated the effect of residual sulfur compounds left by chemical cleaning on the potential for causing tube damage. It was determined in that study (32) that the cleaning process developed by the Steam Generators Owners Group (SGOG) "did not increase the susceptibility of tubing materials to degradation" nor "aggravate existing tubing faults." The applicability of this study to the CR-3 pit-like IGA should be evaluated to determine if additional testing is needed prior to carrying out future chemical cleaning operations.

Section 6

REFERENCES

1. BWNT Document No. 1222047A-00, "UT-360 Final Report: Crystal River 3 Tube Pull "B" SG, September, 1992," October 1, 1992.

2. H. L. Smith, "Crystal River 3 Eddy Current Review on Selected Tubes," BWNT Report 1208687, January, 1991.

3. K. Krzywosz, "Review of Successive Eddy Current Data on Pulled Steam Generator Tubes from Crystal River Unit 3," EPRI NDE Center Letter Report, March 24, 1993.

4. J. C. Brown, "Crystal River-3 Evaluation of First Span Defect Indications," BWNT Document 51-1218868-00.

5. B. Cochet and B. Flesch, "Crack Stability Criteria in Steam Generator Tubes", Structural Mechanics in Reactor Technology, Volume D: Experience with Structures and Components in Operating Reactors, 9th International Conference,Lausanne Switzerland, August 1987, pp. 413 - 419.

6. D. Azodi, H. Schulz and R. Arenz, "Crack Stability Criteria in Steam Generator Tubes", Structural Mechanics in Reactor Technology, Volume D: Experience with Structures and Components in Operating Reactors, 9th International Conference,Lausanne, Switzerland, August 1987, pp. 413 - 419.

7. D.W. Koch and B.P. Miglin, "Literature Review - OTSG Secondary-Side Tube IGA/SCC Evaluation," BWNT Document No. 51-1177882-00, January 1990.

8. A.K. Agrawal, et. al., "Evaluation of Alloy 600 Tube A77-34 from Steam Generator A of Arkansas Nuclear One, Unit 1, EPRI Report No. NP-4504-LD, Project S304-11, March 1986.

9. R.L. Jones, et.al., "The Origin of the Extensive Cracking of the Steam Generator Tubing at TMI Unit 1," Corrosion/83, Paper No. 141, April 1983.

10. A.K. Agrawal, et.al., "Failure Analysis of Inconel 600 Tubes from OTSG A and B of Three Mile Island Unit-1", Battelle Columbus Laboratories, June 1982.

11. Inman, S.C., "Examination of OTSG Tubes B73 and B112-19 from ANO-1 - Final Report," RDD:84:5303-04:02, June 10, 1983.

12. E.B.S. Pardue, et.al., "Evaluation of the Lower Tubesheet Region of an Oconee 1 Steam Generator Tube," EPRI NP-3026-LD, July 1983.

13. S.L. Harper, et.al., "The Role of Sulfur in the Corrosion of NSG," Proceedings of the Third International Symposium on the Environmental Degradation of Materials in Nuclear Power Systems - Water Reactors," August 1987.

14. P.L. Daniel, "Sulfur Induced Corrosion in Nuclear Steam Generators", B&W Report No. RDD:83:2341, September 1983.

15. J.F. Hall, "Destructive Examination of Steam Generator Tubes Removed from Millstone Point Unit 2," EPRI NP-4737-LD, July 1986.

16. S.C. Inman, et.al., "Examination of Steam Generator Tube Sections from the Millstone Point Unit 2 Nuclear Power Plant," EPRI NP-4829-LD, October 1986.

17. D.E. Powell and L.J. Laskowski, "Destructive Examination Results of Steam Generator Tubing Removed from Connecticut Yankee during 1984 Refueling Outage," Proceedings of the Third International Symposium on the Environmental Degradation of Materials in Nuclear Power Systems - Water Reactors," Traverse City, MI, August 1987.

18. G.O. Hayner et al., "Examination of Tubes Removed from St. Lucie Unit 1 and Investigation of the Causes of Corrosion", Proceedings of the Third International Symposium on the Environmental Degradation of Materials in Nuclear Power Systems - Water Reactors, Traverse City, MI, August 1987, pp. 449 - 459.

19. J.F. Newman, "Stress Corrosion of Alloy 600 and 690 in Acidic Sulfate Solutions at Elevated Temperatures", EPRI Report No. NP-3043, Project S191-1, October 1983.

20. W.H. Cullen, et.al., "IGA/IGSCC of Alloy 600 in Acidic Sulfate and Chloride Solutions," Proceedings of the Fifth International Symposium on the Environmental Degradation of Materials in Nuclear Power Systems - Water Reactors, Monterey, CA, August 1991, pp. 780-788.

21. W.E. Allmon and S.J. Potterton, "Conditions for the Chemical Reduction of Sulfates in an Aqueous Environment," 1985 Nuclear Chemistry Technology Update, Lynchburg, VA, November 20-22, 1985.

22. B. Sala, et.al., "Chemistry of Sulfur in High Temperature Water - Reduction of Sulfates," Proceedings of the Fifth International Symposium on the Environmental Degradation of Materials in Nuclear Power Systems - Water Reactors, Monterey, CA, August 1991, pp. 502-510.

23. P. Combrade, et.al., "Effect of Sulfur on the Protective Layers on Alloys 600 and 690 in Low and High Temperature Environments," Proceedings of the Fourth International Symposium on the Environmental Degradation of Materials in Nuclear Power Systems - Water Reactors, Jekyll Island, GA, August 1989, pp. 5-79 - 5-95.

24. R.C. Post, "OTSG -Subtask 1, Nondestructive Exam," BWNT Document No. 51-1155549-00, June 14, 1985.

25. J.B. Lumsden and P.J. Stocker, "The Relationship Between Surface Oxide Compositions and the Chemistries in Steam Generator Crevices", Proceedings of the Fourth International Symposium on the Environmental Degradation of Materials in Nuclear Power Systems - Water Reactors, Jekyll Island, GA, August 1989, pp. 6-38 - 6-51.

26. T. Sakai, et.al., "A Study of the Oxide Thin Film on Alloy 600 in High Temperature Water," Proceedings of the Fourth International Symposium on the Environmental Degradation of Materials in Nuclear Power Systems - Water Reactors, Jekyll Island, GA, August 1989, pp. 6-52 - 6-68.

27. R. Bandy et al., "Low Temperature Stress Corrosion Cracking of Alloy 600 Under Two Different Conditions of Sensitization", Corrosion Science, Volume 23, No. 9, 1983, pp. 995 - 1006.

28. M.J. Bell, "Report on Root Cause Investigation - Crystal River 3," February 1994.

29. A.K. Agrawal, et.al., "Pitting of Alloy 600 Steam Generator Tubes in Indian Point No. 3," Proceedings of the international symposium on the Environmental Degradation of Materials in Nuclear Power Systems - Water Reactors, Myrtle Beach, SC, August 22-25, 1983, pp. 223-242.

30. Personal conversations with R.H. Thompson, FPC.

31. M.W. Kendig and H.S. Isaacs, "Corrosion of Alloy 600 by Cationic Resin Beads", Nuclear Technology, Volume 55, October 1981, pp. 191 - 195.

32. G.T. Upperman, "Autoclave Tests - Inconel Specimens in Decomposed Powdex Cation Solution", B&W Report No. LR 73:6328-72:1, March 1973.

33. Jevec, J.M., et.al., "Assessment of Sulfur in Chemical Cleaning of PWR Steam Generators," EPRI Report No. NP-5026, February 1987.

EPRI REPORT

APPENDIX A

EDDY CURRENT EXAMINATION OF PULLED STEAM GENERATOR TUBES

B&W NUCLEAR SERVICE COMPANY

Special Products & Inspection Services

EDDY CURRENT EXAMINATION OF PULLED STEAM GENERATOR TUBES CRYSTAL RIVER UNIT 3

Throughout package - this statement that this cannot be reproduced. Need authorized letter from Company for reproduction for Quality.

TABLE OF CONTENTS

DISTRIBUTION

CR-3	R.E. THOMPSON
EPRI	K.J. KRZYWOSZ
BWNS-LTC	K.R. REDMOND
BWNS-SPIS	P.A. SHERBURNE
	H.L. SMITH
	DOCUMENT CONTROL (original)

B&W NUCLEAR SERVICE COMPANY
Special Products & Inspection Services

EDDY CURRENT EXAMINATION OF PULLED STEAM GENERATOR TUBES CRYSTAL RIVER UNIT 3

Prepared by: for H. L. Smith Date: 9-11-92

Reviewed by: T. E. Washburn Date: 9-11-92

Approved by: T. A. Richards Date: 9/11/92

1.0 INTRODUCTION

In May, 1992, sections of six tubes were removed from the "B" Once Through Steam Generator (OTSG) of Florida Power Corporations Crystal River Unit 3 Nuclear Station. These tubes are identified as 41-44, 52-51, 90-28, 97-91, 106-32 and 109-30. This report summarizes the bobbin coil and rotating probe results of field and laboratory eddy current examinations that were performed on these tube sections as well as provides plots of the results. A detailed description of the pulled tube sections (tube no's, lengths, regions of interest, etc.) are provided in attachments 1 through 6.

2.0 SUMMARY

The prime objectives of the examination were flaw detection and characterization, accurate location and variations in signal response with various examination techniques. The field bobbin coil eddy current examinations recorded multiple indications in the freespan region between the lower tubesheet secondary face (LTSF) and the first tube support plate (TSP). Both bobbin and/or 3-coil motorized rotating pancake coil (MRPC) examinations, performed in the laboratory, identified multiple indications in each of the tubes as reported in the field examinations. A few indications were detected in the sections of tubes where no field results existed. It is very likely that these indications are a result of the tube pull activities. The process of removing the sections of tubing did not, however, affect the multiple indications reported in the field.

3.0 EXAMINATION

Bobbin coil and MRPC probe examinations were performed prior to and following the tube pull process. The goal of this report is to provide both pre and post eddy current data in attempts to characterize any tube degradation, particularly damage associated with low signal-to-noise ratio (S/N) indications in the boiling/free span regions, for correlation with field/lab eddy current data.

The probes used for this study were Zetec .510" mag-bias universal long cone high frequency (M/ULC/HF) and Zetec .520" MRPC 3-coil probes. Eddy current data was acquired and analyzed using Zetec DDA-4 and Eddynet programs, respectively.

As was done with the field data, the bobbin differential 600 kHz primary frequency was used to normalize the voltages of all channels by setting the peak-to-peak voltage of the 4 x 100% drilled through wall (TW) holes in the calibration standard to six (6) volts.

The MRPC absolute 200 kHz primary frequency was used to normalize the voltages of all channels by setting the peak-to-peak voltage of the single 100% TW hole in the calibration standard to ten (10) volts. This normalization method is different from the field exam due to the lack of an EDM calibration standard. The alternate method specified in the guidelines was used. A difference in the measured voltage between the field and lab MRPC exams will be observed.

Table 1 lists the calibration standard used in this study. Tables 2 and 3 show the system configuration for the different probes used. As-built calibration documentation can be found in Figure 1 following Table 5.

After performing the analysis of the laboratory eddy current data, the results were compared to those obtained in the field. Tables 4 and 5 show this comparison. Graphics depicting the data derived from this comparison can be found in Appendix A for bobbin field and laboratory and Appendix B for MRPC field and laboratory results.

4.0 AXIAL AND CIRCUMFERENTIAL POSITION INFORMATION

A tube specimen holder fabricated specifically for use in securing tube specimens during eddy current examination was used for this task. A drawing is provided in Figure 2 which shows the holder and gives details on the procedure followed for positioning tubes in it for the examination.

The holders fixed and moveable grippers produce the signals used to establish the measurement scaling used to derive the axial position information of the flaws detected. The signal produced by the notch cut and copper piece attached to the tube specimen provide the landmarks used to calculate the circumferential position of the flaws detected.

The axial location of flaws is measured in inches and referenced to the bottom tube end. The circumferential location is measured in degrees and referenced to the notch cut at the zero degree location. The copper piece attached to the specmien is the zero degree location. Degrees increase in a positive manner with clockwise rotation when viewing the specimen from the copper end. Circumferential position information is presented in Table 5.

5.0 CONCLUSION

5.1 The damage mechanism present is volumetric (non-cracklike) in nature and is believed to be possible shallow outside diameter pitting.

5.2 Of the thirty (30) tube specimens examined with the bobbin coil probe the areas of interest were sections 2, 3 and 4 for all 6 pulled tubes. Section 2 consisted of the freespan area from the LTSF to the first TSP. All flaw indications reported in the field for Sections 2 were confirmed during the laboratory examination. The signature of the signals were consistent with the field data such that the tube pull process appears to not have damaged the indications of interest. The phase, amplitude and % TW of the indications correlated well with both field and laboratory examinations. An additional 15 flaw-like indications were reported during the laboratory examination for tubes 41-44, 90-28, 97-91, and 109-30. Sections 3 for tube 52-51 and 4 for all remaining tubes were reported as no detectable degradation (NDD). The area of interest for these tubes was the first TSP.

5.3 For the MRPC examination only the sections with areas of interest were examined. Thirty-eight (38) flaw indications were reported in the field and (23) flaw indications were confirmed during the laboratory examination. The field calls reported as NDD in the lab data were due to the indications not responding as a real flaw but exhibited more deposit or non-flaw characteristics.

5.4 For both bobbin and MRPC examinations the majority of flaws reported in the field were confirmed in the laboratory with no change. No new or different modes of degradation were detected.

B&W NUCLEAR SERVICE COMPANY

Special Products & Inspection Services

ATTACHMENT 1

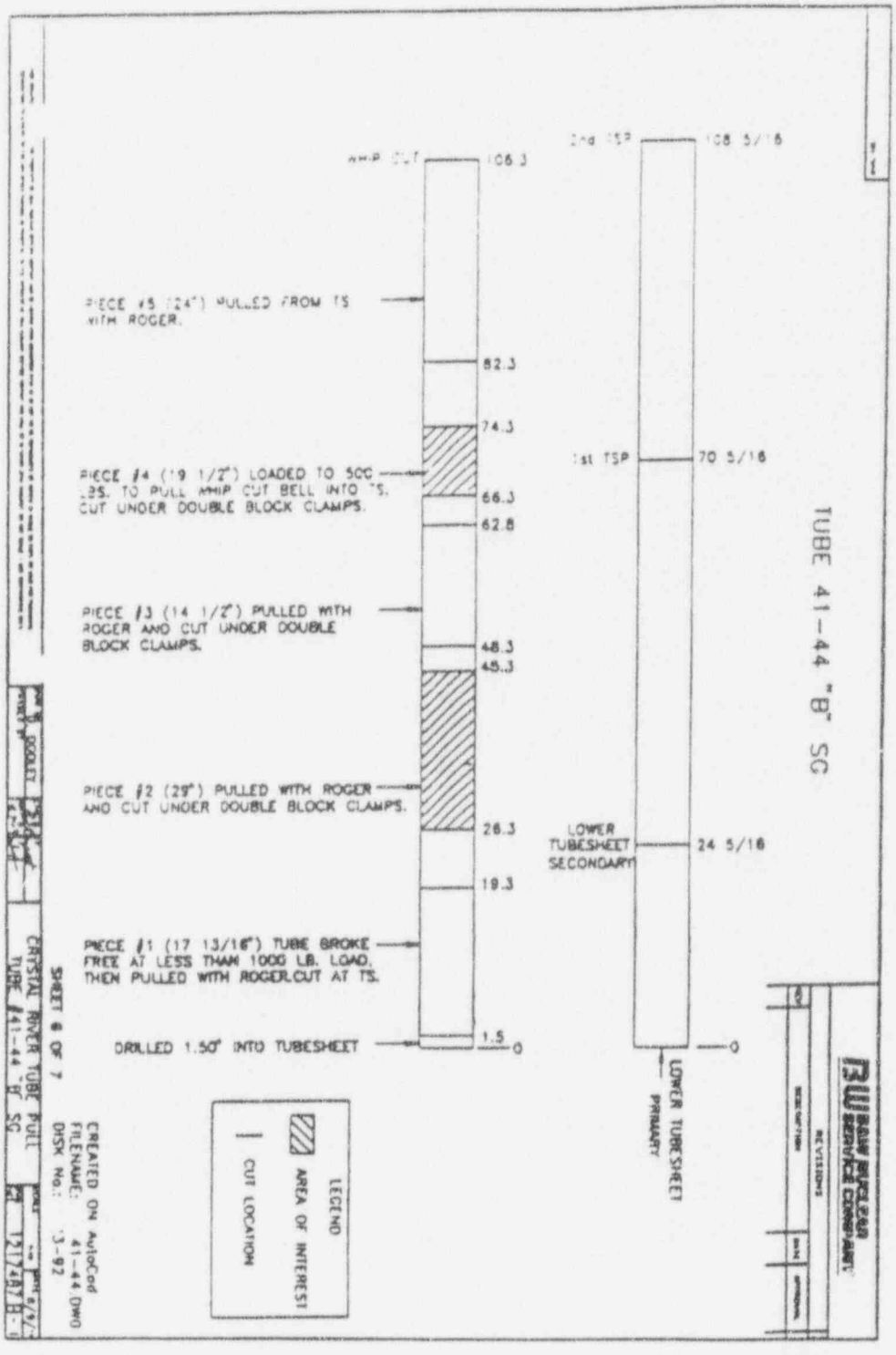

B&W NUCLEAR SERVICE COMPANY

Special Products & Inspection Services

ATTACHMENT 2

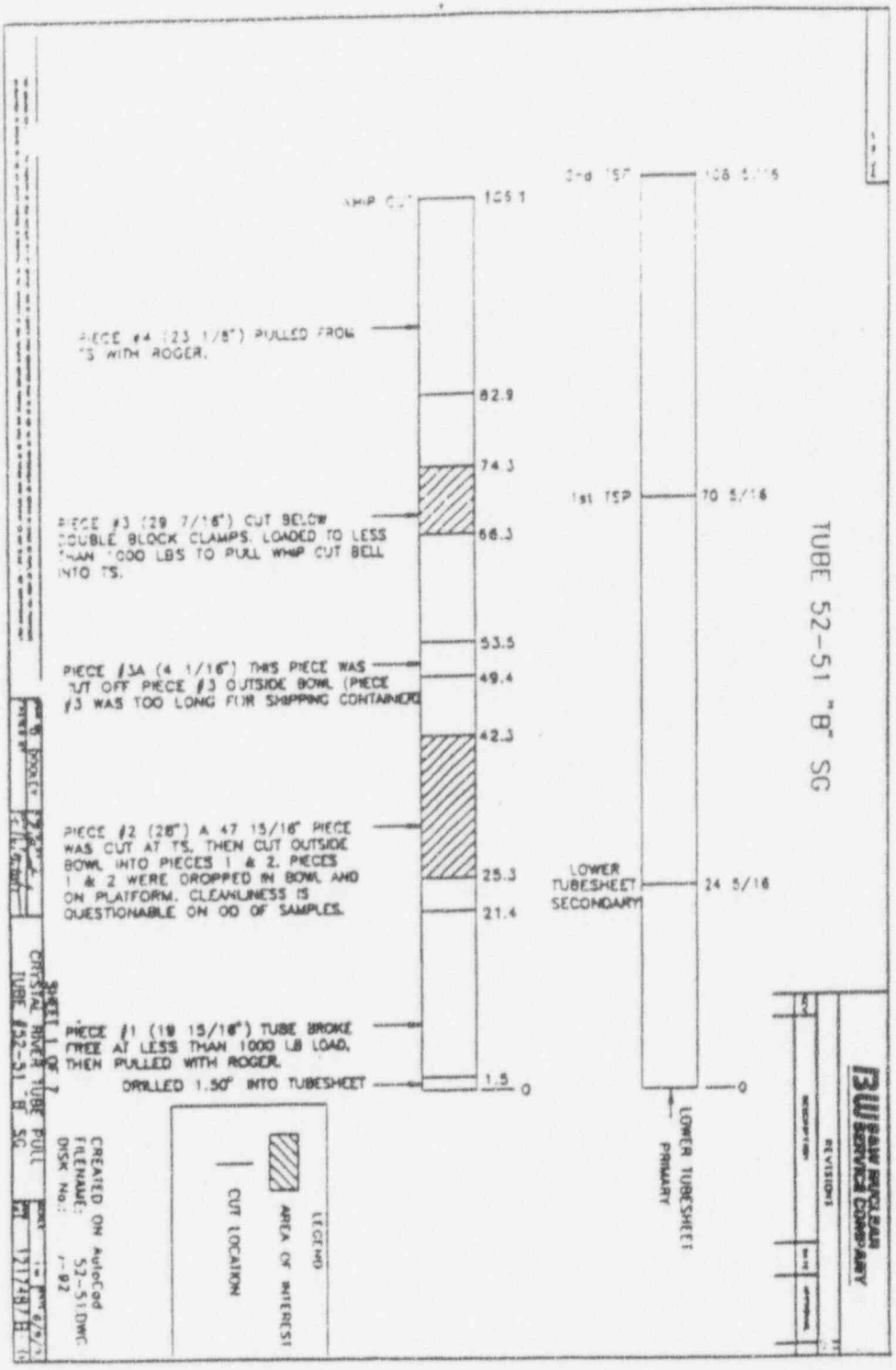

B&W NUCLEAR SERVICE COMPANY

Special Products & Inspection Services

ATTACHMENT 3

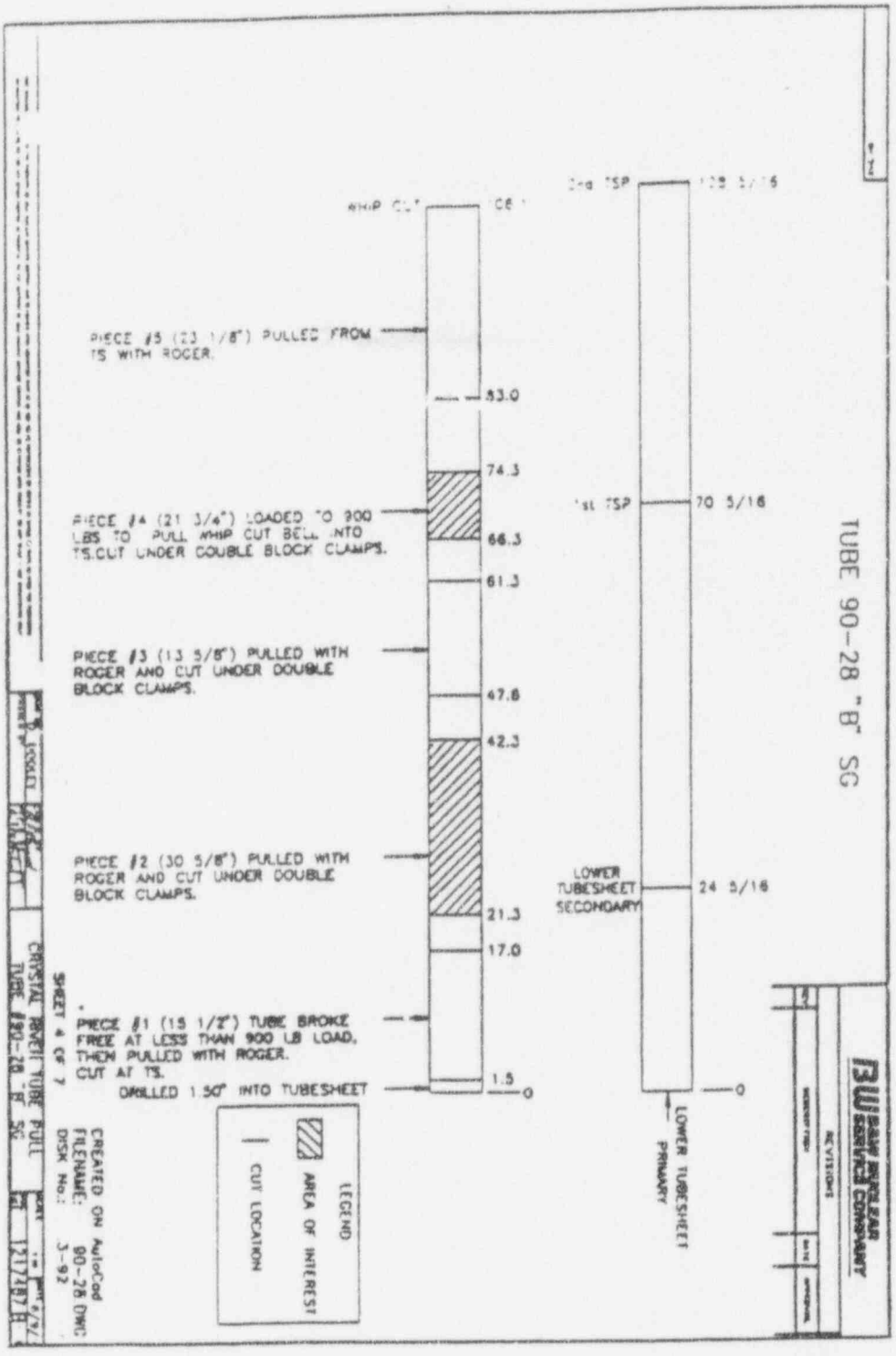

B&W NUCLEAR SERVICE COMPANY

Special Products & Inspection Services

ATTACHMENT 4

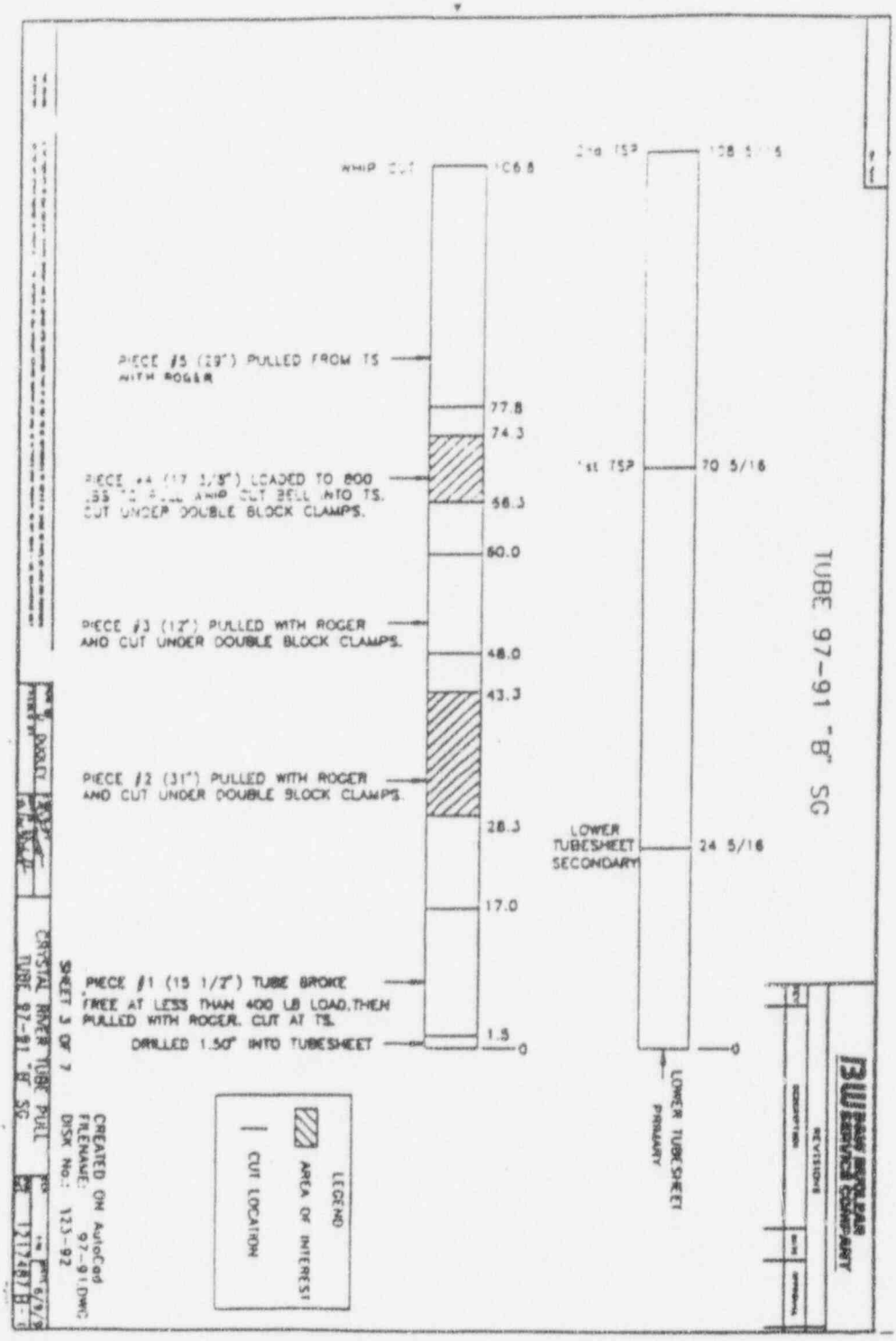

EDDY CURRENT EXAMINATION OF
PULLED STEAM GENERATOR TUBES
CRYSTAL RIVER UNIT 3

B&W NUCLEAR SERVICE COMPANY

Special Products & Inspection Services

ATTACHMENT 5

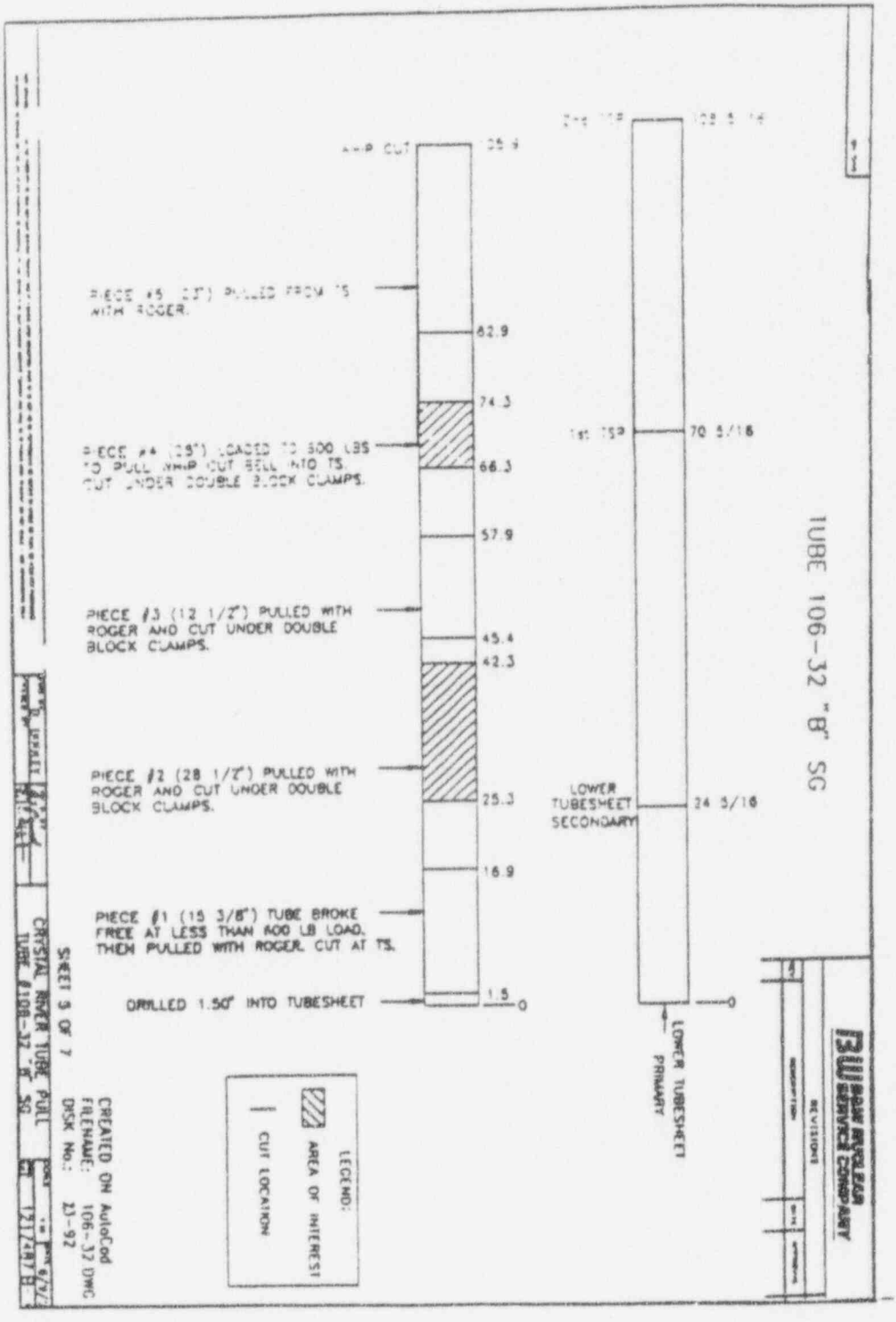

B&W NUCLEAR SERVICE COMPANY

Special Products & Inspection Services

ATTACHMENT 6

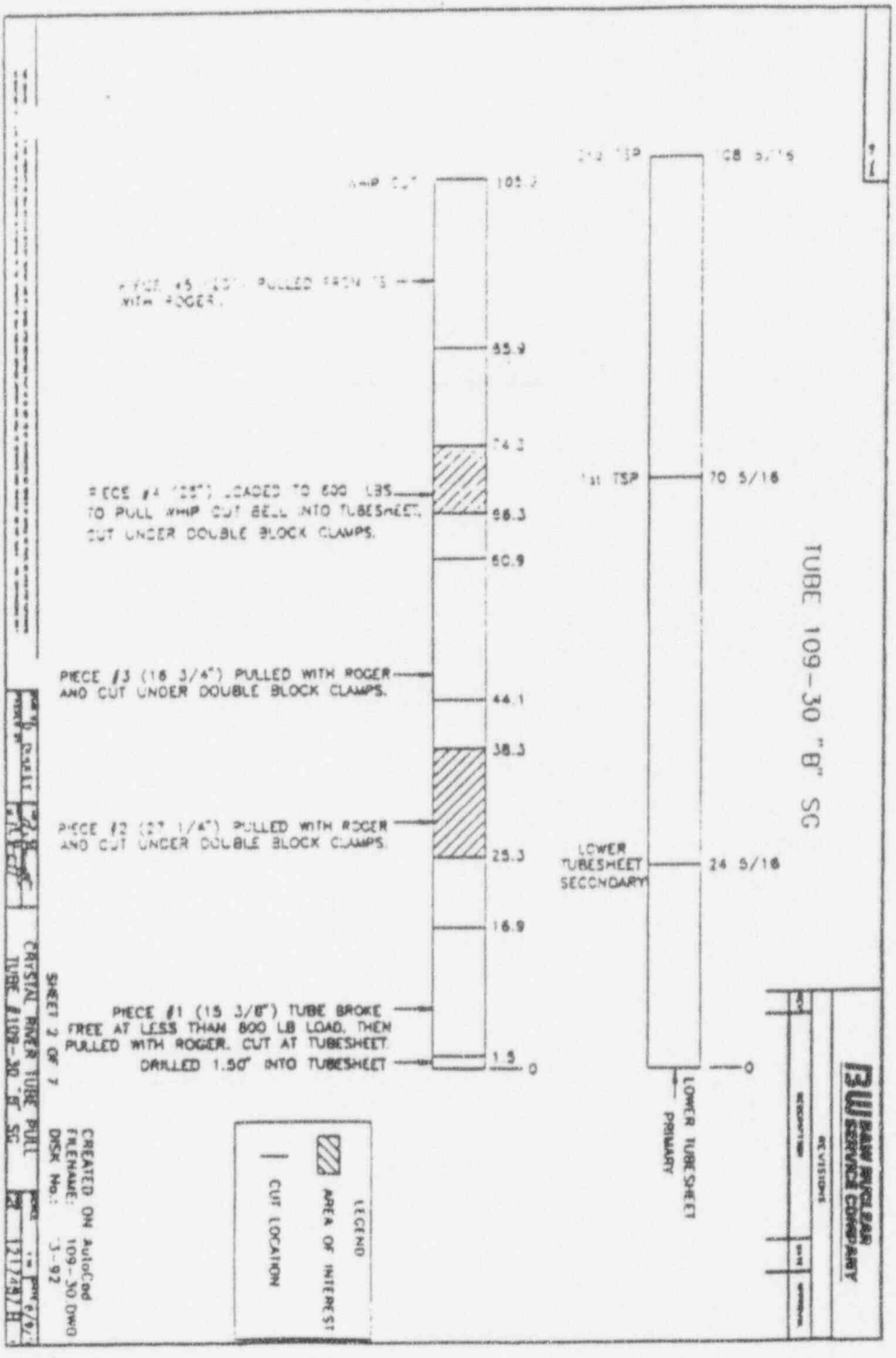

EDDY CURRENT EXAMINATION OF PULLED STEAM GENERATOR TUBES
CRYSTAL RIVER UNIT 3

DATE: 9/8/92
DWG: 1217887
REV: 0

B&W NUCLEAR SERVICE COMPANY
Special Products & Inspection Services

TABLE 1
CALIBRATION STANDARD

Calibration Standard	Reference Number
0.6285 ASME	1217345B-0

TABLE 2
SYSTEM CONFIGURATION FOR ZETEC .510 BOBBIN PROBE M/ULC/HF

	COILS							
Frequency	1	2	3	4	5	6	7	8
600	X				X			
400	X				X			
200	X				X			
35	X				X			

TABLE 3
SYSTEM CONFIGURATION FOR ZETEC .520 3-COIL PROBE

	COILS							
Frequency	1	2	3	4	5	6	7	8
300	X				X		X	
200	X				X		X	
100	X				X		X	
35	X			X		X		X

TABLE 4

BOBBIN

FIELD VS. LABORATORY EDDY CURRENT

SPECIMEN		FIELD RESULTS				LABORATORY RESULTS			
ROW-TUBE-PIECE	AREA OF INTEREST	LOCATION	VOLTS	PHASE	1992 %TW	AXIAL LOCATION++	VOLTS	PHASE	1992 %TW
41-44-2	26.3" TO 45.3"	LTSF + 6.86"	0.89	118	S/N	BTH +11.92"	0.75	120	S/N
		LTSF +12.12"	0.62	117	S/N	BTH +16.76"	0.80	120	S/N
		LTSF +15.53"	0.85	126	S/N	BTH +20.64"	0.72	120	S/N
						BTH + 9.70"*	0.45	124	S/N
						BTH +10.63"*	0.48	118	S/N
						BTH +13.86"*	0.26	119	S/N
						BTH +22.81"*	0.59	140	S/N
52-51-2	25.3" TO 42.3"	LTSF + 5.79"	0.98	148	S/N	BTH + 8.64"	0.97	154	S/N
		LTSF + 8.03"	0.52	78	S/N	BTH +10.91"	0.79	87	S/N
		LTSF + 9.22"	0.95	149	S/N	BTH +12.21"	1.02	130	S/N
		LTSF +10.12"	0.47	75	S/N	BTH +16.97"	0.35	107	S/N
90-28-2	21.3" TO 42.3"	LTSF + 6.38"	1.00	107	S/N	BTH +13.32"	0.91	99	S/N
		LTSF + 7.88"	1.73	121	46	BTH +14.78"	1.66	122	36
		LTSF +10.35"	1.07	119	S/N	BTH +17.21"	1.06	126	S/N
						BTH + 7.98"*	0.44	144	S/N
						BTH +17.65"*	0.46	100	S/N
						BTH +18.61"*	0.46	116	S/N
						BTH +18.99"*	1.07	132	S/N
						BTH +19.72"*	0.66	143	S/N
						BTH +21.39"*	1.12	130	S/N
						BTH +21.92"*	0.65	91	S/N
						BTH +23.66"*	1.08	164	S/N
97-91-2	28.3" TO 43.3"	LTSF + 8.28"	0.88	90	76	BTH +15.54"	0.75	113	44
		LTSF + 8.56"	0.65	110	S/N	BTH +15.82"	0.79	124	S/N
		LTSF +14.28"	0.71	106	63	BTH +19.19"	0.64	91	62
						BTH +21.89"*	0.93	103	52
						BTH + 5.58"*	0.51	161	S/N
106-32-2	25.3" TO 42.3"	LTSF + 5.76"	0.84	135	S/N	BTH + 9.13"	0.50	136	S/N
		LTSF + 8.22"	0.34	138	S/N	BTH +12.89"	0.70	167	S/N
		LTSF + 9.48"	0.55	156	S/N	BTH +14.19"	0.74	144	S/N
		LTSF +10.91"	0.48	147	S/N	BTH +10.80"	0.56	155	S/N
		LTSF +11.24"	0.34	131	S/N	BTH + 8.76"	0.71	122	S/N
		LTSF +12.82"	0.57	162	S/N	BTH + 7.27"	0.67	153	S/N
		LTSF +14.34"	0.30	110	S/N	BTH + 5.90"	0.73	160	S/N
109-30-2	25.3" TO 33.3"	LTSF + 5.66"	0.79	150	S/N	BTH +13.11"	0.80	159	S/N
		LTSF + 7.99"	0.94	133	30	BTH +15.39"	0.94	131	27
		LTSF + 9.22"	0.31	132	S/N	BTH +16.62"	0.35	138	S/N
		LTSF + 9.78"	0.60	150	S/N	BTH +17.17"	0.54	148	S/N
						BTH +25.45"*	0.33	131	S/N

*ADDITIONAL LOCATIONS REPORTED DURING LAB ANALYSIS

++AXIAL LOCATION IS MEASURED FROM THE BOTTOM TUBE END

NOTE: ALL PIECE 4'S FOR EACH TUBE EXHIBITED NO DETECTABLE DEGRADATION (NDD)

TABLE 5

MRPC

FIELD VS. LABORATORY EDDY CURRENT

SPECIMEN		FIELD RESULTS				LABORATORY RESULTS				CIRCUMFERENTIAL LOCATION TOP(NOTCH) = 0 DEGREES++
ROW-TUBE-PIECE	AREA OF INTEREST	LOCATION	VOLTS	PHASE	1992 %TW	AXIAL LOCATION++	VOLTS	PHASE	1992 %TW	
41-44-2	26.3" TO 45.3"	LTSF + 4.99"	1.44	115	S/N				NDD	
		LTSF + 5.93"	2.02	37	S/N				NDD	
		LTSF + 7.20"	2.06	125	S/N	BTH +14.11"	0.77	74	S/N	130 DEG
		LTSF +11.89"	2.59	29	S/N	BTH +19.78"	1.76	39	S/N	0 DEG
		LTSF +13.37"	1.61	72	S/N	BTH +21.62"	0.86	60	S/N	270 DEG
		LTSF +15.50"	1.89	65	S/N	BTH +24.26"	1.23	59	S/N	0 DEG
		LTSF +17.63"	2.04	67	S/N	BTH +26.74"	0.92	111	S/N	270 DEG
52-51-2	25.3" TO 42.3"	LTSF + 5.90"	0.17	108	S/N				NDD	
		LTSF + 6.22"	1.83	108	S/N	BTH + 8.14"	0.88	103	S/N	100 DEG
		LTSF + 8.01"	0.24	57	S/N	BTH +10.68"	1.13	64	S/N	180 DEG
		LTSF + 8.47"	2.42	45	S/N				NDD	
		LTSF + 9.25"	0.12	52	S/N				NDD	
		LTSF + 9.75"	1.61	30	S/N				NDD	
		LTSF +10.00"	0.14	142	S/N	BTH +13.00"	0.35	125	S/N	0 DEG
		LTSF +10.57"	0.90	70	S/N				NDD	
90-28-2	21.3" TO 42.3"	LTSF + 6.21"	0.41	12	S/N				NDD	
		LTSF + 6.33"	2.09	85	S/N	BTH +13.22"	0.96	91	S/N	130 DEG
		LTSF + 7.79"	3.93	15	S/N	BTH +14.89"	0.92	86	S/N	90 DEG
		LTSF + 7.95"	0.23	22	S/N	BTH +17.25"	0.71	70	S/N	210 DEG
		LTSF + 9.12"	0.31	57	S/N	BTH +18.54"	1.47	76	S/N	200 DEG
		LTSF +10.15"	2.70	54	S/N	BTH +21.28"	0.58	52	S/N	220 DEG
						BTH +23.07"*	0.76	45	S/N	290 DEG
97-91-2	28.3" TO 43.3"	LTSF + 8.66"	0.35	82	S/N	BTH +15.82"	1.09	117	S/N	310 DEG
		LTSF + 8.95"	0.17	72	S/N	BTH +15.51"	1.00	114	S/N	310 DEG
		LTSF +12.15"	0.21	43	S/N	BTH +19.17"	1.74	69	S/N	310 DEG
		LTSF +14.84"	0.36	57	S/N	BTH +21.88"	1.41	71	S/N	340 DEG
						BTH +19.27"*	0.51	68	S/N	310 DEG
106-32-2	25.3" TO 42.3"	LTSF + 5.77"	0.32	101	S/N	BTH +12.74"	1.12	133	S/N	180 DEG
		LTSF + 6.35"	0.37	92	S/N	BTH +14.00"	0.94	73	S/N	320 DEG
		LTSF + 8.17"	0.25	101	S/N	BTH +16.12"	0.61	127	S/N	180 DEG
		LTSF + 8.85"	0.19	8	S/N				NDD	
		LTSF + 9.09"	0.20	87	S/N	BTH +16.36"	0.84	97	S/N	160 DEG
		LTSF + 9.81"	0.12	80	S/N				NDD	
		LTSF +10.13"	0.27	93	S/N				NDD	
		LTSF +10.78"	0.15	45	S/N				NDD	
		LTSF +11.88"	0.14	61	S/N				NDD	
		LTSF +12.12"	0.12	41	S/N				NDD	
		LTSF +13.41"	0.13	76	S/N	BTH +18.20"	0.69	88	S/N	350 DEG
						BTH +17.77"*	0.92	132	S/N	170 DEG
109-30-2	25.3" TO 33.3"	LTSF + 8.47"	0.13	67	S/N	BTH +16.59"	0.42	58	S/N	150 DEG
		LTSF + 9.66"	0.28	88	S/N				NDD	

*ADDITIONAL LOCATIONS REPORTED DURING LAB ANALYSIS

+AXIAL LOCATION IS MEASURED FROM THE BOTTOM TUBE END

++CIRCUMFERENTIAL LOCATION IS MEASURED IN DEGREES. THE COPPER PIECE ATTACHED TO THE SPECIMEN IS THE ZERO-DEGREE LOCATION. DEGREES INCREASE IN A POSITIVE MANNER WITH CLOCKWISE ROTATION WHEN VIEWING THE SPECIMEN FROM THE COPPER PIECE.

B&W NUCLEAR SERVICE COMPANY

Special Products & Inspection Services

FIGURE 1

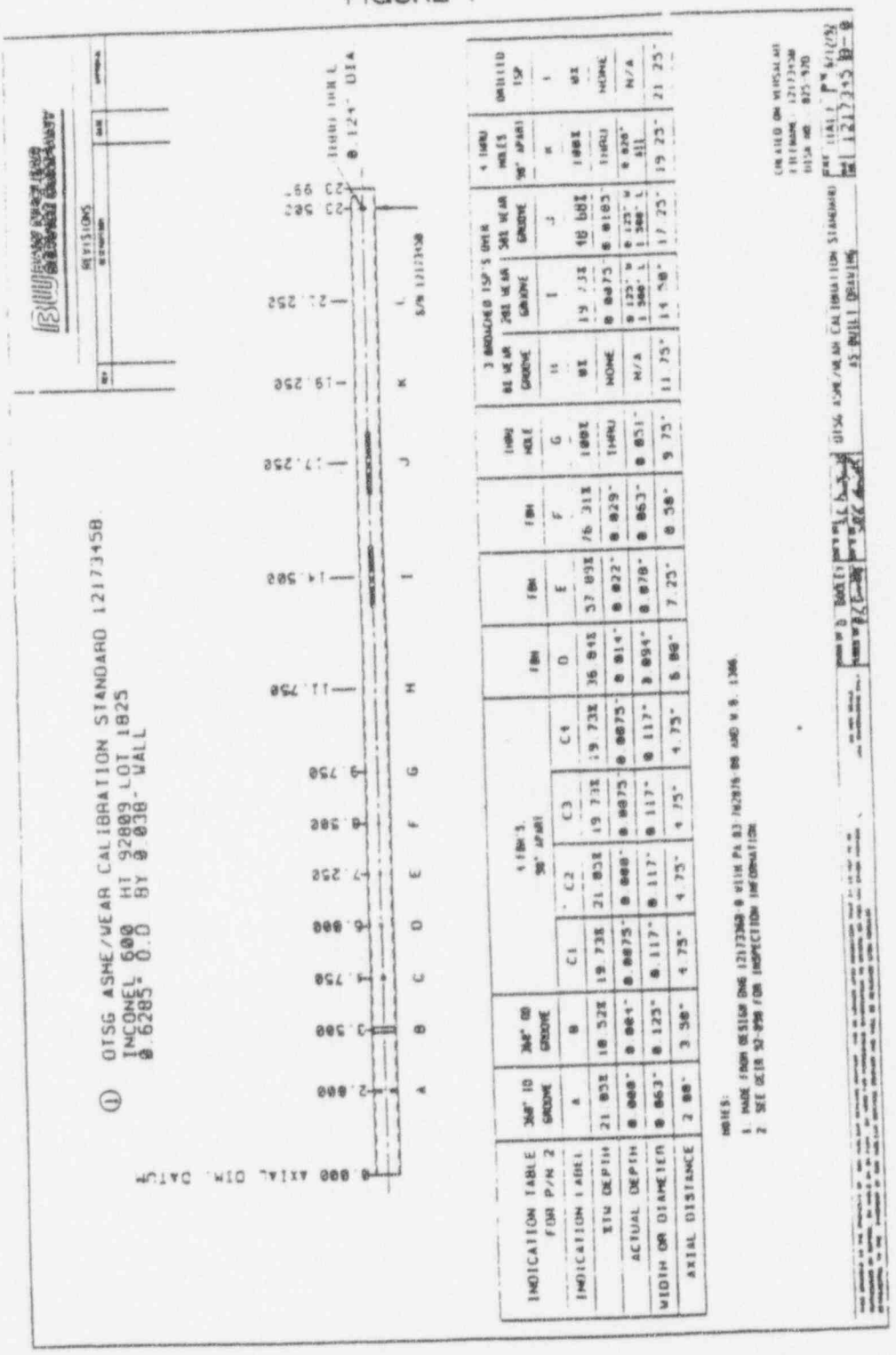

B&W NUCLEAR SERVICE COMPANY
Special Products & Inspection Services

FIGURE 2

TUBE SAMPLE HOLDER DESCRIPTION

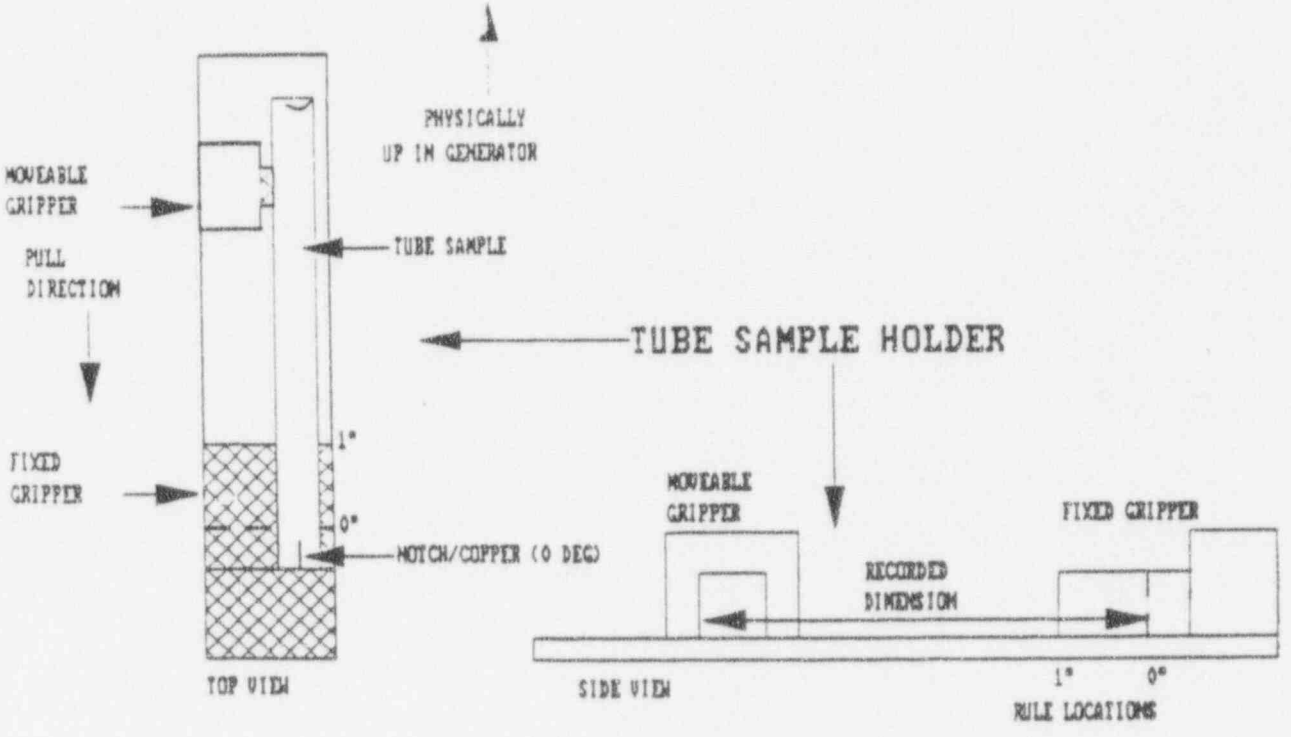

NOTES:

1. Notched at tube lower end as installed in generator.
2. Notch positioned up in all cases at fixed holder end/probe driver end.
3. All measurements in inches.

EPRI REPORT

APPENDIX B

EPRI NDE CENTER REVIEW OF ECT DATA

EPRI NDE CENTER

Electric Power Research Institute
Nondestructive Evaluation Center — *Leadership in Technology Transfer*

March 24, 1993

Mr. Paul Sherburne
B&W Nuclear Service Company
155 Mill Ridge Road
Lynchburg, VA 24502-4341

SUBJECT: Review of Successive Eddy Current Data on Pulled Steam Generator Tubes From Crystal River Unit 3

Dear Paul:

To resolve questions involving occurrence and growth, if any, of patches of intergrannular attack (IGA) noted in the pulled steam generator tubes at Crystal River Unit 3 (CR3), the subject data review was performed at the EPRI NDE Center.

Also, issues related to eddy current flaw detection and sizing capabilities were addressed in this letter report.

Please contact me if you have any questions upon reviewing the contents of this letter report.

Sincerely,

Kenji Krzywosz
Manager, Heat Exchanger Inspection
EPRI NDE Center

KK:mph

cc: P. Paine, EPRI
M. Behravesh, EPRI
R. Thompson, FPC
R. Stone
F. Ammirato
G. Henry

1300 Harris Boulevard • Charlotte, North Carolina 28262 • Telephone: (704) 547-6100
(P.O. Box 217097, Charlotte, North Carolina 28221) • FAX: (704) 547-6168

Evaluation of Pulled Steam Generator Tubes from Crystal River 3

Background

In order to ascertain if the noted patches of intergrannular attack (IGA) were attributed to a one-time occurrence or continuing activity at Crystal River Unit 3 (CR3), three successive eddy current outage data were reviewed. Of the six pulled tubes from "B" steam generator, only three tubes were identified as having been eddy current tested in '89, '90, and '92 outages. They were tubes 52-51, 109-30, and 106-32. Consequently, their analysis results were analyzed and compared. Since the B&W data analysis guidelines call for the use of the 600 kHz differential channel to report quantifiable indications with a signal-to-noise ratio of 5, this channel was selected for comparison. To compare three successive outage data acquired by different diameter size probes and varying lengths of extension cable, eddy current signals from a 100% calibration hole were normalized to 5 volts peak-to-peak at phase angle of 40^0. All flaw locations were referenced in the positive upward direction from the lower tube sheet interface toward the first tube support plate location.

IGA Status and Occurrence

Attachment A shows data comparison of signal amplitude and phase angle measurements from 21 indications representing IGA patches. There were no new detectable IGA indications based on the review of three successive outage data. The same number of eddy current indications confirmed as IGA patches by metallurgical test results in 1992/1993 were also present in 1989. Consequently, the observed IGA patches were already present prior to 1989.

Any growth or active damage form typically results in higher eddy current signal amplitude, accompanied by reduction in the phase angle. The net result is the overall increase in the percent wall loss. Evaluation results showed just the opposite effect of decreased signal amplitude. The percent wall loss, however, increased slightly. This amplitude reduction is attributed more likely to a combined effect of tube conditions, signal quality, and differences in the eddy current measurements. The increased percent wall loss of 9 percent is also considered well within the sizing error band. Therefore, it is concluded that the IGA patches have not grown, but remained stable and dormant.

Eddy Current Flaw Detection

To determine the capability of eddy current to detect IGA patches, all of the reported metallurgical test results were tabulated in Attachment B along with the associated bobbin

coil analysis results. Due to the active bobbin coil area with axial extent of around 0.200 inch, any multiple metallurgical test results of less than 0.200-inch apart were combined as one flaw for comparison. The following correction factors were added to the bobbin coil locations in order to compare with the reported metallurgical test results: 2.91 inches for Tube 52-51; 7.41 inches for Tubes 109-30 and 106-32; and 7.31 inches for tube 90-28.

Figure 1 shows a distribution of IGA patches by different percent wall losses from primarily the following three tubes: Tubes 52-51, 106-32, and 90-28. Only two points were available for inclusion from Tube 109-30. There was a total of 23 IGA patches exhibiting 40% and greater wall losses, while the remaining 30 IGA patches exhibited less than the 40% repair limit. The IGA distribution peaked in the 40-49% wall loss range. Using the information presented in the figure, the percentage of IGAs detected by bobbin coils was next plotted at each respective flaw depth range. This IGA percent detection by bobbin coils is shown as Figure 2. In general, the plot shows any IGAs in excess of 45% wall loss are reliably detected 80% of the time.

Next, the IGA detection capability of bobbin coils was compared to the motorized rotating pancake coil (MRPC). The tabulated number of respective eddy current indications by each tube was compared to the number of metallurgical test results.

Tube	Bobbin Coils	MRPC	Met Results
90-28	11	13	18
106-32	12	17	22
109-30	2	2	2
52-51	7	9	11
Total	32	41	53
% Detected	60	77	

Based on the comparison, the IGA patches were better detected with the MRPC. One drawback is its slow inspection speed. The reported number of MRPC indications were previously included in my January 12, 1993, correspondence to Rocky Thompson. It should be noted that the number of bobbin coil indications also increased. This increase was attributed to 1989 bobbin coil data, which clearly confirmed some of the questionable indications not originally reported from the May, 1992, field data.

Eddy Current Flaw Sizing

To evaluate the accuracy of bobbin coils to size IGA patches, eddy current depth estimates were compared with metallurgical test results. Table B also shows the comparative analysis results by each outage. Tube 90-28 test results were also included in the '92 outage analysis. Sizing accuracy was evaluated using a linear regression analysis by comparing eddy current estimates to metallurgical test results. Three statistically derived values were

evaluated. These include correlation coefficient, root-mean-square (RMS) error, and slope of the linear regression (best fit) line. Flaw sizing accuracy increases as the value of best-fit slope and correlation coefficient increases. However, sizing precision decreases with increasing RMS error values. For optimal flaw sizing, a correlation coefficient of greater than 80% with RMS error of less than 20% is desirable. Under this condition, the slope of the best-fit line generally falls between 0.8 and 1.2.

Calculated statistical values from Attachment B show that 600 kHz eddy current analysis procedure offers no reliable flaw sizing. The tabulated statistical values are listed below.

Linear Regression Analysis by Each Outage

	3/18/89	4/30/90	5/14/92	5/14/92
Correlation Coefficient	1%	-8%	8%	25%
Root-Mean-Square (RMS) Error	28%	34%	31%	27%
Slope of Best Fit Line	0.032	-0.314	0.278	0.646
Mean Met Wall Loss (X)	40%	40%	40%	36%
Mean Eddy Current Wall Loss (Y)	30%	33%	33%	30%
No. of Flaws	21	21	21	32

Even after including 11 additional points from Tube 90-28, the best statistical values obtained were 25% correlation and 27% RMS error with a slope of 0.646. These results, illustrated graphically as Figure 3, show high degrees of scatter in sizing IGA patches. A similar comparison at 400 kHz showed no improvements in flaw sizing. If axial positions associated with the reported metallurgical test results and eddy current analysis results were indeed accurate, no viable eddy current analysis procedure was demonstrated for estimating IGA wall losses. It should be mentioned that this condition is not unique to CR3 but applicable to the whole industry. Currently, no reliable procedure exists for estimating IGAs.

Summary

Review of the successive eddy current data indicated that observed IGA patches were already present in 1989. No evidence of growth as applied to either existing or new IGAs was noted. IGA patches were better detected than sized. In addition, the MRPC detected IGA patches better than bobbin coils. No reliable IGA depth estimate was demonstrated with the bobbin coil.

Observations

Signal quality of the '89 data was superior in comparison to the '92 data, despite the smaller diameter probe size. The latest data was "noisier". Consequently, the 400 kHz data in both differential and absolute forms was better suited for identifying IGA patches than the

600 kHz data. For sizing IGA patches, the 600 kHz data should still be used in the free-span regions. Therefore, truly high frequency probes which operate optimally at 600 kHz should be used after factoring the known length of the probe extension cable. Adding extension cable without considering its effect on probe performance will result in the lowering of the optimal operating frequency and reduced eddy current sensitivity.

Attachment A - Comparative Analysis of Eddy Current Signals

52-51 Locations(A)	3/18/89 Volt/Phase/%(B)	4/30/90 Volt/Phase/%(B)	5/14/92 Volt/Phase/%(B)	Met Locations/%(C)
6.38/6.43/6.21	0.89/148/2	0.62/153/0	0.62/148/16	9.12-9.34/34
8.66/8.64/8.48	0.47/94/66	0.57/92/68	0.33/79/82	11.39-11.57/53(2)
9.89/9.87/9.66	0.88/139/17	0.75/136/21	0.61/150/13	12.57-12.78/52(2)
10.77/10.73/10.59	0.19/80/77	0.24/47/96	0.30/66/89	13.50-13.68/45(2)
12.2/12.07/11.91	0.19/66/86	0.22/45/97	0.16/62/91	14.82-15.11/40(2)
12.95/12.86/12.72	0.43/161/0	0.26/162/0	0.32/164/0	15.63-15.86/33(2)
14.53/14.5/14.32	0.33/119/43	0.29/105/57	0.35/152/9	17.23-17.44/33
109-30 Locations	**3/18/89 Volt/Phase/%**	**4/30/90 Volt/Phase/%**	**5/14/92 Volt/Phase/%**	**Met Locations/%**
6.04/6.29/6.13	0.67/153/0	0.67/157/0	0.54/153/8	No met
8.34/8.54/8.46	0.75/125/36	0.66/126/35	0.65/137/31	15.75-15.95/50
9.52/9.77/9.66	0.33/131/28	0.27/129/31	0.23/135/33	No met
10.09/11.13/10.16	0.43/141/13	0.50/135/23	0.35/132/37	17.5-18.54/40
10.91/11.13/-	0.18/126/35	0.16/117/45	-	No met
12.72/12.95/12.87	0.13/45/97	0.27/53.93	0.18/26/60	No met
14.84/15.17/15.15	0.32/20/50	0.36/28/70	0.20/32/74	No met
106-32 Locations	**3/18/89 Volt/Phase/%**	**4/30/90 Volt/Phase/%**	**5/14/92 Volt/Phase/%**	**Met Locations/%**
6.32/6.32/6.35	0.62/141/13	0.86/147/2	0.58/138/30	13.73-13.76/49(3)
6.87/6.80/6.96	0.83/164/0	0.93/165/0	0.63/176/0	14.21-14.37/51(2)
7.58/7.57/7.71	0.35/145/6	0.42/132/25	0.40/167/0	14.98-15.12/25(4)
8.01/7.97/8.09	0.39/11/27	0.38/15/37	0.26/22/51	15.38-15.50/24
8.69/8.67/8.78	0.33/126/35	0.27/124/35	0.23/138/30	16.08-16.19/40(2)
8.94/8.91/9.01	0.19/74/81	0.21/39/95	0.14/82/80	16.32-16.42/29
9.71/9.68/9.73	0.49/150/0	0.60/145/4	0.29/152/9	17.09-17.14/38
9.98/9.97/---	0.46/139/16	0.50/146/4	0.34/157/1	17.38-17.39/40
11.34/11.33/11.44	0.35/127/34	0.53/146/4	0.32/150/13	18.74-18.85/42(2)
11.71/11.71/11.78	0.55/134/24	0.65/134/22	0.24/133/36	19.12-19.19/46(2)
13.09/13.20/13.34	0.57/133/25	0.58/140/14	0.36/150/13	20.5-20.75/39(3)
14.63/14.56/14.81	0.22/101/61	0.43/117/44	0.20/110/59	21.97-22.22/36(3)

Notes: (A) Eddy current flaw locations of respective tube from each outage
(B) 600 kHz eddy current data and flaw depth estimates
(C) Adjusted locations and associated met results, (X) indicates multiple # of indications

	3/18/89	4/30/90	5/14/92	Difference
Average Peak-to-Peak Volt	0.472	0.499	0.366	-23%
Average Phase Angle	120	117	127	+6%
Average Percent Wall Loss	30	33	33	+9%

Attachment B - IGA Detection and Sizing by Eddy Current

52-51 Locations (A)	3/18/89 Volt/Phase/% (B)	4/30/90 Volt/Phase/% (B)	5/14/92 Volt/Phase/% (B)	Met Locations/% (C)
6.38/6.43/6.21	0.89/148/2	0.62/153/0	0.62/148/16	9.06/34
8.66/8.64/8.48	0.47/94/66	0.57/92/68	0.33/79/82	11.37,11.63/53
9.89/9.87/9.66	0.88/139/17	0.75/136/21	0.61/150/13	12.63/52
10.77/10.73/10.59	0.19/80/77	0.24/47/96	0.30/66/89	13.50,13.63/45
NDD				14.0/13%
12.2/12.07/11.91	0.19/66/86	0.22/45/97	0.16/62/91	14.88,15.06/40
12.95/12.86/12.72	0.43/161/0	0.26/162/0	0.32/164/0	15.69/33
NDD				16.69/18
14.53/14.5/14.32	0.33/119/43	0.29/105/57	0.35/152/9	17.25/33
NDD				17.94/26
NDD				19.13/32

109-30 Locations	3/18/89 Volt/Phase/%	4/30/90 Volt/Phase/%	5/14/92 Volt/Phase/%	Met Locations/%
6.04/6.29/6.13	0.67/153/0	0.67/157/0	0.54/153/8	No met
8.34/8.54/8.46	0.75/125/36	0.66/126/35	0.65/137/31	15.88-15.96/50
9.52/9.77/9.66	0.33/131/28	0.27/129/31	0.23/135/33	No met
10.09/11.13/10.16	0.43/141/13	0.50/135/23	0.35/132/37	17.5-17.56/40
10.91/11.13/-	0.18/126/35	0.16/117/45	-	No met
12.72/12.95/12.87	0.13/45/97	0.27/53.93	0.18/26/60	No met
14.84/15.17/15.15	0.32/20/50	0.36/28/70	0.20/32/74	No met

106-32 Locations	3/18/89 Volt/Phase/%	4/30/90 Volt/Phase/%	5/14/92 Volt/Phase/%	Met Locations/%
NDD				12.75/14
6.32/6.32/6.35	0.62/141/13	0.86/147/2	0.58/138/30	13.81,13.94/49
6.87/6.80/6.96	0.83/164/0	0.93/165/0	0.63/176/0	14.38/51
NDD				14.63,14.81/18
7.58/7.57/7.71	0.35/145/6	0.42/132/25	0.40/167/0	15.00-15.19/25
8.01/7.97/8.09	0.39/11/27	0.38/15/37	0.26/22/51	15.44/24
8.69/8.67/8.78	0.33/126/35	0.27/124/35	0.23/138/30	16.18,16.19/40
8.94/8.91/9.01	0.19/74/81	0.21/39/95	0.14/82/80	16.44/29
9.71/9.68/9.73	0.49/150/0	0.60/145/4	0.29/152/9	17.19/38
9.98/9.97/---	0.46/139/16	0.50/146/4	0.34/157/1	17.50/40
NDD				17.94,18.0/16
NDD				18.19,18.25/22
NDD				18.36-18.56/36
11.34/11.33/11.44	0.35/127/34	0.53/146/4	0.32/150/13	18.75/42
11.71/11.71/11.78	0.55/134/24	0.65/134/22	0.24/133/36	19.13,19.25/46
NDD				19.81/19
13.09/13.20/13.34	0.57/133/25	0.58/140/14	0.36/150/13	20.69/31
NDD				20.94,21.06/39
14.63/14.56/14.81	0.22/101/61	0.43/117/44	0.20/110/59	21.81,22.13/36
NDD				22.31-22.50/22
NDD				23.00,23.13/31
NDD				24.00,24.13/17

Attachment B (Cont'd)

90-28 Locations	5/14/92 Volt/Phase/%	Met Locations/%
6.46	0.73/109/59	13.56,13.69/56
7.98	1.26/123/44	15.31/50
10.39	0.75/122/46	17.63,17.69/53
10.65	0.32/124/43	17.88/46
NDD		18.25/18
11.59	0.25/115/53	18.80,19.06/27
11.93	0.79/138/24	19.25/45
NDD		19.75/45
12.76	0.42/144/14	20.31/23
NDD		20.44/28
NDD		20.69/53
14.36	0.90/128/38	21.50,21.56/49
14.84	0.35/112/56	21.88,22.06/62
NDD		22.56/30
15.78	0.09/130/36	23.00/30
NDD		23.56/49
16.50	0.50/158/0	23.63/24
NDD		24.69/51

Notes: (A) Eddy current flaw locations of respective tube from each outage
(B) 600 kHz eddy current data and flaw depth estimates
(C) Actual met locations and met results
NDD - No detectable degradations

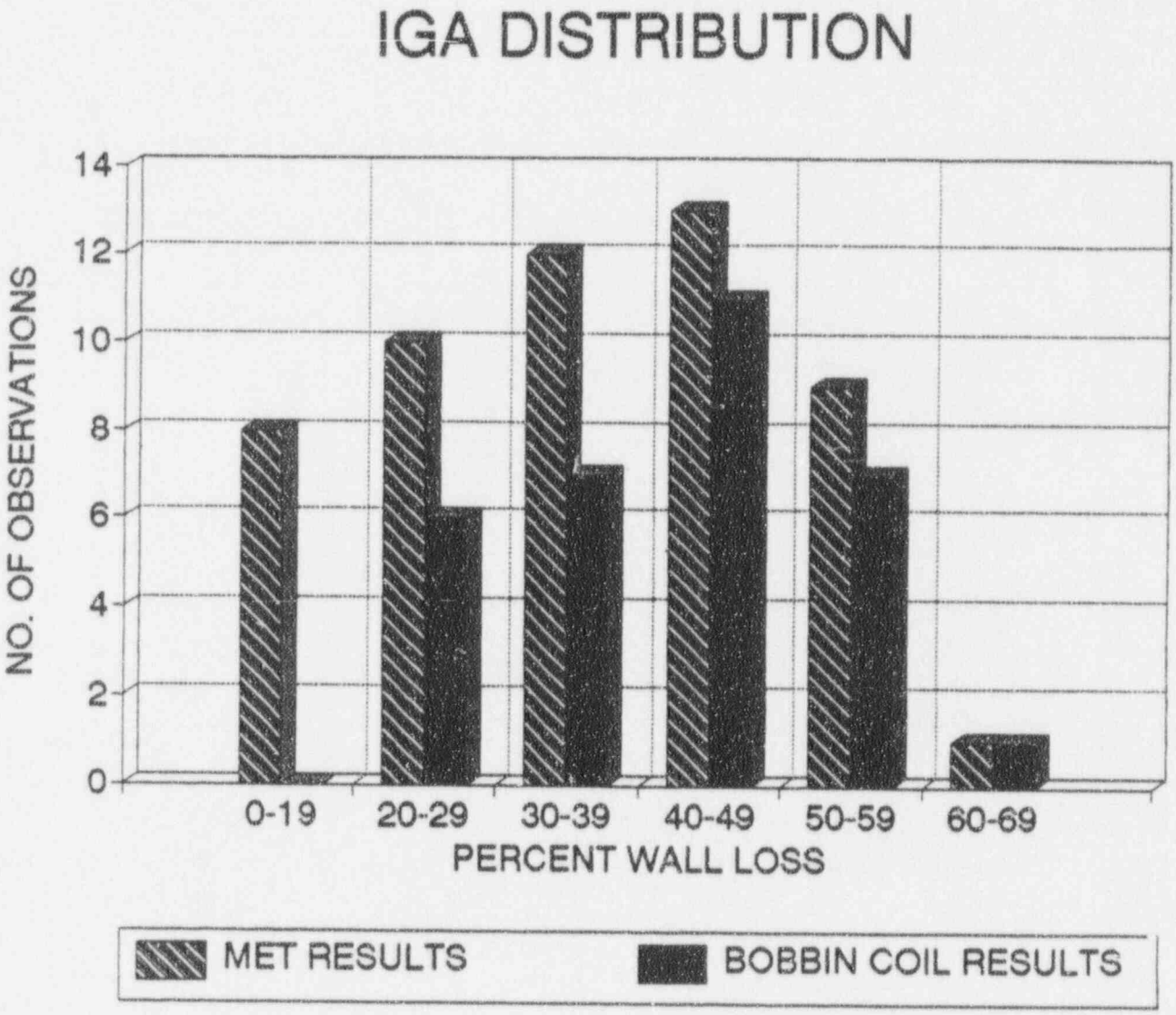

Figure 1 - IGA distribution by depths based on the metallurgical and eddy current test results from the four pulled tubes

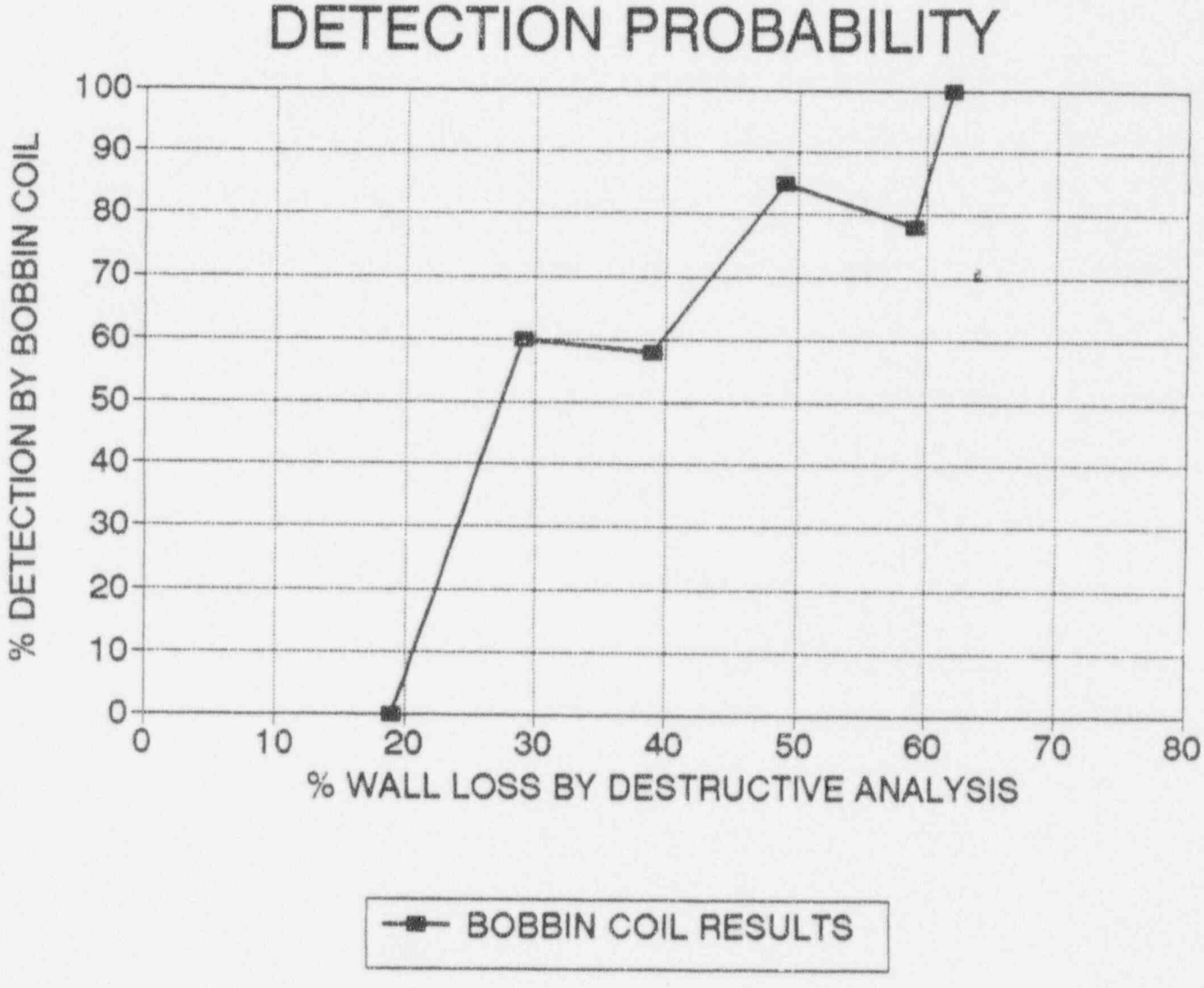

Figure 2 - IGA percent detection at various depths by bobbin coils

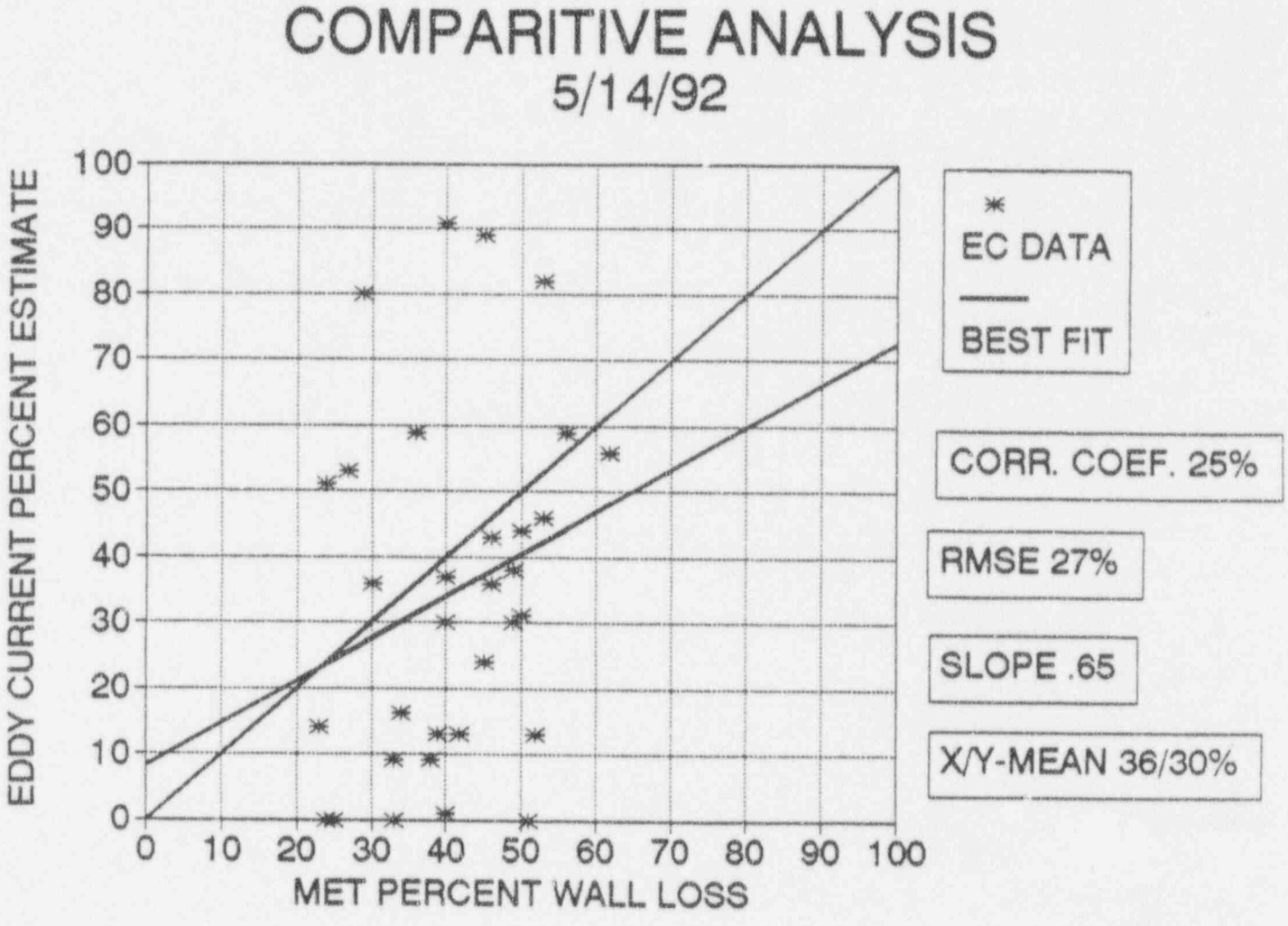

Figure 3 - Linear regression analysis of eddy current bobbin coil estimates versus metallurgical test results

EPRI REPORT

APPENDIX C

CHEMISTRY SUPPORT FOR CRYSTAL RIVER-3 PULLED TUBE EXAMINATION

Appendix C

CHEMISTRY SUPPORT FOR CRYSTAL RIVER UNIT 3 PULLED TUBE EXAMINATION

Prepared by

Adams & Hobart
Consulting Engineers
46738 Fremont Boulevard
Fremont, CA 94538

1.0 Introduction

1.1 Scope of Work

Adams & Hobart was contracted by Florida Power Corporation and the Electric Power Research Institute to support Babcock & Wilcox with the pulled tube evaluation for Crystal River Unit 3. That support consisted of the following tasks:

A. Review accessible chemistry data from 1977 through 1982 and attempt to correlate water chemistry history with pulled tube destructive examinations and surface analyses.

B. Review hideout return chemistry data from 1988 to the present to evaluate the risk of initiating or propagating IGA under current operation conditions.

Information from both tasks was integrated to develop an hypothesis of plant operating chemistry and tube degradation.

1.2 Background

Eddy current (ECT) inspections of the Crystal River Unit 3 "B" steam generator had shown indications located at 1 to 2 feet above the upper surface of the lower tubesheet (tubing freespan) and at the seventh, eighth, and ninth tube supports (tube-tube support crevices). The extent of some of these indications required utility personnel to plug a number of tubes. There had been no visual indications that would confirm the ECT results.

This tailored collaboration project involved pulling several tubes from the affected steam generator for detailed non-destructive and destructive testing. The main body of this report and the other supporting appendices discuss the results of those tests.

In conjunction with the examinations of pulled tubes, a review of historical chemistry data was conducted. This review was intended to identify any chemistry trends or transients that might correspond to the ECT indications.

In order to place the historical data review in the proper context, a summary of chemistry-related operating practices and plant design/configuration changes is presented below.

- **MSR drains** were routed forward from 1977 through 1978. In 1978 the MSR drains were permanently routed back to the condenser.
- **Condenser** was originally tubed with 70/30 Cu/Ni and frequently experienced leaks. Retubing of one waterbox at a time with titanium was begun in March 1992. The last two waterboxes will be retubed in 1994.
- **Full-flow, deep-bed condensate polishers** are operated with a 2:1 volume ratio of cation:anion resins. Five beds are on-line during normal operation, with one spare to use for pH control.
- **Condensate polisher resin** regeneration was stopped in about 1979. At this time, the plant began operating the polishers in the ammonium cycle and discarding resins when the effluent sodium or chloride concentration was 2 to 3 ppb.
- **Feedwater pH (25°C)** has been increased gradually — starting in 1985 at approximately 9.1, increasing to approximately 9.45 by 1987, and in the range of 9.6 to 9.8 in 1993 with morpholine AVT chemistry.
- **AVT pH control agents** have been changed with time.

  1977-1989: Ammonia AVT

  July 1989-March 1993: Morpholine AVT

  - Low morpholine (10-20 ppm), 1989-June 1992
  - High morpholine (50-100 ppm), June 1992-March 1993

  April 1993-Fall 1993: Ethanolamine/morpholine AVT (3-5 ppm ETA/3-5 ppm morpholine)

2.0 Data Available for Evaluation

Chemistry data for three blocks of time were used in this study:

- Fuel cycles 1 through 4 (January 1977, just prior to commercial operation, through Spring 1982),
- Fuel cycle 8 (June 1990 through April 1992), and
- Fuel cycle 9 (July 1992 through May 1993).

Crystal River plant personnel put forth a significant effort to retrieve archived chemistry data to facilitate this review and evaluation. Data were provided to Adams & Hobart in the following forms:

Secondary Cycle Chemistry Logs

ChemRad Reports

Hideout Return Study Data Logs

Impurity Transport Study Data Logs

REDAS Data Logs

Spreadsheets of operating chemistry data for Cycles 8 and 9

A detailed listing of data available to this study is presented in Section C.1, Table C.1-1.

As is the usual case with historical data reviews, data from early plant operations are sketchy and do not cover all impurity species that are considered currently to be important with respect to steam generator corrosion. However, the data records that were required during those years were found to be complete and in order.

Supplemental chemistry information was obtained from published reports of plant and industry studies. Those reports that were found to contain useful data also are listed in section C.1, in Table C.1-2.

3.0 Data Evaluation

3.1 Task A: 1977 Through 1982

Insufficient data were available to perform an historical analysis of operating transients or wet layup chemistry for this time period. An effort was made to evaluate early operating chemistry in terms of: (a) concentrations of impurities; (b) evidence of any identifiable impurity excursions; (c) presence of any relationships between pH, concentrations of hydrazine, concentrations of dissolved oxygen, and concentrations of ionic impurities; and (d) comparisons with more recent chemistry. The following paragraphs address these issues for sodium, chloride, cation conductivity, pH, and hydrazine.

3.1.1 Sodium

Figure 3-1 presents hotwell and feedwater sodium concentrations versus time for the three periods investigated during this study: January 1977 through April 1982, June 1990 through May 1992, and July 1992 through May 1993. There were no feedwater data available for the 1977 through 1982 time period.

There was one very high hotwell sodium concentration (500 ppb) at plant startup (1977), and it is probable that there was a corresponding elevated feedwater value. Blowdown sodium concentrations were approximately 100 ppb and 40 ppb for steam generators A and B, respectively, during this same 1977 startup time period (see Figure 3-2), which indicates that feedwater did experience elevated concentrations.

Hotwell and feedwater sodium data are shown on an expanded scale in Figure 3-3. From this presentation it can be seen that both hotwells experienced increases in sodium concentration between July 1992 and May 1993. However, the condensate polishers were able to maintain feedwater in the range of 0.5 to 2.5 ppb, except for a significant spike (4 ppb) during the May 1993 startup, corresponding to the initial introduction of ethanolamine (ETA) as a pH control agent.

A cyclical trend in feedwater sodium can be seen in Figure 3-3. Peaks in concentration of about 2 to 3 ppb occurred in June 1990, December 1990, March 1991, June 1991, August 1991, March 1992, September 1992, January 1993, and May 1993.

3.1.2 Chloride

Figure 3-4 illustrates hotwell and feedwater chloride concentrations during the three time periods studied. Hotwell B experienced elevated chloride concentrations in 1982 (1 to 12 ppb) and during much of the 1990 and 1992 time frame (10 to 42 ppb). The condensate polishers were able to maintain feedwater concentrations at less than 3 ppb, except for one sample in June 1990, as shown on the expanded scale of Figure 3-5. It is possible that this anomalous value (9 ppb) was from a contaminated sample.

A cyclical trend in feedwater chloride is evident in Figure 3-5. Peaks in concentration of approximately 2 ppb occurred in June 1990, December 1990, March 1991, June 1991, August 1991, March 1992, September 1992, November 1992, March 1993, and May 1993. These peaks correspond almost exactly with the cycle peaks for sodium (section 3.1.1).

There is nothing in the historical chloride data that appears to explain any pre-1988 steam generator tube corrosion.

3.1.3 Cation (Acid) Conductivity

From Figure 3-6 it can be seen that cation conductivity of both hotwells and feedwater has decreased during the life of the plant. (It should be noted that there are no hotwell cation conductivity available for the period, June 1992 through June 1993.) The patterns of hotwell chloride concentrations and cation conductivity observed from Figures 3-4 and 3-6 do not appear to be similar. An examination of feedwater chloride concentrations and cation conductivity on the expanded scales of Figures 3-5 and 3-7 does not indicate a relationship. Therefore, it appears that some non-chloride, acidic species (e.g., sulfate, phosphate, nitrate, and/or organic acids) historically have controlled secondary cycle cation conductivity. It also is apparent that the concentrations of non-chloride, acidic species in the hotwells were highest during early years of plant operation.

The concentration of chloride during early plant operation was not sufficient to account for all the measured cation conductivity. Chloride concentrations of around 0.4 ppb only provide 0.06 μS/cm of cation conductivity, while 1.0 to 1.5 μS/cm were measured periodically between 1977 to 1982. If sulfate were the predominant anionic species contributing to those cation conductivity spikes, it would have had to present at a concentration of about 170 ppb.

3.1.4 Comparison of Feedwater pH and Sodium

Figure 3-8 compares feedwater pH and sodium for the three time periods studied, except that there are no sodium data for 1977 through 1982. There does not appear to be a cyclical pattern of pH corresponding to that of sodium concentration for 1990 through 1993. The slight upward trend in pH (9.4 to 9.6) in 1992 does correspond to an upward trend in sodium concentration (1 to 1.5 ppb). However, after the brief December 1992 outage, the sodium concentration dropped by about 0.5 ppb, with no corresponding drop in pH.

3.1.5 Comparison of pH and Chloride

Figure 3-9 compares feedwater chloride and pH for the three time periods studied. There is no clear relationship between pH and chloride. While both experienced fluctuations during the April 1993 startup, there was no pH fluctuation in February and March 1993 to account for the changes in chloride. During the 1977 startup there was no high value of chloride recorded in response to the high pH.

3.1.6 Hydrazine

In Figure 3-10, it can be seen that a very high concentration of feedwater hydrazine (approximately 20 ppm) was recorded during the 1977 plant startup. This concentration of hydrazine decomposing to ammonia could have caused a high leakage of sodium from the condensate polishers, which could have shown up in the condenser hotwell as the elevated value observed (500 ppb). In addition, there is a cycling in

hydrazine concentration evident in 1990 through 1992 that might be suggestive of a relationship with feedwater chloride concentrations.

Feedwater chloride versus hydrazine concentrations are plotted in Figure 3-11. The general decrease in chloride concentration during the two periods, 1990 through 1992 and 1992 through 1993, does correspond with a decrease in hydrazine concentration. The short-term increase in chloride concentration between January and June 1991 may relate to a slight increase in hydrazine concentration during the same period. However, there is no apparent drop in hydrazine concentration that would correlate with the sudden drop in chloride concentration in July 1991.

Higher concentrations of hydrazine (50-100 ppb) were typical in the 1977 to 1989 time frame than during the rest of the plant history. Following the conversion to morpholine for pH control in July 1989, hydrazine concentrations were decreased to a nominal 30 ppb. This change was made in order to maintain a sufficiently high morpholine concentration to reduce corrosion product transport, without producing excessively high feedwater pH.

3.1.7 Dissolved Oxygen

Figure 3-12 shows a comparison of feedwater and deaerator effluent dissolved oxygen and hydrazine. During the 1977 plant startup, the deaerator effectively reduced the dissolved oxygen (filled symbols on Figure 3-12) but the hydrazine level was kept high (open symbols). An expanded plot is shown in Figure 3-13. The high hydrazine concentrations relative to oxygen would have created a very reducing environment in the steam generators, whereby any sulfate species present could have been reduced.

3.1.8 Summary of Historical Chemistry Review

While sulfate was not monitored between 1977 and 1986, cation conductivity was high and not accounted for by measured chloride concentrations. This indicates that acid species may have been available in sufficient concentrations to produce an acidic environment in the concentrating films on the steam generator tubes.

It can only be speculated about whether or not the non-chloride anionic material was predominantly sulfate, or whether other species such as phosphates or organic acids were present in relatively high concentrations. However, the possibility of high concentrations of sulfate (potentially as high as 170 ppb) does potentially support the B&W postulate that resin-related sulfonates and sulfates were generated by the condensate polishers during early years of operation.

High concentrations of hydrazine were also present during early plant operation. The combination of acidic chemistry, possible presence of sulfur, and documented presence of high concentrations of hydrazine in feedwater during those early years supports the B&W postulate that reduced sulfur species were responsible for steam generator tube damage prior to 1988.

A second issue, not particularly related to this project's objectives, is the apparently anomalous behavior of chloride observed in historical data. It would be expected that decomposition of hydrazine to ammonia would increase condensate pH and shift

demineralizer equilibrium to result in chloride throw. This means that chloride in feedwater should be related to both changes in hydrazine and pH. However, elevated feedwater chloride concentrations appear to be more related to hydrazine concentrations than pH during the past few years and hydrazine and pH did not track together well. It is not apparent why hydrazine concentrations do not parallel pH and why chloride concentration trends are more similar to hydrazine trends than pH. One possibility for this behavior could be that the hydrazine has had chloride contamination. If that were the case, both pH and hydrazine concentrations would affect chloride. However, hydrazine solutions (purchased as 35 wt %) would have to contain chloride contamination roughly on the order of 12,000 ppm in order to affect feedwater concentration by the 1 ppb transients observed. Plant personnel have not analyzed incoming hydrazine for chloride, but they believe the certified analyses should be close enough in accuracy to assure that these high concentrations do not exist.

3.2 Task B: 1988 Through 1992

3.2.1 Transient Periods

Available operating data for these two recent operating cycles were obtained from spreadsheets containing secondary chemistry data. The data were reviewed to identify three types of chemistry transients: hotwell high sodium and chloride; hotwell high sodium and low chloride; and condensate demineralizer effluent high sodium and low chloride, with no evidence of high sodium in the condenser hotwell. High sodium and chloride concentrations in the condenser hotwell would most probably be the result of a condenser tube leak. High sodium and low chloride concentrations in the hotwell could be indicative of sodium throw from the makeup water plant, while high sodium and low chloride concentrations in the demineralizer effluent could be indicative of sodium throw from those demineralizers. The transients shown in section C.2, Table C.2-1, were identified from review of the data.

For each of the transients shown in Table C.2-1, where feedwater chemistry data were available, MULTEQ runs were performed to estimate deposit/crevice chemistry. Recorded feedwater data used in this analysis consisted of concentrations of sodium, chloride, sulfate, formate and acetate.[1] It should be noted that chemistry data were not available for some strong acid and strong base species (e.g., potassium, calcium, magnesium, phosphate). Neither were concentrations of silica available, although recent measurements of MSR drains samples indicate that feedwater concentrations should be on the order of only 2 ppb. Although it is a weakly ionized species, silica is important because formation and precipitation of silicates in basic solutions can impact predicted crevice chemistry. Because of the incomplete data, there is a large degree of uncertainty in the MULTEQ predictions. The results are summarized in Table 3-1. Detailed results are shown in section C.2, Table C.2-2.

Crevice pH estimates are shown in Tables 3-1 and C.2-2 for two conditions: a concentration factor of 1000, which should be indicative of under-deposit conditions,

[1] Additional feedwater chemistry data available include cation conductivity and dissolved oxygen, pH, ammonium, hydrazine, and morpholine concentrations.

and a boiling point elevation of 7 °C, which should be indicative of OTSG tube-tube support crevices. Because of the inherent uncertainty in results, given the limited data sets available, the predicted crevice conditions were used only qualitatively. Therefore, there was no need to interpolate to establish an estimated pH for a boiling point elevation of precisely 7 °C. The notations, "Insufficient data to evaluate", were used for three situations: (a) there was no sulfate concentration available; (b) the observed transient occurred mid-way between weekly feedwater sample analyses; and (c) no or limited analytical data were recorded for the week. When weak organic acid concentrations were not available but adjacent data points appeared stable, they were estimated.

Summary – Transient Chemistry, 1988-1992

Recent transient data provide circumstantial evidence of neutral under-deposit chemistry for both steam generators, but acid-sulfate crevice chemistry in steam generator A and a nearly equal times of acid-sulfate and neutral/caustic crevice (tube-tube support) chemistry in steam generator B. The acidic chemistry predicted in both steam generators is due to relatively high concentrations of sulfate present.

TABLE 3-1

Summary of MULTEQ pH Predictions
From Feedwater Chemistry Data During Transients

Condenser High Na and Cl

		CF=10^3 (Under Deposit)		ΔBP=~7°C	
Date	FW Train	pH	NpH	pH	NpH
10/1/90	A	6.98	5.74	9.42	5.02
	B	5.52	5.74	2.53	5.12
12/19/90	A	4.76	5.73	2.23	5.01
3/26/91	A	6.35	5.74	5.93	5.15
	B	6.22	5.74	4.21	5.14
5/21/91	A	6.96	5.74	6.29	5.02

TABLE 3-1, cont'd.

Summary of MULTEQ pH Predictions
From Feedwater Chemistry Data During Transients

Condenser High Na and Low Cl					
		CF=10^3 (Under Deposit)		ΔBP=~7℃	
Date	FW Train	pH	NpH	pH	NpH
9/18/90	A	4.33	5.74	0.05	5.06
	B	4.39	5.74	1.01	5.18
10/1/90	A	6.98	5.74	9.42	5.02
10/8/90	A	4.66	5.75	0.47	5.20
10/30/90	B	5.81	5.74	3.52	5.17
1/22/91	A	4.58	5.74	0.54	5.21
	B	4.94	5.74	1.02	5.13
3/12/91	A	4.20	5.74	0.45	5.20
	B	4.67	5.74	0.93	5.16
3/19/91	A	5.92	5.74	3.44	5.16
	B	6.40	5.74	5.66	4.99
7/9/91	A	6.19	5.74	3.71	5.04
	B	6.71	5.74	9.35	4.95
7/16/91	A	6.73	5.74	9.35	5.13
7/23/91	B	6.46	5.74	5.30	5.03
8/20/91	A	5.91	5.74	3.42	3.65
	B	6.94	5.74	9.39	5.04
9/3/91	B	5.98	5.74	3.76	5.25
9/10/91	A	6.20	5.74	3.76	5.16
	B	6.78	5.74	9.23	5.10
9/18/91	A	4.55	5.74	0.20	5.09
	B	5.13	5.74	1.30	5.19
9/24/91	B	6.08	5.74	3.80	5.21
10/1/91	B	7.23	5.72	9.01	5.14
3/10/92	A	6.79	5.74	9.23	5.06
	B	6.44	5.74	6.41	5.12

While only one data point was available that represented potential sodium throw from the condensate demineralizers, there were several instances where elevated sodium in the hotwell passed through the demineralizers. With only two exceptions, all cases of high sodium in the hotwell and/or condensate demineralizer effluent coincided with acidic-concentrating feedwater for Train A. However, only half of the cases of high sodium in the hotwell and/or condensate demineralizer effluent coincided with acid-concentrating Train B feedwater. The apparent difference in steam generator chemistries could reflect simply the uncertainty in analytical results.

There is a potential for significant amounts of feedwater-borne sulfate to adsorb on oxide surfaces inside the steam generator. Adsorbed sulfate would not be available for influencing pH in flow-restricted areas of the steam generator. However, the sulfate levels are high enough to indicate that the water would be probably acid-concentrating, even with removal of some sulfate by adsorption.

3.2.2 Investigation of Sulfate

The relatively high levels of sulfate (2-3.3 ppb) observed in feedwater during analysis of recent chemistry transients prompted an investigation of its origin. Operating chemistry data from Cycle 9 were examined to determine if the feedwater sulfate corresponds to condenser inleakage. Condenser hotwell samples are not rou inely analyzed for sulfate, so Figure 3-14 compares concentration of hotwell sodium with concentration of feedwater sulfate. There is no apparent correlation between those data.

To obtain more detailed and accurate information on the behavior of sulfate in the secondary cycle, a special sulfate analysis test was initiated by Crystal River-3 personnel in January 1993. Figures 3-15 through 3-17 plot data from that test. Figure 3-15 compares concentrations of sulfate in feedwater with those in the hotwells. The measured concentrations track closely, with the "A" hotwell and "A" feedwater train showing similar trends and the "B" hotwell and "B" feedwater train behaving similarly. Plant personnel have commented that this correlation cannot always be observed. It is interesting to note that there is no obvious and consistent bias between hotwell and feedwater concentrations, although the full-flow, deep-bed condensate polishers were in use.

Sulfate concentration in the condensate demineralizer effluent header does not trend particularly well with those in the feedwater trains, as can be seen in Figure 3-16. If the header were well mixed, there were no removal of sulfate by the condensate demineralizers, and the sample analyses were accurate and precise, the common condensate demineralizer effluent concentration would always be positioned between the hotwell concentrations.

To investigate whether the condensate demineralizers were either removing or throwing sulfate, mass flows were determined using hotwell (influent) sample points CE-2 and CE-3 and feedwater (effluent) sample points CE-9 and CE-10. Results are presented in Figure 3-17. It is apparent that during the test period the demineralizers were neither removing nor contributing ionic sulfate. That could indicate that either that the demineralizers were in equilibrium with the condensate with respect to sulfate,

or that the top portion of the beds were removing sulfate while the lower portion of the beds were releasing sulfate.

To determine whether the demineralizers are throwing colloidal resin particles or soluble sulfonates from resin decomposition, the concentrations of sulfate in high pressure heater drains (condensed extraction steam) was compared with those in feedwater. The results, shown in Figure 3-18, are inconclusive. While there are four peaks in heater drains sulfate concentration that are higher than feedwater concentrations, many of the sample points show concentrations that are slightly lower. This could reflect a routine loss of sulfate by adsorption on secondary plant piping and steam generator surfaces, with periodic throw of organic sulfonates from cation resin. However, this possibility can not be proven with the data.

3.2.3 Analysis of Water Treatment Plant Effluent and Cooling Water

While it is expected that condenser leakage of cooling water from the Gulf of Mexico would result in the addition of acidic-concentrating species to Crystal River's secondary coolant, samples of circulating water were analyzed to verify that assumption. The results are shown in Section C.3, Table C.3-1. Not surprisingly, the Crystal River circulating water is virtually identical to published results for sea water. Major impurities include sodium, calcium, bromine, magnesium, potassium, silicon, sulfur/sulfate, strontium, and chlorine/chloride. The molar concentration of chloride exceeds that of sodium, but is balanced by the other cations present. When Crystal River circulating water chemical data are used in MULTEQ with a dilution factor of 1E6, the resultant pH predictions are:

Under deposit (CF=1E3)	pH=4.79	NpH=5.72
Sludge pile (BPE=11)	pH=2.81	NpH=4.87

Precipitates predicted are $MgSO_4$ and AlO(OH). Condenser leakage would produce an acid-concentrating secondary coolant, as expected.

Demineralization of a fresh water source usually produces water that is caustic-concentrating. In order to determine whether that is the case at Crystal River where makeup water is drawn from deep wells, samples of water treatment plant effluent were analyzed. The results are presented in Section C.3, Table C.3-2. Crystal River makeup water is remarkably high purity. MULTEQ pH predictions for concentration of this water are:

Under deposit (CF=1E3)	pH=6.50	NpH=5.74
Sludge pile (BPE=8.72)	pH=5.36	NpH=4.85

Precipitates predicted are NiO, $ZnSO_4$, ZnO, SiO_2, and PbO. In the absence of condenser leakage, secondary coolant should be neutral to slightly basic.

3.2.4 Hideout Return Studies (1988-1992)

Currently, EPRI recommends that three types of plant hideout return data be input to MULTEQ when studying crevice chemistry conditions: prompt return concentrations, cumulative hot soak quantities, and cumulative cooldown return quantities. However,

the shutdown/cooldown sequence historically used at Crystal River-3 has not included a true hot soak and insufficient data have been obtained historically to compute total return quantities. The prompt return data discussed below was obtained just after draindown, at the start of feed and bleed operation. Because a careful industry-wide study of this type data for once-through units has not been conducted, there is a great deal of interpretation required of the data and results. Consequently, there is also a significant uncertainty in the conclusions drawn. Total return during feed and bleed operation for the March 1992 shutdown have been used in MULTEQ to obtain additional insights. Total return data for the March 1993 shutdown were not available at the time this report was prepared.

Results For October 1988 Outage. Analytical data records are sketchy from this shutdown, so there is considerable uncertainty in the MULTEQ output. Under deposit and sludge pile pH predictions are shown in Table 3-2.

Table 3-2

MULTEQ pH Predictions From
1988 Hideout Return Data

Steam Generator A

RCS T = 533 °F (initial shutdown):

Input Species	Concentration
Na^+	40 ppb
Fe^+	57
Cl^-	84
$SO_4^=$	93
H_3SiO_4	189.6

Predicted pH	NpH	ΔBP	CF
3.82	5.69	-	10^3
0.86	5.06	5.71	-

RCS T = 440 °F (sludge pile soak):

Input Species	Concentration
Na^+	8 ppb
Fe^+	40
Cl^-	-
$SO_4^=$	9
H_3SiO_4	72

Predicted pH	NpH	ΔBP	CF
7.64	5.73	-	10^3
9.73	4.87	7.83	-

Table 3-2, cont'd.

MULTEQ pH Predictions From
1988 Hideout Return Data, cont'd.

Steam Generator B

RCS T = 533 °F (initial shutdown):

Input Species	Concentration
Na^+	60 ppb
Fe^+	17
Cl^-	25
$SO_4^=$	17
H_3SiO_4	254

Predicted pH	NpH	ΔBP	CF
8.45	5.69	-	10^3
9.56	4.99	5.01	-

RCS T = 440 °F (sludge pile soak):

Input Species	Concentration
Na^+	25 ppb
Fe^+	34
Cl^-	-
$SO_4^=$	8
H_3SiO_4	66

Predicted pH	NpH	ΔBP	CF
8.36	5.71	-	10^3
9.86	4.91	5.85	-

These data could indicate that steam generator A has acid chemistry in its upper areas, but caustic conditions within the sludge pile. They could also indicate that steam generator B has caustic conditions throughout the steam generator. However. the data are sufficiently incomplete to preclude the drawing of firm conclusions.

It should be noted that no chloride was detected for the samples during the sludge pile soak (RCS temperature of 440 °C). Apparently the chloride concentration was below the laboratory's limit of quantification (probably 1-2 ppb). Inclusion of the actual concentration would have resulted in a slightly lower calculated pH than those shown in Table 3-2. However, the water should still have been slightly basic concentrating.

Results For October 1991 Mid-Cycle Outage. Analytical data records also are sketchy from this shutdown, so there is considerable uncertainty in the MULTEQ output. Under deposit and sludge pile pH predictions are shown in Table 3-3.

Table 3-3

MULTEQ Results From 1991
Hideout Return Data

Steam Generator A

RCS T = 552 °F (initial shutdown):

Input Species	Concentration
Na^+	1 ppb
Cl^-	0.42
$SO_4^=$	3.01
H_3SiO_4	7.9

Predicted pH	NpH	ΔBP	CF
5.47	5.74	-	10^3
2.02	5.17	3.89	-

RCS T = 534 °F (18 hr after shutdown):

Input Species	Concentration
Na^+	1.1 ppb
Cl^-	0.5
$SO_4^=$	2.32
H_3SiO_4	7.9

Predicted pH	NpH	ΔBP	CF
5.21	5.74	-	10^3
0.91	5.09	4.78	-

Steam Generator B

RCS T = 533 °F (initial shutdown):

Input Species	Concentration
Na^+	0.5 ppb
Cl^-	-
$SO_4^=$	4.23
H_3SiO_4	-

Predicted pH	NpH	ΔBP	CF
4.64	5.74	-	10^3
0.81	5.13	4.00	-

RCS T = 537 °F (18 hrs after shutdown):

Input Species	Concentration
Na^+	0.5 ppb
Cl^-	-
$SO_4^=$	1
H_3SiO_4	-

Predicted pH	NpH	ΔBP	CF
6.32	5.75	-	10^3
9.81	5.04	5.38	-

These data could indicate that steam generator B has acid chemistry in its upper areas, but caustic conditions within the sludge pile. They could also indicate that steam

generator A has acid conditions throughout the steam generator. However, the data are sufficiently incomplete to preclude the drawing of firm conclusions.

Results For March 1992 Trip. Analytical data records are sketchy from this shutdown, so there is considerable uncertainty in the MULTEQ output. Under deposit and sludge pile pH predictions are shown in Table 3-4.

Table 3-4

MULTEQ Results From 1992 Trip
Hideout Return Data

Steam Generator A

Initial shutdown:

Input Species	Concentration
Na^+	0.2 ppb
Cl^-	-
$SO_4^=$	4.89
H_3SiO_4	-

Predicted pH	NpH	ΔBP	CF
4.37	5.74	-	10^3
-0.09	5.00	4.58	-

9.5 hr after shutdown:

Input Species	Concentration
Na^+	280 ppb
Cl^-	25
$SO_4^=$	12.45
H_3SiO_4	390

Predicted pH	NpH	ΔBP	CF
9.21	5.62	-	10^3
9.98	4.88	7.63	-

Steam Generator B

Initial shutdown:

Input Species	Concentration
Na^+	0.5 ppb
Cl^-	-
$SO_4^=$	4.72
H_3SiO_4	-

Predicted pH	NpH	ΔBP	CF
4.55	5.74	-	10^3
0.09	5.10	4.48	-

Table 3-4, cont'd.

MULTEQ Results From 1992 Trip
Hideout Return Data, cont'd.

Steam Generator B, cont'd.

RCS T = 537 °F (18 hrs after shutdown):

Input Species	Concentration
Na^+	850 ppb
Cl^-	60
$SO_4^=$	41.3
H_3SiO_4	565

Predicted pH	NpH	ΔBP	CF
9.54	5.54	-	10^3
10.14	4.90	8.24	-

These data could indicate that both steam generators A and B have acid chemistry in their upper areas, but caustic conditions within the sludge pile. However, the data are sufficiently incomplete to preclude the drawing of firm conclusions.

Results For April-June 1992 Refueling Outage. The results in Table 3-5 were obtained using initial concentrations and total returns from feed and bleed in MULTEQ. Details of data used as input to MULTEQ and outputs for specific data sets are shown in Section C.4, Table C.4-1.

The notation, "B&W Data," denotes MULTEQ runs that were made using data generated exclusively by B&W chemistry analyses. The notation, "FPC plus B&W Data," denotes runs there were made using a combination of data generated by B&W and FPC plant laboratory chemistry analyses.

An examination of the steam generator feed and bleed return quantities versus time plots indicates that the following precipitates or associated species might be present: sodium hydroxide, sodium silicate, sodium sulfate, potassium sulfate, and potassium silicate.

There is no obvious correlation between these possible precipitates and any one of the data sets used to predict crevice pH with MULTEQ, above. However, Adams & Hobart postulates that the tendency of initial feed and bleed concentrations to predict neutral to acidic pH indicates that tube-tube support plate crevice areas probably have neutral to acidic chemistry. The feed and bleed total return quantities represent a soak of the tubesheet deposits. Hence, the MULTEQ pH predictions from total feed and bleed return would reflect dissolution of a sodium silicate precipitate from the sludge pile and the back-diffusion of soluble sodium hydroxide remaining after volatilization of HCl.

Table 3-5

Summary of MULTEQ Results
From 1992 Shutdown Hideout Return

	CF=10^3 (Under Deposit)		ΔBP=~7°C	
Date/Time	pH	NpH	pH	NpH
SG A				
4/30/92, 0607 -B&W Data	7.06	5.73	6.52	5.13
-FPC plus B&W Data	3.95-7.07	5.73	0.51-6.27	5.09-5.22
Total Return	7.86	5.73	9.99	4.87
SG B				
4/30/92, 0609 -B&W Data	3.80	5.74	0.85	5.41
-FPC plus B&W Data	3.32-4.08	5.72-5.74	0.37-0.64	5.24
Total Return	8.84	5.68	10.15	5.11

Preliminary Results From March 1993 Mid-Cycle Outage. Chemical analyses and operational data from the March 1993 outage have not been completely evaluated, to date. However, some preliminary observations can be made from studying the raw data.

Expanded sampling and analysis was performed during the power-down in order to detect whether the combination of turbine wash and hideout return impurities would provide insight into the sludge pile and under-deposit chemistry environments. Chemistry data from three times during the power-down are presented in Table 3-6.

TABLE 3-6

Selected Power-Down Chemical Analysis Results

			Concentration, ppb												
Sample Point	Date	Time	Na^+	K^+	Ca^{++}	Mg^{++}	Li^+	F^-	Cl^-	$SO_4^{=}$	NO_3^-	PO_4^{-3}	SiO_2	OAc^-	HCO_2^-
Feedwater-A	3/3/93	1300	2.4	0.1	<0.1	<0.1	<0.5	<0.1	0.1	<0.1	3.6	<5	<3	<1	9
		2230	1.5	0.1	<0.1	<0.1	<0.5	<0.1	0.2	1.5	<2	<5	<3	<1	7.4
	3/4/93	0130	2.2	0.2	<0.1	<0.1	<0.5	<0.1	0.4	2.2	<2	<5	<3	<1	7
Feedwater-B	3/3/93	1300	2	0.1	<0.1	<0.1	<0.5	<0.1	1.2	1.1	<2	<5	<3	<1	5.4
		2230	1.8	0.2	<0.1	<0.1	<0.5	<0.1	1.2	1.4	<2	<5	<3	<1	6.2
	3/4/93	0130	1.3	0.1	<0.1	<0.1	<0.5	<0.1	1.3	1.6	<2	<5	<3	<1	8.5
HP Heater	3/3/93	1300	3.1	0.1	<0.1	<0.1	<0.5	<0.1	0.6	<0.1	2.9	<5	<3	<1	9.3
Drains		2230	0.8	0.2	<0.1	<0.2	<0.5	<0.1	0.2	1.2	<2	<5	<3	<1	4.2
	3/4/93	0130	0.7	0.1	<0.1	<0.1	<0.5	<0.1	<0.1	<0.1	<2	<5	<3	<1	7.4
MSR Drains	3/3/93	1300	18	0.5	<0.1	<0.1	<0.5	2.8	16	1.9	<2	<5	18	94	110
		2230	15	0.5	<0.1	<0.1	<0.5	2.4	10	1.4	<2	<5	22	150	90
	3/4/93	0130	18	0.4	<0.1	<0.1	<0.5	4.2	19	2.8	<2	<5	24	250	170
LP Heater	3/3/93	1300	0.5	<0.1	<0.1	<0.1	<0.5	<0.1	<0.1	<0.1	<2	<5	<3	<1	<1
Drains		2230	0.4	0.1	<0.1	<0.1	<0.5	<0.1	<0.1	0.9	<2	<5	<3	<1	<1
	3/4/93	0030	3.1	0.3	<0.1	<0.1	<0.5	<0.1	1.5	1	<2	<5	5.3	<1	<1

Although increased chloride concentrations were present in low pressure heater drains during the latter part of the power-down, increased sodium concentrations were also present. In the low pressure heater drains sample at 0030 on March 4, 0.135 μmoles/L of sodium were present and only 0.042 μmoles/L of chloride. This does not support the hypothesis that HCl was volatilizing and leaving soluble NaOH in the steam generator sludge pile. The MSR drains samples had relatively steady and high concentrations of chloride during the entire power-down, but there was a slight excess of sodium present. Thus, the turbine and MSR wash that occurred during power-down appeared to contain sodium chloride and, possibly, sodium hydroxide, rather than hydrochloric acid.

Mass balances have not been constructed for this shutdown, to date. However, an examination of the concentration data leads to the conclusion that significant amounts of NaOH did not return from the sludge pile during power-down and cooldown. The only strongly ionized species observed during hideout return were sodium, potassium, chloride and sulfate. Selected data during the cooldown are presented in Table 3-7. MULTEQ predictions of concentrated pH from these data are listed in Section C.5, Table C.5-1 and summarized in Table 3-8. The under-deposit and sludge pile pH predictions for both steam generators are neutral or acidic at all three points of time evaluated, although relatively high concentrations of sodium were present. Sufficient amounts of sodium were complexed with sulfate in every case so that the remaining ionic sodium could be balanced in charge by free anions (such as nitrate, acetate, chloride, and bisulfate). While there was no notable difference in predicted pH conditions for the two steam generators, concentrations of sulfate returning from OTSG-B were significantly higher during cooldown than from OTSG-A (approximately 5 times higher).

TABLE 3-7

Selected Cooldown Chemistry Analysis Results

			Concentration, ppb											
Sample Point	Date	Time	Na^+	K^+	Ca^{++}	Mg^{++}	Li^+	F^-	Cl^-	$SO_4^{=}$	NO_3^-	PO_4^{-3}	SiO_2	OAc^-	HCO_2^-
OTSG-A	3/4/93	0225	2.6	1.2	<0.1	<0.1	<0.5	<0.1	0.1	1.9	3.6	<5	10	36	41
		1030	0.1	<0./1	<0.1	<0.1	<0.5	<0.1	<0.1	0.7	<2	<5	<3	13	9.9
		1830	8.5	1.3	<0.1	<0.1	<0.5	<0.1	2.1	1.7	<2	<5	9.1	460	93
	3/5/93	0630	3.6	0.4	<0.1	<0.1	<0.5	<0.1	1.4	2.6	<2	<5	24	160	75
OTSG-B	3/4/93	0225	3.1	0.3	<0.1	<0.1	<0.5	<0.1	3.5	11	<2	<5	5.1	110	21
		1030	0.2	<0.1	<0.1	<0.1	<0.5	<0.1	<0.1	<0.1	<2	<5	<3	2.7	4.9
		1830	1.3	<0.1	<0.1	<0.1	<0.5	<0.1	<0.1	1.6	2.1	<5	<3	<1	<1
	3/5/93	0630	53	2.1	<0.1	<0.1	<0.5	0.3	11	12	<2	<5	58	630	340

TABLE 3-8

MULTEQ Results for Selected Cooldown Chemistry Results

	CF=10^3 (Under Deposit)		ΔBP=~7°C	
Date/Time	pH	NpH	pH	NpH
SG A				
3/4/93, 0225	5.82	5.74	5.10	5.43
3/4/93, 1030	5.10	5.75	2.04	5.62
3/4/93, 1830	5.41	5.73	4.84	5.45
3/5/93, 0630	5.34	5.72	4.93	5.54
SG B				
3/4/93, 0225	4.12	5.73	1.22	5.42
3/4/93, 1030	6.02	5.75	5.62	5.47
3/4/93, 1830	5.97	5.74	3.16	5.07
3/5/93	6.02	6.59	5.30	5.35

These results appear to be significantly different than the results from the previous shutdown. While the 1992 shutdown produced acid-concentrating water during power-down and initial cooldown, the quality of the hideout return changed to caustic-concentrating during the cooldown. This recent 1993 shutdown produced only acid-concentrating water during both power-down and cooldown. However, relatively high

concentrations of sodium began appearing during the subsequent layup. Chemistry analysis data and MULTEQ results from the layup are presented in Table 3-9.

TABLE 3-9

MULTEQ Results for 1993 Shutdown Layup

OTSG B, 3/20/93, 1830

Input Species	Concentration
Na^+	190 ppb
Cl^-	10
$SO_4^=$	150
F^-	-
OAc^-	4.44
HCO_2^-	97.1
H_3SiO_4	544

Predicted pH	NpH	ΔBP	CF
8.77	5.65	-	10^3
9.58	5.00	6.56	-

Na_2SiO_5 precipitated.

$NaSO_4$, Na_2SO_4, $NaHSO_4$, HSO_4^-, HOAc, HCO_2H, $H_6(SiO_3)_4$, and H_4SiO_4 in solution.

OTSG B, 3/21/93, 1200

Input Species	Concentration
Na^+	228 ppb
Cl^-	15
$SO_4^=$	120
F^-	-
OAc^-	8.6
HCO_2^-	101
H_3SiO_4	635

Predicted pH	NpH	ΔBP	CF
8.90	5.64	-	10^3
9.65	4.98	7.11	-

Na_2SiO_5 precipitated.

NaOH, $NaSO_4$, $NaHSO_4$, Na_2SO_4, HSO_4^-, HOAc, HCO_2H, H_2SiO_4, $H_6(SiO_3)_4$, and H_4SiO_4 in solution.

OTSG B, 3/22/93, 1200

Input Species	Concentration
Na^+	293 ppb
Cl^-	13
$SO_4^=$	113
F^-	-
OAc^-	3.1
HCO_2^-	101.4
H_3SiO_4	785

Predicted pH	NpH	ΔBP	CF
9.02	5.62	-	10^3
9.72	4.94	7.56	-

Na_2SiO_5 precipitated.

NaOH, $NaSO_4$, $NaHSO_4$, Na_2SO_4, HSO_4^-, HOAc, HCO_2H, H_2SiO_4, $H_6(SiO_3)_4$, and H_4SiO_4 in solution.

TABLE 3-9, cont'd.

MULTEQ Results for 1993 Shutdown Layup

OTSG A, 3/24/93, 0900

Input Species	Concentration
Na^+	249 ppb
Cl^-	47
$SO_4^=$	153
F^-	32.5
OAc^-	12
HCO_2^-	50
H_3SiO_4	296

Predicted pH	NpH	ΔBP	CF
8.79	5.63	-	10^3
9.42	4.95	7.72	-

Na_2SiO_5 precipitated.

NaOH, $NaSO_4$, $NaHSO_4$, Na_2SO_4, HSO_4^-, HOAc, HF, HF_4, HCO_2H, H_2SiO_4, $H_6(SiO_3)_4$, and H_4SiO_4 in solution.

OTSG A, 3/25/93, 0745

Input Species	Concentration
Na^+	330 ppb
Cl^-	88
$SO_4^=$	220
F^-	-
OAc^-	163
HCO_2^-	91
H_3SiO_4	424

Predicted pH	NpH	ΔBP	CF
8.73	5.62	-	10^3
9.35	5.09	3.92	-

SiO_2 precipitated.

NaOH, $NaSO_4$, $NaHSO_4$, Na_2SO_4, HSO_4^-, HOAc, HCO_2H, H_2SiO_4, $H_6(SiO_3)_4$, and H_4SiO_4 in solution.

OTSG A, 3/26/93, 1215

Input Species	Concentration
Na^+	403 ppb
Cl^-	89
$SO_4^=$	79
F^-	-
OAc^-	23.5
HCO_2^-	118
H_3SiO_4	593

Predicted pH	NpH	ΔBP	CF
9.16	5.60	-	10^3
9.69	5.01	4.75	-

No precipitates.

NaOH, $NaSO_4$, $NaHSO_4$, Na_2SO_4, HSO_4^-, HOAc, HCO_2H, H_2SiO_4, $H_6(SiO_3)_4$, and H_4SiO_4 in solution.

TABLE 3-9, cont'd.

MULTEQ Results for 1993 Shutdown Layup

OTSG A, 3/27/93, 1155

Input Species	Concentration
Na^+	472 ppb
Cl^-	102
$SO_4^=$	74
F^-	-
OAc^-	14.9
HCO_2^-	99.5
H_3SiO_4	746

Predicted pH	NpH	ΔBP	CF
9.21	5.59	-	10^3
9.71	4.99	4.95	-

Na_2SiO_5 precipitated.

NaOH, $NaSO_4$, $NaHSO_4$, Na_2SO_4, HSO_4^-, HOAc, HCO_2H, H_2SiO_4, $H_6(SiO_3)_4$, and H_4SiO_4 in solution.

OTSG B, 3/31/93, 1215

Input Species	Concentration
Na^+	608 ppb
Cl^-	31
$SO_4^=$	228
F^-	-
OAc^-	5.68
HCO_2^-	109.3
H_3SiO_4	1438

Predicted pH	NpH	ΔBP	CF
9.19	5.58	-	10^3
9.71	5.00	4.89	-

Na_2SiO_5 precipitated.

NaOH, $NaSO_4$, $NaHSO_4$, Na_2SO_4, HSO_4^-, HOAc, HCO_2H, H_2SiO_4, $H_6(SiO_3)_4$, and H_4SiO_4 in solution.

OTSG A, 4/1/93, 0833

Input Species	Concentration
Na^+	642 ppb
Cl^-	109
$SO_4^=$	113
F^-	2.13
OAc^-	18
HCO_2^-	107
H_3SiO_4	1017

Predicted pH	NpH	ΔBP	CF
9.27	5.57	-	10^3
9.74	4.95	5.91	-

Na_2SiO_5 precipitated.

NaOH, $NaSO_4$, $NaHSO_4$, Na_2SO_4, HSO_4^-, HOAc, HF, HCO_2H, H_2SiO_4, $H_6(SiO_3)_4$, and H_4SiO_4 in solution.

TABLE 3-9, cont'd.

MULTEQ Results for 1993 Shutdown Layup

OTSG B, 4/8/93, 1056

Input Species	Concentration
Na^+	716 ppb
Cl^-	64
$SO_4^=$	291
F^-	-
OAc^-	15.2
HCO_2^-	107.7
H_3SiO_4	1630

Predicted pH	NpH	ΔBP	CF
9.20	5.57	-	10^3
9.69	4.98	5.49	-

Na_2SiO_5 precipitated.

NaOH, $NaSO_4$, $NaHSO_4$, Na_2SO_4, HSO_4^-, HOAc, HCO_2H, H_2SiO_4, $H_6(SiO_3)_4$, and H_4SiO_4 in solution.

OTSG A, 4/13/93, 0115

Input Species	Concentration
Na^+	741 ppb
Cl^-	284
$SO_4^=$	251
F^-	3
OAc^-	55
HCO_2^-	47
H_3SiO_4	1203

Predicted pH	NpH	ΔBP	CF
9.12	5.56	-	10^3
9.54	4.96	6.28	-

Na_2SiO_5 precipitated.

NaOH, $NaSO_4$, $NaHSO_4$, Na_2SO_4, HSO_4^-, HOAc, HF, HCO_2H, H_2SiO_4, $H_6(SiO_3)_4$, and H_4SiO_4 in solution.

OTSG B, 4/15/93, 2000

Input Species	Concentration
Na^+	690 ppb
Cl^-	120
$SO_4^=$	227
F^-	-
OAc^-	6
HCO_2^-	46
H_3SiO_4	1002

Predicted pH	NpH	ΔBP	CF
9.28	5.57	-	10^3
9.72	4.95	5.76	-

Na_2SiO_5 precipitated.

NaOH, $NaSO_4$, $NaHSO_4$, Na_2SO_4, HSO_4^-, HOAc, HCO_2H, H_2SiO_4, $H_6(SiO_3)_4$, and H_4SiO_4 in solution.

TABLE 3-9, cont'd.

MULTEQ Results for 1993 Shutdown Layup

OTSG B, 4/16/93, 2230

Input Species	Concentration
Na^+	617 ppb
Cl^-	285
$SO_4^=$	238
F^-	-
OAc^-	5.7
HCO_2^-	27.8
H_3SiO_4	967

Predicted pH	NpH	ΔBP	CF
9.05	5.58	-	10^3
9.50	4.98	5.55	-

Na_2SiO_5 precipitated.

NaOH, $NaSO_4$, $NaHSO_4$, Na_2SO_4, HSO_4^-, HOAc, HCO_2H, H_2SiO_4, $H_6(SiO_3)_4$, and H_4SiO_4 in solution.

OTSG B, 4/17/93, 1320

Input Species	Concentration
Na^+	663 ppb
Cl^-	268
$SO_4^=$	216
F^-	-
OAc^-	374
HCO_2^-	43
H_3SiO_4	1069

Predicted pH	NpH	ΔBP	CF
8.86	5.57	-	10^3
9.33	4.96	6.81	-

Na_2SiO_5 precipitated.

NaOH, $NaSO_4$, $NaHSO_4$, Na_2SO_4, HSO_4^-, HOAc, HF, HCO_2H, H_2SiO_4, $H_6(SiO_3)_4$, and H_4SiO_4 in solution.

3.2.5 Summary, Task B (1988-1992)

The general trend seen from evaluation of transient data is for Crystal River-3 steam generator chemistry to be acidic, even during periods of high sodium concentration indicative of sodium throw from the condensate polishers or makeup plant demineralizers. The trend seen from evaluation of hideout return data is for bulk water sampled immediately upon shutdown to be acid-concentrating, while steam generator water samples after a soak of the sludge pile area are basic-concentrating.

This shift in chemistry would suggest that Crystal River-3 steam generator tube support plate crevices may be neutral to acidic in pH presently, while there is some possibility that chemistry in the tubesheet sludge pile region is caustic. A caustic sludge pile could be due to volatilization of acidic anion species. This would support the hypothesis developed by metallurgists that freespan corrosion, judged to be an acidic attack, was a one-time event should not be progressing currently.

There is no indication of a significant difference in chemistries between SG A and B, except that hideout quantities of sulfate may be higher in SG B.

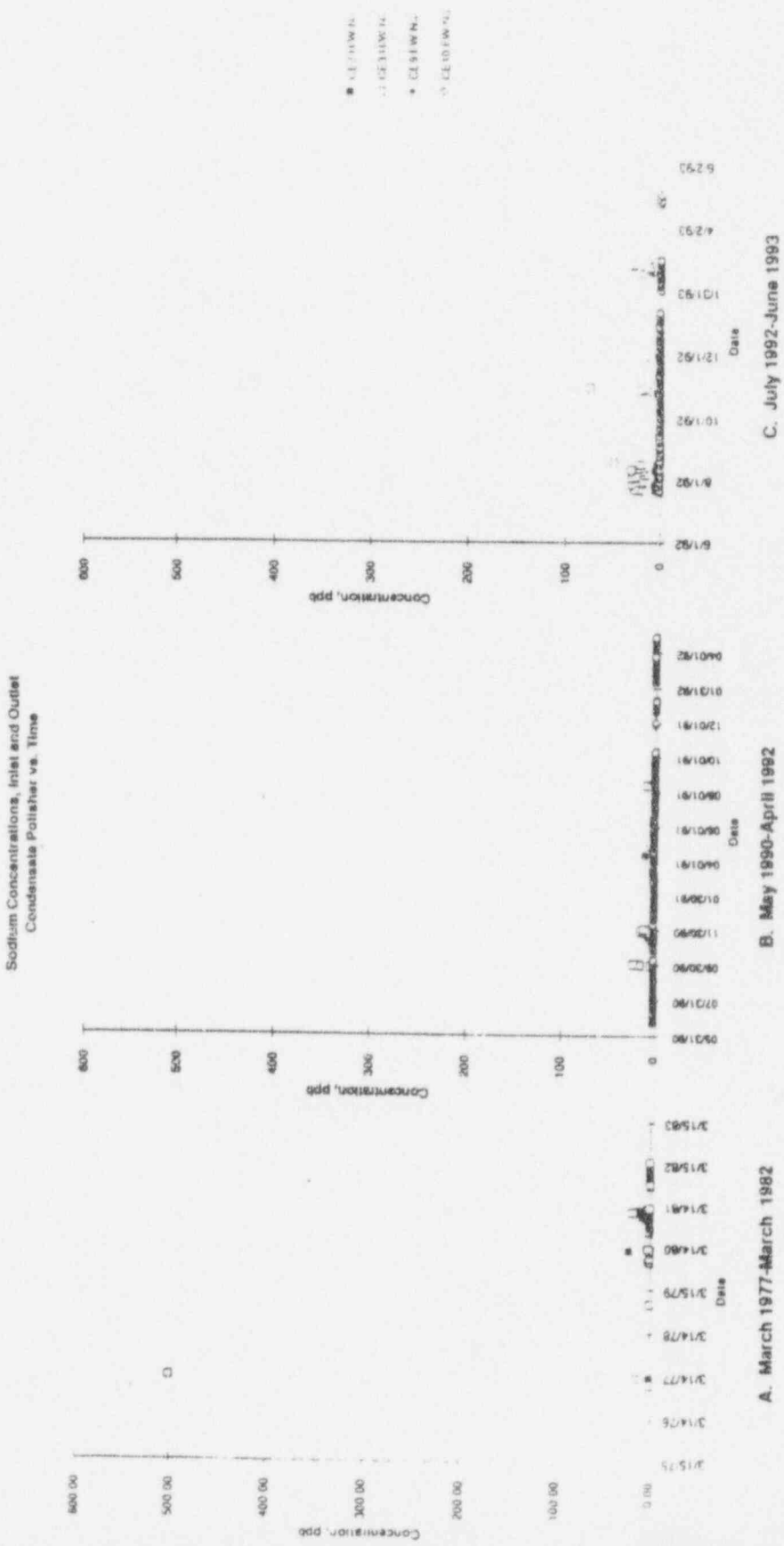
Sodium Concentrations, Inlet and Outlet
Condensate Polisher vs. Time
Concentration, ppb
Date
A. March 1977-March 1982
B. May 1990-April 1992
C. July 1992-June 1993

Figure 3-1

Figure 3-2

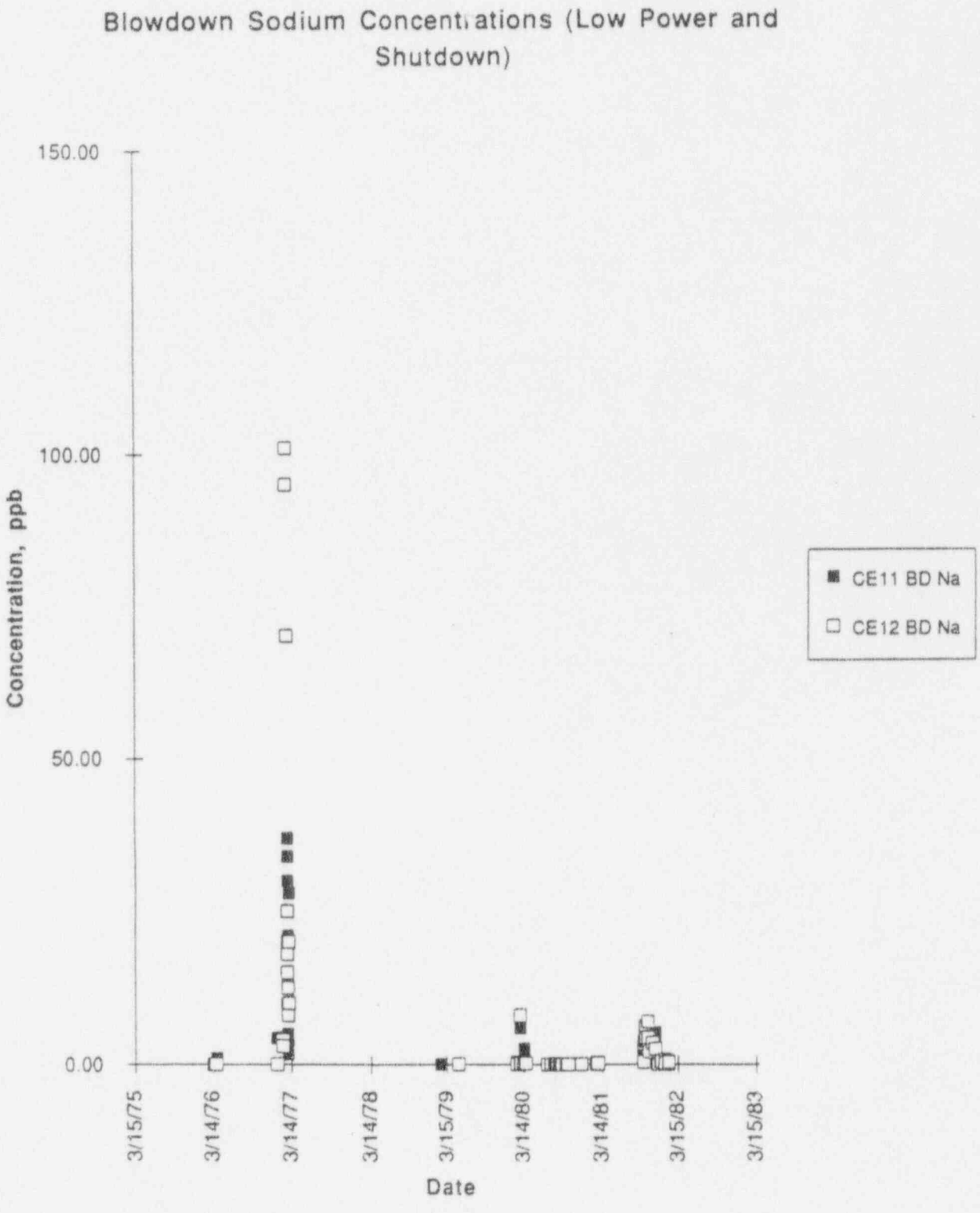
Blowdown Sodium Concentrations (Low Power and Shutdown)
150.00
100.00
50.00
0.00
Concentration, ppb
CE11 BD Na
CE12 BD Na
3/15/75
3/14/76
3/14/77
3/14/78
3/15/79
3/14/80
3/14/81
3/15/82
3/15/83
Date

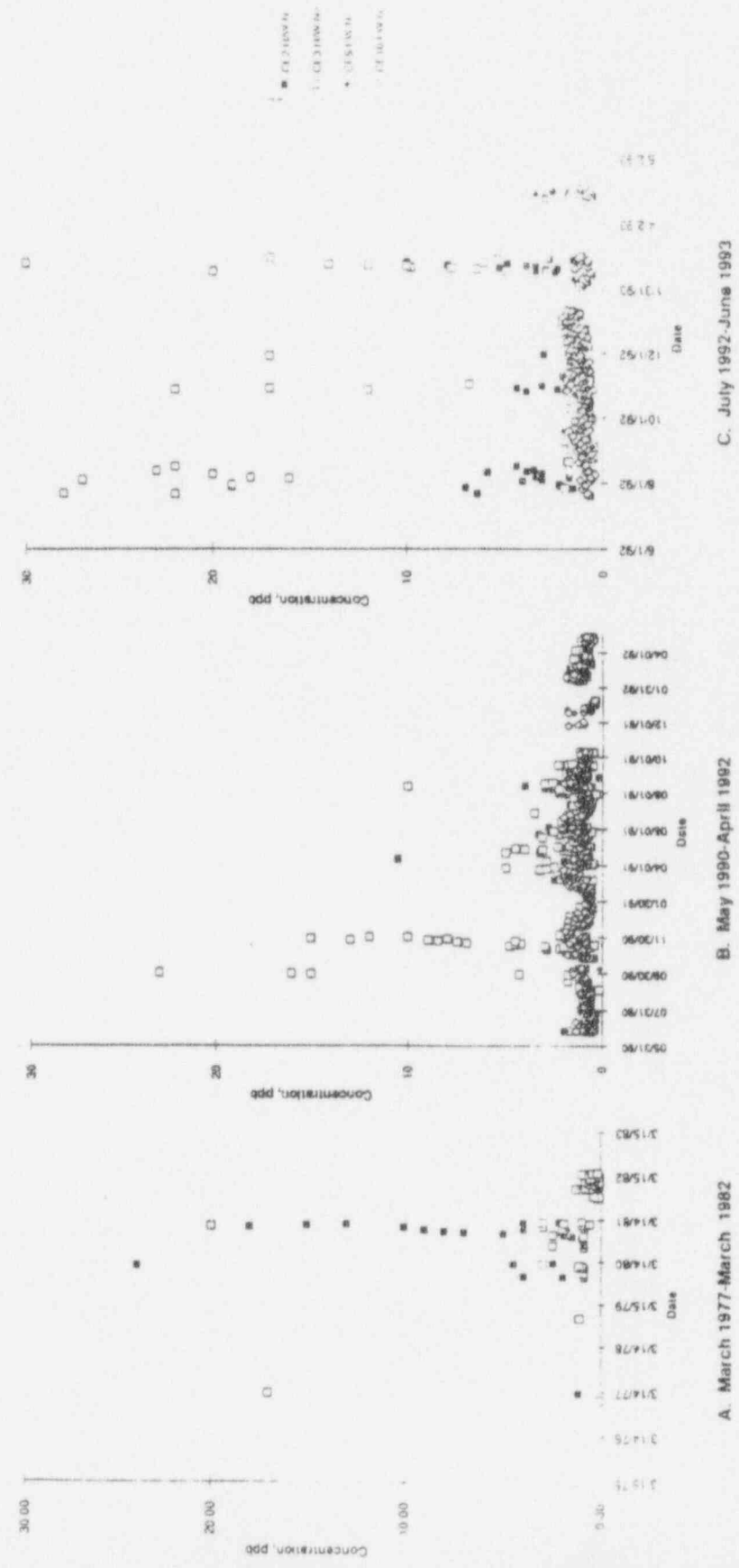
Sodium Concentrations, Inlet and Outlet
Condensate Polisher vs. Time
Concentration, ppb
Date
A. March 1977-March 1982
B. May 1990-April 1992
C. July 1992-June 1993

Figure 3-3

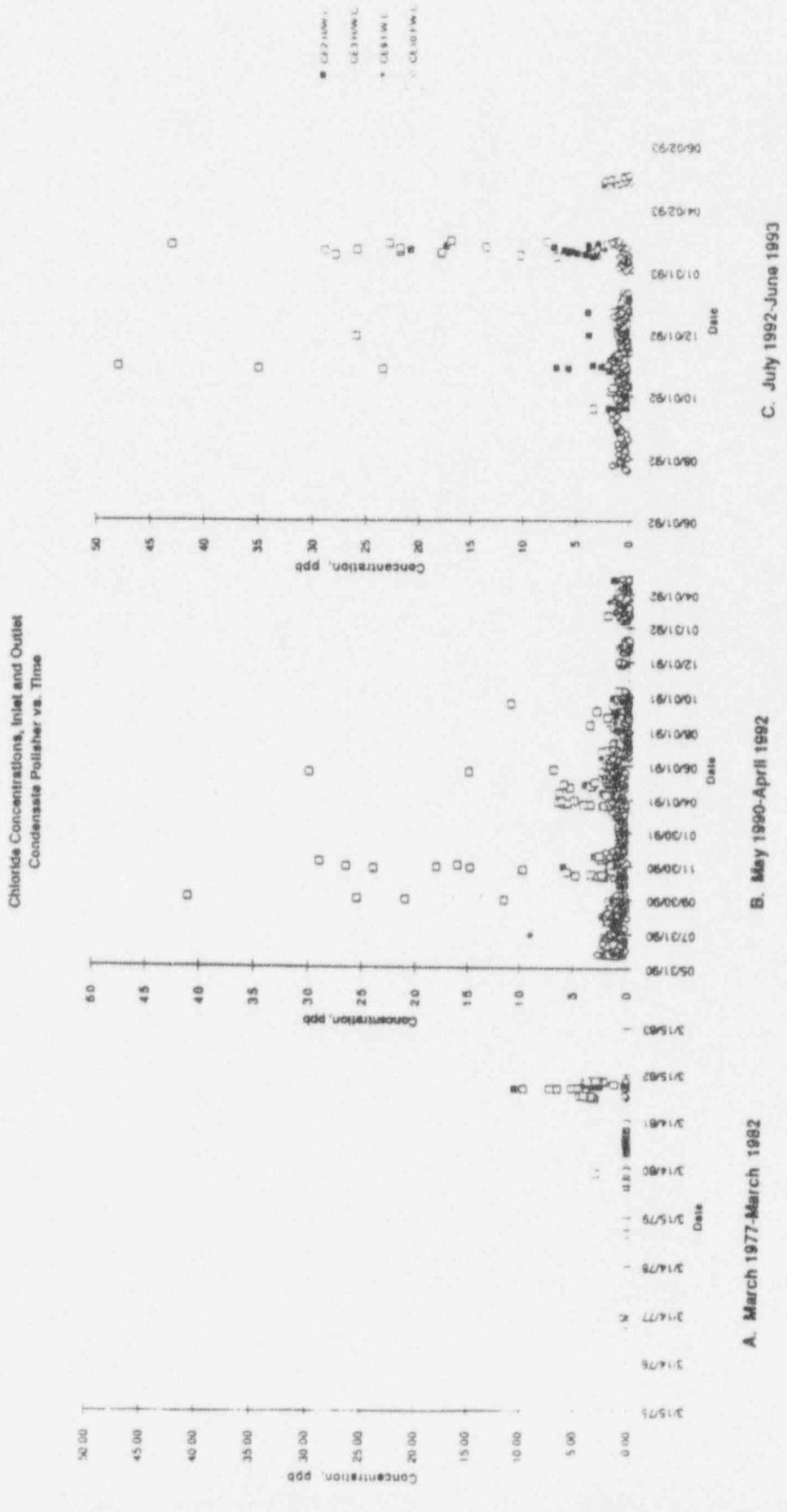
Chloride Concentrations, Inlet and Outlet
Condensate Polisher vs. Time
Concentration, ppb
Date
A. March 1977-March 1982
B. May 1990-April 1992
C. July 1992-June 1993

Figure 3-4

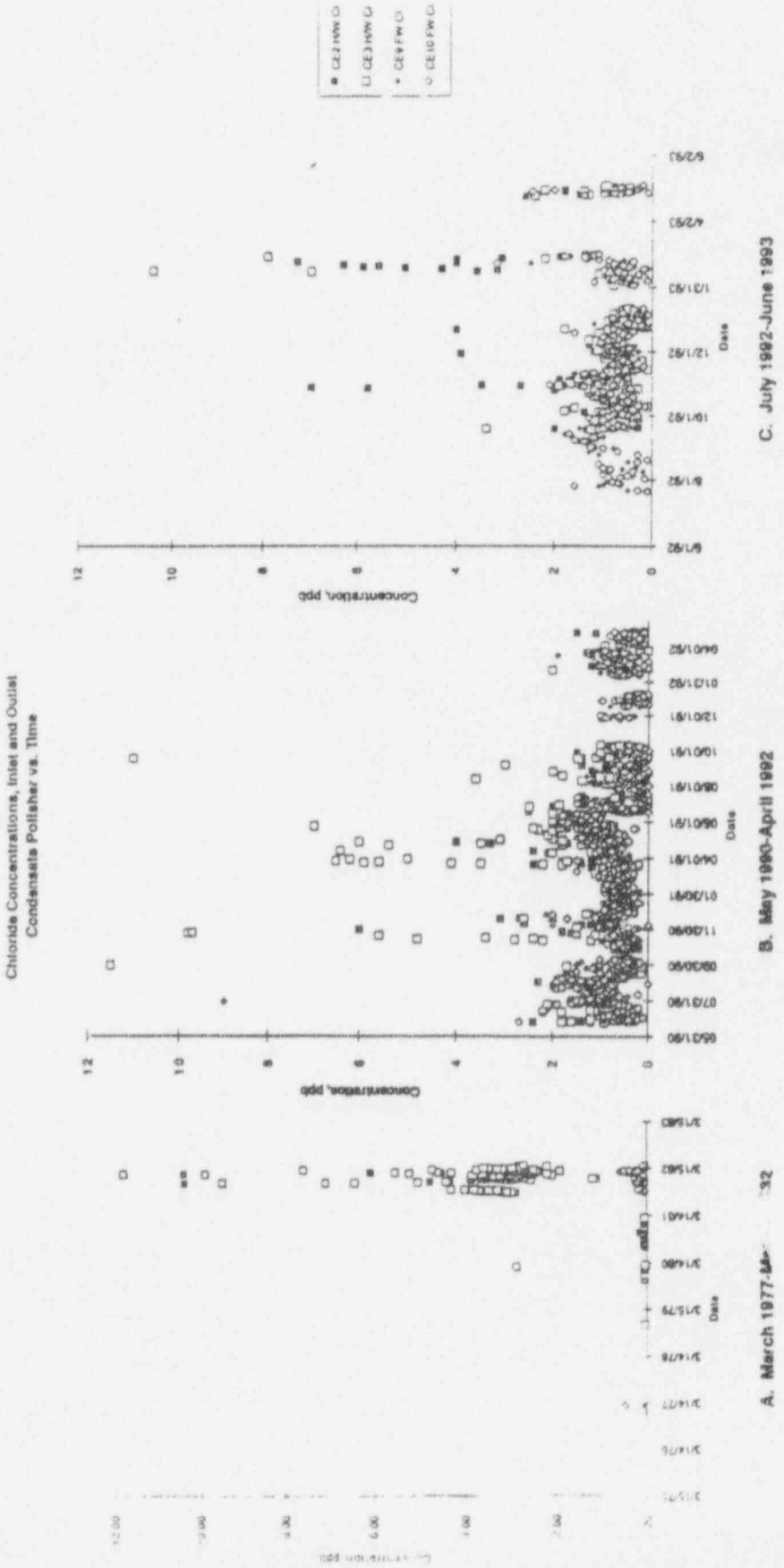
Chloride Concentrations, Inlet and Outlet
Condensate Polisher vs. Time
Concentration, ppb
Date
C. July 1992-June 1993
B. May 1990-April 1992
A. March 1977-

Figure 3-5

Figure 3-6

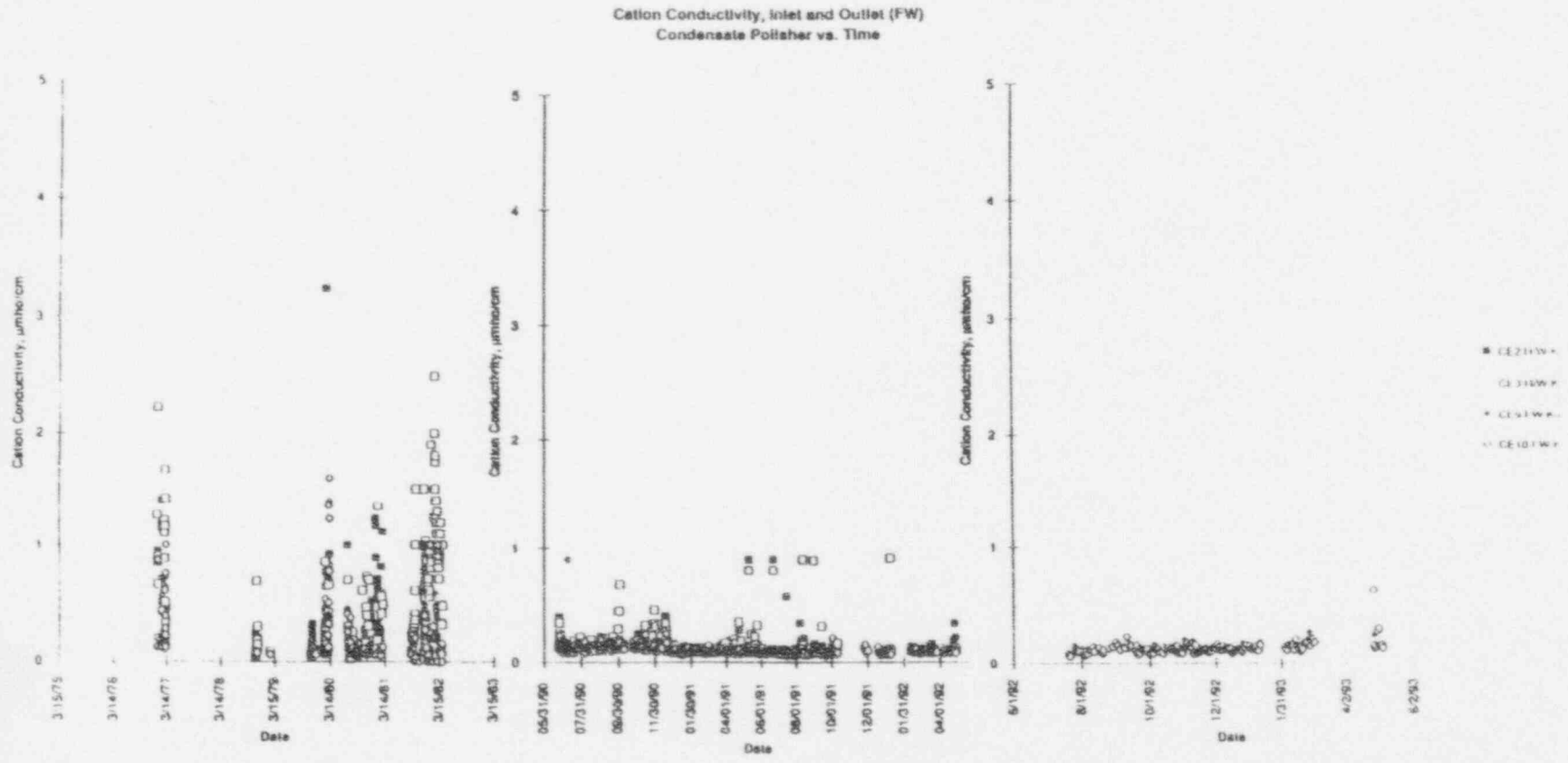
Cation Conductivity, Inlet and Outlet (FW)
Condensate Polisher vs. Time
Cation Conductivity, µmho/cm
Date
A. March 1977-March 1982
B. May 1990-April 1992
C. July 1992-June 1993

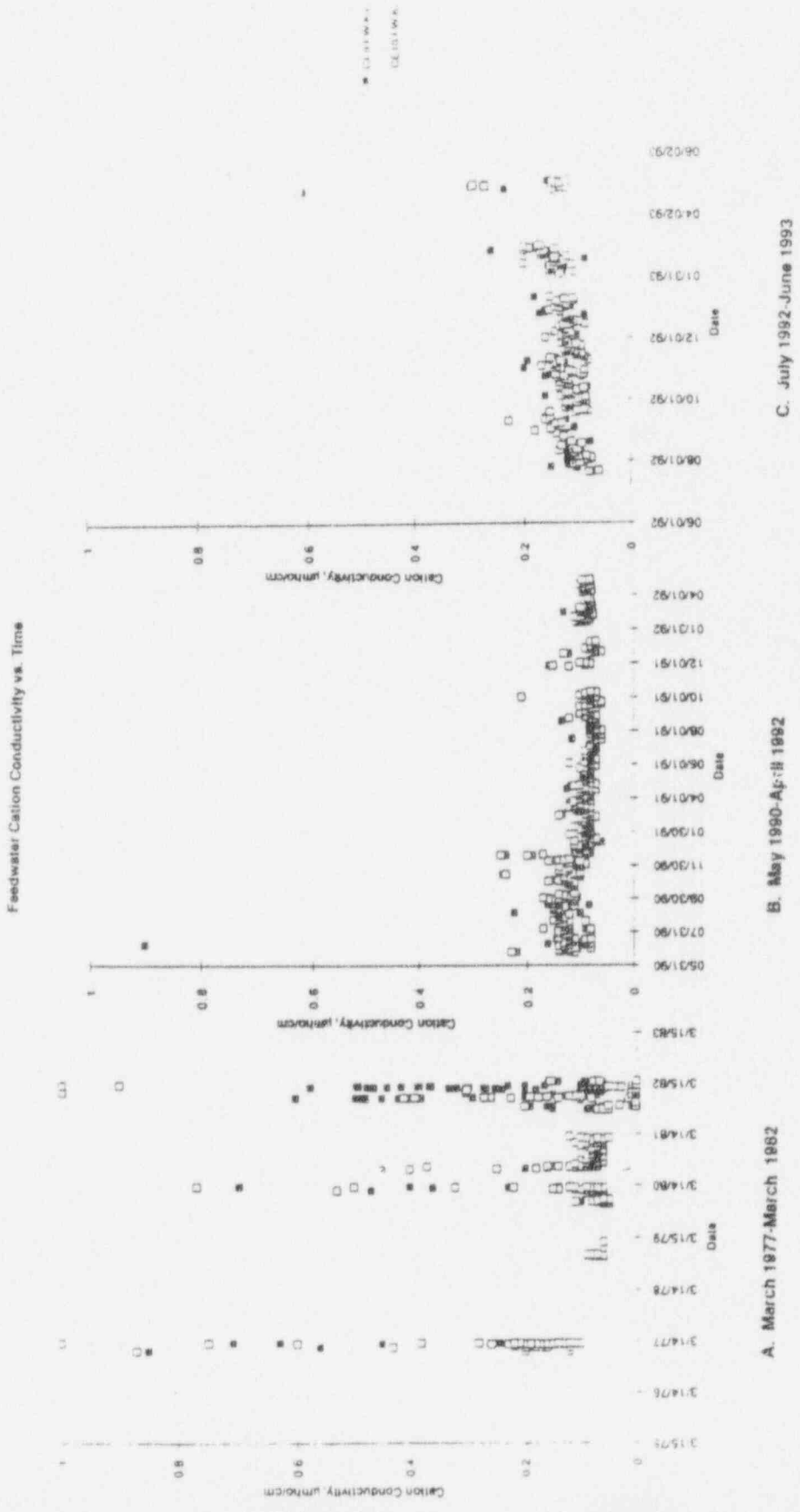
Feedwater Cation Conductivity vs. Time
Cation Conductivity, µmho/cm
Date
A. March 1977-March 1982
B. May 1990-April 1992
C. July 1992-June 1993

Figure 3-7

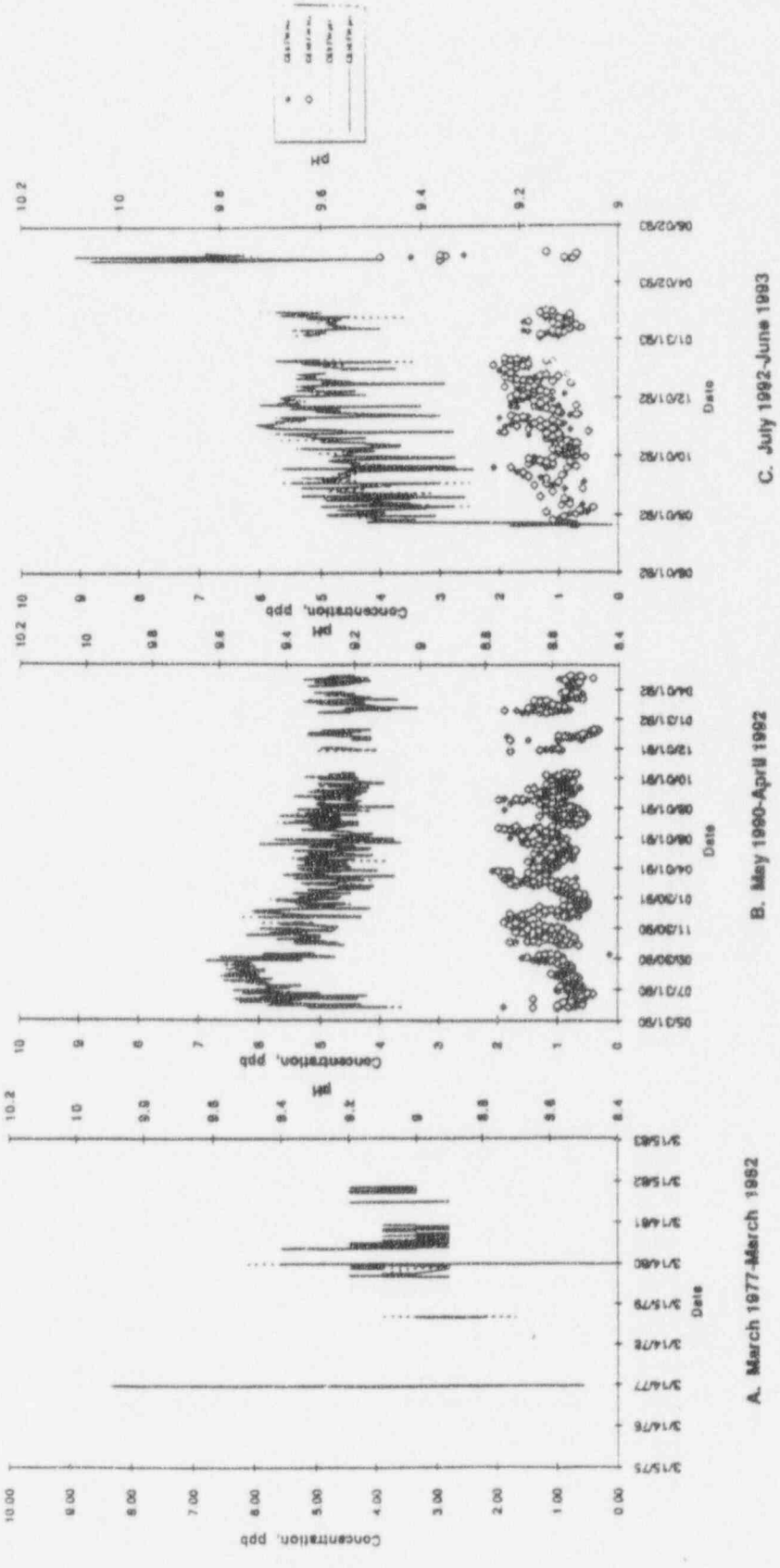

Figure 3-8
Feedwater pH and Na vs. Time

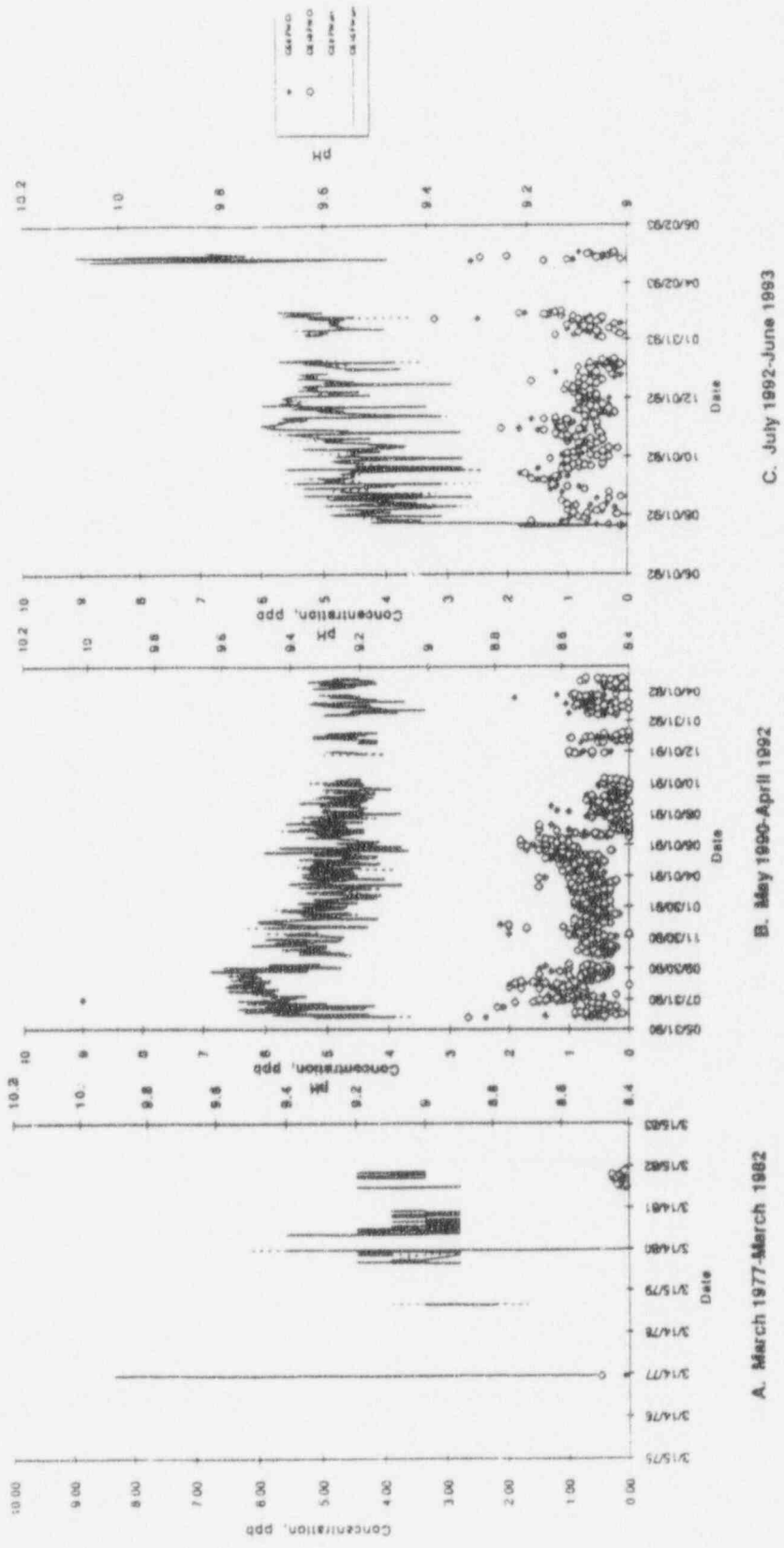

Figure 3-9
Feedwater pH and Cl vs. Time

Figure 3-10

Variation of Feedwater and Deaerator Effluent Hydrazine with Time

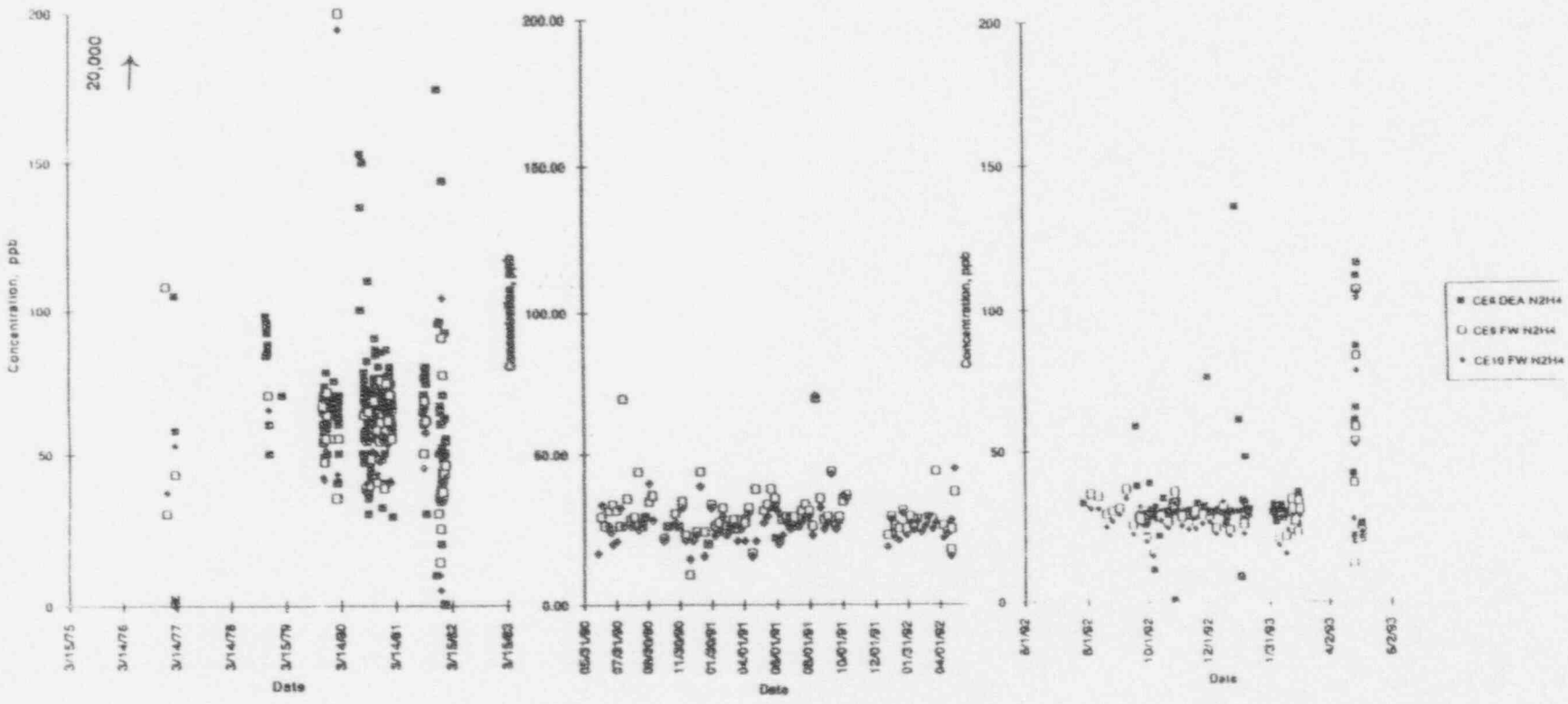

A. March 1977-March 1982

B. May 1990-April 1992

C. July 1992-June 1993

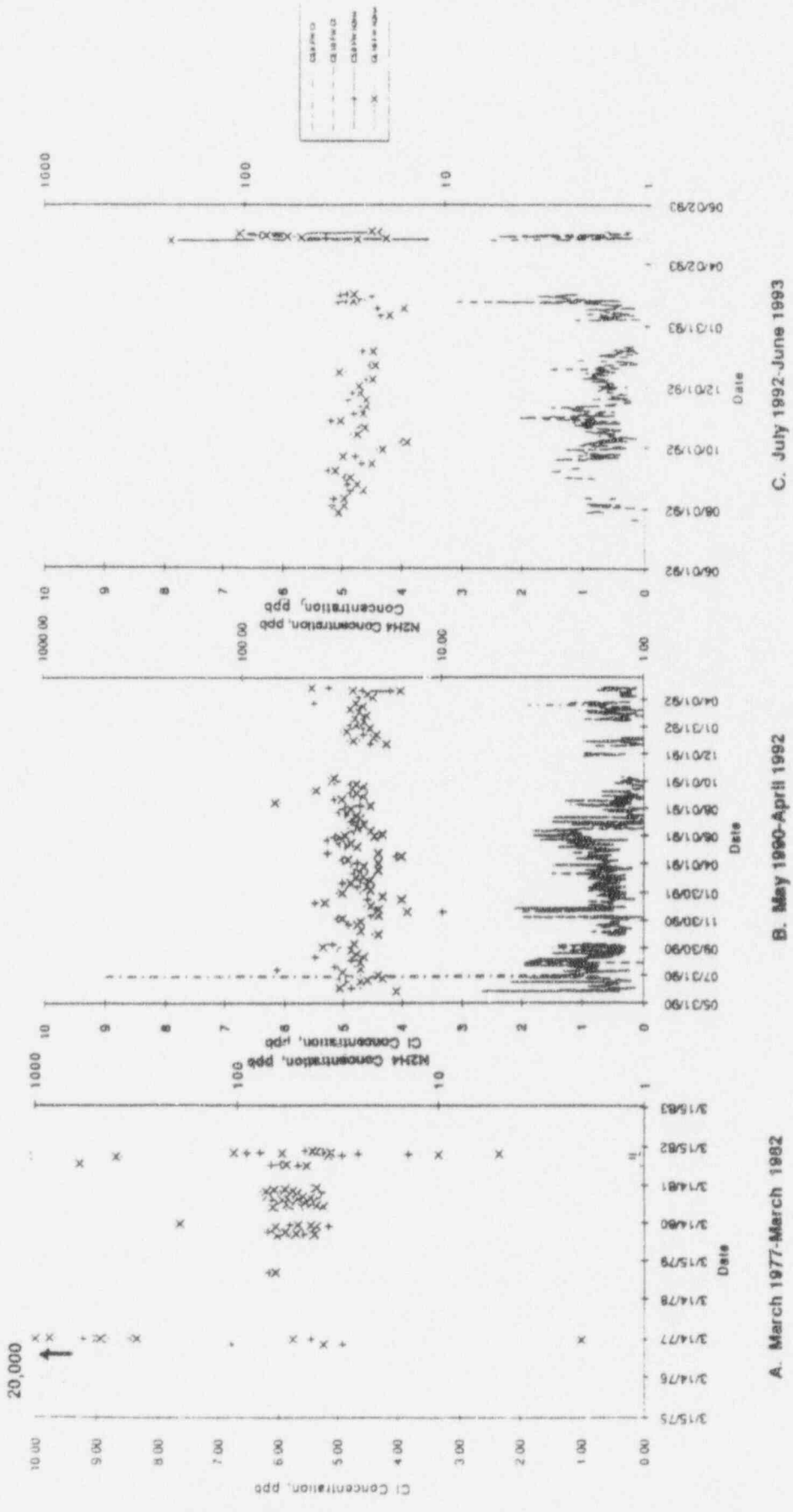

Figure 3-11
Feedwater N_2H_4 and Cl vs. Time

Figure 3-12

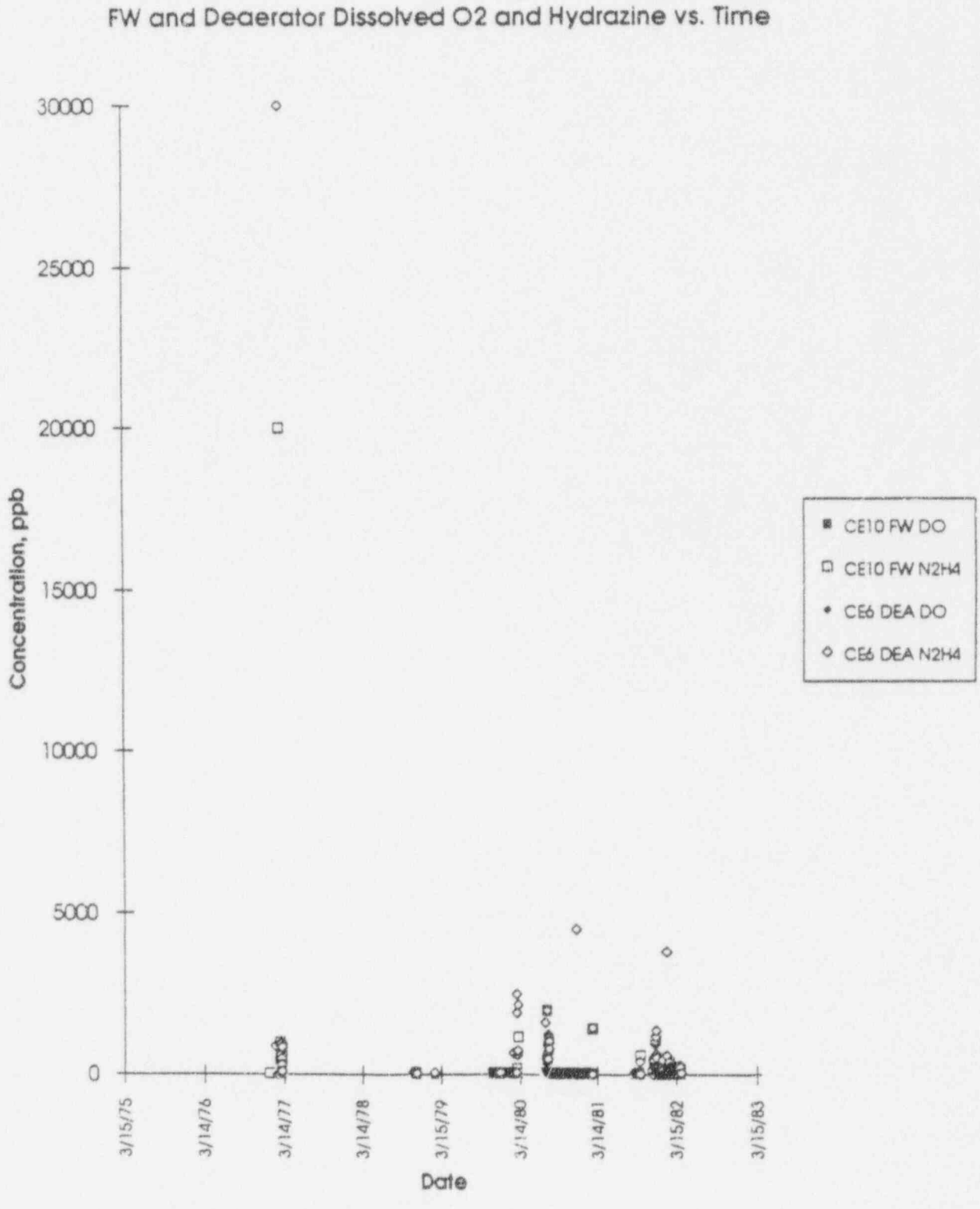
FW and Deaerator Dissolved O2 and Hydrazine vs. Time
Concentration, ppb
30000
25000
20000
15000
10000
5000
0
3/15/75
3/14/76
3/14/77
3/14/78
3/15/79
3/14/80
3/14/81
3/15/82
3/15/83
Date
CE10 FW DO
CE10 FW N2H4
CE6 DEA DO
CE6 DEA N2H4

Figure 3-13

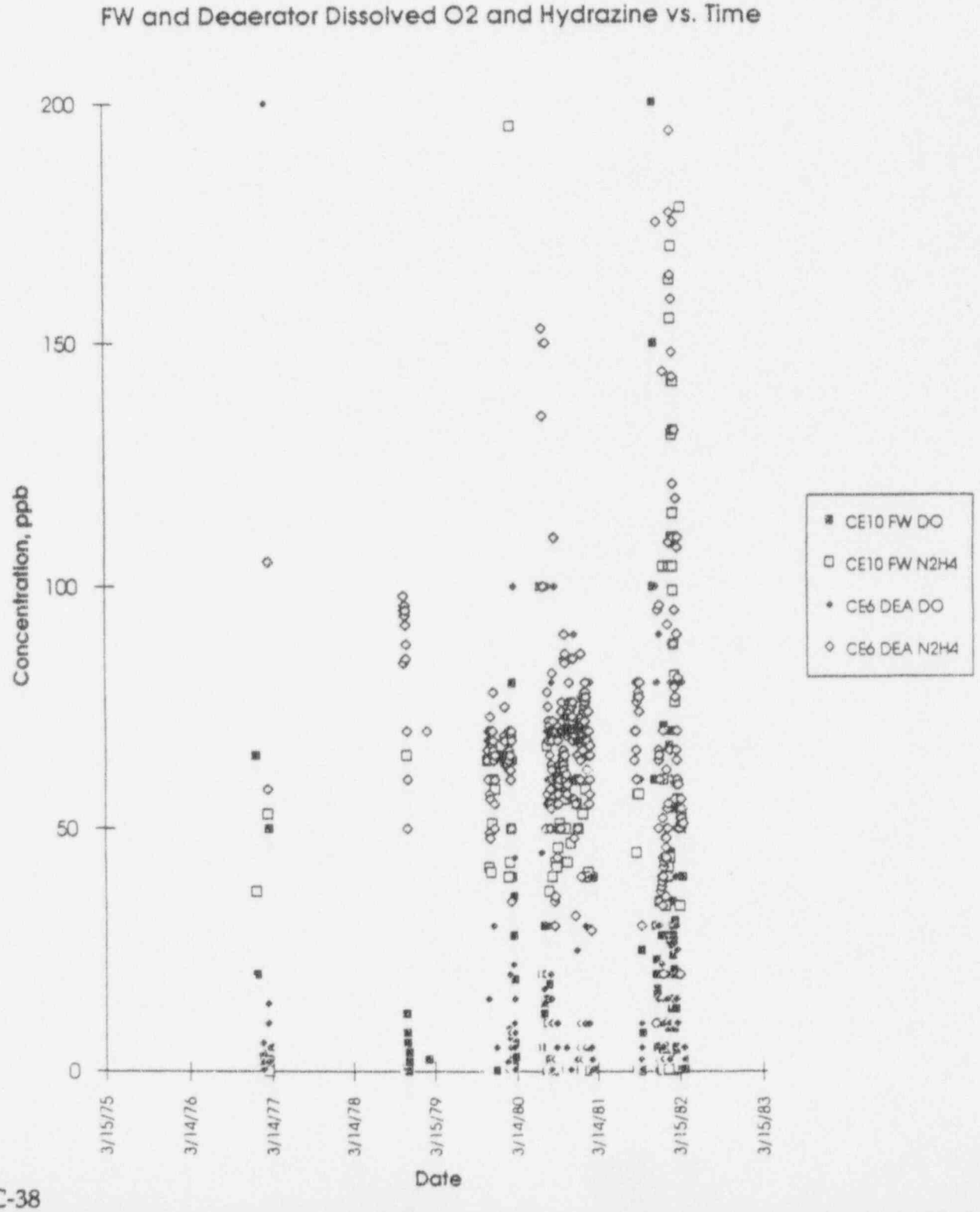
FW and Deaerator Dissolved O2 and Hydrazine vs. Time
Concentration, ppb
200
150
100
50
0
3/15/75
3/14/76
3/14/77
3/14/78
3/15/79
3/14/80
3/14/81
3/15/82
3/15/83
Date
CE10 FW DO
CE10 FW N2H4
CE6 DEA DO
CE6 DEA N2H4

Figure 3-14

CYCLE 9 Sulfate Trends

Comparison of Hotwell Na and FW SO4

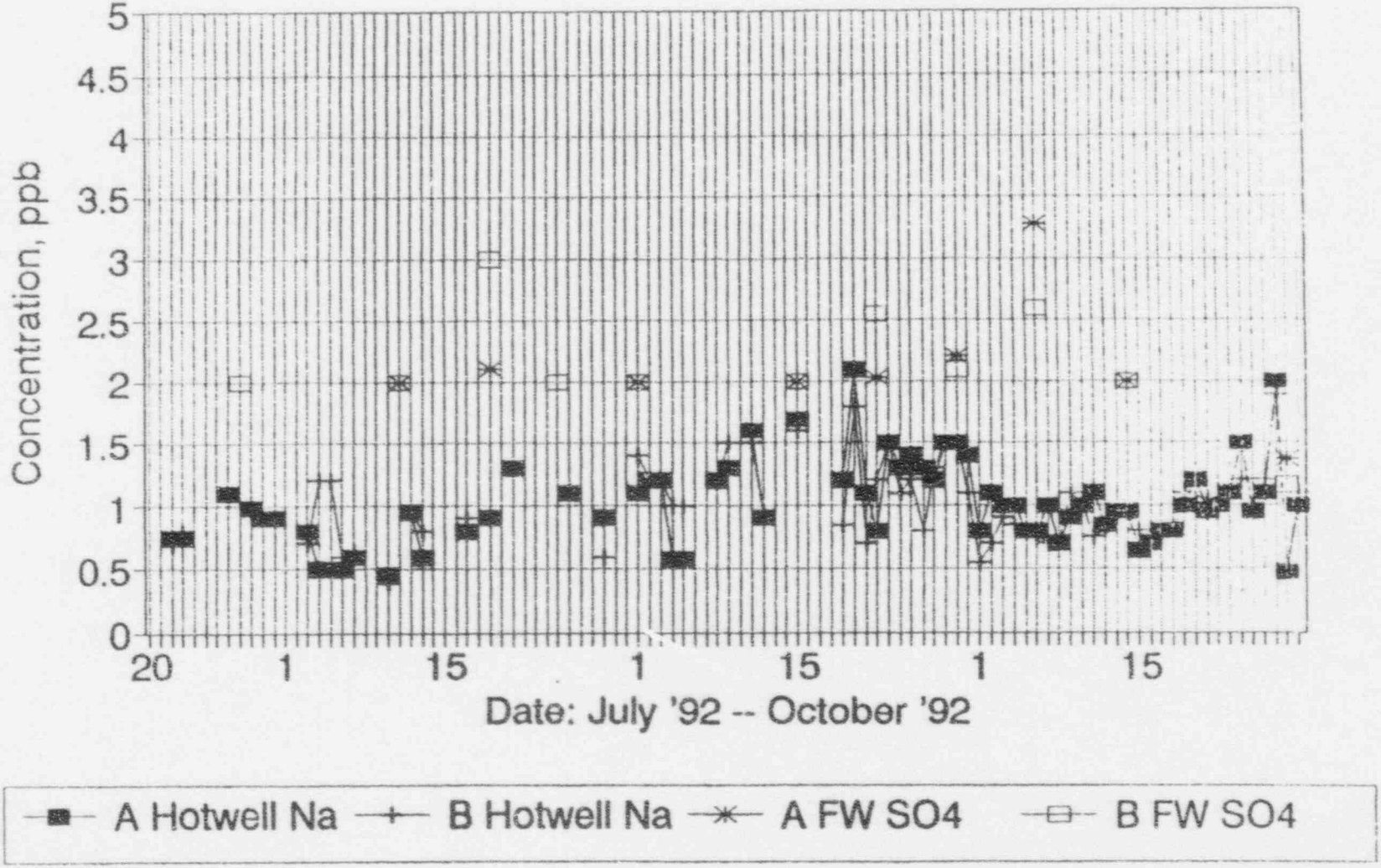

Figure 3-15

1993 Sulfate Trends

Comparison of Hotwell and Feedwater

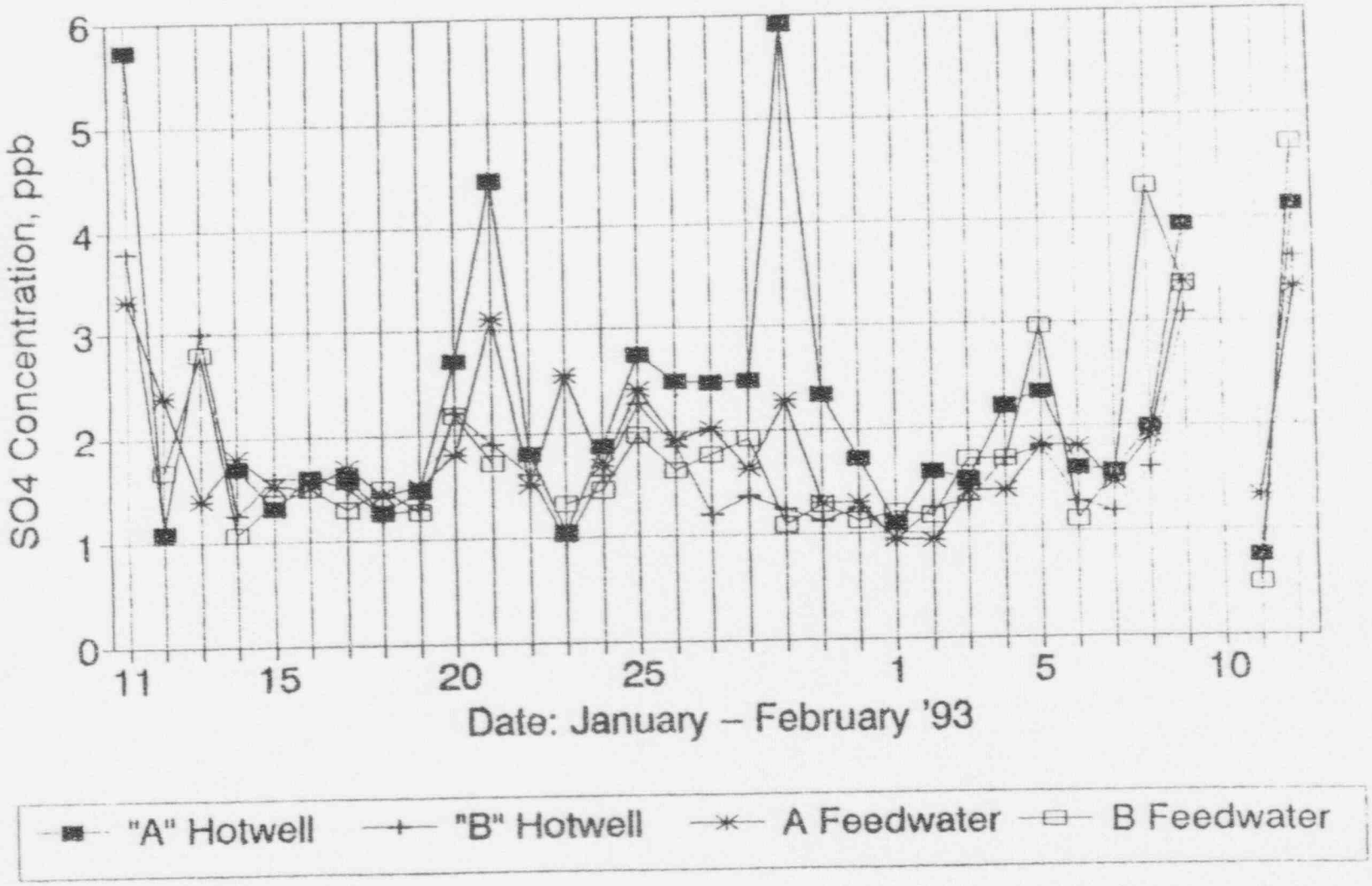

Figure 3-16

1993 Sulfate Trends

Comparison of Common CD Effl and FW

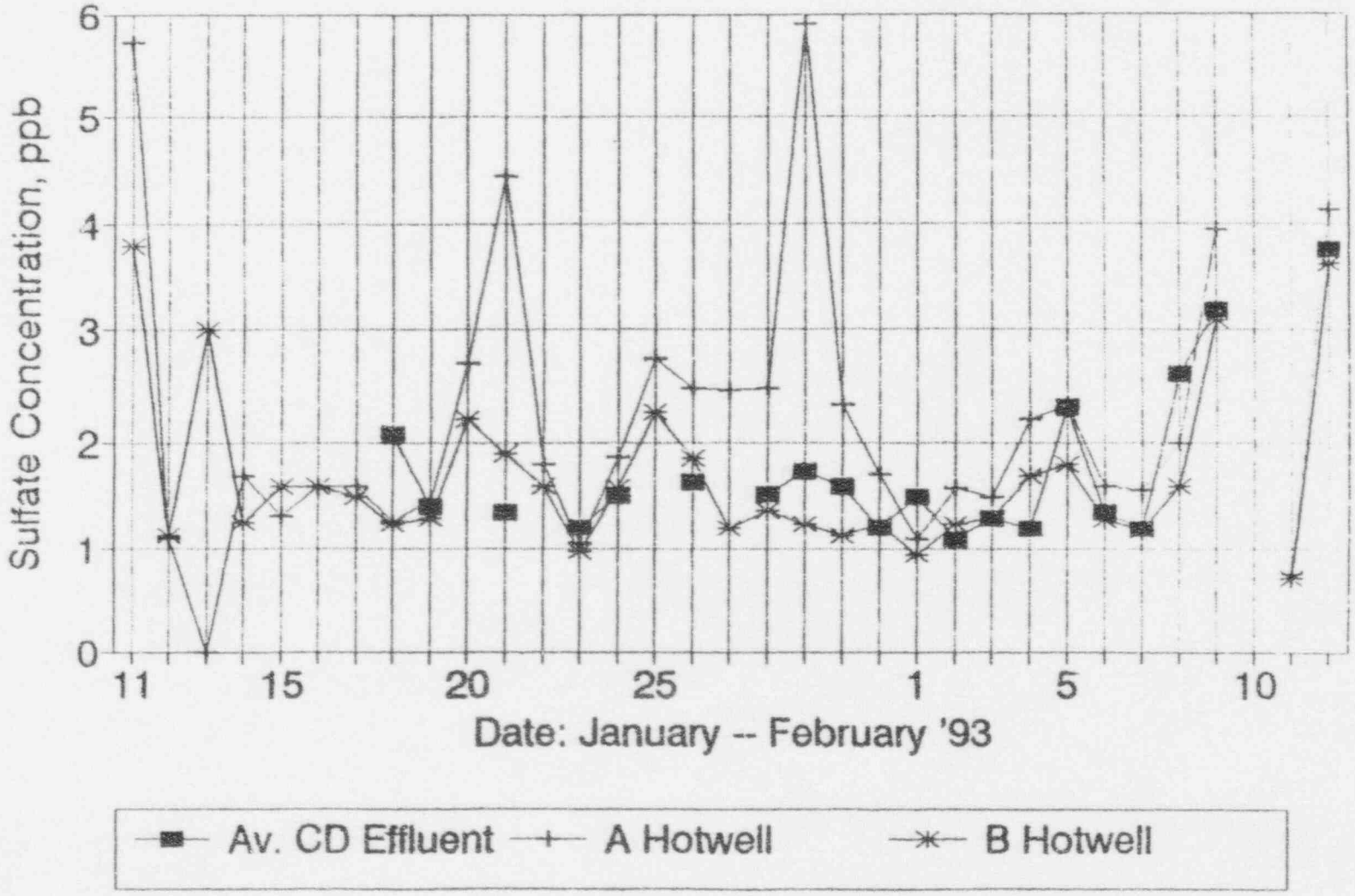

Figure 3-17

Condensate Demin Sulfate Mass Flows

Comparison of CD Inlet and Outlet

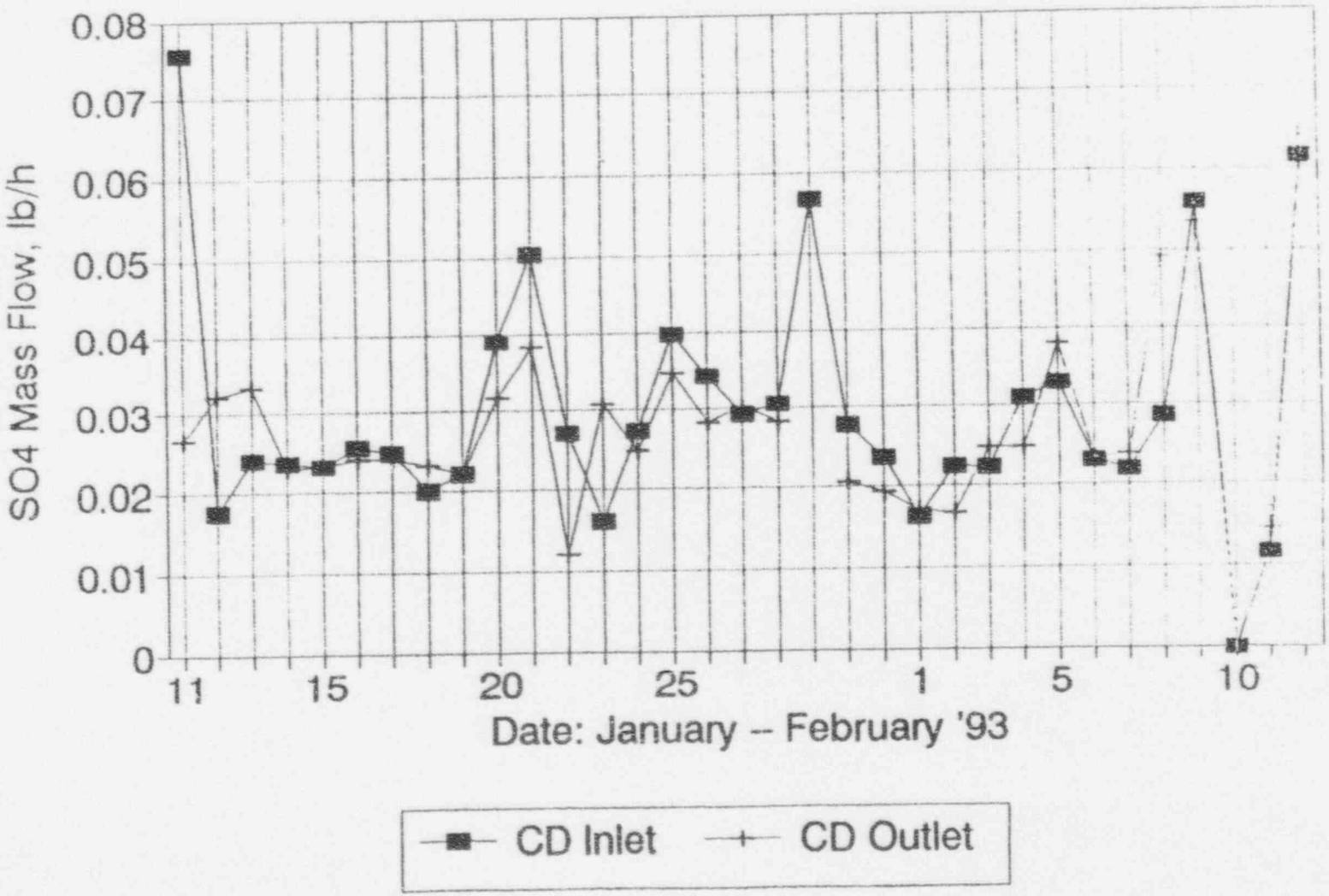

Figure 3-18

1993 Sulfate Trends

Comparison of Heater Drains and FW

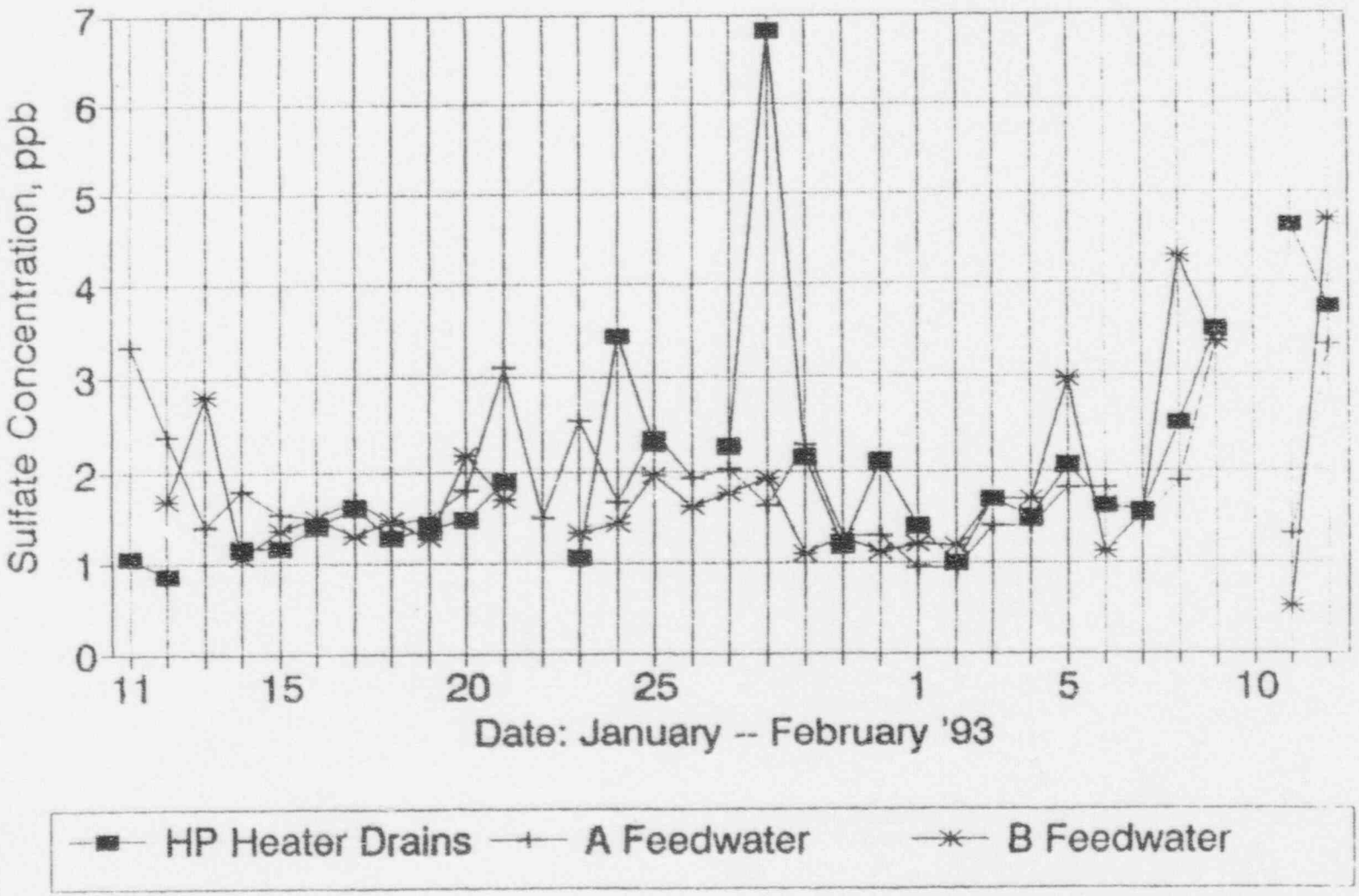

4.0 Conclusions and Recommendations

4.1 Cause of Tube Degradation Below First Tube Support

While this chemistry review cannot prove conclusively what may have caused the steam generator tube degradation observed at Crystal River-3, observations that were made can support the B&W postulate that reduced sulfur species from resin decomposition promoted an acidic attack of tubing early in the operating history of the plant. Specifically:

- There was evidence of high concentrations of non-chloride anions at initial plant startup (cation conductivity peaks of 1 to 1.5 µS/cm between 1977 and 1982, with a maximum of only 0.06 µS/cm accounted for by chloride). Those anions may have been sulfate. Approximately 170 ppb sulfate would balance the measured cation conductivity. In any case, the non-chloride acid species would tend to make steam generator under-deposit and crevice chemistry acid-concentrating.
- Exceptionally high concentrations of hydrazine were present in feedwater at initial plant startup (spikes of 1000 to 20,000 ppb during the period from 1977 through 1982, Figure 3-12, average of approximately 60 ppb, Figure 3-10), without comparable concentrations of oxygen. Therefore, the hydrazine was available for reducing any sulfate present in the steam generators during that period of time.

4.2 Status of Degradation Mechanism

The low-temperature (< 180 °F), acidic, reduced sulfur attack on the tubing freespan below the first tube support should not be progressing at present. While there is not a lot of industry experience with interpretation of hideout return data from once through steam generators, a careful evaluation of data from multiple shutdowns indicates that under-deposit areas on tubing may have neutral to acidic chemistry at present, while the sludge pile region appears to have caustic chemistry. The sludge pile chemistry environment would not support continuation of the reduced sulfur acid attack below the first tube support.

4.3 Recommendations

4.3.1 Crystal River-3 personnel should continue to carefully monitor hideout return chemistry and be alert to the possibility of acidic conditions recurring in the lower portion of the steam generator.

One question that arose early during this project was what might be the cause of caustic chemistry in the sludge pile, when all feedwater data appeared to support a postulate of acid-concentrating solutions in flow-restricted areas of the steam generator. There was no evidence of hideout return of acidic species in the steam piping or turbines this past outage, which would be indicative of continual concentration of sodium hydroxide within the steam generator due to partitioning of acidic species into the steam.

The historical data gave evidence of one very significant hotwell sodium excursion at initial plant startup, which could have been a result of steam carryover of sodium from

throw off the condensate polishers due to high hydrazine concentrations. No feedwater sodium data are available to evaluate this hypothesis. However, the presence of caustic species in sludge pile hideout returns may be an indication that sodium is leaching out from an inventory accumulated in the past, rather than being left behind as acidic species partition into steam during current operations. If this is the case, decreasing quantities of sodium should be observed in hideout return during each outage.

To the extent that the sludge pile chemistry becomes less caustic with time, as determined by hideout return studies, Florida Power Corporation personnel should be alert to the possibility of acidic attack resuming below the first tube support in the future.

4.3.2 Crystal River-3 personnel should make efforts to improve condensate polisher operation and reduce the baseline concentration of sulfate in the secondary cycle.

There are two indications that the condensate polishers are throwing sulfonated organics and fines from cation resins at present: (a) a possible bias in sulfate concentrations between steam generators A and B, and (b) the steady-state leakage of a few ppb of sulfate from the condensate polishers, which was no observed during one earlier period of the plant's operation. Crystal River-3 personnel have determined that this may indicate the presence of a cation resin layer on the bottom of the polisher vessels. Other plants have had some success in addressing this problem by putting in an anion resin layer underneath the mixed bed and by using a new type of non-segregating resin that has been developed.

Due to the possibility that steam generator sludge pile chemistry may become less caustic with time, it would be advisable for Crystal River-3 to make reasonable attempts to reduce the sulfate concentrations in feedwater.

4.3.3 Crystal River-3 personnel should be cautious in adopting high hydrazine chemistry.

Because feedwater appears to be acid-concentrating under nearly all condensate polisher operating conditions to date and the cause of caustic solutions in the sludge pile has not been identified conclusively, there is a good probability that sludge pile, tube support crevice, and under-deposit chemistry environments may all be acidic at some point in the future. If that should occur, the presence of significant excesses of hydrazine would promote reduction of sulfates and could re-initiate reduced-sulfur, acid attack in the freespan below the first tube support.

4.3.4 Crystal River-3 personnel should investigate the possibility of chloride and sodium contamination of supplied bulk hydrazine.

While sodium concentrations related reasonably positively to pH, which would indicate condensate polisher throw of sodium at elevated pH, there was some cycling of sodium concentration that did not appear in pH trends. This same cycling was observed in chloride concentrations, and peaks in chloride concentration usually did not appear related to high pH. The concentration of hydrazine may have exhibited some of the same type cycling observed in sodium and chloride. Therefore, sodium and chloride

contamination of the hydrazine may be indicated. The vendor for hydrazine furnishes a certified analysis with each shipment. However, verbal reports from both the power and semiconductor industries assert that even chemicals of certified quality are often out of specification. While chloride concentration in hydrazine would have to be on the order of 12,000 ppm to account for feedwater transients of 1 ppb, the possibility of hydrazine contamination should be checked at least periodically at Crystal River.

C.1
Data Available for Study

Table C.1-1 lists the data, and their sources, available to this study. Data for the period spanning 1976 through 1982 were obtained from printouts of microfiche data logs. Data for 1990 through 1993 were provided on magnetic media by Florida Power Corporation.

TABLE C.1-1
Data Used In Evaluation

		Conductivity		Concentrations		
Stream	Dates	K_s	K_a	Na^+	Cl^-	SiO_2
Sec Cycle Chem Log	2/1/77-3/4/77					
	2/3/82-3/4/82					
Condenser H/W, CE-2						
Condenser H/W, CE-3			X	X	X	
Condensate Demin Effluent, CE-5			X	X	X	
Feedwater, CE-9			X	X		X
Feedwater, CE-10			X	X		X
Blowdown, CE-11 (<15% power)			X	X	X	X
Blowdown, CD-12 (<15% power)			X	X	X	X

TABLE C.1-1, cont'd.
Data Used In Evaluation

Stream	Dates	Conductivity K_s	Conductivity K_a	Concentrations Na^+	Concentrations Cl^-	Concentrations SiO_2
Chem Rad Report	3/15/76-3/31/76					
	1/1/77-1/10/77					
	11/4/78-11/20/78					
	2/13/79					
	11/7/79-3/30/80					
	7/3/80-7/30/80					
	8/5/80-12/28/80					
	1/5/81-2/28/81					
	9/4/81-10/1/81					
	11/5/81-11/6/81					
	11/21/81-1/21/82					
	1/23/82-4/6/82					
Condenser H/W, CE-2		X	X			
Condenser H/W, CE-3		X	X			
Condensate Demin Effluent, CE-5		X	X	X	X	X
Feedwater, CE-9			X			X
Feedwater, CE-10			X			X

TABLE C.1-1, cont'd.
Data Used In Evaluation

Stream	Dates	Conductivity K_s	Conductivity K_a	Concentrations Na^+	Concentrations Cl^-	SiO_2
Chem Rad Report	5/10/79					
	5/18/80					
	9/9/81					
	9/28/81-10/1/81					
	10/3/81-10/7/81					
	10/8/81-10/10/81					
	10/21/81-10/27/81					
	10/29/81					
	11/11/81-11/12/81					
	11/22/81					
	11/24/81					
	11/26/81					
	1/10/82-1/11/82					
Blowdown, CE-11 (<15% power)			X	X	X	
Blowdown, CD-12 (<15% power)			X	X	X	

TABLE C.1-1, cont'd.
Data Used In Evaluation

Stream	Dates	Conductivity K_s	Conductivity K_a	Concentrations Na^+	Concentrations Cl^-	Concentrations $SO_4^=$	Concentrations SiO_2
H/O Return Study	10/9/88 10/11/88						
Blowdown, CE-11 (<15% power)				X	X	X	X
Blowdown, CE-12 (<15% power)				X	X	X	X
H/O Return Study	10/11/91- 10/13/91						
Feedwater, CE-9				X	X		
Feedwater, CE-10				X	X		
Blowdown, CE-11 (<15% power)				X	X	X	X
Blowdown, CE-12 (<15% power)				X	X	X	X
H/O Return Study (outage startup)	11/17/91- 11/18/91						
Feedwater, CE-9			X	X	X		
Feedwater, CE-10			X	X	X		
Blowdown,[2] CE-11 (<15% power)					X	X	X
Blowdown,[3] CE-12 (<15% power)					X	X	X

[2] Also potassium, calcium, magnesium, fluoride, acetate, formate.
[3] Also potassium, calcium, magnesium, fluoride, acetate, formate.

TABLE C.1-1, cont'd.
Data Used In Evaluation

Stream	Dates	Conductivity K_s	Conductivity K_a	Concentrations Na^+	Concentrations Cl^-	Concentrations $SO_4^=$	Concentrations SiO_2
CH-450, Bulk Water (H/O Ret.)	3/37/92-4/2/92						
Blowdown, CE-11 (<15% power)			X	X	X	X	X
Blowdown, CE-12 (<15% power)			X	X	X	X	X
H/O Return Study (H/O Return)	4/30/92-5/1/92						
Feedwater, CE-9			X	X	X		
Feedwater, CE-10			X	X	X		
Blowdown,[4] CE-11 (<15% power)			X		X	X	X
Blowdown,[5] CE-12 (<15% power)			X		X	X	X
H/O Return Study (H/O Return)[6]	3/3/93-3/5/93						
HP Heater Drains, CE-7				X	X	X	X
Feedwater, CE-9				X	X	X	X
Feedwater, CE-10				X	X	X	X
LP Heater Drains, CE16/17				X	X	X	X
MSR Drains, CE-100				X	X	X	X
Blowdown, CE-11				X	X	X	X
Blowdown, CE-12				X	X	X	X

[4] Also potassium, calcium, magnesium, fluoride, acetate, formate.
[5] Also potassium, calcium, magnesium, fluoride, acetate, formate.
[6] Also potassium, calcium, magnesium, lithium, fluoride, nitrate, phosphate, acetate, and formate for all streams sampled this outage.

TABLE C.1-1, cont'd.
Data Used In Evaluation

Stream	Dates	Conductivity K_s	Conductivity K_a	Concentrations Na^+	Concentrations Cl^-	Concentrations $SO_4^=$	Concentrations SiO_2
Supplemental Data Sheet (Drain after water slap)		5/18/92					
Blowdown[7]				X	X	X	
Transport Study	7/11/91-10/15/91						
IP Htr Drains, CE-7					X		
Steam, CE-13				X	X		
Steam, CE-14				X	X		
LP Htr Drains, CE-16				X	X		
LP Htr Drains, CE-20				X	X		

[7] Also fluoride, acetate, formate.

TABLE C.1-1, cont'd.
Data Used In Evaluation

Stream	Dates	Conductivity K_s	Conductivity K_a	Concentrations Na^+	Concentrations Cl^-	Concentrations $SO_4^=$	Concentrations SiO_2
REDAS Data	7/1/91-10/11/91						
Condenser H/W, CE-2		X	X	X	X		
REDAS Data	6/29/91-7/12/91						
Condenser H/W, CE-3							X
REDAS Data	5/27/91-7/12/91						
Cond Demin Effl, CE-5		X	X	X	X		X
REDAS Data	7/1/91-10/4/91						
IP Htr Drains, CE-7				X			X
REDAS Data	6/29/90-10/4/91						
IP Htr Drains, CE-7				X			X
MSR Drains, CE100		X	X	X	X		
REDAS Data	8/1/91-10/11/91						
Feedwater[8], CE-9			X	X	X		X
Feedwater[9], CE-10			X	X	X		X

[8] Also sulfate, formate, acetate for 7/2/91-10/8/91.
[9] Also sulfate, formate, acetate for 7/2/91-10/8/91.

TABLE C.1-1, cont'd.
Data Used In Evaluation

Stream	Dates	Conductivity K_s	Conductivity K_a	Concentrations Na^+	Concentrations Cl^-	Concentrations SiO_2
Secondary Cycle Chemistry Spreadsheets	6/24/90-4/30/92					
Condenser H/W, CE-2		X	X	X	X	
Condense. H/W, CE-3		X	X	X	X	
Cond Demin Effl, CE-5		X	X	X	X	
Feedwater,[10] CD-9			X	X	X	X
Feedwater,[11] CD-10			X	X	X	X
	7/20/92-11/6/92					
Condenser H/W, CE-2				X	X	
Condenser H/W, CE-3				X	X	
Feedwater,[12] CD-9			X	X	X	X
Feedwater,[13] CD-10			X	X	X	X

[10] Also acetate and formate.
[11] Also acetate and formate.
[12] Also acetate and formate.
[13] Also acetate and formate.

TABLE C.1-1, cont'd.
Data Used In Evaluation

Stream	Dates	Conductivity K_s	Conductivity K_a	Concentrations Na^+	Concentrations Cl^-	Concentrations $SO_4^=$
Secondary Cycle Chemistry Spreadsheets, cont'd.						
	1/11/93-2/9/93					
Cond Demin Effl, CE-5						X
IP Htr Drains, CE-7						X
Feedwater, CD-9						X
Feedwater, CD-10						X
Steam, CE-13						X
Steam, CE-14						X
LP Htr Drains, CE-16/20						X
MSR Drains, CE100						X

TABLE C.1-2
Supplemental Chemistry Data From Reports

Stream	Dates	Conductivity K_s	Conductivity K_a	Concentrations Na^+	Concentrations Cl^-	Concentrations SiO_2
OTSG Secondary Chemistry Study: Fourth Progress Report (Draft) August-October 1978						
Condensate Demin Inlet	9/15/78-10/31/78	X	X	X		
Condensate Demin Effluent	9/15/78-10/31/78	X	X	X		
Feedwater	1/1/78-10/31/78		X	X		
Blowdown (Startup)	9/6/79-9/29/78		X	X	X	X
OTSG Secondary Chemistry Study: Fifth Progress Report (Preliminary) November 1978-January 1979						
Condensate Demin Inlet	9/1/78-1/31/79		X	X		
Condensate Demin Effluent	9/1/78-1/31/79		X	X		
CD Bed A Effluent	10/1/78-10/31/78	X				
CD Bed B Effluent	10/1/78-10/31/78	X				
Blowdown (Startup & HSB)	12/30/78 1/6/79 1/17/79 1/30/79		X	X	X	X

TABLE C.1-2
Supplemental Chemistry Data From Reports, cont'd.

Stream	Dates	Conductivity K_s	Conductivity K_a	Concentrations Na^+	Concentrations Cl^-	Concentrations SiO_2
OTSG Secondary Chemistry Study: Sixth Progress Report (Preliminary) February -July 1979						
Condensate Demin Inlet	9/15/78-4/30/79		X	X		
Condensate Demin Effluent	9/15/78-4/30/79		X	X		
CD Bed A Effluent	10/1/78-10/31/78	X				
CD Bed B Effluent	10/15/78-11/5/78	X				
CD Beds A-F Eff's	2/1/79-4/30/79		X			
Blowdown (Layup)	4/24/79-5/7/79		X	X	X	X
Blowdown[14] (Shutdown)	4/23/79			X	X	
Chemistry Evaluation OTSG Water Slap Process Preliminary Report						
Pre-Slap Swipes[15]	1985			X	X	X
Liquid-Lower TS[16]	1985			X	X	X
Tube Support Plates[17]	1985	X	X	X	X	X

[14] Also sulfate.
[15] Also iron, copper, calcium, magnesium, silicon, fluoride, nitrate, phosphate, sulfate.
[16] Also iron, copper, calcium, magnesium, silicon, fluoride, nitrate, phosphate, sulfate.
[17] Also iron, copper, calcium, magnesium, silica, fluoride, nitrate, phosphate, sulfate.

C.2
Chemistry Transients Identified From Data

Many of the impurity concentrations in the following table are within the normal ranges encountered at Crystal River-3. They were selected as "transient" points for this study because they represented peaks above a baseline that could be defined for several days.

TABLE C.2-1

Secondary Cycle Chemistry Transients

Condenser High Na and Cl			
CE-2			
December 19, 1990	Na=1.8 ppb	Cl=3.1 ppb	DO=106 ppb
August 9, 1991	Na=2.70	Cl=1.35	DO=14.60
October 28, 1992	Na=2.4	Cl=5.8	DO=3.05
CE-3			
October 1, 1990	Na=16	Cl=25.5	DO=1.94
November 27, 1990	Na=13	Cl=14.8	DO=2.87
December 19, 1990	Na=1.8	Cl=2.6	DO=4.82
March 26, 1991	Na=3.2	Cl=5.6	DO=2.83
May 21, 1991	Na=1.3	Cl=15	DO=5.33
October 28, 1992	Na=12	Cl=23.5	DO=3.98
Condensate Demineralizer Effluent High Na and Low Cl			
CE-5			
June 24, 1990	Na=1.0 ppb	Cl=0.08 ppb	K_s=3.02 µS/cm
October 8, 1990	Na=1.6	Cl=0.15	K_s=6.48
November 27, 1990	Na=1.9	Cl=0.8	K_s=6.58
December 11, 1990	Na=1.9	Cl=0.5	K_s=4.82
January 5, 1991	Na=1.9	Cl=0.8	K_s=5.84
January 11, 1991	Na=1.2	Cl=0.8	K_s=5.13
February 12, 1991	Na=1.1	Cl=0.65	K_s=4.68
February 27, 1991	Na=1.8	Cl=0.5	K_s=4.3
May 1, 1991	Na=1.3	Cl=0.7	K_s=4.39
May 17, 1991	Na=1.4	Cl=1.2	K_s=4.51
December 18, 1991	Na=1.7	Cl=0.4	K_s=3.19

TABLE C.2-1, cont'd.

Secondary Cycle Chemistry Transients, cont'd.

Condenser High Na and Low Cl

CE-2			
September 18, 1990	Na=1.2 ppb	Cl=0.8 ppb	DO=1.33 ppb
October 1, 1990	Na=1.5	Cl=0.7	DO=1.52
October 30, 1990	Na=0.95	Cl=0.4	DO=2.86
November 16, 1990	Na=1.9	Cl=0.4	DO=2.5
January 5, 1991	Na=1.6	Cl=0.8	DO=2.47
March 4, 1991	Na=1.5	Cl=0.4	DO=2.78
March 12, 1991	Na=1.3	Cl=0.8	DO=3.3
March 19, 1991	Na=1.6	Cl=0.3	DO=3.13
March 29, 1991	Na=1.4	Cl=0.4	DO=2.14
June 18, 1991	Na=1.7	Cl=2.5	DO=1.74
July 8, 1991	Na=1.5	Cl=0.3	DO=1.57
July 23, 1991	Na=1.1	Cl=0.4	DO=1.61
July 31, 1991	Na=2.3	Cl=0.3	DO=2.38
August 20, 1991	Na=1.2	Cl=0.4	DO=3.15
September 3, 1991	Na=1.2	Cl=0.6	DO=2.72
September 10, 1991	Na=1.4	Cl=0.5	DO=2.46
September 18, 1991	Na=1.7	Cl=0.05	DO=2.51
October 1, 1991	Na=1.1	Cl=0.2	DO=2.72
CE-3			
September 10, 1990	Na=0.95	Cl=0.5	DO=1.91
September 18, 1990	Na=1.80	Cl=0.6	DO=1.58
October 8, 1990	Na=1.2	Cl=0.6	DO=1.76
November 6, 1990	Na=1.9	Cl=0.5	DO=2.57
December 4, 1990	Na=1.6	Cl=1.0	DO=2.68
January 5, 1991	Na=1.7	Cl=0.8	DO=3.08
January 22, 1991	Na=1.2	Cl=0.6	DO=3.58
March 4, 1991	Na=1.5	Cl=0.5	DO=3.65
March 12, 1991	Na=1.3	Cl=1.0	DO=3.52
March 19, 1991	Na=1.7	Cl=0.4	DO=3.88
June 18, 1991	Na=1.7	Cl=0.46	DO=1.83
July 9, 1991	Na=0.6	Cl=0.2	DO=2.08
July 16, 1991	Na=1.0	Cl=0.3	DO=0.34
July 23, 1991	Na=0.8	Cl=0.3	DO=1.76

TABLE C.2-1, cont'd.

Secondary Cycle Chemistry Transients, cont'd.

Condenser High Na and Low Cl, cont'd.

CE-3, cont'd.

July 30, 1991	Na=0.35	Cl=0.1	DO=7.2
August 8, 1991	Na=2.2	Cl=0.5	DO=2.26
August 20, 1991	Na=1.3	Cl=0.1	DO=2.27
September 3, 1991	Na=0.9	Cl=0.4	DO=2.17
September 10, 1991	Na=0.99	Cl=0.59	DO=4.38
September 24, 1991	Na=0.9	Cl=0.2	DO=0.41
February 18, 1991	Na=1.8	Cl=0.6	DO=2.7
March 10, 1991	Na=1.1	Cl=0.55	DO=2.59
March 21, 1991	Na=1.5	Cl=0.9	DO=3.05
April 14, 1991	Na=0.8	Cl=0.5	DO=1.94

TABLE C.2-2

Feedwater Chemistry Data
For Periods of Chemistry Transients

Condenser High Na and Cl

		Feedwater Impurity Concentration, ppb						MULTEQ Estimated
Date	Train	Na	Cl	SO_4	Formate	Acetate	H_3SiO_4[18]	pH/NpH
10/1/90	A	1.5	0.4	1	2.57	2	7.9	6.98/5.74, CF=10^3 9.42/5.02, D BP=4.49 °C
	B	1.5	0.5	4.57[19]	17.7[20]	5.8[21]	7.9	5.52/5.74, CF=10^3 2.53/5.12, D BP=5.70 °C
11/27/90	A/B	Insufficient data to evaluate.						
12/19/90	A	1.7	2	2.17	24	7	7.9	4.76/5.73, CF=10^3 2.23/5.01, D BP=6.57 °C
	B	Insufficient data to evaluate.						
3/26/91	A	1.1	0.45	1.5	7.5	4.87	7.9	6.35/5.74, CF=10^3 5.93/5.15, D BP=2.99 °C
	B	1.3	0.55	2.2	9.46	8.11	7.9	6.22/5.74, CF=10^3 4.21/5.14, D BP=2.99 °C
5/21/91	A	1.6	0.25	1.17	4.74	4.79	7.9	6.96/5.74, CF=10^3 6.29/5.02, D BP=4.81 °C
	B	Insufficient data to evaluate.						
8/9/91	A/B	Insufficient data to evaluate.						
10/28/92	A/B	Insufficient data to evaluate.						

[18] Estimate.
[19] From October 2, nearest available data point.
[20] From October 2, nearest available data point.
[21] From October 2, nearest available data point.

TABLE C.2-2, cont'd.

Feedwater Chemistry Data
For Periods of Chemistry Transients

Condensate Demineralizer Effluent High Na

Date	Train	Feedwater Impurity Concentration, ppb Na	Cl	SO_4	Formate	Acetate	H_3SiO_4	MULTEQ Estimated pH
6/24/90	A/B	Insufficient data to evaluate.						
10/8/90	A	0.14	0.65	0.9	4.5	2	7.9	4.66/5.75, CF=10^3 0.47/5.20, Δ BP=2.74 °C
	B	Insufficient data to evaluate.						
11/27/90	A/B	Insufficient data to evaluate.						
12/11/90	A/B	Insufficient data to evaluate.						
1/5/91	A/B	Insufficient data to evaluate.						
1/11/91	A/B	Insufficient data to evaluate.						
2/12/91	A/B	Insufficient data to evaluate.						
2/27/91	A/B	Insufficient data to evaluate.						
5/1/91	A/B	Insufficient data to evaluate.						
5/17/91	A/B	Insufficient data to evaluate.						
12/18/91	A/B	Insufficient data to evaluate.						

Condenser High Na and Low Cl

Date	Train	Feedwater Impurity Concentration, ppb Na	Cl	SO_4	Formate	Acetate	H_3SiO_4	MULTEQ Estimated pH
9/10/90	A	0.75	0.5	3.29	2[22]	2[23]	7.9	4.78/5.74, CF=10^3 0.95/5.22, Δ BP=3.19 °C
	B	Insufficient data to evaluate.						
9/18/90	A	1	0.6	7.05	2.8	2	7.9	4.33/5.74, CF=10^3 0.05/5.06, Δ BP=6.87 °C
	B	1	1.5	4	10	11.9	7.9	4.39/5.74, CF=10^3 1.01/5.18, Δ BP=4.23 °C
10/1/90	A	1.5	0.4	1	2.57	2	7.9	6.98/5.74, CF=10^3 9.42/5.02, Δ BP=4.49 °C
	B	Insufficient data to evaluate.						

[22] Estimate.
[23] Estimate.

TABLE C.2-2, cont'd.

Feedwater Chemistry Data
For Periods of Chemistry Transients

Condenser High Na and Low Cl, cont'd.

		Feedwater Impurity Concentration, ppb						MULTEQ
Date	Train	Na	Cl	SO_4	Formate	Acetate	H_3SiO_4	Estimated pH
10/8/90	A	0.14	0.65	0.9	4.5	2	7.9	4.66/5.75, CF=10^3 0.47/5.20, Δ BP=2.76 °C
	B	Insufficient data to evaluate.						
10/30/90	A	Insufficient data available.						
	B	1	0.5	2.02	8	15.5	7.9	5.81/5.74, CF=10^3 3.52/5.17, Δ BP=3.33 °C
11/6/90	A/B	Insufficient data available.						
11/16/90	A/B	Insufficient data available.						
12/4/90	A/B	Insufficient data available.						
1/5/91	A/B	Insufficient data available.						
1/22/91	A	0.5	0.6	2.97	7.9	6.1	7.9	4.58/5.74, CF=10^3 0.54/5.21, Δ BP=2.86 °C
	B	0.5	0.4	2	8.1	6.1	7.9	4.94/5.74, CF=10^3 1.02/5.13, Δ BP=6.71 °C
3/4/91	A/B	Insufficient data available.						
3/12/91	A	1.3	0.9	8.99	5.6	9.3	7.9	4.20/5.74, CF=10^3 0.45/5.20, Δ BP=2.71 °C
	B	1.3	0.7	5.3	6.3	11.3	7.9	4.67/5.74, CF=10^3 0.93/5.16, Δ BP=5.55 °C
3/19/91	A	1.2	0.4	2.9	4.7	8.1	7.9	5.92/5.74, CF=10^3 3.44/5.16, Δ BP=3.82 °C
	B	1.2	0.3	1.9	5.5	7.8	7.9	6.40/5.74, CF=10^3 5.66/4.99, Δ BP=6.85 °C
3/29/91	A/B	Insufficient data available.						
6/18/91	A/B	Insufficient data available.						
7/9/91	A	0.95	0.1	2.15	2.8	7.2	7.9	6.19/5.74, CF=10^3 3.71/5.04, Δ BP=6.66 °C
	B	0.8	0.1	0.72	3	2	7.9	6.71/5.74, CF=10^3 9.35/4.95, Δ BP=6.64 °C
7/16/91	A	Insufficient data available.						
	B	1	0.2	1	3	2	7.9	6.73/5.74, CF=10^3 9.35/5.13, Δ BP=2.91 °C

TABLE C.2-2, cont'd.

Feedwater Chemistry Data
For Periods of Chemistry Transients

Condenser High Na and Low Cl, cont'd.

		Feedwater Impurity Concentration, ppb						MULTEQ
Date	Train	Na	Cl	SO_4	Formate	Acetate	H_3SiO_4	Estimated pH
7/23/91	A	Insufficient data available.						
	B	1.1	0.2	2	8.6	2	7.9	6.46/5.74, CF=10^3 5.30/5.03, Δ BP=5.60 °C
7/31/91	A/B	Insufficient data available.						
8/8/91	A/B	Insufficient data available.						
8/20/91	A	1.2	0.1	3.71	5[24]	3[25]	7.9	5.91/5.74, CF=10^3 3.42/5.21, Δ BP=3.65 °C
	B	1.7	0.1	2.08	2	2	7.9	6.94/5.74, CF=10^3 9.39/5.04, Δ BP=4.45 °C
9/3/91	A	Insufficient data available.						
	B	0.8	0.2	2	3.5	3.6	7.9	5.98/5.74, CF=10^3 3.76/5.25, Δ BP=2.36 °C
9/10/91	A	1.4	0.3	3.29	5[26]	3[27]	7.9	6.20/5.74, CF=10^3 3.76/5.16, Δ BP=3.86 °C
	B	1.4	0.15	1.83	3	3	7.9	6.78/5.74, CF=10^3 9.23/5.10, Δ BP=3.71 °C
9/18/91	A	1.2	0.2	7.05	2.8	5[28]	7.9	4.55/5.74, CF=10^3 0.20/5.09, Δ BP=6.92 °C
	B	1.2	0.2	4.93	2.28	2	7.9	5.13/5.74, CF=10^3 1.30/5.19, Δ BP=4.81 °C
9/24/91	A	Insufficient data available.						
	B	0.9	0.3	2	2	2	7.9	6.08/5.74, CF=10^3 3.80/5.21, Δ BP=2.61 °C
10/1/91	A	Insufficient data available.						
	B	0.95	0.4	1	2.84	2	7.9	7.23/5.72, CF=10^3 9.01/5.14, Δ BP=2.77 °C

[24] Estimate.
[25] Estimate.
[26] Estimate.
[27] Estimate.
[28] Estimate.

TABLE C.2-2, cont'd.

Feedwater Chemistry Data
For Periods of Chemistry Transients

Condenser High Na and Low Cl, cont'd.

		Feedwater Impurity Concentration, ppb						MULTEQ
Date	Train	Na	Cl	SO_4	Formate	Acetate	H_3SiO_4	Estimated pH
3/10/92	A	1.4	0.4	1.33	3[29]	3.4	7.9	6.79/5.74, CF=10^3 9.23/5.06, D BP=6.92 °C
	B	1.2	0.6	1.48	3	3.9	7.9	6.44/5.74, CF=10^3 6.41/5.12, D BP=3.34 °C
4/14/92	A/B	Insufficient data available.						

[29] Estimate.

C.3
Detailed Analytical Results of Impurity Source Water Samples

TABLE C.3-1

Comparison of Crystal River Circulating Water Impurities With Published Impurities in Sea Water

	Concentrations, ppb		
Species	Circulating Water #1	Circulating Water #2	Sea Water[30]
Aluminum	10	13	10
Antimony	0.12	0.18	0.33
Argon	-	-	600
Arsenic	≤LOQ (2)	≤LOQ (2)	3
Barium	12	13	30
Beryllium	0.26	0.20	6E-4
Bismuth	≤LOQ (0.04)	≤LOQ (0.04)	0.017
Boron	2500	2500	4600
Bromine	41,000	43,000	65,000
Bromide	ND	-	-
Cadmium	≤LOQ (0.1)	0.40	0.11
Calcium	300,000	300,000	400,000
Carbon	-	-	28,000
Cerium	≤LOQ (0.4)	≤LOQ (0.4)	0.4
Cesium	0.26	0.15	0.5
Chlorine	-	-	19,000,000
Chloride	16,470,000	-	-
Chromium	≤LOQ (10)	≤LOQ (10)	0.05
Cobalt	3.2	3.3	0.27
Copper	≤LOQ (40)	≤LOQ (40)	3
Dysprosium	0.060	≤LOQ (0.5)	-
Erbium	0.080	≤LOQ (0.05)	-
Europium	≤LOQ (0.06)	≤LOQ (0.06)	-
Fluorine	-	-	1300
Fluoride	ND	-	-

[30] CRC Handbook of Chemistry & Physics, 69th Edition, Weast, R.C., ed., CRC Press, Inc., Boca Raton, 1988.

TABLE C.3-1, cont'd.

Comparison of Crystal River Circulating Water Impurities
With Published Impurities in Sea Water

Species	Concentrations, ppb Circulating Water #1	Circulating Water #2	Sea Water[31]
Gadolinium	0.070	≤LOQ (0.06)	-
Gallium	0.33	≤LOQ (0.05)	0.03
Germanium	≤LOQ (0.3)	0.90	0.07
Gold	≤LOQ (0.03)	0.050	0.011
Hafnium	0.11	≤LOQ (0.07)	≤LOQ (8E-3)
Helium	-	-	6.9E-3
Holmium	≤LOQ (0.02)	0.030	-
Hydrogen	-	-	1.08E8
Iodine	36	43	60
Indium	≤LOQ (0.05)	≤LOQ (0.05)	≤LOQ (20)
Iridium	≤LOQ (0.2)	≤LOQ (0.2)	-
Iron	80	56	10
Krypton	-	-	2.5
Lanthanum	≤LOQ (0.04)	≤LOQ (0.04)	0.012
Lead	0.48	0.46	0.03
Lithium	110	98	180
Magnesium	1,150,000	-	1,350,000
Manganese	≤LOQ (5)	≤LOQ (5)	2
Mercury	0.29	≤LOQ (0.2)	0.03
Molybdenum	6.9	8.4	10
Neodymium	≤LOQ (0.06)	0.060	-
Neon	-	-	0.14
Nickel	33	24	5.4
Niobium	≤LOQ (0.07)	≤LOQ (0.07)	0.01
Nitrogen	-	-	500
Nitrate	ND	-	-
Osmium	0.040	≤LOQ (0.03)	

[31] CRC Handbook of Chemistry & Physics, 69th Edition, Weast, R.C., ed., CRC Press, Inc., Boca Raton, 1988.

TABLE C.3-1, cont'd.

Comparison of Crystal River Circulating Water Impurities
With Published Impurities in Sea Water

Species	Concentrations, ppb Circulating Water #1	Circulating Water #2	Sea Water[32]
Oxygen	-	-	8.57E8
Palladium	≤LOQ (0.07)	0.080	-
Phosphorus	-	-	70
Phosphate	ND	-	-
Platinum	≤LOQ (0.04)	≤LOQ (0.04)	-
Potassium	1,079,000	-	380,000
Praseodymium	≤LOQ (0.04)	≤LOQ (0.04)	-
Protactinium	-	-	2E-6
Radium	-	-	6E-8
Radon	-	-	6E-13
Rhenium	0.080	0.080	-
Rhodium	0.22	0.18	-
Rubidium	84	84	120
Ruthenium	≤LOQ (0.05)	0.060	
Samarium	0.12	≤LOQ (0.07)	-
Selenium	20	20	0.09
Scandium	1.9	1.2	-
Silicon	950	920	3000
Silver	≤LOQ (0.06)	0.15	0.3
Sodium	7,967,000	-	10,500,000
Strontium	5600	5800	8100
Sulfur	-	-	885,000
Sulfate	2,040,000	-	-
Tantalum	≤LOQ (0.03)	0.030	≤LOQ (2.5E-3)
Tellurium	≤LOQ (0.2)	≤LOQ (0.2)	-
Terbium	0.050	≤LOQ (0.02)	-
Thallium	≤LOQ (0.1)	≤LOQ (0.1)	≤LOQ (0.01)
Thorium	≤LOQ (0.06)	≤LOQ (0.06)	0.05
Thulium	0.030	≤LOQ (0.02)	-
Tin	1.4	1.1	3
Titanium	≤LOQ (50)	≤LOQ (50)	1

[32] CRC Handbook of Chemistry & Physics, 69th Edition, Weast, R.C., ed., CRC Press, Inc., Boca Raton, 1988.

TABLE C.3-1, cont'd.

Comparison of Crystal River Circulating Water Impurities
With Published Impurities in Sea Water

Species	Concentrations, ppb Circulating Water #1	Circulating Water #2	Sea Water[33]
Tungsten	0.12	0.060	0.1
Uranium	2.3	2.5	3
Vanadium	≤LOQ (4)	≤LOQ (4)	2
Xenon	-	-	0.052
Ytterbium	0.90	≤LOQ (0.05)	-
Yttrium	≤LOQ (0.05)	0.21	0.3
Zinc	17	17	10
Zirconium	0.14	0.040	0.022

[33] CRC Handbook of Chemistry & Physics, 69th Edition, Weast, R.C., ed., CRC Press, Inc., Boca Raton, 1988.

TABLE C.3-2

Chemical Analysis of Crystal River Water Treatment Plant Effluent

Species	Concentrations, ppb Water Plant Effluent #1	Water Plant Effluent #2
Aluminum	≤LOQ (0.3)	≤LOQ (0.3)
Ammonium	0.62	0.73
Antimony	0.12	≤LOQ (0.1)
Arsenic	≤LOQ (2)	≤LOQ (2)
Barium	0.070	0.040
Beryllium	≤LOQ (0.09)	≤LOQ (0.09)
Bismuth	≤LOQ (0.04)	≤LOQ (0.04)
Boron	≤LOQ (0.3)	≤LOQ (0.3)
Bromine	7.0	5.5
Bromide	≤LOQ (1)	-
Cadmium	≤LOQ (0.1)	≤LOQ (0.1)
Calcium	≤LOQ (1)	≤LOQ (1)
Cerium	≤LOQ (0.4)	≤LOQ (0.4)
Cesium	≤LOQ (0.07)	≤LOQ (0.07)
Chloride	0.80	-
Chromium	≤LOQ (0.2)	≤LOQ (0.2)
Cobalt	≤LOQ (0.05)	≤LOQ (0.05)
Copper	≤LOQ (0.2)	≤LOQ (0.2)
Dysprosium	≤LOQ (0.05)	≤LOQ (0.05)
Erbium	≤LOQ (0.05)	≤LOQ (0.05)
Europium	≤LOQ (0.06)	≤LOQ (0.06)
Fluoride	0.05	-
Gadolinium	≤LOQ (0.07)	≤LOQ (0.07)
Gallium	≤LOQ (0.05)	≤LOQ (0.05)
Germanium	≤LOQ (0.1)	≤LOQ (0.1)
Gold	≤LOQ (0.03)	≤LOQ (0.03)
Hafnium	≤LOQ (0.04)	≤LOQ (0.02)
Holmium	≤LOQ (0.02)	≤LOQ (0.02)
Iodine	2.4	2.1
Indium	≤LOQ (0.05)	≤LOQ (0.05)

TABLE C.3-2, cont'd.

Chemical Analysis of Crystal River Water Treatment Plant Effluent

	Concentrations, ppb	
Species	Water Plant Effluent #1	Water Plant Effluent #2
Iridium	≤LOQ (0.2)	≤LOQ (0.2)
Iron	≤LOQ (10)	≤LOQ (10)
Lanthanum	≤LOQ (0.04)	≤LOQ (0.04)
Lead	0.070	≤LOQ (0.07)
Lithium	≤LOQ (0.4)	≤LOQ (0.4)
Magnesium	2.9 [≤LOQ (1)][34]	≤LOQ (0.3)[≤LOQ (1)]
Manganese	0.12	≤LOQ (0.07)
Mercury	≤LOQ (0.1)	≤LOQ (0.1)
Molybdenum	≤LOQ (0.09)	≤LOQ (0.09)
Neodymium	≤LOQ (0.06)	≤LOQ (0.05)
Nickel	0.85	≤LOQ (0.5)
Niobium	≤LOQ (0.07)	≤LOQ (0.07)
Nitrate	≤LOQ (1)	-
Osmium	≤LOQ (0.02)	≤LOQ (0.02)
Palladium	≤LOQ (0.09)	≤LOQ (0.09)
Phosphate	≤LOQ (1)	-
Platinum	≤LOQ (0.04)	≤LOQ (0.04)
Potassium	≤LOQ (0.5)	≤LOQ (0.5)
Praseodymium	≤LOQ (0.04)	≤LOQ (0.04)
Rhenium	≤LOQ (0.04)	≤LOQ (0.04)
Rhodium	≤LOQ (0.03)	≤LOQ (0.03)
Rubidium	≤LOQ (0.06)	≤LOQ (0.06)
Ruthenium	≤LOQ (0.05)	≤LOQ (0.04)
Samarium	≤LOQ (0.07)	≤LOQ (0.07)
Selenium	≤LOQ (0.07)	≤LOQ (0.07)
Scandium	0.13	0.12
Silicon	≤LOQ (50)	≤LOQ (50)
Silver	≤LOQ (0.06)	≤LOQ (0.06)

[34] Results obtained by ICP-MS [IC]

TABLE C.3-2, cont'd.

Chemical Analysis of Crystal River Water Treatment Plant Effluent

Species	Concentrations, ppb Water Plant Effluent #1	 Water Plant Effluent #2
Sodium	0.33	0.28
Strontium	≤LOQ (0.08)	≤LOQ (0.08)
Sulfate	0.52	-
Tantalum	≤LOQ (0.03)	≤LOQ (0.03)
Tellurium	≤LOQ (0.2)	≤LOQ (0.2)
Terbium	≤LOQ (0.2)	≤LOQ (0.2)
Thallium	≤LOQ (0.1)	≤LOQ (0.1)
Thorium	≤LOQ (0.06)	≤LOQ (0.06)
Thulium	≤LOQ (0.02)	≤LOQ (0.02)
Tin	0.12	0.060
Titanium	≤LOQ (0.3)	≤LOQ (0.3)
Tungsten	≤LOQ (0.02)	≤LOQ (0.02)
Uranium	≤LOQ (0.02)	≤LOQ (0.02)
Vanadium	≤LOQ (0.04)	≤LOQ (0.04)
Ytterbium	≤LOQ (0.05)	≤LOQ (0.05)
Yttrium	≤LOQ (0.05)	≤LOQ (0.05)
Zinc	1.6	≤LOQ (0.04)
Zirconium	≤LOQ (0.04)	≤LOQ (0.04)
Acetate	0.31	-
Propionate	≤LOQ (0.3)	-
Glycolate	≤LOQ (0.1)	-
Formate	0.18	-

C.4
Detailed Results From MULTEQ Evaluation of 1992 Hideout Return Data

TABLE C.4-1

MULTEQ pH Preductions From
1992 Hideout Return Data

SG A, 4/30/92, 0607 -- B&W Analytical Data

Input Species	Concentration	Predicted pH	NpH	ΔBP	CF
K^+	11.8 ppb	7.06	5.73	-	10^3
Cl^-	4.0	6.52	5.13	9.82	-
NO_3^-	3.3	No precipitates. No combined species			
OAc	8.6	in solution.			
HCO_2	34				

SG A, 4/30/92, 0607 -- FPC (B&W) Analytical Data

Input Species	Concentration	Predicted pH	NpH	ΔBP	CF
K^+	(11.8)[35] ppb	6.81	5.73	-	10^3
Cl^-	3.75	5.56	5.11	5.04	-
NO_3^-	(3.3)	K_2SO_4 precipitate. Potassium sulfate			
$SO_4^=$	2.12	in solution.			
F^-	0.18				
OAc	8.63				
HCO_2	9.67				

[35] Numbers in parentheses were obtained by B&W.

SG A, 4/30/92, 0607 -- FPC (B&W) Analytical Data, Sensitivity Run #1

Input Species	Concentration	Predicted pH	NpH	ΔBP	CF
Na^+	[1][36] ppb	3.95	5.73	-	10^3
K^+	[1] ppb	0.51	5.22	4.82	-
Cl^-	3.75	No precipitates. Potassium sulfate,			
NO_3^-	(3.3)	sodium sulfate, silica fluoride in solution.			
$SO_4^=$	2.12				
F^-	0.18				
OAc	8.63				
HCO_2	9.67				
H_3SiO_4	[15]				

SG A, 4/30/92, 0607 -- FPC (B&W) Analytical Data, Sensitivity Run #2

Input Species	Concentration	Predicted pH	NpH	ΔBP	CF
Na^+	[1] ppb	7.07	5.73	-	10^3
K^+	(11.8)	6.29	5.09	5.05	-
Cl^-	3.75	SiO_2, K_2SO_4 precipitated. Na_2SiF_6			
NO_3^-	(3.3)	precipitating next cycle of concentration.			
$SO_4^=$	2.12	Sodium sulfate, potassium sulfate, silica			
F^-	0.18	fluoride in solution.			
OAc	8.63				
HCO_2	9.67				
H_3SiO_4	[15]				

SG A, **Total Return** (Feed & Bleed) -- B&W (FPC) Analytical Data

Input Species	Grams/ppb	Predicted pH	NpH	ΔBP	CF
Na^+	6.1	7.86	5.73	-	10^3
Cl^-	0.13	9.99	4.87	7.96	-
NO_3^-	0.02	$Na_2Si_2O_5$, Na_2SiO_3 precipitated. Na_2SO_4			
$SO_4^=$	0.26	precipitating next cycle of concentration.			
H_3SiO_4	[10.3]	Sodium sulfate in solution.			

[36] Numbers in brackets are arbitrary concentrations input for sensitivity studies.

SG B, 4/30/92, 0609 – B&W Analytical Data

Input Species	Concentration	Predicted pH	NpH	ΔBP	CF
Na	0 ppb	3.80	5.74	-	10^3
K	0	0.85	5.41	3.33	-
Cl	3.9				
NO_3	3.0	No precipitates predicted. No complex			
OAc	27.5	species in solution.			
HCO_2	34.0				

SG B, 4/30/92, 0609 – FPC (B&W) Analytical Data

Input Species	Concentration	Predicted pH	NpH	ΔBP	CF
K^+	0 ppb	3.32	5.72	-	10^3
Cl^-	3.13	0.37	5.24	3.08	-
NO_3^-	(3.0)				
$SO_4^=$	1.51	No precipitates. No complex species			
F^-	0.20	in solution.			
OAc	8.71				
HCO_2	2.00				

SG B, 4/30/92, 0609 – FPC (B&W) Analytical Data, Sensitivity Run #1

Input Species	Concentration	Predicted pH	NpH	ΔBP	CF
Na^+	[1] ppb	4.08	5.74	-	10^3
K^+	[1] ppb	0.64	5.24	3.10	-
Cl^-	3.13	No precipitates. Silica fluoride			
NO_3^-	(3.0)	in solution.			
$SO_4^=$	1.51				
F^-	0.20				
OAc	8.71				
HCO_2	2.00				
H_3SiO_4	[12.2]				

SG B, 4/30/92, 0609 – FPC (B&W) Analytical Data, Sensitivity Run #2

Input Species	Concentration	Predicted pH	NpH	ΔBP	CF
Na^+	[1] ppb	4.08	5.74	-	10^3
K^+	[1] ppb	0.64	5.24	3.10	-
Cl^-	3.13				
NO_3^-	(3.0)	No precipitates. Silica fluoride			
$SO_4^=$	1.51	in solution.			
F^-	0.20				
OAc	8.71				
HCO_2	2.00				
H_3SiO_4	[23.4]				

SG B, **Total Return** (Feed & Bleed) – B&W (FPC) Analytical Data

Input Species	Grams/ppb	Predicted pH	NpH	ΔBP	CF
Na^+	23	8.84	5.68	-	10^3
Ca^{++}	0.13	10.15	5.11	2.77	-
Cl^-	0.62				
NO_3^-	0.76	Na_2SiO_3 precipitated. Na_2SO_4			
$SO_4^=$	0.03	in solution.			
H_3SiO_4	(5.3)				

C.5
Detailed Results From MULTEQ Evaluation of 1992 Hideout Return Data

TABLE C.5-1

MULTEQ Results for 1993 Shutdown Cooldown

OTSG A, 3/4/93, 0225

Input Species	Concentration	Predicted pH	NpH	ΔBP	CF
Na^+	2.6 ppb	5.82	5.74	-	10^3
K^+	1.2 ppb	5.10	5.43	3.81	-
Cl^-	0.1				
NO_3^-	3.6	Silica precipitated for under-deposit case.			
$SO_4^=$	1.9	$NaSO_4$, Na_2SO_4, $NaHSO_4$, KSO_4, HSO_4, HOAc,			
F^-	-	HC_2OH, and H_4SiO_4 in solution.			
OAc	36				
HCO_2	41				
H_3SiO_4	15.6				

OTSG A, 3/4/93, 1030

Input Species	Concentration	Predicted pH	NpH	ΔBP	CF
Na^+	0.1 ppb	5.10	5.75	-	10^3
K^+	-	2.04	5.62	3.10	-
Cl^-	-				
NO_3^-	-	No precipitates.			
$SO_4^=$	0.7	$NaSO_4$, $NaHSO_4$, HSO_4, HOAc,			
F^-	-	and HC_2OH in solution.			
OAc	13				
HCO_2	9.9				
H_3SiO_4	-				

OTSG A, 3/4/93, 1830

Input Species	Concentration
Na^+	8.5 ppb
K^+	1.3 ppb
Cl^-	2.1
NO_3^-	-
$SO_4^=$	1.7
F^-	-
OAc	460
HCO_2	93
H_3SiO_4	14.2

Predicted pH	NpH	ΔBP	CF
5.41	5.73	-	10^3
4.84	5.45	7.38	-

No precipitates.
$NaSO_4$, Na_2SO_4, $NaHSO_4$, HSO_4, HOAc, HC_2OH, and H_4SiO_4 in solution.

OTSG A, 3/5/93, 0630

Input Species	Concentration
Na^+	3.6 ppb
K^+	0.4 ppb
Cl^-	1.4
NO_3^-	-
$SO_4^=$	2.6
F^-	-
OAc	160
HCO_2	75
H_3SiO_4	37.4

Predicted pH	NpH	ΔBP	CF
5.34	5.72	-	10^3
4.93	5.54	3.17	-

No precipitates.
$NaSO_4$, $NaHSO_4$, Na_2SO_4, HSO_4, HOAc, HC_2OH, and H_4SiO_4 in solution.

OTSG B, 3/4/93, 0225

Input Species	Concentration
Na^+	3.1 ppb
K^+	0.3 ppb
Cl^-	3.5
NO_3^-	-
$SO_4^=$	11
F^-	-
OAc	110
HCO_2	21
H_3SiO_4	8

Predicted pH	NpH	ΔBP	CF
4.12	5.73	-	10^3
1.22	5.42	6.10	-

Silica precipitated for under-deposit case.
$NaSO_4$, Na_2SO_4, $NaHSO_4$, KSO_4, HSO_4, HOAc, HC_2OH, and H_4SiO_4 in solution.

OTSG B, 3/4/93, 1030

Input Species	Concentration	Predicted pH	NpH	ΔBP	CF
Na^+	0.2 ppb	6.02	5.75	-	10^3
K^+	-	5.62	5.47	3.59	-
Cl^-	-				
NO_3^-	-	No precipitates.			
$SO_4^=$	-	HOAc and HC_2OH in solution.			
F^-	-				
OAc	2.7				
HCO_2	4.9				
H_3SiO_4	-				

OTSG B, 3/4/93, 1830

Input Species	Concentration	Predicted pH	NpH	ΔBP	CF
Na^+	1.3 ppb	5.97	5.74	-	10^3
K^+	-	3.16	5.07	4.56	-
Cl^-	-				
NO_3^-	2.1	No precipitates.			
$SO_4^=$	1.6	$NaSO_4$, Na_2SO_4, $NaHSO_4$, HSO_4			
F^-	-	in solution.			
OAc	-				
HCO_2	-				
H_3SiO_4	-				

OTSG B, 3/5/93, 0630

Input Species	Concentration	Predicted pH	NpH	ΔBP	CF
Na^+	53 ppb	6.02	6.59	-	10^3
K^+	2.1 ppb	5.30	5.35	4.67	-
Cl^-	11				
NO_3^-	3.6	No precipitates.			
$SO_4^=$	12	$NaSO_4$, Na_2SO_4, $NaHSO_4$, KSO_4, HSO_4, HOAc,			
F^-	0.3	HF, HF_2, HC_2OH, and H_4SiO_4 in solution.			
OAc	630				
HCO_2	340				
H_3SiO_4	90				

APPENDIX B

MPR STRUCTURAL ANALYSIS

MPR
ASSOCIATES INC
ENGINEERS

February 24, 1994

Ms. Phyllis Dixon
Florida Power Corporation
Crystal River Energy Complex
15760 West Power Line Street
Crystal River, Florida 34428-6708

Subject: CR-3 Steam Generator

Dear Ms. Dixon:

Enclosed as requested is our report "Evaluation of Crystal River Unit 3 (CR-3) Steam Generator Tube Wall Degradation," dated February 24, 1994.

Please call if you have any questions or comments.

Sincerely,

Sterling J. Weems

Enclosure

320 KING STREET ALEXANDRIA, VA 22314-3238 703-519-0200 FAX 703-519-0224